GEOCHEMICAL MODELLING OF THE SPECIATION, TRANSPORT, DISPERSAL AND FATE OF METAL CONTAMINANTS IN WATER SYSTEMS IN THE VICINITY OF TAILINGS STORAGE FACILITIES

Bronwyn Patricia Camden Grover

A Thesis submitted to the Faculty of Science, University of the Witwatersrand, Johannesburg, in fulfilment of the requirements for the degree of Doctor of Philosophy

Johannesburg, 2016

DECLARATION

I declare that this thesis is my own, unaided work. It is being submitted for the Degree of Doctor of Philosophy at the University of the Witwatersrand, Johannesburg. It has not been submitted before for any degree or examination at any other University.

_____

Bronwyn P.C. Grover

_____ day of _____ 20_____ in _____

ABSTRACT

Gold mining of the Witwatersrand Basin reefs has been responsible for the rise of Johannesburg as an economic centre of South Africa. While mining provided a base for business and infrastructure development for the region, it has also generated social and environmental problems for the country. Tailings storage facilities (TSFs), a common sighting around Johannesburg and across the entire basin, have been built to contain the processed waste following extraction of gold from the pyrite containing quartzite ore. When the fine grained waste is exposed to atmospheric conditions, oxidation of remnant sulphides occurs resulting in acidic, metal rich and sulphate rich plumes that enter the environment through surface and groundwater systems.

This thesis sought to better understand the release, transport, dispersal and fate of metals emanating from TSFs and their remnant footprints on the Witwatersrand. These metals included aluminium, copper, chromium, iron, manganese, nickel and uranium and are known to be toxic to humans depending on their concentration and speciation. Traditionally, analytical methods have been employed in studies focussing on the characterisation of some of these processes in the region. While these studies have generally conducted quantitative assessment of the extent of pollution, little comprehensive interrogation and fingerprinting of the processes that are influential in determining the potential risk posed by metals has been done. This has largely been due to the shortcomings of analytical methods to determine these. To this end, this research has employed geochemical modelling to complement the traditional analytical methods.

The approach to study the release of metals from TSFs involved assessment of the partitioning of metals within tailings and their potential release using batch and sequential extraction methods. Processes of metal release within the tailings were simulated through geochemical modelling (using the PHREEQC and Geochemist's Workbench codes). The simulations were based on the percolation of rainwater through these layers and the changes in its chemistry along the path. The potential seepage of this plume along the path was then

correlated to observed efflorescent mineral crusts that are temporary sinks for metals and are a common feature in the vicinity of the tailings and water bodies such as ponds and streams. The potential impact of the mineral crusts on the water chemistry of receiving water systems following their dissolution was assessed using forward geochemical modelling. The transport of the metals in groundwater was also studied. This involved simulations of the transition in chemistry of a plume from a TSF along an aquifer of known composition. This was based on a 1-D reactive transport model constructed using information from sequential extraction work on the aquifer rock (to identify the key minerals to consider) and site data (mainly flow rates) from previous studies. The processes occurring in the removal of metals from acid mine drainage (AMD) through a permanent sink in the form of a pump-and-treat plant in the Central Goldfield of the basin were simulated using PHREEQC.

The findings from the research showed that two different plumes were produced from an abandoned TSF as a result of rainwater percolation, notably a plume produced from the dissolution of secondary salts formed in the oxidised layer and a sulphuric acid rich plume in the unoxidised layer. These differences were apparent in the geochemical composition of the mineral crusts collected on the walls of tailings dumps and from a pond into which the plumes were draining. On dissolution, mineral crusts were found to produce acidic solutions with crusts containing predominantly Fe producing pH values below 3. The simulated dissolution of various types of mineral crusts gave insight into the impact of minerals present in the smallest amount. This showed that the bulk mineralogy as determined by analytical techniques such as PXRD and remote sensing could not be used with confidence to deduce the impact of the mineral crusts on receiving water bodies.

The characteristics of surface plumes released from tailings TSF were compared to other water systems in the area around Soweto, with complementary interpretation conducted using chemometric methods. From principal component analysis (PCA), surface water systems were found to form

distinct groups largely influenced by mineral solubility, alkalinity and dissolved oxygen content.

The 1-D reactive transport simulations involved acidic, metal and sulphate rich water ingressing the aquifer (below the TSF). Several scenarios were modelled including simulations with different dolomite contents; allowing for surface complexation and the presence of cation exchange surfaces. At a point 500 m from the water ingress in the dolomite rich aquifer, Fe and Mn were largely precipitated out (as confirmed by sequential extraction results on the aquifer rock) while the sulphate concentration was reduced by almost half. On the other hand, Ca concentrations were conservative largely because of continuous dissolution of dolomite and precipitation of gypsum along the flow path.

The simulations of the high density sludge treatment plant involved forward modelling of the treatment process with the sludge responsible for the removal of trace metals from the incoming acid mine drainage. The model can be of use for cost and process optimisation at the facility.

This research has had notable outputs in the form of publications; models on metal release, transport and attenuation; and models on pump-and-treat processes. These will form an important repository of information and for benchmarking any further studies related to AMD.

ACKNOWLEDGEMENTS

I am very grateful to have been supervised by Professor Hlanganani Tutu. His continuous encouragement, support and advice have been hugely appreciated throughout this work. Thank you Prof Tutu, I cannot express how thankful I am for all the opportunities and knowledge you've given me access to.

My co-supervisor, Dr Raymond Johnson has been a mentor in geochemical modelling and my time spent with him in The United States of America was very beneficial and interesting. His continued patience in teaching modelling and his expert opinions are highly appreciated.

I am grateful to the National Research Foundation for funding this research (Innovation Doctoral Scholarship, number 86340).

The Environmental Analytical Chemistry Group has been a second home to me for several years. I am immensely appreciative towards Professor Ewa Cukrowska, Professor Luke Chimuka and Professor Hlanganani Tutu for welcoming me into their research group and for all of their support and expertise during my studies. Within the research group, I am grateful to have built friendships with the staff and fellow postgraduates. In particular, I'd like to thank Julien, Elysee, Thuthuka, Phatsimo, Charlene, Xoliswe, Nikita, Bongani, Kgabo, Stanley, Somandla and Dikeledi for their good spirit, willingness to help and support.

Thank you to the School of Chemistry, University of the Witwatersrand. I'd like to thank the previous and current Head of School, Professor Joseph Michael (2012) and Professor Dean Brady (2013- 2016), for their support.

The United States Geological Survey (USGS) hosted me for a six week voluntary internship in 2013 under the guidance of Dr R.H. Johnson. I learnt so much during this time and was lucky to meet and interact with many passionate professionals.

Powder X-ray diffraction was run following training and discussion with Professor Dave Billing. Thank you for your guidance. Thank you to the postgraduates in the PXRD laboratory (Wilson, Robert and Stewart) for their assistance.

The School of Animal Plant and Environmental Sciences were of assistance at and after sampling expeditions. In particular, I'd like to thank Isabel Weiersbye for her guidance and discussion as well as Peter Dye for his assistance during and after sampling.

Thank you to AngloGold Ashanti for access to their property for sampling.

The cooperation and openness of Peter Walters and Mintails Pty (Ltd) were greatly appreciated. Thank you to Anthony Turton for his organization of sampling expeditions at this site, his reference material and his passion and interest in this work.

I was incredibly fortunate to attend the International Mine Water Association conferences held in Golden, United States of America (2013); Xuzhou, China (2014) and Santiago, Chile (2015). The experience of presenting and the advice received from "the geochemical legends" at these conferences have been invaluable to this work and to me personally.

I am appreciative of my peers and friends at Young Water Professional South Africa for their support and expertise at YWP conferences and workshops. Thank you to Water Institute of South Africa and Water Research Commission for their research material and discussion at events, workshops and conferences.

I am thankful to have been on the committee of both ChemSoc and Whizz Bang within the School of Chemistry. This gave the opportunity of engaging with different research groups within the School and I'd like to thank Jean, Robyn, Amy, Monika, Jess, Hendrik and Evah for their discussions and advice.

I was fortunate to supervise two students during their Research Assistantship Projects, Papi Mthombeni and Nicole Pretorius. I'd like to thank the School of

Chemistry for giving me the opportunity to work with these enthusiastic individuals as well as the many undergraduates that I've demonstrated and tutored over the years. They taught me much more than I could've taught them.

I met some very special students in the first year of my BSc and I am so fortunate to have had them as friends all the way through to end of my PhD. These friends and the friends that I have made during my studies have been empathetic and supportive. To my best friends, Lindsay and Jean, thank you for everything.

My family has been kind, patient and supportive from the very start of my studies and I would not have been able to do this without their unceasing love and encouragement. Thank you to the Camden-Smith (Peter, Pam, Darrel, Taryn and Michael), the Bartram (Sam, Shaun, Jaydee and Peter), the Grover (Avril, Richard and Terence) and the Sequeira (Mandy, Sean, Alex and Cameron) families, I am so blessed to be a daughter, sister or aunt to you. A special thank you to my mom, Pam Camden-Smith, and Samantha Bartram for proofreading and editing numerable abstracts and journal articles, your input was greatly appreciated.

My husband, Stephen Grover, has been a source of endless encouragement throughout my studies. I cannot describe how thankful I am for everything that he has done, for his incredibly good sense of humour and for his love.

Lastly; I'd like to extend a heartfelt expression of gratitude to my dad, Peter Camden-Smith. He has given me so much more than his support and assistance throughout my research; he has encouraged and nursed a love of science and our natural world from the beginning. I've met many incredible people throughout my travels and conferences, yet my dad remains the most passionate and knowledgeable person I've ever known.

CONTENTS

DECLARATION i
ABSTRACT ii
ACKNOWLEDGEMENTS v
LIST OF FIGURES xi
LIST OF TABLES xvi
CHAPTER ONE- Introduction 1
1.1 Introduction to the Witwatersrand Gold Fields 2
1.1.1 Discovery of the Witwatersrand Goldfields 2
1.1.2 Geology and mining of the Witwatersrand Supergroup 3
1.1.2 Economic Significance of the Region 6
1.1.4 Water Resources 6
1.1.5 Environmental Problems Related to Mining Activities 7
1.2 Hypothesis 8
1.3 Aims and objectives 9
1.4 Structure of thesis 10
CHAPTER TWO- Literature review 14
2.1 Evolution, mobility and remediation of metals in mining-impacted waters 14
2.1.1 Acid mine drainage and the release of metal contaminants 14
2.1.2 Elemental speciation and mobility of metals in mining-impacted waters 17
2.1.3 Remediation of Acid Mine Drainage 18
2.2 Theory and applications of geochemical modelling 23
2.2.1 Speciation-solubility models 23
2.2.2 Forward modelling 25
2.2.3 Inverse modelling 26
2.2.4 Reaction path modelling 27
2.2.5 Coupled transport and reaction modelling 29
CHAPTER THREE- Methodology 33
3.1 Sampling 35
3.1.1 Sampling Sites 35
3.1.2 Water Sampling Procedure 45
3.1.3 Water Sample Preservation 46
3.1.4 Solid Material Sampling 46

3.1.5 Solid Material Preservation 47
3.2 Sample Preparation 47
3.2.1 Leaching studies 49
3.2.2 Dissolution and evaporation of soluble sampled material (i.e. efflorescent crusts) 54
3.2.3 Acidic microwave digestion of solid material 55
3.3 Analytical Techniques 56
3.3.1 Analysis of Water and Prepared Samples 56
3.3.2 Analysis of Solid Material 65
3.4 Strategy for constructing geochemical models 67
3.4.1 Establishment of the goals of the model 67
3.4.2 Site selection and determination of the water flow system 68
3.4.3 Compilation of field and laboratory data 68
3.4.4 Selection of geochemical models 68
3.4.5 Assemblage of chemical properties 69
3.4.6 Selection of a computer code 73
3.4.7 Construction of a model 74
3.4.8 Verification and validation of models 74
3.4.9 Interpretation of modelling results 77
CHAPTER FOUR - Evolution of metal pollutants from tailings storage facilities 78
4.1. Mineralogy of tailings material 78
4.2. Batch and Sequential Leaching of Tailings Material 79
4.2.1. Journal article 1: Geochemical modelling of the evolution and fate of metal pollutants arising from an abandoned gold mine tailings facility in Johannesburg 80
4.2.2. Journal article 2: Fractionation of metals in gold mine tailings: implications for release and mobility to the surroundings 81
4.2.3. Journal article 3: Leachability of metals from gold tailings by rainwater: an experimental and geochemical modelling approach 103
CHAPTER FIVE- Distribution pathways of pollutants from tailings storage facilities: transport, dispersal and fate 104
5.1 Groundwater systems 105
5.1.1. Conference proceedings 1: The release and transport of metals arising from gold mining tailings storage facilities in the Witwatersrand, South Africa 107
5.1.2 One dimensional reactive transport model of a metal and sulphate plume emanating from an active TSF 124

5.2 Surface water systems 131
5.2.1 Conference proceedings 2: Chemical Transformations of Metals Leaching from Gold Tailings 132
5.2.2 Occurrence and distribution of metals in surface water systems 133
5.3 Temporary and Permanent Sinks 156
5.3.1 Evaporation barriers 157
5.3.1.1 Conference proceedings 3: Investigating the potential impact of efflorescent mineral crusts on water quality: complementing analytical techniques with geochemical modelling 158
5.3.1.2 Journal article 4: Mineralogy and geochemistry of efflorescent minerals on mine tailings and their potential impact on water quality 159
5.3.2 AMD Treatment Plants 160
5.3.2.1 Journal article 5: Investigating the removal of trace metals in a high density sludge treatment plant using a geochemical modelling approach 160
5.4 Overview of modelling 173
5.4.1 Book chapter: Geochemical modelling of water quality and solutes transport from mining environments 173
CHAPTER SIX- General conclusions and recommendations 175
REFERENCES 180
APPENDICES 196

LIST OF FIGURES

Figure 1.1: Geological map showing of the surface and subsurface extent of the West Rand and Central Rand Group (from Frimmel, 2005) 3

Figure 1.2: Map showing the relative position of the different Witwatersrand Goldfields and active gold mines (after Vorster, 2000) 5

Figure 2.1: One dimensional representation of a coupled transport and reaction model (from Crawford, 1999) 30

Figure 3.1: Outline of sample preservation, preparation and analysis 34

Figure 3.2: Photographs of the tailings pond and edge of TSF located in Germiston during: a) the dry season and b) the wet season 36

Figure 3.3: Proposed scheme of surface water and groundwater flow from TSF to pond to stream (from Camden-Smith and Tutu (2014)) 36

Figure 3.4: a) Samples of unoxidised material b) Samples of oxidised material c) Evaporated pond section from which efflorescent crust samples were taken d) Tailings pond 37

Figure 3.5: Idealised sampling plan for groundwater plumes emanating from an active tailings storage facility 39

Figure 3.6: a) Excavator digging linear pit b) Saturated zone exposed at the bottom of pit 39

Figure 3.7: Google Earth map of the area showing where water (red markers) and solid samples (labeled as “pit”) were collected 40

Figure 3.8: Google Earth overview of the sampled region 42

Figure 3.9: Photograph of the tailings storage facility 42

Figure 3.10: Photograph of tailings run off pond 42

Figure 3.11: Photograph of tailings run off pond (in foreground) and pollution control dam (in background) 43

Figure 3.12: Photograph of wetland adjacent to the pollution control dam 43

Figure 3.13: Google Earth image of the September 2012 water sampling excursion 44
Figure 3.14: Different leaching approaches (adapted from Rao, Sahuquillo & Lopez Sanchez, 2008) 49
Figure 3.15: Processes of metal pollutant evolution and transportation from a tailings storage facility that were considered in geochemical models 68

Figure 5.1: Map of sulphate plumes at the Vaal study site. Boreholes in the vicinity of Plume 1 were sampled (Figure extracted from report by GCS (Pty) Ltd, 2011) 106
Figure 5.2: Aluminium partitioning in sediments impacted by underground AMD plume 111
Figure 5.3: Calcium partitioning in sediments impacted by underground AMD plume 111
Figure 5.4: Copper partitioning in sediments impacted by underground AMD plume 112
Figure 5.5: Magnesium partitioning in sediments impacted by underground AMD plume 112
Figure 5.6: Manganese partitioning in sediments impacted by underground AMD plume 112
Figure 5.7: Nickel partitioning in sediments impacted by underground AMD plume 113
Figure 5.8: Zinc partitioning in sediments impacted by underground AMD plume 113
Figure 5.9: Boreholes sampled for water at the end of the dry season at the active western TSF situated in plume 1. Solid sampling was undertaken at Pit and Borehole B. 115
Figure 5.10: Boreholes sampled for water at the end of the dry season at the eastern TSF footprint situated in plume 3. 115
Figure 5.11: Input for inverse model between borehole A with infiltrating rainwater and borehole B 122

Figure 5.12: Input for basic reactive transport model (model A) 126
Figure 5.13: Additional input script for the inclusion of reactive surface modelling into the reactive transport model (model B) 126
Figure 5.14: Additional input script for the inclusion of cation exchange surfaces into the reactive transport model (model C) 127
Figure 5.15: 1-D PHREEQC reactive transport modelled output of pH within the plume at 15 years (55 steps). Models with high dolomite content are in the foreground and low dolomite models are set further back 128
Figure 5.16: 1-D PHREEQC reactive transport modelled output of pH within the plume at 50 years (180 steps) 128
Figure 5.17: 1-D PHREEQC reactive transport modelled output of dissolved iron within the plume at 15 years (55 steps) 129
Figure 5.18: 1-D PHREEQC reactive transport modelled output of dissolved iron within the plume at 50 years (180 steps) 130
Figure 5.19: 1-D PHREEQC reactive transport modelled output of precipitated iron hydroxide from the plume at 15 years (55 steps) 130
Figure 5.20: 1-D PHREEQC reactive transport modelled output of precipitated iron hydroxide from the plume at 50 years (180 steps) 131
Figure 5.21: Modified Google Earth image of tailings spillage stream and stream showing flow directions (sampling undertaken in September 2012, satellite imagery from 3 October 2012) 138
Figure 5.22: Modified Google Earth map showing the relative positions of a sampled stream and its sampled tributary. The tributary flows along the southern edge of a TSF and through a residential area (sampling undertaken in September 2012, satellite imagery from 1 140
Figure 5.23: Photograph showing foam and rapids at the sampling site of sample stream 3 140

Figure 5.24: Modified Google Earth image showing positioning of trench samples along the southern edge of a TSF (sampling undertaken in September 2012, satellite imagery from 3 October 2012) 142

Figure 5.25: Photograph showing colour change in trench surrounding TSF. Water is flowing from left to right. Before the outlet, water was orange with a pH of 3.5; water decanting from the pipe has a pH of 9.6; water after the pipe is blue/green with a pH of 3.6 142

Figure 5.26: Modified Google Earth map showing the relative positions of samples from Fleuhof dam, Florida Lake and the tailings paddock. (sampling undertaken in September 2012, satellite imagery from 9 December 2012) 143

Figure 5.27: Photograph of seepage emanating from freshly exposed residual tailings material following reprocessing of the TSF 144

Figure 5.28: Piper diagram plot of Soweto samples 146

Figure 5.29: Scree plot of Pearson principal component analysis of Soweto samples 147

Figure 5.30: Analysed variables plotted on first and second principal component axes showing a grouping of transition metals along the first axis and a partial grouping of alkali and alkali earth metals along the second axis 149

Figure 5.31: Observations (samples) plotted on first and second principal component axes showing a grouping of acidic samples taken from within the trenches or near to trenches surrounding TSF and lesser polluted streams and dams 150

Figure 5.32: Geochemist's Workbench calculated saturation indices of a selection of minerals within the spillage stream samples 151

Figure 5.33: Geochemist's Workbench calculated saturation indices of a selection of minerals within the stream samples collected in Soweto 152

Figure 5.34: Geochemist's Workbench calculated saturation indices of a selection of minerals within the samples collected from a trench collecting leachates bordering a TSF in Soweto 153

Figure 5.35: Geochemist's Workbench calculated saturation indices of a selection of minerals within the tailings paddock run off sample 154

Figure 5.36: Geochemist's Workbench calculated saturation indices of a selection of minerals within dam and lake samples collected within Soweto 154

LIST OF TABLES

Table 3.1: Outline of the BCR sequential leach (adapted from Rauret et al. (1999)) 54

Table 3.2: Preparation of 1000 mg L-1 anion stock solution for IC calibration (as recommended by ASTM International, 2010) 63

Table 3.3: Comparison of the models for determining ion activity coefficients 72

Table 5.1: BCR sequential extraction results for the borehole sample (sampled at 10 m). Values are the average of three replicates and analytical error <10% 109

Table 5.2: Field measurements and alkalinity determinations of borehole samples from plume 1 and plume 3 116

Table 5.3: Anion and metal concentrations within borehole samples from plume 1 and plume 3 118

Table 5.4: Charge balance and selected saturation indices of borehole water samples 120

Table 5.5: Results of inverse modelling between borehole A with infiltrating rainwater and borehole B 124

Table 5.6: Description of Soweto sampling sites 135

Table 5.7: Field determined physio-chemical parameters and lab based alkalinity titrations of Soweto water samples 136

Table 5.8: Quantification of anion and metal concentrations in Soweto water samples 137

Table 5.9: Factor loading of the first four principal components for the Soweto samples 148

`

CHAPTER ONE- INTRODUCTION

The Witwatersrand gold fields have been mined since their discovery in 1886. The abundance of gold in the area has been both a blessing and a curse for the past and present citizens of South Africa. The region flourished economically and the business hub of Africa was founded in Johannesburg, the site of the first gold discovery. Unfortunately, the mining of this famous deposit has come at a price, with both negative social and environmental implications. Despite the decrease in mining activity over the past two decades, the environmental impacts resulting from flooding of abandoned or decommissioned mine workings and tailings storage facilities continues. Acid mine drainage is a well documented worldwide environmental concern resulting from the oxidation of sulphide minerals within exposed rock or waste material. The subsequent generation of acidic, metal rich water along with its release into and effects on the environment has been the topic of numerous discussions and research endeavours spanning the physical, social and political sciences. This research seeks to better understand the release, transport and dispersal of metals in acid mine drainage emanating from tailings storage facilities on the Witwatersrand gold fields through a combination of analytical and geochemical modelling techniques.

Chapter One provides a brief introduction to the discovery, geology, mining and economic significance of the Witwatersrand gold fields followed by an overview of water resources in Johannesburg and environmental problems related to mining activities. The hypothesis, aims and objectives, and research questions are defined and the structure of the thesis is presented.

`

1.1 Introduction to the Witwatersrand Gold Fields

This section details the discovery of the gold in South Africa and then details the discovery and significance of the all important economical gold reefs within the Central Rand Group. The geology of the area was studied through the search for new or extended reefs and the current placement of towns and cities in the region is a consequence of these discoveries. This section also discusses water resources and water concerns within the area. A shallow water table was originally present in the region and once underground mining was initiated, large volumes of water were pumped away from the workings and a multitude of environmental concerns has arisen due to this.

1.1.1 Discovery of the Witwatersrand Goldfields

South Africa's gold mining history did not start with the discovery of the Witwatersrand gold reefs. Alluvial gold eroded from the Witwatersrand was discovered by Pieter Jacob Marais in 1853. However, it was not until 1874 that the first mine was opened by the Nil Desperandum Co-operative Quartz Company near what is today Magaliesburg (Durand, 2012). The Timeball Hill Formation quartzites of the Transvaal Supergroup were mined at this location near Blaauwbank (Durand, 2012). This deposit was generally considered uneconomical, although it was occasionally mined up until the 1960s (Lednor, 1986). Mining of the same formation also occurred at Broederstroom (Janisch, 1986). Both of these sites are situated in what is today the North West province.

In 1886, George Harrison discovered the Main Reef. The Central Rand Goldfield lies south of Johannesburg and hosts the site of the discovery made by Harrison on Langlaagte farm in February 1886 (Werdmuller, 1986). Gold bearing conglomerates were discovered by Fred Struben in 1884, prior to the major discovery by George Harrison (Lednor, 1986). However, these were low grade conglomerates of the West Rand group and as such the discovery of the Witwatersrand is attributed to Harrison for his identification of the economically important Main Reef (Lednor, 1986). The Main Reef discovery shaped the future of the Witwatersrand Goldfields. The Main Reef and the other reefs of the Central Rand Group are hosts to the richest and most

`

extensive gold deposit in the world. The Main Reef was extensively explored and mining camps gave rise to the towns and cities that continue to function today. These include Roodepoort, Krugersdorp, Germiston, Boksburg, Nigel, Brakpan, Carletonville and Johannesburg (Durand, 2012).

1.1.2 Geology and mining of the Witwatersrand Supergroup

The world renowned Witwatersrand gold ore deposit is hosted in a sedimentary rock sequence which was deposited approximately 2.8 billion years ago into a large inland basin. It is comprised of two stratigraphic groups; the West Rand Group and the Central Rand Group (Figure 1.1). Shales and quartzites in equal proportions make up the West Rand Group whereas quartzites and conglomerates with few shale units make up the younger Central Rand Group (McCarthy, 2006).

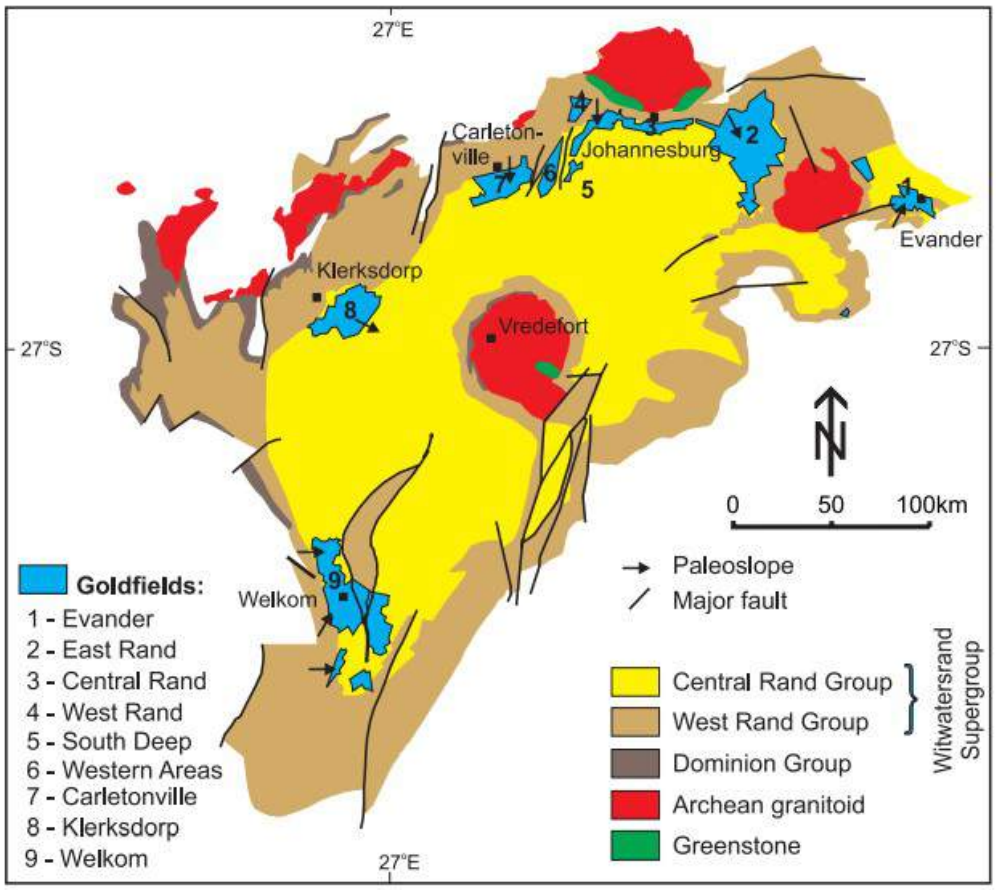

Figure 1.1: Geological map showing of the surface and subsurface extent of the West Rand and Central Rand Group (from Frimmel, 2005)

`

The Central Rand Group hosts the gold bearing conglomerates from which 1600 million ounces of gold have been extracted. The quartz pebble conglomerate horizons contain about 3% pyrite and a range of other sulphide ore minerals in lesser abundance such as arsenopyrite (FeAsS), cobaltite (CoAsS), galena (PbS), pyrrhotite (FeS) and gersdofite (NiAsS) (Naicker, Cukrowska, & McCarthy, 2003). Oxide ore minerals include uraninite (UO_2), brannerite ($UO_3Ti_2O_4$) and chromite ($FeCr_2O_4$) (Naicker et al., 2003).

The region hosts various goldfields as shown in Figure 1.2. The Central Rand Goldfield hosts the original discovery site and has hosted approximately 46 mines since its discovery.

Faults known as the Witpoortjie Gap separate the Central Rand Goldfield from the West Rand Goldfield (McCarthy, 2006). The West Rand goldfields include Krugersdorp, Randfontein and Westonaria. Uranium was extracted from the West Rand during the 1950s (Lednor, 1986). The East Rand Goldfield lies east of Johannesburg around Springs, it was discovered in 1887 on the farm Varkensfontein, was developed between 1888 and 1940 and is largely mined out now (de Jager, 1986). Uranium oxide, silver and osmiridium have also been extracted the goldfield (de Jager, 1986). The Carletonville Goldfield (also known as the West Wits Line) was discovered in the 1930s with the use of geophysical methods and drilling as it is almost entirely covered by the Transvaal Supergroup (McCarthy, 2006). This goldfield is considered to be one of the premier regions in the world for gold and uranium (Engelbrecht, 1986). The Welkom Goldfield was discovered in 1946 also through the use of geophysical methods as it is entirely covered by the Karoo Supergroup. The Klerksdorp Goldfield was mined from early on but it was the discovery of the Vaal Reef in the 1940s that allowed the region to blossom. Exploration of the Evander Goldfield (east of the East Rand Goldfield) began in 1902, however the first significant reef was only found in 1951 after an aeromagnetic survey (McCarthy, 2006). This goldfield is also covered by Karoo Supergroup rocks (McCarthy, 2006).

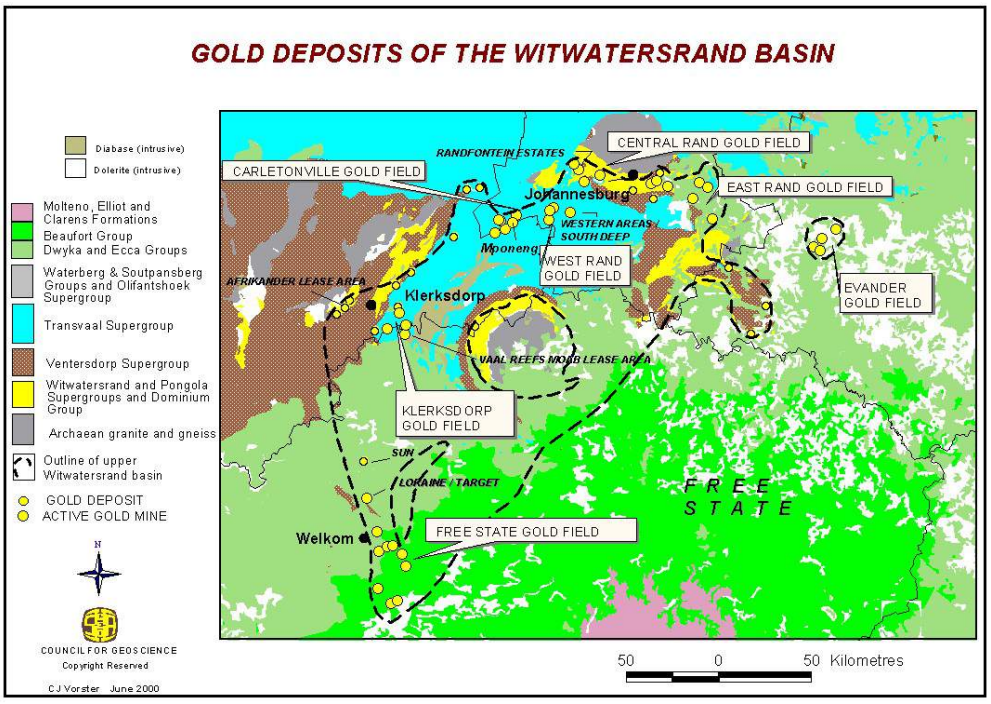

Figure 1.2: Map showing the relative position of the different Witwatersrand Goldfields and active gold mines (after Vorster, 2000)

The challenges that the Witwatersrand goldfields presented were plentiful; mining operations could not remain as small isolated entities and small mining operations were sold or merged into large mining companies such as Crown Mines Limited and Consolidated Gold Fields of South Africa Limited (Durand, 2012). The underground ore deposits presented many infrastructure challenges. Underground mining using shafts and stopes was perfected on the Witwatersrand and the world's deepest mines are found in the region (Durand, 2012). Specialised crushing equipment was required for crushing of the hard, conglomerate rock host and the gold required chemical extraction as opposed to the mechanical methods generally used for alluvial deposits. Initially, a mercury amalgam was used to extract the gold ore (Tutu, McCarthy, & Cukrowska, 2008). Stamp mills were erected to crush the ore and by 1895, the Witwatersrand was home to 2870 stamps (Durand, 2012). Processed waste was collected in steep sand dumps with material transported by donkey drawn coco pans. The mercury amalgam method became inefficient as deeper, unoxidised ores were encountered (Tutu et al., 2008). In 1890, the MacArthur-Forrest cyanidation process for gold extraction was

`

developed by Scottish chemists and implemented in 1915 (Tutu et al., 2008; Durand, 2012). Finer millings were required for this process and a fine, alkaline slurry was produced as waste. This waste was piped to slimes dams which are square in plain view, flat and have straighter walls than their sand dump counterparts.

1.1.2 Economic Significance of the Region

South Africa is a country blessed with mineral wealth. Of the world's mineral resources in 2009, South Africa was estimated to host 89% of the world's platinum group metals as well as significant major reserves of hafnium (42%), chromite (37%), manganese (19%), rutile (18%), gold (13%), ilmenite (9%), phosphate (9%) and nickel (9%) (Yager, 2011).

The Witwatersrand goldfields have produced 48 000 tonnes of gold which is 35% of the world's total gold production (Robb, 2005). In 2009, South Africa produced 9% of the world's gold (Yager, 2011). South Africa's gold production has been on a long term decline since its peak in the 1970s and gold production between 2008 and 2007 had decreased by 16% (Yager, 2011). The constant decline has been attributed to the challenges of mining at deep depths, safety issues, lower ore grades and power supply constraints (Yager, 2011).

This world famous resource of gold has fuelled South Africa's economy, provided a source of employment for thousands and generated a centre for development. In 1999, 51% of people employed in the mineral industry (a total of 437 028 people) worked in gold production. In 2009, gold production employed 32.5% of the total 491 222 employed in the mineral industry (Yager, 2011).

1.1.4 Water Resources

Unlike many of the major cities of the world, Johannesburg does not lie on a major river or lake. Groundwater was initially plentiful but considered a problem in the area and it was necessary to pump water away from active underground mine workings. At present, the Vaal Dam supplies the region with most of its water.

`

After the Anglo-Boer War, the Vaal Barrage was built, between 1916 and 1923, to supply a growing Johannesburg with water (Durand, 2012). The water supply became insufficient and the Vaal Dam was built in 1938 with a capacity of 994 GL. As the region expanded so did the Vaal Dam and by 1985, the capacity was increased to 3364 GL (Durand, 2012).

The Vaal River is the major feed into Vaal Dam. The Vaal River flows from the eastern escarpment, across the country and into the Atlantic Ocean and supplies water for major mining regions such as the Witwatersrand, Sishen, Welkom and Postmasburg (McCarthy, 2011). The intense demand placed on the Vaal River has necessitated interbasin transfers from the Orange and Tugela Rivers (McCarthy, 2011).

Ground water resources lie in the dolomites of the Malmani Subgroup of the Transvaal Supergroup, however these have been polluted in the region with the influx of sewage, industrial waste and the efflux of mine water (Durand, 2012). The proximity of these dolomites to the gold bearing reefs of the Witwatersrand required the continuous dewatering of gold mining operations. In order to maintain low groundwater levels, millions of litres of water were pumped from the mines daily. This has led to the drying up of springs, the subsidence of land, the change in groundwater flow patterns, flooding of streams and the modification or creation of wetlands (Durand, 2012).

1.1.5 Environmental Problems Related to Mining Activities

The discovery and extraction of materials by humans has occurred for centuries. The void generated in the ground where the material was removed must be filled with air, water or solid material. This alteration of the natural state is destined to have an impact on the environment surrounding the void and adjacent to the void. For example, removing rock during underground mining generates a void filled with air and oxidation processes occur. The subsequent flooding of the void transports the products of oxidation away from the void where they have the potential to affect unmined regions.

The mechanical and chemical processes to extract ore minerals from host rock produce waste material which requires storage. Water and air interact

`

with the exposed rock in underground mine workings and waste material on surface in the form of sand dumps and tailings storage facilities. The oxidation of sulphide minerals can lead to the generation of acid mine drainage. This can lead to the release of a range of possible pollutants into the environment. The impact and prevalence of pollutants released into the environment will depend on the pH and redox nature of the receiving waters as well as several other factors including the presence of living organisms and the presence of inorganic binding surfaces. Pollutants of concern include uranium, iron, nickel, cobalt, copper, chromium, arsenic, mercury, zinc, manganese, aluminium and lead. Other elements of interest include gold, titanium, silica, major cations (such as sodium, magnesium, calcium, etc) and some lanthanides. Anions of concern are sulphate, cyanide, phosphate, chloride and nitrate. The chemistry of acid mine drainage is discussed in greater detail in Chapter Two.

1.2 Hypothesis

This research is based on the hypothesis that tailings storage facilities (TSFs) in the Witwatersrand Basin are potential sources of metal pollutants in water systems in the vicinity of such facilities. Transport and dispersal of these pollutants depends on their speciation and a number of factors, for example pH, temperature, the presence of organic matter and presence other complexing ligands or surfaces. However, analytical techniques alone are not sufficient to interrogate and understand the behaviour of these pollutants. Potential release and dispersal of pollutants involves complex processes which are difficult to observe analytically, making modelling a useful tool to use in predicting such processes. Thus, geochemical and chemometric modelling can be applied to enhance understanding regarding the release, transport and dispersal of pollutants released from tailings storage facilities in the Witwatersrand Basin. Moreover, decisions regarding remediation of polluted water and soil systems can be made based on results from modelling techniques.

`

1.3 Aims and objectives

The central aim of this research was to assess the release of metal contaminants from tailings storage facilities, their transport and their dispersal in the water systems around Johannesburg.

This broad aim was achieved through the following specific objectives:

i) Identifying the potential sources of pollutants (i.e. active slimes dams, dormant slimes dams and footprints).

ii) Conducting leaching tests on material collected from the above-mentioned sources.

iii) Establishing, from geochemical modelling, the likely reaction processes following release of the pollutants e.g. reactions on contact with rainwater, reactions related to mixing of different water plumes, precipitation reactions and adsorption reactions.

iv) Assessing impacted water systems with respect to prevalent pollutants and making predictive models of pollutant behaviour based on the prevailing conditions through the use of 1-dimensional modelling.

v) Establishing pollutant distribution patterns and spatial variability based on geographical information systems and chemometric techniques.

vi) Assessing the use of geochemical and chemometric models as decision-making tools in planning for remediation and rehabilitation strategies.

`

1.4 Structure of thesis

This thesis fulfils the recommended requirements for submission through publication in that it contains three peer reviewed journal articles that have been published in scientific journals. Additionally, three peer reviewed conference proceedings have been published; a reviewed and published book chapter in "Research and Practices in Water Quality", InTech and two submitted journal articles that are pending review have been included into the thesis. The journal articles, conference proceedings and book chapter form part of the Results and Discussion chapters (Chapters Four and Five).

The thesis consists of the following chapters:

- Chapter One- Introduction

  This chapter provided a history of gold mining on the Witwatersrand and highlighted the main environmental problems related to it. The hypothesis, aims and objectives of this research were described.

- Chapter Two- Literature Review

  In this chapter, a brief literature review is presented. The pertinent literature for each journal article is discussed in the introduction section of the article. As such, to avoid redundancy Chapter Two sought to provide a general overview of metal speciation and mobility in mining impacted waters and an introduction to the theory and applications of geochemical modelling.

- Chapter Three- Methodology

  A description of sampling sites, sampling practice, sample preparation and analytical techniques is presented in this chapter. This chapter provides a more comprehensive description of analytical techniques than is detailed in journal articles. A section of the compilation of a geochemical model from conceptualisation to interpretation is also included.

`

- Chapter Four- Evolution of metal pollutants from tailings storage facilities

This chapter focuses on the release of metal pollutants from tailings storage facilities (TSFs). Publications which are discussed and presented in this chapter include:

  - B.P.C Camden-Smith and H. Tutu (2014). Geochemical modelling of the evolution and fate of metal pollutants arising from an abandoned gold mine tailings facility in Johannesburg. *Water Science and Technology* 69(5). doi: 10.2166/wst.2014.028
  - B.P.C Grover, P. Mthombeni and H. Tutu (pending revision). Fractionation of metals in gold mine tailings: implications for release and mobility to the surroundings. Submitted to *Toxicological and Environmental Chemistry*
  - B.P.C Grover, R.H. Johnson and H. Tutu (2016). Leachability of metals from gold tailings by rainwater: an experimental and geochemical modelling approach. *WaterSA* 42(1) doi: 10.4314/wsa.v42il.05

- Chapter Five- Distribution pathways of pollutants from tailings storage facilities: transport, dispersal and fate

This chapter investigates and discusses the water aided transport and dispersal of metal pollutants from TSFs. There are additional results and discussion included in this chapter that expands on the content presented in the journal articles. The following publications are included in this chapter:

  - B. Camden-Smith, P. Mthombeni, R.H. Johnson, I.M. Weiersbye and H. Tutu (2014). The release and transport of metals arising from gold mining tailings storage facilities in the Witwatersrand, South Africa. In W. Sui, Y. Sun and C Wang (Ed.), *International*

Mine Water Association Proceedings: "*Interdisciplinary Responses to Mine Water Challenges,"* Xuzhou, China

- B. Camden-Smith, N. Pretorius, A. Turton, P. Camden-Smith and H. Tutu (2015). Chemical Transformations of Metals Leaching from Gold Tailings. In *Agreeing on solutions for more sustainable mine water management-Proceedings of the 10th ICARD and IMWA Annual Conference*, Santiago, Chile. GECAMIN
- B. Camden-Smith, R. Johnson, R. Richardson, D. Billing and H. Tutu (2013). Investigating the potential impact of efflorescent mineral crusts on water quality: complementing analytical techniques with geochemical modelling. In A. Brown, L. Figueroa, & C. Wolkersdorfer (Ed.), *International Mine Water Association Proceedings: Reliable Mine Water Technology (Vol I).* (pp. 281-287). Denver, Colorado, USA.
- B.P.C Grover, R.H. Johnson, D.G. Billing, I.M. Weiersbye and H. Tutu (2015). Mineralogy and geochemistry of efflorescent minerals on mine tailings and their potential impact on water chemistry. *Environmental Science and Pollution Research* (pp. 1-11) doi: 10.1007/s11356-015-5870-z
- B.P.C Grover, P.M.C. Camden-Smith and H. Tutu (pending revision). Investigating the removal of trace metals in a high density sludge treatment plant using a geochemical modelling approach. Submitted to *Water Science and Technology.*
- B. Camden-Smith, R.H. Johnson, P. Camden-Smith and H. Tutu (2015). Geochemical Modelling of Water Quality and Solutes Transport from Mining Environments. In: Research and Practices in Water Quality, Dr. Teang Shui Lee (Ed.), ISBN: 978-953-51-2163-3, InTech. Available from: http://www.intechopen.com/books/research-and-practices-in-water-quality/geochemical-modelling-of-water-quality-and-solutes-transport-from-mining-environments

`

- Chapter Six- General Conclusions and Recommendations

Although conclusions are presented in each journal article, this chapter describes the overall conclusions of the thesis and suggests where future work is required.

- References

A complete list of references, including references in journal articles, is included.

- Appendices

Supplemental material is included in this section.

`

CHAPTER TWO- LITERATURE REVIEW

A brief, general literature review is presented in this chapter. Literature relevant to each journal article and conference proceeding is discussed in the introduction of that particular publication. In the first section of this chapter, the mechanisms for the release of metals and acidic water from mines and mining waste, the transport and dispersal of these products in the environment, and potential and implemented remediation schemes that have been investigated across the world are discussed. The second section covers an introduction to geochemical modelling, outlines the theories involved, and discusses some applications that have been published in the literature over recent years.

2.1 Evolution, mobility and remediation of metals in mining-impacted waters

The metal pollutants of interest in this research arise from abandoned and active gold mining tailings storage facilities. Decant of acidic water from these facilities releases contaminants into surrounding water bodies (Section 2.1.1). The chemical characteristics of receiving water bodies affect the oxidation state of the incoming transition metals and provide ligands for the complexing and chelation of the metal ions. Therefore, the chemistry of both the carrying solution and the receiving solution dictates how mobile a metal is (Section 2.1.2). Natural remediation of metal concentrations has been noted in mining impacted regions. There are methods to aid nature in the attenuation of metal pollutants, these remediative schemes often make use of reactions that would occur naturally but aim to perform them more effectively (Section 2.1.3).

2.1.1 Acid mine drainage and the release of metal contaminants

Acidic waters are a natural phenomenon of leaching occurring when oxygenated water is transported through or over sulphide containing rock (acid rock drainage). Mining provides additional pathways for the leaching of metals from material and for the release of these metals into the environment.

`

Acid mine drainage is a problem that affects both gold and coal mining and is not confined to South African borders. South African regions under current stress from acid mine drainage are the Witwatersrand Gold Fields, Mpumalanga and KwaZulu-Natal Coal Fields and the O'Kiep Copper District (Northern Cape) (Expert Team of the Inter-Ministerial Committee, 2010). It is of greatest concern in the Witwatersrand Basin. In 2009, it was predicted that the potential volume of acid mine drainage released within in the Witwatersrand was 350 ML/day (CSIR, 2009).

Acid mine drainage comes in several forms, the two most publicised forms being: 1) flooding within and decant of water from mines due to ceasing of pumping during mine closures (Expert Team of the Inter-Ministerial Committee, 2010) and 2) discharge from waste rock piles, tailings storage facilities and ore stock piles (CSIR, 2009). The presence of abandoned mines and active mines generally affects relatively small areas (Salomons, 1995). Surface mine waste is the main source of mining related contaminants because the leaching processes which releases acidity and metals are accelerated by providing mineralised material access to oxygen (Salomons, 1995).

Regardless of the form of acid mine drainage in the Witwatersrand, the generation of the acid follows the same mechanism. Surface mine waste is exposed to several weathering processes and agents, such as freeze-thaw cycles, solar radiation, atmospheric oxygen, rainwater and microbial activity (Diehl, Hageman & Smith, 2008). The physical and chemical processes associated with weathering render small sized particles with a higher surface to mass ratio than unweathered particles and result in a host of reactive, readily soluble secondary phases.

The initial acid producing reaction occurs during the oxidation of pyrite (reaction 2.1). The gold mining TSFs on the Witwatersrand contain between <0.5 and 2 weight percentage of pyrite (Yibas et al., 2012). The outer surface of the TSF is oxidized first. Oxygen is not capable of diffusing through the entire tailings material and so a zone of oxidation is developed. This zone of

`

oxidation is TSF dependent. It commonly varies between 1.5 m to 5 m below the outer surface of the TSF and a zone of lesser oxidation can occur up to an additional 4 m below this (Yibas et al., 2012). Factors affecting the diffusion of oxygen in the tailings include grain size of the material and the degree of water saturation of the material. Fine grained particles may have a larger surface area which increases the rate of the reaction but their closer packing prevents oxygen advection and diffusion (Salomons, 1995). Therefore, coarse grained waste often produces more acid (Salomons, 1995). Even though tailings are often initially alkaline as the cyanide extraction process requires a high pH, there is an insufficient buffering capacity and inevitably the pH starts to decrease from this first reaction. The discharge of this acidified water causes the oxidation of iron (II) by atmospheric oxygen (reaction 2) (Tutu, McCarthy, & Cukrowska, 2008). Abiotic oxidation of the dissolved iron (II) is a slow process at low pH and the rate increases as pH increases. This is due to the species distribution of iron (II) with respect to pH and their relative reaction rates (Salmon & Malmstrom, 2004).

FeS_2 (s) +7/2 O_2 (aq) +H_2O → $2SO_4^{2-}$ (aq) + Fe^{2+} (aq) + $2H^+$ (aq) ... (reaction 2.1)

Fe^{2+} (aq) + ¼ O_2 (aq) + H^+ → Fe^{3+} (aq) + ½ H_2O … (reaction 2.2)

The iron (III) ions released from reaction 2 have two possible paths depending on the pH of the solution. If the pH is lower than 3.5, the Fe^{3+} ions remain in solution and oxidises more pyrite (reaction 2.3) (Salmon & Malmstrom, 2004). The alternative occurs at pH greater than 3.5 where the iron (III) ions precipitate as $Fe(OH)_3$ (reaction 2.4) (Tutu et al., 2008). In unsaturated tailings material, the precipitation of iron may occur directly within the tailings material (Sracek et al., 2011). This leads to the co-precipitation of other metals that would not normally precipitate at such low pH.

$FeS_2(s) + 14Fe^{3+}(aq) + 8H_2O \rightarrow 15Fe^{2+}(aq) + 2SO_4^{2-}(aq) + 16H^+(aq)$ … (reaction 2.3)

`

$Fe^{3+} + 3H_2O \rightleftharpoons Fe(OH)_3\ (s) + 3H^+$ … (reaction 2.4)

Pyrite can contain a percentage of trace metals, such as arsenic, cobalt, lead, nickel and zinc. The inclusion of these metals into the crystal lattice of pyrite leads to instability in the lattice and can increase the solubility of pyrite (Diehl, Hageman & Smith, 2008). Dissolution of pyrite can release these metals into surrounding water systems (Salmon & Malmstrom, 2004).

The pH of the leaching solution released following oxidation can be buffered by dissolution of calcite or other carbonate minerals and through the weathering of aluminosilicate minerals (Salmon & Malmstrom, 2004). The mineralogy of the TSF on the Witwatersrand goldfields is predominantly quartz, mica, chlorite and chloritoid. Some dams also contain a small percentage of pyrophyllite and potassium feldspar (Yibas et al., 2012). Precipitation and dissolution of secondary hydroxides and sulphates could also affect the pH of the resulting solution (Salmon & Malmstrom, 2004).

2.1.2 Elemental speciation and mobility of metals in mining-impacted waters

The mobility and potential impact of contaminants in mine drainage is dependent on four major factors: the occurrence of the contaminant; sufficient abundance of the contaminant; the reactivity of the contaminant and the presence of a hydrological flow path (Nordstrom, 2011). The conservative (non-reactive) or non-conservative (reactive) nature of an element in water systems depends on the pH and redox potential of the solution, the composition of the solution, temperature, flow rate of the water and the presence and influence of microbiological organisms (Nordstrom, 2011).

Most metal cations; with the common exceptions being iron (III) and sulphate forms of lead and barium; tend to exist in solution in acidic waters (Nordstrom, 2011). In surface waters, iron (II) is rapidly oxidised to iron (III) and forms insoluble micro- or nano-precipitates such as goethite, schwertmannite and ferrihydrite. Other metals, such as lead, copper, zinc, cadmium and arsenic, adsorb onto the surface of these precipitates

`

(Nordstrom, 2011). The pH and temperature affect adsorption equilibria. Sorption can also be affected by the presence of sulphates and is sensitive to the type of substrate (Nordstrom, 2011). A change in redox conditions can remobilise adsorbed metals by converting the iron (III) precipitates into soluble iron (II) complexes (Salomons, 1995). Iron (III) can also be reduced to soluble iron (II) by solar radiation (Nordstrom, 2011). However, in reducing conditions the formation of insoluble sulphides could reduce mobility of iron once more (Salomons, 1995). Amorphous aluminium hydroxides also precipitate from acidic waters (Nordstrom, 2011). The pK1 value for the hydrolysis of aluminium is 5. At a pH significantly lower than this value, Al exists in solution primarily as a free ion and is conservative (Bigham and Nordstrom, 2000). These hydroxides can also adsorb metals though not as well as the hydroxy iron oxide precipitates and particulate organic carbon (Nordstrom, 2011).

Dissolved organic carbon enters water bodies as a product of the degradation of animal and plant tissue (Salomons, 1995). The functional groups chelate metal ions, can form stable organic-metal complexes (in particular with humic and fulvic acids) and can result in the increase in the amount of dissolved metals solution. However, due to the chelating of metal ions, their toxicity might decrease. For example, the increased dissolved copper concentration when organic ligands are present corresponds with a decreased toxic inorganic copper concentration (Salomons, 1995).

As well as being affected by seasonal and flow changes, some streams that are affected by acid mine drainage have been noted to have diel (24 hour) metal concentration variations (Nordstrom, 2011). The factors that might be responsible for this include daily pH variations, temperature fluctuations, photoreduction of iron and algal growth and associated metal uptake (Nordstrom, 2011).

2.1.3 Remediation of Acid Mine Drainage

Common treatment efforts for areas affected by acid mine drainage are discussed, these can be grouped into chemical and biological treatment

techniques. This section focuses on passive treatment methods. Active treatment of acid mine drainage involving high density sludge (HDS) pump-and-treat plants is discussed in detail in Section 5.3.2.

Chemical techniques include the use of dry covers and water covers to hinder the reactions which produce acid; the direct treatment of the tailings in efforts to curb the release of acid and the installation of permeable reactive barriers into groundwater paths to hinder the transport of contaminants from an impacted site. Biological treatment options could involve the use of wetlands to provide an organic-rich environment to reduce metal mobility, the use of metal hyperaccumulating plants to uptake metals from impacted soils and the use of passive surface compost reactors. An overview of treatment techniques can be found in Blowes et al. (2003) and Johnson and Hallberg (2005).

2.1.3.1 Tailings Remediation

A mercury amalgam extraction technique was initially used during the early stages of mining of the Witwatersrand gold reefs. This process was replaced by a more effective cyanide recovery process when unoxidised ores were encountered. The cyanide recovery process required lime for pH regulation (a pH of 10 was required for optimal extraction) (Tutu, McCarthy & Cukrowska, 2008). Therefore, the initial tailings to enter a slimes dam were alkaline however, the buffering capacity was insufficient and acidic conditions prevailed after the oxidation of pyrite (Tutu, McCarthy & Cukrowska, 2008). The more recent “Carbon in Leach” and “Carbon in Pulp” gold recovery methods also utilise cyanide. Ferrous sulphide or ferrous chloride is added after extraction of gold in order to neutralise cyanide (Durand, 2012). Excess cyanide is leached into the surrounding environment through tears in the protective lining of the tailings (Durand, 2012).

The addition of extra calcium carbonate (limestone) has been used as a remediative possibility. Two moles of calcium carbonate is required to neutralise the acid produced from one mole of pyrite (Salomons, 1995). However, iron hydroxide and calcium sulphate (gypsum) precipitate during the reaction and coat the limestone particles (Salomons, 1995). This prevents

`

the core of particle from reacting. Despite this, limestone is an inexpensive option for the treatment of acid mine drainage. A pulsed limestone bed reactor has been investigated. This adds carbon dioxide to increase the rate of the neutralisation reaction and causes particle-particle abrasion which removes coatings on the grains (Hammarstrom, Sibrell & Belkin, 2003).

Addition of phosphate containing minerals such as apatite to mine waste has also been investigated. Following the initial acid forming reactions, ferric ions are precipitated as ferric phosphate and can no longer act as an oxidising agent. Similar to the addition of limestone, the mineral grains can be coated and their effectiveness decreased. As such, a soluble phosphate technology involving hydrogen peroxide has been developed by Evangelou (1998) (Johnson & Hallberg, 2005).

2.1.3.2 Wet and Dry Tailings Covers

Preventing acid mine drainage from tailings could entail limiting oxygen access. In some locations, depending on local conditions, it might be possible to flood the tailings (Salomons, 1995). Following this, it is believed that long term neutralisation of tailings can occur through the acid consuming dissolution reaction of silicate minerals (Salomons, 1995). Covering tailings with water has been predicted to lead to a reduced oxidation rate of 99.1 % (Romano et al., 2003). However the construction and maintenance of stable wet covers is a complex and costly undertaking (Romano et al., 2003).

Another remediation option involves covering the tailings with layers of clay, gravel, topsoil and vegetation as this prevents erosion of the tailings into local waterways (Salomons, 1995). The clay layer acts as a sealing layer although in areas with extreme climates (either heavy rain or high temperatures), this layer can crack and the method becomes less effective (Swanson et al., 1997; Johnson & Hallberg, 2005).

2.1.3.3 Limestone drains and reactive barrier remediation

Anoxic and oxic limestone drains, open limestone channels and limestone diversion walls have been researched or employed as treatment options for

`

acid mine drainage (Cravotta III & Trahan, 1999). Acid mine drainage is passively treated in these systems through the dissolution of calcite. The process raises the pH and, in the case of oxic systems, accelerates the rate of chemical oxidation of ferrous ions. This leads to the precipitation of hydroxide and carbonate minerals (Johnson & Hallberg, 2005).

Permeable reactive barriers (PRM) have been shown to be successful for the treatment of contaminated groundwater. The barriers are a combination of chemical and biological processes (Johnson & Hallberg, 2005). Installation of a PRM involves digging a trench and filling the void with a combination of organic material and limestone. The permeable nature allows water to flow through the barrier unimpeded (Johnson & Hallberg, 2005). This provides a reducing environment in which sulphate is reduced and dissolved metal contaminants are removed though metal sulphide precipitation (Benner et al, 1999; Younger et al., 2003). The limestone neutralises the acidic water and increases the alkalinity of the resulting water (Benner et al, 1999).

2.1.3.4 Wetland Remediation

Wetlands are capable of removing metals from mine drainage with the potential to release them later on. Metal removal occurs through adsorption or cation exchange; by precipitation of hydroxides, carbonates or sulphides and by biological uptake (Sheoran & Sheoran, 2006). Bacterial processes are one of the processes responsible for removal. Iron oxidizing bacteria such as *Acidithiobacillus ferrooxidans* utilise energy obtained from the conversions of the Fe^{2+}/Fe^{3+} redox couple (Stanton, 2008). The *Desulfovibrio* reduce sulphate to sulphide during the decomposition of organic matter (Stanton, 2008). The abundant organic matter present in wetlands combined with the high sulphate concentration from incoming mine drainage promotes bacterial growth. The reducing conditions provided by the aqueous sulphide are characteristic of wetlands and some metals are reduced to their immobile forms. Problems that been identified with wetland remediation include little system control, seasonal variations, an inability to assess their performance

`

and their inefficiency when used in isolation (Johnson & Hallberg, 2002; precipitation (Neculita, Zagury & Bussière, 2007).

2.1.3.5 Phytoremediation

Phyto-technology has been investigated by the University of the Witwatersrand in conjunction with Anglo Gold Ashanti South Africa as a remediation tool for the rehabilitation of tailings dams, polluted soil and groundwater.

Phytoremediation involves using plants and soil micro flora as well as non-living biomass to improve the quality of soil and water (Weiersbye, 2008). Plants naturally take up metals from soil and water, as most of these elements act as macro- and micro-nutrients essential for growth. Included in this metal uptake could be metals considered as pollutants. Most plants suffer toxicity effects when exposed to metal concentrations lower than what would be required for efficient phytoremediation of contaminants (Terry, Sambukumar, & LeDuc, 2003). Metal hyperaccumulators on the other hand are plant species that are capable of accumulating high concentrations of metal pollutants in their tissues (Soriano & Fereres, 2003), this makes them applicable for mine remediation purposes, where metal concentrations can be very high.

2.1.3.6 Passive bioreactors

Bioreactors provide a low cost, effective means to reduce sulphate quantities in AMD using sulphate reducing bacteria (Neculita, Zagury & Bussière, 2007). The simple flow through reactors consist of an AMD flowing over a carbon containing solid reactive mixture which both supports the microbial attachments and provides a site for sulphide precipitation (Neculita, Zagury & Bussière, 2007). Metal removal occurs through the precipitation of metal sulphides (as noted for Zn, Cu and Cd) and the precipitation or co-precipitation of metal hydroxides (for Fe, Mn, and Al) (Zaluski et al., 2003). The reducing and alkalinity producing system (RAPS) is a variation of the simple bioreactor system in which AMD flows downward through two layers (Younger et al., 2003). It follows the same reactions as those which occur

within the permeable reactive barriers. In the first layer, AMD filters through compost in which oxygen is removed and iron and sulphate are reduced. In the second layer, the partially treated AMD reacts with calcite to increase its alkalinity.

2.2 Theory and applications of geochemical modelling

Environmental reactions that affect water quality generally occur at low temperature (0-100°C) and under approximately atmospheric pressure. The processes of interest include dissolution and precipitation of minerals; speciation and complexation of inorganic and organic matter; evaporation, dilution or mixing of water bodies; adsorption or desorption of solute; ion exchanges; reduction-oxidation of constituents; reaction with or production of gases and reactions catalysed by light or biological organisms (Nordstrom, 2007).

Geochemical modelling seeks to model these processes through the use of mass action and mass balance equations. Geochemical reaction models, also known as batch models, neglect transport aspects and can be conceptualised by that of a stirred tank reactor in which the distribution of a chemically reactive species is mathematically calculated (Crawford, 1999). Coupled transport and reaction models include modelling of the transport of chemical constituents down a flow path (Crawford, 1999). Geochemical reaction models can be subdivided into forward models, inverse models and reaction path models. Speciation-solubility models are incorporated into the geochemical reaction models and are briefly discussed. Many studies involving geochemical modelling have been conducted since the 1960s and a few studies illustrating the use of the different geochemical models are summarised. These select studies have been chosen for discussion here as similar methodologies or modelling approaches have been implemented into the case studies for the thesis.

2.2.1 Speciation-solubility models

Speciation-solubility models are used to define the distribution of stable species in the system and to determine the saturation states of minerals within

`

the system (Zhu & Anderson, 2002). Most models assume local equilibria in order to solve the equations involved in determining the species spectrum. This assumption is often valid as the reactions which affect the bulk chemistry of natural water bodies occur relatively fast with reference to the time scale of interest (van der Lee & De Windt, 2001). Chemical equilibrium can be solved in two ways, either by minimising the Gibbs' free energy of a system or by using mass action equations combined with equilibrium constants. The second method is used by the majority of programming software because of a lack of consistent Gibbs' free energy data (Crawford, 1999).

A technical article was published by van der Sloot and van Zomeren (2012) which involved the use of speciation-solubility modelling. The software LeachXS Orchestra was used along with a modified MINTEQA2 database to determine the chemical speciation of 30 elements and the saturation of 80 minerals in a study to characterise the release of metals from different tailings and waste rock sites. They conducted pH dependent leach tests and upflow percolation tests which were analysed with inductively coupled plasma-optical emission spectroscopy (ICP-OES), ion chromatography (IC) and total organic carbon analyser. Amorphous and crystalline iron oxide was selectively extracted using a technique involving dithionite and amorphous aluminium oxide was selectively extracted using oxalate extraction. The speciation modelling inputs included the fixed element availabilities, a selection of minerals, the active iron and aluminium oxide sites, particulate organic material and reactive dissolved organic carbon (which was defined as a polynomial function of pH). Modelling of the pH dependent leach tests was undertaken and then verified against the measurements for a liquid to solid ratio of 10. The model was iteratively optimised and produced a chemical speciation fingerprint for each site. This fingerprint was then used to predict the release of metals at a low liquid to solid ratio of 0.2. This low ratio can be compared to the first fraction obtained from the percolation tests because it should ideally represent the pore water which seeps from landfills. There was good correlation between predicted low liquid to solid leachates and the first

`

fractions of the column tests. Combined with the good agreement between the model and measured values for the pH dependent leach tests suggest that the same processes for metal release operate over a range of liquid to solid leaching ratios. Furthermore, the results obtained across the waste sites are similar and imply that leaching processes are generic even though the sites had different mineralogy. This was interpreted by stating that leaching occurs on the surface of particles. These particles have undergone oxidation on their surface and might have different phases to that present in the core of the grain and because similar phases result from oxidation of a range of sulphide minerals, leaching profiles are the similar (van der Sloot & van Zomeren, 2012).

2.2.2 Forward modelling

In forward modelling, the final composition of a solution after a reaction or equilibration is calculated (Crawford, 1999). It is of particular use in performance testing or design studies (Crawford, 1999).

Thermodynamic models utilises equilibrium constraints and are assumed to be valid for homogeneous reactions in which there is sufficient residence time for equilibrium to be reached. Heterogeneous reactions such as the dissolution and precipitation of minerals, their adsorptive properties are often kinetically controlled and models should ideally be adjusted accordingly.

An interesting example of an application of forward modelling is a study conducted by Tonkin, Balistrieri and Murray (2002). The team compared model predictions of metal removal onto natural oxide particles with experimental results. An acidic solution from a mining district in northern Idaho was mixed in fractions ranging from 1:1000 to 1:2 with an ambient surface solution collected from a river. The precipitates that formed from mixing were analysed by XRD. The formation of solution complexes, precipitation of solid phases and the sorption of metals onto iron and aluminium oxide surfaces were simulated. The precipitated material was mostly amorphous but there were trends noted in the crystalline portion (schwertmannite was the major phase for solutions with pH 2.9-3.1, goethite

`

was the major phases for solutions with pH 3.1-3.8 and solutions with pH 6.0-6.3 had minor goethite and trace schwertmannite). With these results in mind, amorphous and crystalline iron oxide and aluminium oxide surfaces were defined as the equilibrium solid phases in the mixing simulations. A diffuse double layer surface complexation model was used with PHREEQC 2.2 as the code and a modified MINTEQA2 database. The pE values for the water samples had to be calculated. The pE value for the acidic mine water sample was optimised by comparing the ratio of iron (II) to a calculated iron (III) (total iron less iron (II)) with the ratio of predicted iron speciation. The pE value for the ambient water sample was calculated using the measured pH and an assumption that the solution was in equilibrium with atmospheric oxygen. When the defined equilibrium phases in the model were hydrous ferric oxide and the crystalline minerals observed using XRD; the predicted amounts of iron precipitates (ferrihydrite, goethite and schwertmannite) correlated within a factor of 1.5 with the experimental results. For the simulation of metal adsorption onto particles of schwertmannite, goethite and amorphous iron oxide; a universal single set of surface parameters (that of hydrous ferric oxide) was chosen. The simulated values of adsorption correlated well with experimental data for lead and copper. Arsenic, molybdenum and antimony values did not correlate well which suggests that perhaps there are other removal mechanisms operating which cannot be included in the simple model of using universal HFO parameters (Tonkin, Balistrieri & Murray, 2002).

2.2.3 Inverse modelling

Inverse modelling is also known as mass balance modelling. Given that the composition of water samples along the same flow path and the mineralogy of the rock through which the water flows are known, inverse modelling can provide a set of possible reactions which occurred to transform a combination of initial water samples into a final composition (Nordstrom, 2007). Mass balance equations are utilised and neither thermodynamic properties nor kinetic restraints are considered (Zhu & Anderson, 2002).

`

Inverse modelling was used in a study by Nordstrom et al. (1992) of the ground water chemistry at the Osamu Utsumi uranium mine, Morro do Ferro thorium and rare earth element deposits in Brazil. Ground and surface water samples were collected over a three year period and analysed using a range of techniques including ICP-OES, flame atomic absorption spectrometry, ferrozine colorimetry, ion chromatography, potentiometric titrations, Gran's plot titration, nephelometry and mass spectrometry. Speciation and saturation indices calculations were done using the WATEQ4F code and a modified WATEQ4F database. Ion plots and saturation indices were used as they are indicative of which reactions are responsible for the observed chemistry. In this study, it was clear that barite solubility was strongly controlled by the sulphate concentration; this was attributed to the common ion effect. Mass balance calculations (inverse modelling) between dilute recharge water (pure water was used) and ground water samples were done using BALANCE (based on BALINPT, precursor to NETPATH). Models revealed the dissolution of fluorite, calcite, potassium feldspar, albite, chlorite and manganese oxides; the oxidation and dissolution of pyrite and sphalerite and the precipitation of kaolinite, cryptocrystalline quartz and ferrihydrite. Models could have been both refined and complicated by including clay minerals. Once one or more probable models were obtained, the thermodynamic feasibility of, and the degree to which equilibrium prevails in the models, were determined using forward modelling and the code PHREEQE (the precursor to PHREEQC) with the modified WATEQ4F database. Saturation indices as obtained from the speciation-solubility models and mass transfers from the inverse models were used. The same composition and pH (within measurement uncertainty) of the water samples were obtained. This showed that the models were thermodynamically sound (Nordstrom et al, 1992).

2.2.4 Reaction path modelling

Reaction path models track reaction progress in small incremental steps. At each step, the species distribution and saturation indices are calculated and equilibrium is maintained by the dissolution or precipitation of defined

`

minerals (Crawford, 1999). These models are used to describe forward reaction processes, for example the addition of gases or minerals to a water system, the mixing of chemically unique water bodies and the removal of minerals or components from a system (for example, evaporation of water) (Zhu & Anderson, 2002).

The reaction path models are branched into four different types, namely titration models, buffering models, flush models and kinetic reaction path models (Zhu & Anderson, 2002). The first three models consider the reactions in a stepwise manner and as such time is not included as a factor in the calculations (Crawford, 1999). Kinetic reaction path models include kinetic aspects and can relate reaction progress to time (Crawford, 1999). Kinetic reaction path modelling is ideal although not always possible due to the deviation between laboratory determined and natural surface area changes and reaction rates of dissolution and precipitation reactions (Apollaro, Marini & De Rosa, 2007).

Reaction path modelling was used by Apollaro, Marini and De Rosa (2007) to predict the water chemistry of streams and groundwater at a site in Calabria, Italy. The software EQ3/6 (version 7.2) and modified COM database was used. Rainwater, stream water and spring water samples were collected and analysed using acidimetric titration for alkalinity determination; ion chromatography for anion analysis; ICP-OES for calcium, magnesium, sodium and potassium analysis and ICP-MS (mass spectrometry) for trace analysis. A stoichiometric approach was taken and reaction rates and surface areas were not considered. Two solid reactants were involved in the modelling, phyllitic rock (comprised of quartz, muscovite, chlorite and albite) and calcite (also present in phyllitic rock but considered separately due to faster dissolution but also present in a lower abundance). Titration simulations were undertaken which involved the incremental dissolution of amounts of phyllite and calcite in an initial solution of rainwater. At each step a selection of secondary minerals were allowed to precipitate (based on knowledge of the weathering and as indicated through activity plots) and the

`

solution was re-equilibrated. The minerals that were allowed to precipitate were gibbsite, kaolinite, amorphous silica, illite, hydroxide solid solution and carbonate solid solution. The sampled water was satisfactorily reproduced through reaction path modelling (Apollaro, Marini & De Rosa, 2007).

Examples of geochemical modelling can be found outside of the traditional environmental applications. The dissolution of chrysotile and tremolite within the human lung was modelled using Geochemists' Workbench and the SUPCRT92 database by Wood, Taunton, Normand and Gunter (2002). Kinetic reaction path modelling was used and reaction constants were taken from available literature. The surface areas of the crystals were calculated using geometry considerations. The effects of organic material were neglected due to a lack of thermodynamic and kinetic data. An open system was simulated using a flush model in which a given mass of solid (quartz, chrysotile and tremolite) was reacted with lung fluid that was removed and replenished daily with fresh solution. A closed system was modelled by mixing the solids with the lung fluid and not allowing for replenishment of fluid or minerals. In both cases, simulations were carried out for a reaction time period of 50 years. Tremolite and chrysotile were both undersaturated in the human lung fluid and chrysotile dissolved faster. The appearance and disappearance of other minerals (such as talc) were also discussed (Wood et al, 2006).

2.2.5 Coupled transport and reaction modelling

Coupled transport and reaction (reactive transport) models are used to show geochemical changes over time along a one, two or three dimensional flow path. This type of model is a forward geochemical reaction model combined with a hydrological model (Crawford, 1999). Programmes, such as PHREEQC, are capable of modelling one dimensional advection, dispersion and chemical reactions (Charlton & Parkhurst, 2002). The concept behind this model is that the flow path is divided into a series of discrete cells. In the first cell a reaction occurs and equilibrium may be calculated (based on the geochemical forward model), this solution is then transported along the flow

`

path to the second volume section (based on the hydrological model) and the process is repeated (Crawford, 1999). This process for one dimension is illustrated in Figure 2.1 in which the beakers represent the solution chemistry as calculated using geochemical model and the arrows represent the water movement as described in a flow model. The uses for reactive transport modelling include the study of migration of contaminants such as metals, radionuclides and organic compounds; the simulation of natural and artificial processes for aquifer remediation and the simulation of laboratory column experiments (Charlton & Parkhurst, 2002).

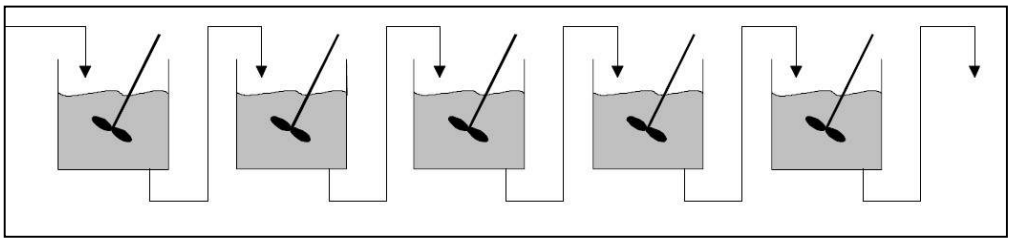

Figure 2.1: One dimensional representation of a coupled transport and reaction model (from Crawford, 1999)

Two examples of the applications of reactive transport modelling are discussed. The first is by Runkel and Kimball (2002) using OTEQ and the second by Johnson (2011) using PHAST. Both programmes were developed by the United States Geological Survey (USGS). OTEQ is a combination of MINTEQ (as the chemical submodel) and OTIS (as the solute transport submodel) (Runkel & Kimball, 2002). PHAST is a combination of PHREEQC (as the chemical submodel) and a simple groundwater flow model (Johnson, 2011).

Runkel and Kimball (2002) used the one dimensional reactive transport modelling program OTEQ to evaluate two remedial alternatives for acid mine drainage at a site in the San Juan Mountains in south-western Colorado. The first remediation scheme involved the addition of calcium carbonate to raise the pH of a closed system in which no oxidation of inflowing iron (II) within the treatment system occurred. The second scheme also used calcium carbonate to raise the pH but allowed for iron (II) oxidation in an open

`

system. Characterisation of the conditions prior to remediation was required and this involved the collection of streamflow estimates and hydrologic parameters (both of which were determined using bromine tracer data) as well as chemical data. Precipitated and adsorbed material can either settle on the streambed or suspend in the water column and for the study site they found that any settling was balanced by resuspension. Therefore, settling velocities were set to zero and precipitated material was transported in the water column downstream. Defined solid phases were gibbsite ($Al(OH)_3$) and ferrihydrite ($Fe(OH)_3$). Sorption onto iron (III) surfaces was simulated using a surface complexation approach and the Dzombak and Morel database. Sorption onto aluminium surfaces was neglected as there was no evidence of aluminium oxide particles in the study area. The remediation simulations both showed a decrease in metal concentrations downstream; however the second remediation scheme shows a greater reduction in most metals, except for arsenic and lead. There is a source of lead downstream from the treatment site. In the first remediation, iron (II) was not oxidized during treatment. This allowed for oxidation further downstream and available sites on iron oxide surfaces for lead sorption. In the second remediation scheme, iron (II) was oxidized during treatment and there was a shortage of sorption sites as the particles move downstream. The authors of the paper also discussed the advantages and disadvantages of the process based approach with mass action equations as compared to rate constant approaches. Briefly summarised the advantages are that solute interactions (in particular, pH and metal oxide precipitation) are considered and that the equations are applicable to pre- and post- remediation situations. Disadvantages include a reliance on extensive, accurate field data which is costly; in some situations inflow might also be from groundwater sources and this requires further assessment and sampling and although a range of pH is taken into account in mass action equations, the chemical changes associated with pH are not (such as different solid phases or sorption characteristics).

Johnson (2011) used reactive transport modelling in PHAST to model the *in situ* recovery of uranium from uranium roll front deposits in two dimensions.

`

Time, flow velocities and mass balances were generic and not site specific but could be added into the model at a later stage. Johnson simulated the deposition of a uranium roll front deposit by starting with a pyrite solid phase and no uraninite or oxygen and introducing uranium-oxygen rich water into the system. The pyrite was a reducing agent and uraninite was precipitated. The pre-mining water conditions were anoxic and no uraninite was deposited, this was shown in the model by an absence of dissolved oxygen and uranium and the presence of solid phase pyrite and uraninite. The *in situ* uranium mining process was modelled by introducing a solution with dissolved oxygen and carbon dioxide along with a five well system (the centre well pumps groundwater out and four surrounding pump processed water in). The result was that uraninite was dissolved and uranium was present in groundwater. Post mining restoration was simulated in two manners; with and without dissolved oxygen. For the case in which oxygen was used in restoration, it was shown that once natural groundwater flows through the site again it would contain uranium and that solid phase uraninite and pyrite would dissolve from original site and precipitate downstream. It was shown that restoration without dissolved oxygen leads to better long term water quality because dissolved uranium was not present in the groundwater and solid phase uraninite and pyrite do not migrate downstream (Johnson, 2011).

There are few comprehensive geochemical models for pollutant evolution, transport and dispersal in the Witwatersrand Basin. Most research work report findings based solely on analytical results and monitoring projects, this oversimplifies the situation and does not account for complex processes. Therefore, this thesis study intended to complement analytical techniques with modelling techniques in order to better understand and to be able to better predict metal evolution, transport and dispersal from tailings storage facilities. The analytical techniques and geochemical modelling approach is discussed in Chapter Three.

`

CHAPTER THREE- METHODOLOGY

This chapter describes the path of a sample taken from the study site, its transportation to the lab, its fate once inside the laboratory and its role in geochemical modelling. The sampling sites and procedure (Section 3.1), sample preservation (Section 3.1), sample treatment (Section 3.2), analytical techniques (Section 3.3) are described. Figure 3.1 outlines the relationships of these aspects. All of the analyses described in this chapter, with the exception of field measurements, were performed within the Environmental Analytical Chemistry laboratories at the School of Chemistry, University of the Witwatersrand. The strategy for constructing a geochemical model and an overview of the considerations involved in the process is discussed in Section 3.4.

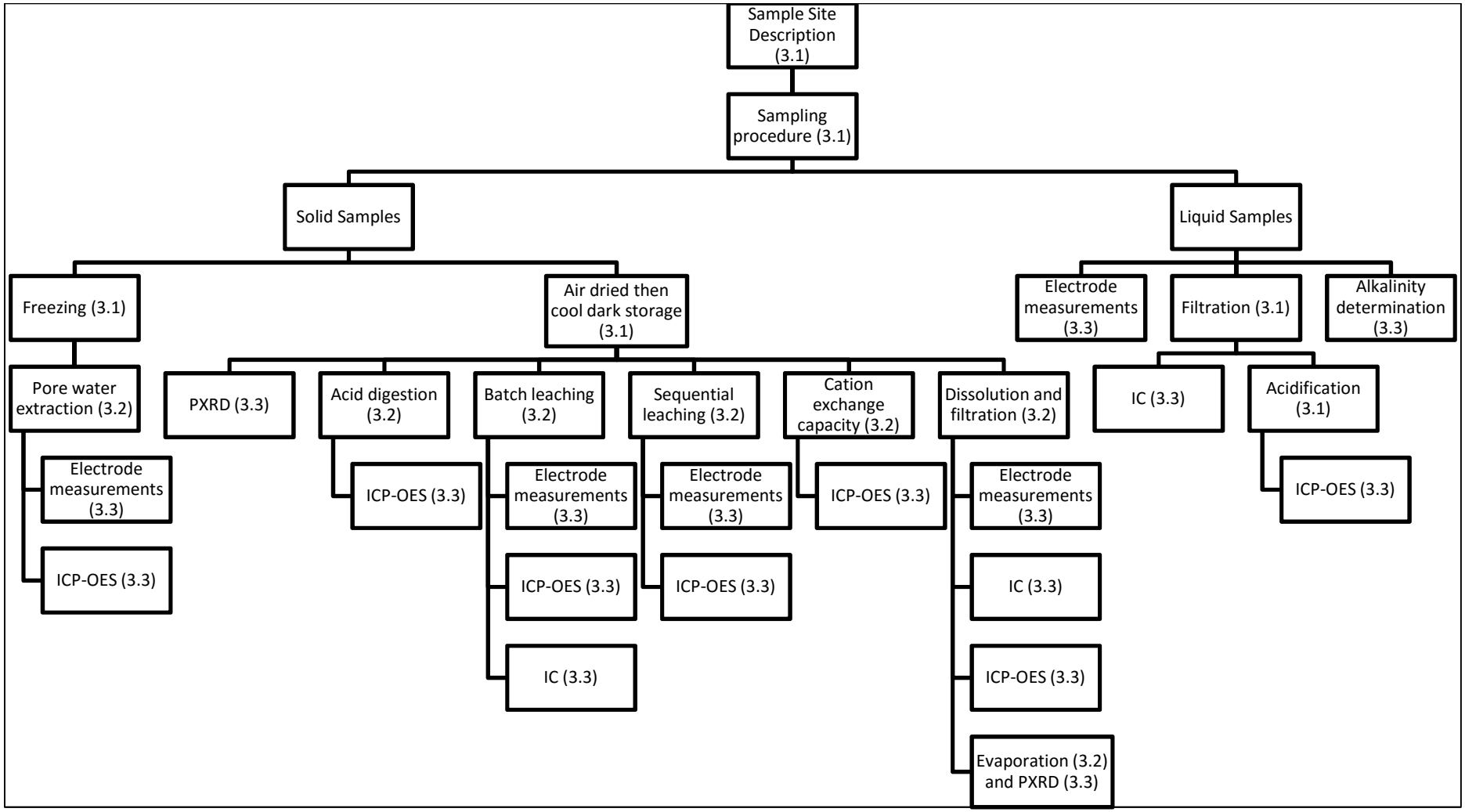

Figure 3.1: Outline of sample preservation, preparation and analysis

`

3.1 Sampling

The samples obtained, their analysis and their interpretation are the backbone of this project. In order to provide a fair comparison of sampling sites, it was of utmost importance that the sampling protocols remained consistent. Unfortunately, due the different nature of the sites this goal was not completely fulfilled. For example, percussion drilling was available at one site whereas augers were the only available means at another site. However, the ideals surrounding sampling at each site were maintained in that each sample was taken with the belief that it was representative of the material surrounding it at the time and every effort was made to ensure that the sample retained its compositional integrity during transport and storage. The sites of sampling, procedures for sampling and methods of sample preservation are discussed in this section.

3.1.1 Sampling Sites

Three different tailings storage facilities (TSF) were sampled during the course of this project, namely: i) a partially reworked and abandoned tailings footprint near Germiston, ii) an active TSF near Potchestroom and iii) a TSF undergoing reprocessing near Roodepoort. Stream water sampling of a region of Johannesburg in which streams are known to be impacted by TSF was conducted in order to determine the extent and speciation of mine related metals in these water bodies. Stream sampling near the partially reworked and abandoned site has taken place annually for many years as part of the third year Environmental Chemistry course. The historic results from this sampling were used to augment the results from this project.

3.1.1.1 Partially reworked and abandoned tailings footprint

An abandoned TSF footprint located near Germiston was sampled during the dry season of 2012 (Figure 3.2a) and during the wet season in 2013 (Figure 3.2b). This site hosted a TSF which was partially reprocessed in 2004. However, due to poor management, the facility was abandoned without rehabilitation. This has resulted in uncontrolled leaching of pollutants into an adjacent natural stream. Leachates drain into a pond within the facility and then seep into the stream via shallow groundwater passages (Figure 3.3).

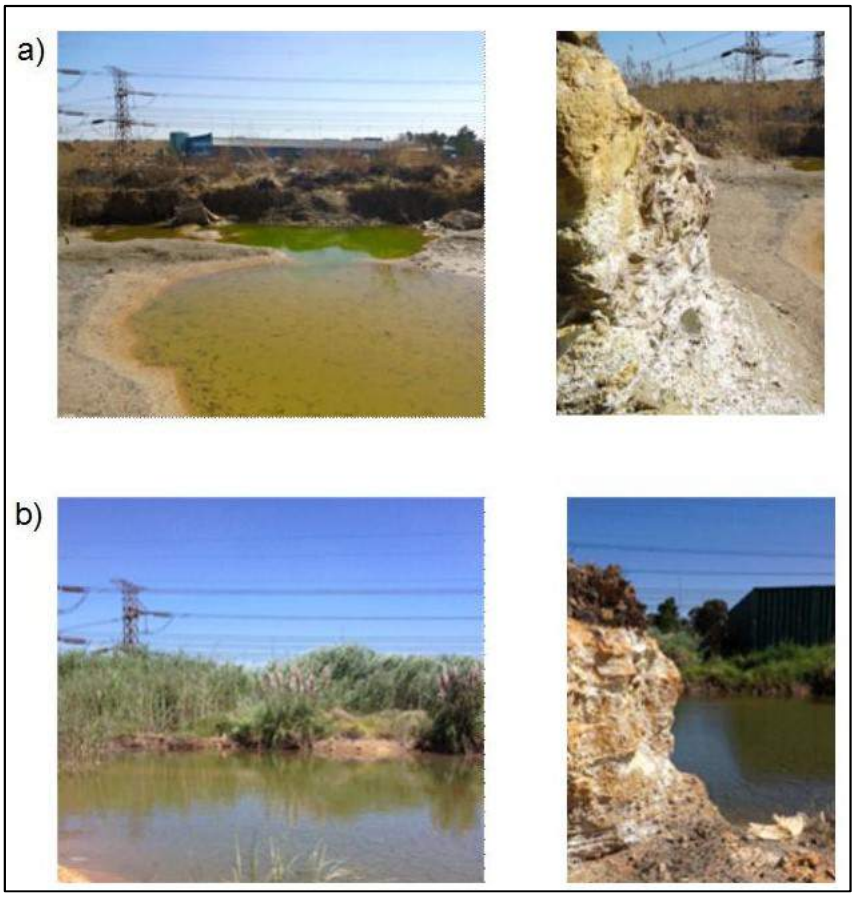

Figure 3.2: tailings pond and edge of TSF located in Germiston during: a) the dry season and b) the wet season

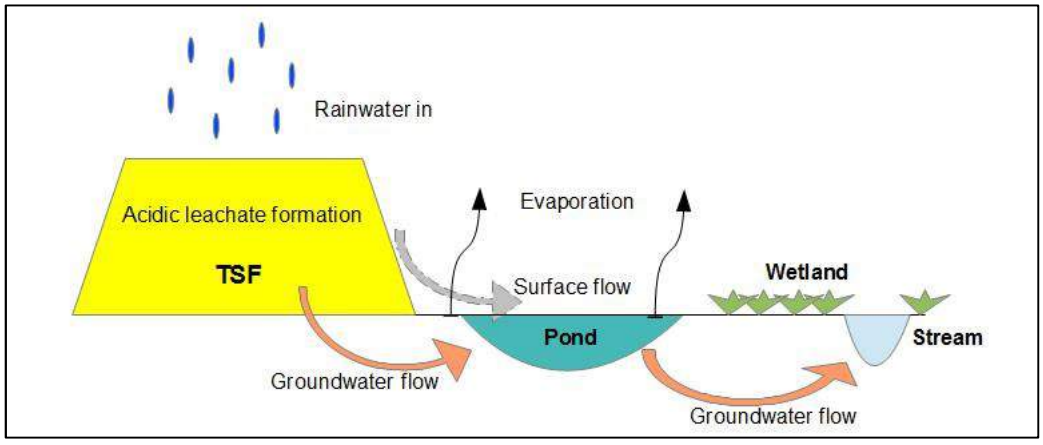

Figure 3.3: Proposed scheme of surface water and groundwater flow from TSF to pond to stream (from Camden-Smith and Tutu (2014))

`

An array of solid samples and three water samples were collected during the dry season in 2012. Unoxidised tailings material was obtained from a recently excavated hole adjacent to the TSF (Figure 3.4a). Partially oxidised tailings material was collected along the side of the TSF (Figure 3.4b). Efflorescent crust was sampled along the sides of the TSF, from an evaporated section of the pond and from an evaporated spillage from a monitoring borehole (Figure 3.4c). Different coloured efflorescent material was sampled separately. Three water samples were obtained from the small pond adjacent to the TSF (Figure 3.4d).

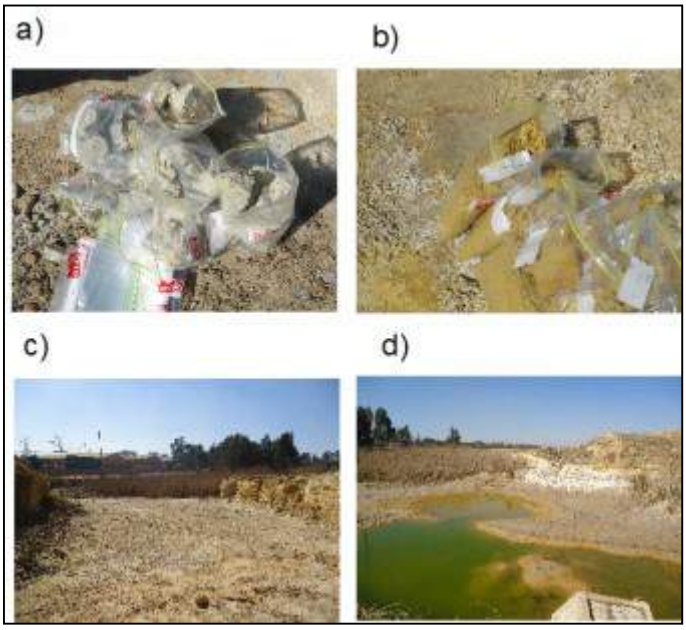

Figure 3.4: a) Samples of unoxidised material b) Samples of oxidised material c) Evaporated pond section from which efflorescent crust samples were taken d) Tailings pond

During the wet season in 2013, sampling of the site was undertaken again. The aim of this sampling was to obtain samples that were representative of the scheme represented in Figure 3.3. Unfortunately, the site was covered in reeds and only water sampling from the dam could take place. However, several water samples were taken from the adjacent pond. These samples were evaporated over a three month period in order to investigate the formation of efflorescent crusts from the pond water.

`

3.1.1.2 Active tailings storage facility

The chemistry of a groundwater plume emanating from an active tailings storage facility site was investigated. Phytoremediation has been investigated as a potential remediative action for this site and there are small plantations of a selection of trees planted on the site for research purposes. This sampling exercise took place in April and August 2013, during the dry season and sampling sites and data were shared with other schools from the University of the Witwatersrand. The aim of this sampling was to sample a transect from the tailings storage facility to the nearby river and to generate a reactive transport model for the site (Figure 3.5). The mining company that manages this facility allowed for a percussion borehole to be drilled, a pit to be excavated and for sampling of water from their monitoring boreholes. It was not possible to collect tailings material from the tailings storage facility; however boreholes adjacent to the tailings storage facility were sampled. The percussion drilling took place in April 2013, solid samples were obtained but water samples were not available. The pit excavation and borehole water sampling took place in August 2013. The previously drilled percussion hole from which solid samples were taken in April 2013 was also sampled for water. Consultants for the mining company had identified several sulphate plumes that were considered liabilities. The boreholes sampled lie within these plumes. Most of the boreholes sampled were covered and locked, however some of the boreholes were open and this has been taken into consideration when interpreting the results of the analysis. The pit was dug as a linear trench (Figure 3.6a). Solid samples in the unsaturated (vadose) zone and water saturated zone were taken (Figure 3.6b).

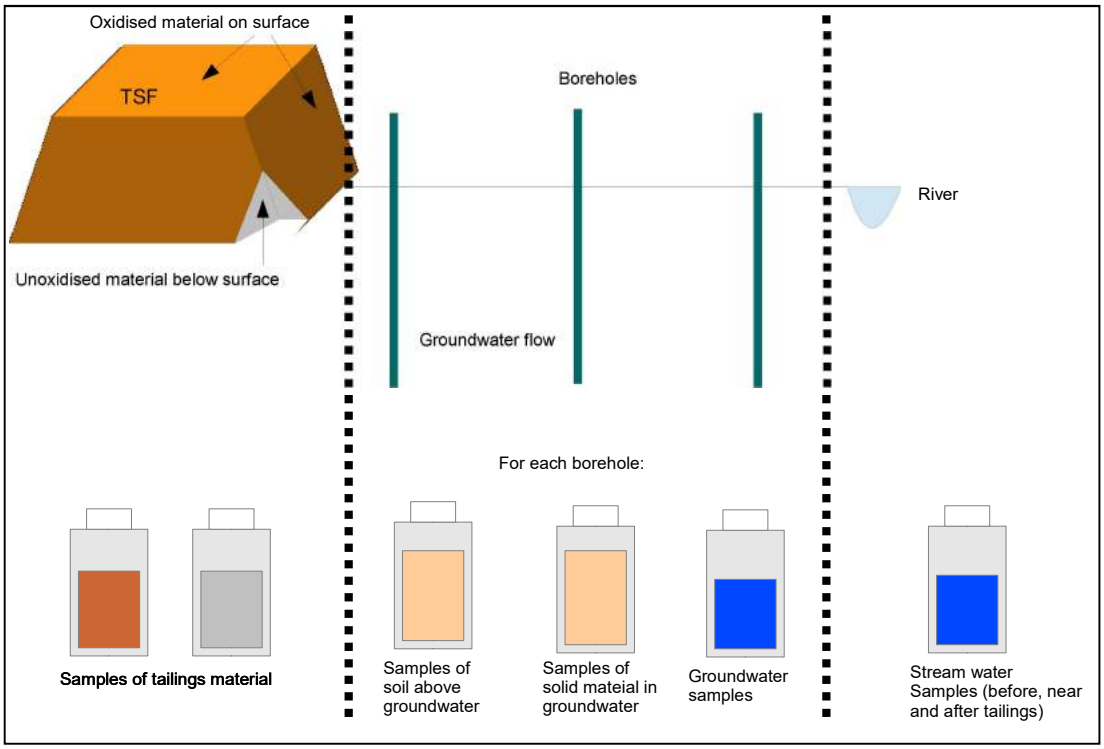

Figure 3.5: Idealised sampling plan for groundwater plumes emanating from an active tailings storage facility

a) b)

Figure 3.6: a) Excavator digging linear pit b) Saturated zone exposed at the bottom of pit

`

The map of the area (Figure 3.7) shows the spatial distribution of the boreholes and pit sampling site. The plumes emanating from the facility have been shown to impact the Schoonspruit and Vaal Rivers. Construction of the TSF shown in Figure 3.7 started in 1954 and was constructed using an upstream semi dry paddock method (GCS (Pty) Ltd, 2011). An emergency dam on the facility, with a capacity of 600 000 m^3, collects surface water drainage. The underlying geology is comprised of weathered (upper 1 – 25 m) and less fractured (25 – 40 m) dolomite and in the west this is underlain by Ventersdorp lavas. The perched aquifer in the study site occurs within the weathered dolomite (GCS (Pty) Ltd, 2011).

Figure 3.7: Google Earth map of the area showing where water (red markers) and solid samples (labelled as "pit") were collected

3.1.1.3 Tailings storage facility undergoing reprocessing

This TSF was in the process of being hydraulically reworked for gold and uranium by a gold mining company at the time of sampling. The site was located between Roodepoort and Randburg and an overview of the sampled area is presented in Figure 3.8. The mining company allowed for sampling of material from the TSF (Figure 3.9), a tailings surface pond that was fed by rainwater leaching the edge of the tailings (Figure 3.10), the acid mine drainage pollution control dam (Figure 3.11) and wetland adjacent to this dam (Figure 3.12). Water

`

sampling took place in January 2014 and water and solid sampling took place in March 2014. There are many tailings storage facilities in the region. This particular sampling scheme was chosen as the pollution control dam was believed to be fed by the sampled TSF (Figure 3.9). Water from the pollution control dam was consistently pumped and treated but the dam wall had been breached on occasion and spillage into the nearby wetland had occurred. The wetland under study is influenced by two TSF. Samples were taken close to the pollution control dam in order to minimize the effect of the second TSF. The pollution control dam has exposed tailings material on the outskirts of one edge. According to a map provided by the company, the pollution control dam was built on the footprint of a reclaimed TSF. A municipal waste dump lies to the east of the TSF. A lined waste water pond is on the edge of this waste dump and collects leachates emanating from the municipal dump. Water from this site is supposed to be pumped out of the pond and processed. However, storm events in which this pond overflows or leaks from this pond could also impact the tailings pollution control dam.

According to a geological report provided by the mining company, the TSF under study was situated on shales and quartzites of the Jeppestown Subgroup of the Witwatersrand Supergroup. The soil surrounding the TSF is predominantly sandy loam with a medium to high filtration rate. The consultants suggest that this type of soil could be leached of acidic and saline pollutants following the rehabilitation of the area thereby leading to a continued output of acidic water even after the removal of the TSF. However, they have stated that the removal and reworking of the TSF in the area will ultimately have a positive impact of the groundwater. They do warn that the TSF should be completely removed to a level lower than the contaminated tailings as only partial removal could have a negative impact. Residual tailing material exposed to the atmosphere could oxidize and release remaining pollutants in the water system.

`

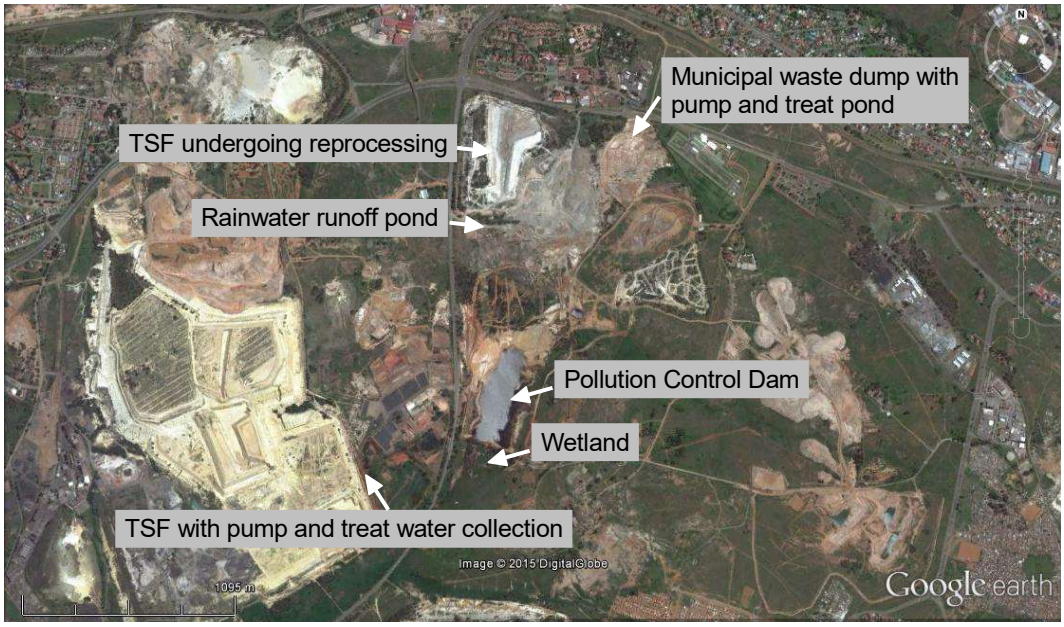

Figure 3.8: Google Earth overview of the sampled region

Figure 3.9: Photograph of the tailings storage facility

Figure 3.10: Photograph of tailings run off pond

`

Figure 3.11: Photograph of tailings run off pond (in foreground) and pollution control dam (in background)

Figure 3.12: Photograph of wetland adjacent to the pollution control dam

3.1.1.4 Regional water sampling

Water samples were taken from dams, lakes, rivers and trenches bordering TSFs across Soweto to assess whether the spatial impact of mine water could be determined using statistical techniques. Most of the samples collected for this purpose were collected in September 2012. A map of the area sampled in September 2012 (Figure 3.13) shows where the sampling took place in the mining impacted region of Soweto.

`

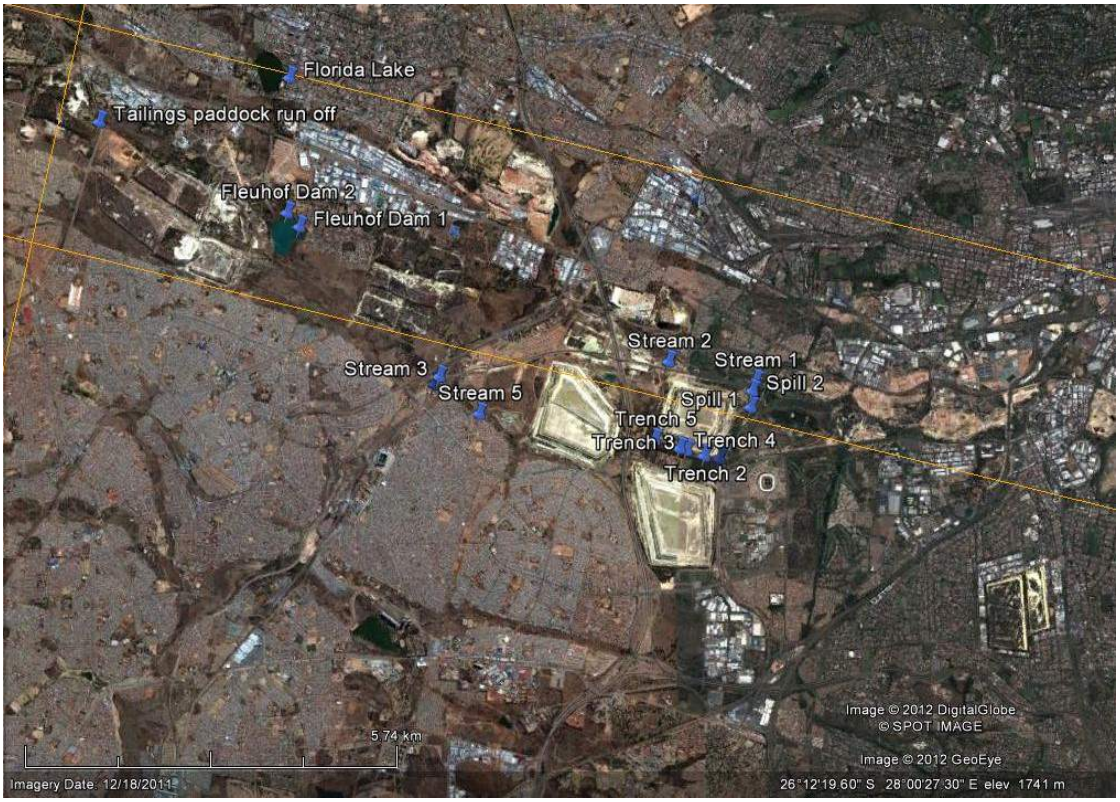

Figure 3.13: Google Earth image of the September 2012 water sampling excursion

3.1.1.5 AMD Treatment Plant

In order to investigate how surface drainage from the TSF differs from the more publicized underground drainage occurring in abandoned shafts, samples from a working treatment plant in the Central Rand Goldfields were acquired in August 2014. Samples of the untreated, acidic underground water were acquired from a high density sludge treatment plant. The company also allowed for samples from the treatment process to be taken. These samples included water samples of the processed water, sludge samples from the gypsum crystallization tank and sludge recycling tank and solid samples of the quick lime and limestone added in the process. Geochemical modelling of these samples were undertaken in order to better understand the treatment process from a chemistry perspective. Once the effects of the underground treatment is understood, it may be possible to see if the same infrastructure could be used to treat surface acid mine drainage.

`

3.1.2 Water Sampling Procedure

Discrete water samples were collected from streams, ponds, dams and the AMD treatment plant. Discrete samples are collected in individual containers and represent the source at time of collection. They are appropriate samples if conditions at the site remain approximately constant, this requires that the rate if fluctuation of analytes of interest is small (Wardencki & Namiesnik, 2002).

There are other types of samples that can be taken for environmental waters. Simple composite samples involve collecting a fixed volume of sample at certain time intervals and putting them in the same container (Wardencki & Namiesnik, 2002). These are used for streams in which there is a high rate of change in analyte concentration. Flow proportional composite samples represent the average conditions during sampling and are flow dependent. Flow proportional samples are collected either by adjusting intervals between samples of fixed volume or by adjusting the volume of sampling collected at constant time intervals (Wardencki & Namiesnik, 2002). A sequential composite sample involves placing a series of samples in one container. It differs from a simple and flow proportional samples in that it is time dependent. It is used for situations in which the analyte concentration is not constant, for example when wastewater is introduced into a stream periodically or when self purification conditions prevail (Wardencki & Namiesnik, 2002). For the purpose of this project, it was decided that discrete water samples were taken because flow rate data could not be obtained in many of the sampling sites or additional permission was required to set up a longer term sampling rig.

Water samples were collected in polypropylene bottles. These bottles were washed, soaked in 10% nitric acid overnight, rinsed with deionised water and dried. Bottles were rinsed with the water of interest at the sampling site, this rinse water was discarded a few metres away from the site of sampling and the bottles were filled with the water of interest.

`

3.1.3 Water Sample Preservation

The physiochemical properties of a water sample such as temperature, colour, pH, redox potential and conductivity can change quickly and as such are measured in the field at the time of sampling. Initially, samples were vacuum filtered with 0.45 µm Millipore filter paper and portions acidified in the laboratory on the same day as sampling. This process was streamlined during the project with filtering of samples done in the field using syringes and disposable 0.45 µm filter units. Three sub samples of the initial bulk water sample were prepared in the field namely: an unfiltered portion for alkalinity titrations; a filtered portion for anion analysis and an acidified, filtered portion for metal analysis. Samples were acidified by adding approximately 0.5 ml of 55% HNO_3 to 25ml of filtered sample. Sub samples were clearly labelled, stored in a cooler box with ice packs and transferred to a refrigerator as soon as possible. Physiochemical properties as mentioned above were determined on the bulk sample prior to partitioning. In general, alkalinity titrations were performed the day after sampling to comply with the recommended maximum 24 hour holding time (Wardencki & Namiesnik, 2002). Unacidified samples for anion analysis have a shorter holding time than the acidified samples for metal analysis. Nitrite has a holding time of only 24 hours; however it was not a significant analyte in this project. Chemically suppressed anion chromatography was performed within 48 hours in order to comply with the maximum holding time of 48 hours for nitrate (Wardencki & Namiesnik, 2002). Acidified, filtered samples could be kept for a longer period of time without deteriorating and were analysed for metal content within one month of sampling. Procedures for preservation, maximum holding time and quantification are summarised as Tables A1 and A2 in the Appendix.

3.1.4 Solid Material Sampling

Solid samples of relevance to this project include tailings material, efflorescent crust, borehole soil and pit soil. Ideal solid samples should have the same quantitative and qualitative composition as the bulk material (Zygmunt & Namiesnik, 2002). This objective was strived for in all but the efflorescent samples in which only the crust was of interest and not the bulk matrix.

`

Sampling of tailings material was undertaken in the same manner as sampling of soil profiles. This is appropriate as tailings material also forms chemically unique horizons (Zygmunt & Namiesnik, 2002). Sampling of discrete layers was required for batch leaching in which the difference between oxidized and unoxidised tailings material was investigated. A section of the tailings storage facility or tailings footprint was chosen and cleaned; this involved removing the outer layer on the side of the tailings footprint. A shovel was used to collect a sample from the centre of each visible horizon. Pit samples near a tailing storage facility were taken in a similar manner. Borehole samples were obtained during percussion drilling. Sampling was done at two metre intervals. The tailings and soil samples were collected in plastic bags and each bag weighed approximately 1.5 kg each). Samples were labelled by placing a sample tag with a description inside each bag. Efflorescent crusts were sampled by scraping the crust off of the surface of tailings material using a shovel.

3.1.5 Solid Material Preservation

Solid samples were air dried in a furnace at 50°C for approximately 5 days. Samples were weighed prior to drying and after drying. The difference between these weights represents the water content of the samples. Dried samples were stored in air tight plastic bags in a cool, dry cupboard. Prior to leaching studies, each dried sample was crushed and a representative portion of the sample was ground until uniform in colour and particle size. This portion was stored in a separate air tight plastic bag. Mud samples, such as those collected at the pit or sludge samples, such as those collected at the AMD treatment plant were ideally dealt with on the day of collection or were frozen shortly after collection. Within one week of sampling, small portions of mud or sludge were centrifuged to extract water. The extracted water was centrifuged once more to remove suspended solids. The supernatant was refrigerated and analysed using the same procedures as for water samples. A portion of the mud or sludge was dried and this dry material was ground and stored as described above.

3.2 Sample Preparation

In order to investigate the release of metals or the total metal content in solid samples, they were leached or digested respectively prior to analysis. This section

`

details the methods by which solid samples were handled in the laboratory. Leaching, acid digestion and dissolution-evaporation techniques were utilized to assess the chemical characteristics of the solid material.

A particular metal ion of interest in solid material can exist as a single phase or combination of phases and the phase affects the mobility of the metal ion. Such phases include water-soluble (including readily soluble salts), ion-exchangeable (bound by weak van der Waals forces in clay), carbonate, adsorbed on or included into amorphous or crystalline iron oxides, sulphides and silicates (Leinz et al., 2000). Figure 3.14 shows the target fractions of each leaching. Note that the percentages portrayed in Figure 3.14 are merely indicators and the actual percentages released for each leaching type is dependent on a multitude of factors including matrix, leaching solution and leaching duration. Complete acid digestion of a portion of the sample allows for the determination of total metal content (Figure 3.14).

Two methods of leaching were employed; batch and sequential. Batch leaching involves weighing a portion of material, adding a particular volume of a solution that will dissolve only specific analytes of interest (for example, readily water soluble analytes or acid soluble analytes) and shaking the mixture for a period of time. Batch leaching allows the contact solution and material to reach equilibrium and hence more is extracted than through column leaching. Sequential leaching follows the same principle as batch leaching, however instead of discarding the material following the first round of leaching, the same material is leached again using a chemically different solution that is intended to allow for the release of an analyte that could not be released for the first solution.

Dissolution of the readily soluble efflorescent crusts was done to assess their chemical composition and dissolution profiles. The solutions were filtered to remove quartz and allowed to evaporate. The evaporation profiles were then modelled and results of modelling compared to the lab results.

`

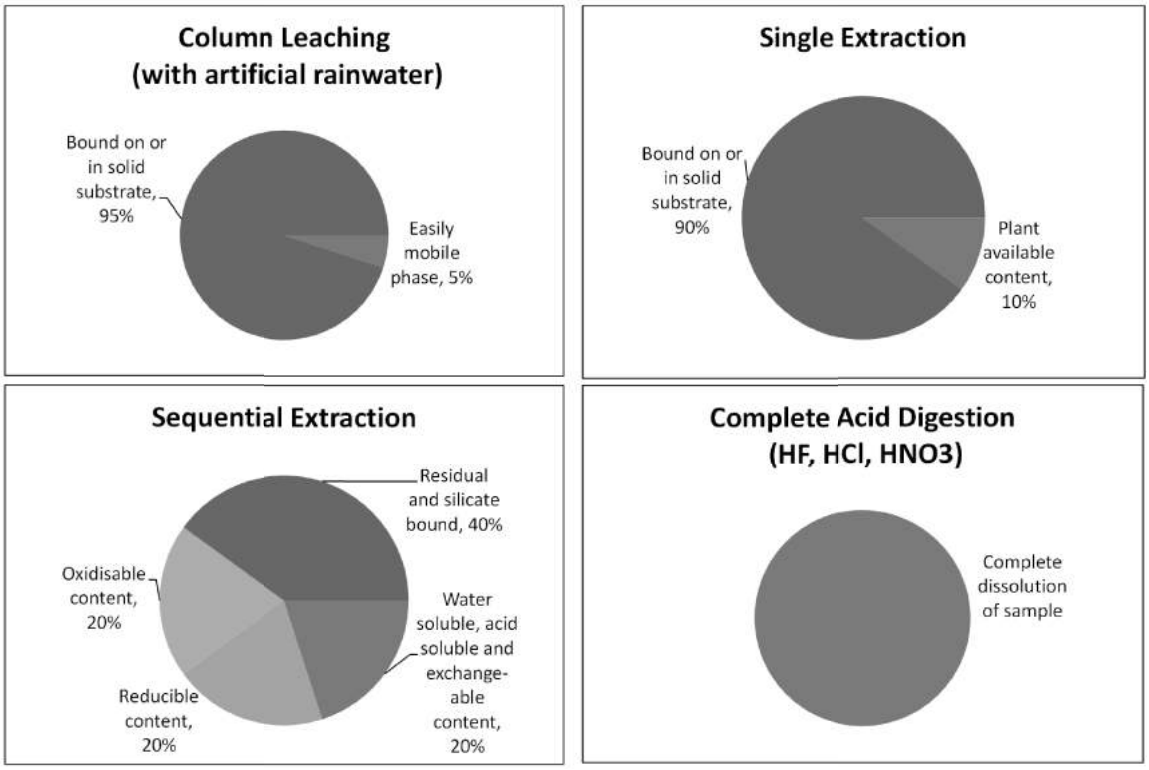

Figure 3.14: Different leaching approaches (adapted from Rao, Sahuquillo & Lopez Sanchez, 2008)

3.2.1 Leaching studies

Natural and anthropogenic materials are capable of releasing several products into the environment when leached with water. Some of these products are of environmental concern. In this project the released metals (common and trace) and anions were of interest.

Batch leaching and sequential leaching use a variety of leaching solutions. These leaching solutions would ideally be specific for metal species that are bound in a certain chemical environment (for example, as carbonates or oxides or silicates). Unfortunately, a lack of selectivity is a common problem and a wide variety of factors influence the leaching of metals from their matrix, such as pH, temperature, leaching time, reagent concentration, stirring or shaking system, particle size distribution and the liquid to solid ratio (Filgueiras, Lavilla, & Bendicho, 2002).

An additional leaching study was conducted to determine the cation exchange capacity. This test follows the same principle as batch leaching.

`

Leachates were analysed using the same methods of analysis for field water samples, i.e. physiochemical measurements (pH, redox, temperature, etc), ion chromatography for anion determination and ICP-OES for metal determination.

3.2.1.1 Twenty four hour leach test

In this method, several leaching solutions were used to leach tailings material. The same ratio of solution to material (20:1) was used. The solutions used were deionised water, artificial rainwater, sulphuric acid (pH 3), calcium chloride (0.01 M), EDTA (0.1 M) and sodium carbonate (0.1 M).

Artificial rainwater was prepared at one hundred times the required concentration and then subsequently diluted. The concentrated rainwater was prepared in a one litre volumetric flask with the following salts: 1.1614 g NH_4NO_3, 0.785 g K_2SO_4, 0.1157 g of Na_2SO_4, 0.1302 g of $MgSO_4.7H_2O$ and 0.4484 g $CaCl_2$ (adapted from Cocksedge, 1988; Maku, 2009).

Similarly to the field leach test (FLT), a 20:1 ratio of leaching solution to solid material was used (Hageman, 2007). Therefore, 20 g of air dried sample was weighed out, the actual mass was recorded to 0.01 g, placed in a wide mouth plastic bottle and leached with 400 ml of leaching solution. The bottles were shaken on an elliptical shaker for 24 hours. The solutions were filtered using Prima PES 0.45 μm filter paper.

Samples for anion analysis are stored in polyethylene bottles, refrigerated and analysis using ion chromatography. Samples for total metal analysis using ICP-OES were acidified with nitric acid and stored in polyethylene bottles. Analysis will follow the same procedure as described for the water samples.

3.2.1.2 Cation exchange capacity leach test

Solid materials that are present in the environment often portray a negative charge for one of two reasons; atomic substitution in their lattice or a pH dependent deprotonation of the surface of clay, amorphous material or organic material (Paschke, 2002). These surfaces act as temporary sinks for cations as they bind to these surfaces through weak attractions and can later be released. The cation exchange capacity (CEC) is a measure of the amount of ions sorbed onto the

`

surface of these clays, etc and is usually measured by saturating material with barium ions. This forces the cations bound to the surfaces into solution and their quantity is then determined. There are several types of cation exchange capacities; the two most common being potential CEC which is measured at a buffered pH of 8.2 (carboxyl groups and humic acids are deprotonated at this pH) and effective pH which measured at the soil's natural pH (Paschke, 2002). A good approximate of the effective pH can be made using an ammonium chloride solution instead of a barium chloride solution (Ross & Ketterings, 1995).

The cation exchange leach test was performed on the soil samples obtained in the vicinity of the active and partially reclaimed tailings storage facilities. An approximate, effective cation exchange capacity was required and not a full compulsive cation exchange capacity. Often, cation exchange capacities are determined in pH buffered solutions, however this can differ significantly from value from capacities determined at the soils natural or field pH. Full methods require two exchanges to ensure that the adsorption is reversible. However, only an estimate was required and as such the method followed was taken from Ross and Ketterings (2011). In this method, the exchangeable cations are measured not necessarily the cation exchange capacity of the soil. Clean, dry 50 ml centrifuge were used and 2.0 g of the soils of interest were weighed into each tube. Triplicate leaching samples were prepared for each sample along with two blank samples. The same soil that had been dried and crushed for the previous leaching studies was used. A 1 M NH_4Cl solution was prepared by transferring and dissolving 53.51 g of the salt into a one litre volumetric flask and filling to the mark with deionised water. Using a measuring cylinder, 20 ml of the solution was added to the soils. The solutions were shaken for one hour and then centrifuged. The supernatant was decanted and kept for ICP-OES analysis.

With the concentrations in mg L^1, the effective cation exchange capacity was calculated as shown in equation 3.1 (Ross & Ketterings, 1995):

$$CEC = \frac{[Ca]}{20} + \frac{[Mg]}{12} + \frac{[K]}{39} + \frac{[Al]}{9} \qquad (3.1)$$

`

3.2.1.3 Sequential extractions

The primary benefit of a sequential extraction over a single, batch type extraction is an improvement in targeting a specific phase (Rao et al., 2008). Sequential extractions involve a series of reagents that attack specific fractions of the study sample (Leinz et al., 2000; Reid, Spencer & Shotbolt, 2011). Many sequential extractions have been developed and tested, however the two most common schemes are the Tessier extraction (Tessier, Campbell & Bisson, 1979) and the BCR method (Rauret et al., 1999).

The BCR sequential extraction, developed by the Standards, Measurements and Testing Programme (formerly the Community Bureau of Reference (BCR)) was used in this work due to the availability of certified reference material (CRM). Currently, there is no CRM available for the Tessier extraction.

Criticisms of sequential extractions include a lack of specificity of attacking reagents; the altering of phases during an extraction; re-adsorption of metals back onto the surface of sediments; decreasing reliability with increased number of extraction steps and complete recovery of trace metals (Li & Thornton, 2001; Reid, Spencer & Shotbolt, 2011). However, many of these problems can be overcome by using consistent procedures (Reid, Spencer & Shotbolt, 2011). Accuracy for the BCR method was assessed using the CRM and by comparing the sum of the extractions with the total value determined by microwave digestion.

Oxidised and unoxidised tailings samples, goethite sand samples, pit samples and percussion borehole samples were subjected to sequential extractions. A portion of the sample was isolated into a sealed bag, lumps of material were broken down and the bag was shaken until it was well mixed. The material was visually homogenous in particle size and no sieving was done to separate size fractions.

The BCR sequential extraction, developed by the Standards, Measurements and Testing Programme (formerly the Community Bureau of Reference (BCR)) was used in this work due to the availability of certified reference material (CRM).

This extraction scheme was developed by the Standards, Measurements and Testing Programme (formerly the Community Bureau of Reference (BCR)) of the

`

European Commission (Rauret et al., 1999). The procedure was improved by Rauret and colleagues (1999) by standardising the volume of acid required in the second step of the extraction. This "improved BCR" scheme is a popular leaching scheme and it has certified reference material (BCR 701) available (Pueyo et al., 2001). This procedure was conducted with a few noteworthy deviations from the prescribed method as described by Rauret et al. (1999). The procedure suggests the use of 80 -100 ml centrifuge tubes. These tubes were not readily available and 50 ml tubes were used instead. The reduced volume of the tubes only affected the third leach step. The procedure recommends an end over end shaker in order to keep the contents in suspension during the leach. However, a horizontal elliptical shaker was the only type of shaker available. A summary of the method is presented in Table 3.1. The solutions for the leaching were prepared as described in the method outlined by Rauret et al. (1999) and Pueyo et al. (2001) with the only deviation being that occasionally only 500 ml of solution was prepared instead of the stated 1 l. This was done to reduce waste. Fresh solutions were prepared for every batch of sequential extractions. In the third leach step, the method prescribes the addition of 50 ml of ammonium acetate solution to the contents. However, 40 ml was added because of the reduced volume of the centrifuge tubes. The reduction of H_2O_2 volume as required in the third step usually had to be completed over a two day period. After each step, the contents were centrifuged for 10 to 15 minutes at 3000 rpm (1891 *g*) within a Hettich® ROTOFIX 32A centrifuge. The supernatant was decanted and kept for ICP-OES analysis. Deionised water (20 ml) was added and the contents were shaken for 15 to 25 minutes then centrifuged again. The rinse water supernatant was discarded. Empty centrifuge tubes were used as procedural blanks and subjected to the same leaching and cleaning procedures. BCR-701 certified reference material was treated to the same leaching procedure as the samples.

`

Table 3. 1: Outline of the BCR sequential leach (adapted from Rauret et al. (1999))

Leach Step	Targeted Fraction	Leaching solution	Volume added (ml)	Duration of leach (hours)	Temperature
1	Water soluble, exchangeable and acid soluble	0.11 M acetic acid	40	16-24	Room
2	Reducible	0.5 M hydroxylamine hydrochloride	40	16-24	Room
3	Oxidisable	H_2O_2 (from supplier)	10 (volume reduced to approximately 3 ml after one hour in bath)	a) 1 b) 1 (occasional manual shaking)	a) Room b) 85°C water bath
		H_2O_2	10 (volume reduced to approximately 1-2 ml after one hour in bath)	1	85°C water bath
		1 M ammonium acetate	40	16 – 24	Room
4	Residual	Acidic Microwave Digestion (see section 3.2.4)			

3.2.2 Dissolution and evaporation of soluble sampled material (i.e. efflorescent crusts)

In order to determine the readily water soluble fractions of the efflorescent crustal material, approximately 3 g of crust was dissolved in 100 ml of deionised water. This was undertaken in a step wise manner. The pH, EC and ORP of 100 ml of deionised water was measured using calibrated electrodes. A pre-weighed portion of the crust (0.50 g - 0.55 g) was added to the beaker. The solution was stirred continuously with a stirrer bar on a magnetic stirrer plate. The pH was recorded at one minute intervals for a period of at least five minutes or until pH and EC remained constant. The EC and ORP were recorded after five minutes. Another portion of the crust was added and the process repeated until six portions of crust had been added. The final solution was gravity filtered using a standard 7 cm filter paper. Undissolved portions were visually described. The solutions were refrigerated. No acidification of samples was required due to the low pH of the

`

solutions. Analysis of the solutions included IC for anions and ICP-OES for metal content. Additional crust was dissolved in deionised water, filtered and added to the initial solutions. The solutions were evaporated at 30°C and the products were dried between 40°C and 50°C.

PXRD was used to determine the mineralogy of the efflorescent crusts prior to dissolution as well as the evaporation products.

3.2.3 Acidic microwave digestion of solid material

Acidic microwave digestion was carried out in order to determine the total metal content present in a solid sample.

Samples were initially ground with a porcelain pestle and mortar. The solid material was dried at 110°C at atmospheric pressure in order to remove adsorbed water (Harris, 2007). Suitable Teflon tubes were used and 0.25 g of sample was weighed out into each tube. In order to completely dissolve the material, a mixture of acids was required. Hydrofluoric acid was used to dissolve silicates (1 ml required). Hydrochloric acid is a non oxidising acid that dissolves many metals, oxides, sulphides, carbonates and phosphates (6 ml required). Nitric acid is an oxidising acid that may dissolve solids that a non-oxidising acid could not (2 ml required) (Harris, 2007). Digestion was carried out in a Teflon-lined bomb in a microwave oven. After digestion, 6 ml of boric acid was added to each Teflon container in order to neutralise the hydrofluoric acid and make the solution safe for storage in glass. The samples were decanted into clean 100 ml volumetric flasks and filled with deionised water to the mark. Three replicate digestions per sample were digested. For every group of digestions performed, two blank digestions and digestion of NCS certified reference material were also performed. The NCS Certified Reference Material (NCS DC73315 (GBW07305)) is a reference material for stream sediment; it was made by the China National Analysis Center for Iron & Steel (2004) and was distributed by Industrial Analytical (Pty) Ltd.

Diluted samples were kept in the refrigerator until analysis by ICP-OES.

`

3.3 Analytical Techniques

In this section, the analytical techniques and equipment used to analyse the water samples, solid samples and leachates are discussed. For water samples and solutions prepared from solid samples (as discussed in the previous section), these techniques included physiochemical electrode measurements of temperature, pH, conductivity, dissolved oxygen and redox potential (E_h); titrations for alkalinity determination; chemically suppressed anion chromatography (IC) for quantitative determination of anions and inductively coupled plasma-optical emission spectroscopy (ICP-OES) for quantitative determination of metal content. Physiochemical electrode measurements of solid samples were also done as well as powder X-ray diffraction to determine the mineralogical composition of the samples.

3.3.1 Analysis of Water and Prepared Samples

This section discusses the analytical techniques used to measure the physical and chemical properties of water samples, leachates from the leaching studies, dissolved crust material and the digested solid material.

3.3.1.1 Determination of physiochemical properties

The physiochemical properties of temperature, colour, pH, redox potential and conductivity discussed here were determined for the water samples and for the batch leachates. Turbidity measurements and dissolved oxygen content were determined for the water samples only. It was important that these measurements were conducted in the field soon after collection of the water samples because they can alter quickly. For the leachates, these measurements were taken prior to preservation of the samples. The Thermo Scientific Orion multiparameter field meter was used for determination of field based properties. The equipment was calibrated and maintained using the manufacturer's suggested buffer solutions.

Temperature of a liquid is an important property as it has influence over the density, surface tension, pH and redox potential (Paschke, 2002). Temperature is measured in the field with an electronic platinum resistance sensor thermometer (Paschke, 2002).

`

The colour of the water can be distinctive of natural impurities within the sample. The colour was described after undissolved particles were removed by sedimentation, filtration or centrifugation. Colour can be qualitatively described through visual means or quantitatively determined through the use of spectrophotometry (Paschke, 2002). For this project, the colour of water samples was described qualitatively.

The pH of a solution is defined as the negative logarithm of the activity of the hydronium ion. It is an important parameter in that it strongly influences the stability, reactivity and mobility of many environmental substances (Paschke, 2002). Accurate determination of the pH is undertaken using a calibrated glass electrode. For laboratory pH measurements, the Knick pH meter 766 Calimatic was used and calibrated with Metrohm pH 4 and pH 7 buffered solutions. For field measurements, the Thermo Scientific Orion or Martini pH 58 field meters were used and calibrated in the field shortly before measurements.

Along with pH, reduction and oxidation (redox) reactions have a control over the speciation and the resulting characteristics of several substances. The redox potential is measured as the difference between an indicator platinum electrode and a reference electrode. The standard hydrogen electrode as a reference is not feasible for field measurements and a calomel electrode is used instead. The resulting redox measurements are then adjusted so as to refer to the standard hydrogen electrode and this allows for comparison and interpretation of results. For field and laboratory ORP measurements, the factory calibrated Martini pH 58 probe was used. The measured redox potential (E_h) is representative of all the redox pairs in an equilibrated system (Paschke, 2002).

The electrical conductivity of a solution is dependent on the concentration of the ions present in the solution as well as their respective mobility through the solution (influenced by the hydration sphere of the ion), the valence of the ion and the temperature of the solution (Paschke, 2002). Adwa AD 32 EC/TDS was used for determination of EC in the laboratory and the calibration of the equipment was checked using a 1288 µS standard solution. The conductivity probe of the

`

Thermo Scientific Orion field multiparameter meter measured the conductivity of the field samples.

Turbidity is a measure of the amount of light that is scattered of light as it passes through a sample. It is caused by suspended matter or colloidal inorganic and organic substances and can be described visually on a range from clear to opaque or quantitatively by nephelometric methods (Paschke, 2002). In this project, the turbidity was visually described.

The presence of oxygen in a solution affects a numerous factors. Oxygen affects the redox potential of a solution which in turn affects the valence state of metal ions in solution (Paschke, 2002). The dissolved oxygen content in field water samples was determined using the RDO optical/ luminescence-based probe of the Thermo Scientific Orion field multiparameter meter. The probe was calibrated using the water saturated air method.

3.3.1.2 Alkalinity determination

Alkalinity is the acid neutralising capacity of a sample of water whereas acidity is the base neutralising capacity (Zhu & Anderson, 2002). Acidity and alkalinity are indications of the carbonate content of the water. The total carbonate concentration of a sample is the sum of the concentrations of the carbonate anion (CO_3^{2-}), bicarbonate anion (HCO_3^-), carbonic acid (H_2CO_3) and dissolved carbon dioxide ($CO_2(aq)$). Carbonate speciation is pH dependent. Below a pH of 6.4 most of the carbonate is mainly present in a hydrated carbonate form or non hydrated carbon dioxide (H_2CO_3 or $CO_2(aq)$), the bicarbonate form dominates between pH 6.4 and 10.3 and above pH 10.3 the carbonate form prevails (Zhu & Anderson, 2002).

Alkalinity of a CO_2-H_2O system is determined by titrating a fixed volume of the water sample with standard acid to an end point of pH 4.5. The two main reactants with the acid are bicarbonate and carbonate anions; hydroxide ions are significant when the solution is either very basic or very dilute. Other bases such as $H_3SiO_4^-$, $H_2BO_3^-$, and HS^- as well as organic compounds can also contribute to alkalinity

`

(Clark & Fritz, 1997). Carbonate alkalinity can be defined as equation 3.2 (Zhu & Anderson, 2002):

$$\text{alkalinity} = m_{HCO_3^-} + 2m_{CO_3^{2-}} + m_{OH^-} - m_{H^+} \qquad (3.2)$$

Guidelines for the alkalinity titration methods were taken from ASTM D1067-06: Standard Test Methods for Acidity or Alkalinity of Water (ASTM International, 2010) and Method 2320: Alkalinity (American Public Health Association, 1999). For this project, only an estimate of alkalinity was required for geochemical modelling. The samples were titrated using standardized hydrochloric acid as a titrant and bromocresol green indicator was used to indicate the end point of pH 4.5. A more accurate method of alkalinity determination includes the use of a pH electrode, the addition small aliquots of titrant and the plotting of a titration curve. Samples with low alkalinity require an alternative extrapolation technique; their determination was not justified and as such this was not undertaken.

For the determination of alkalinity, a solution of approximately 0.02 N HCl was standardized with a primary standard 0.05 N Na_2CO_3 solution. One litre of Na_2CO_3 solution was prepared by dissolving an accurately recorded amount of approximately 2.5 g of salt that had been dried for 4 hours in a furnace at 250°C. One litre of the HCl solution was prepared by diluting 2.00 ml of 32 % HCl with deionised water. Bromocresol green indicator solution was prepared by dissolving 0.1 g of the solid material in 100 ml of deionised water. For the standardisation titrations, 2 drops of bromocresol green indicator was added to a volume of 10 ml of Na_2CO_3 solution and was titrated to colour change. The standardisation titrations were completed in triplicate and the average volume determined. The normality, N (in equivalent $mol.L^{-1}$) of the HCl solution was calculated using the equation 3.3 ,

$$\text{Normality} = \frac{A \times B}{53.00 \times C} \qquad (3.3)$$

Where A is the mass of Na_2CO_3 used to prepare 1 L of primary standard solution (g), B is the volume of Na_2CO_3 solution used in the titrations (in this case, 10 ml)

`

and C is the average volume of the HCl solution delivered to reach end point (ml). The constant 53.00 takes into account the molecular masses.

Ideally the water samples should not be filtered or altered in any way prior to alkalinity titrations. However, many of the water samples collected had significant plant debris or algae content and as the titrations were carried out the day after sample collection it was decided to filter samples on the day of collection using Whatman filter paper. Into a 250 ml conical flask, 100 ml of sample was delivered using a pipette. Bromocresol green indicator was added (2 – 3 drops) and the sample was titrated with the standardised 0.02 N HCl. The titrations were completed in triplicate for each sample.

The alkalinity was calculated using the equation 3.4,

$$\text{Alkalinity} = \frac{\text{A} \times \text{N} \times 50000}{\text{S}} \qquad (3.4)$$

where alkalinity is defined as mg $CaCO_3$ L^{-1}, A is the volume of standard acid delivered (ml), N is the normality of the standard acid ($mol.L^{-1}$) and S is the volume of sample used (in this case, 100 ml).

Using this method , the alkalinity is reported as: "The alkalinity at ___°C to bromocresol green end point was _____ mg $CaCO_3$ L^{-1}" (ASTM International, 2010).

3.3.1.3 Chemically suppressed ion chromatography

Ion chromatography is a high performance equivalent of ion-exchange chromatography (Harris, 2007). The chemically suppressed anion chromatography method was chosen because it provides quantitative determination of a selection of anions in the milligram per litre range, only a small amount of sample (millilitres) is required and the method is able to distinguish between chloride and bromide.

In chemically suppressed-ion anion chromatography, anions are separated using ion exchange in which a "positively" charged stationary phase attracts anions (Harris, 2007). The sample is first pumped through a guard column which protects the separator column from particulates and other contaminants and then to the

`

separator column in which the anions are separated based on their retention characteristics (ASTM International, 2010). A chemical suppressor device is situated between the separator and conductivity detector. The suppressor device is comprised of a column lined with a cation exchange membrane which is regenerated by sulphuric acid (Harris, 2007). This device reduces the background signal caused by the eluent by replacing the cations in the eluent with hydrogen ions (ASTM International, 2010). The anions are converted to their corresponding acidic forms and the sodium bicarbonate and sodium carbonate eluent ions are converted to the carbonic acid which forms dissolved carbon dioxide and water. Therefore, the resulting eluent products have a low electrical conductivity signal and the electrical conductivity cell detector will measure the anion signals from the separated anions in the acidic form (ASTM International, 2010).

Fluoride, chloride, bromide, nitrate, ortho-phosphate and sulphate anions were analysed using chemically suppressed ion chromatography. The standard method ASTM D4327-03: Standard Test Method for Anions in Water by Chemically Suppressed Ion Chromatography was used as a guideline (ASTM International, 2010).

Metrohm equipment was used for analysis of the fluoride, chloride, bromide, nitrate, ortho-phosphate and sulphate concentration of the water samples. A Metrohm 761 Compact IC with suppressor module was used for the analysis. A Metrosep A Supp 5-150 column was used in conjunction with the appropriate guard column. The column was regenerated during the course of the lab work with eluent that was ten times the concentration of the normal eluent. The suppressor was cleaned and regenerated with 1 M H_2SO_4.

Deionised water was obtained from Millipore Direct- Q and had a conductivity of 18.2 $\mu S.cm^{-1}$.

The eluent solution (1.0 mM $NaHCO_3$/ 3.2 mM Na_2CO_3) differs from that described in the method but it was the standard eluent that is prescribed by the column manufacturers, Metrohm. The method states that other eluents can be prepared provided that proper resolution is obtained. Eluent was prepared by

`

dissolving 0.084 g of $NaHCO_3$ and 0.339 g of Na_2CO_3 per one litre of solution. The solution was filtered through 0.45 μm Prima Pes filter paper and degassed in an ultrasonic bath. Eluent was not kept for longer than a month due to possible algae growth.

The membrane suppressor regenerative solution was 50 mM sulphuric acid. It was prepared by diluting 2.75 ml of 96 % H_2SO_4 in a 1 L volumetric flask and filling up to the mark with deionised water.

Multi point calibration was undertaken and series of standard solutions were prepared (1, 5, 10 and 20 ppm with respect to the anion). In order to prepare individual standard solutions, a 1000 mg L^{-1} stock solution of the anions was prepared. Table 3.2 outlines the amount of salt required and the method for preparation. The required amounts of salts were analytically transferred into a single 1 L volumetric flask, dissolved and then diluted to 1 L with deionised water. Standard solutions were prepared daily from the stock solution. A 20 ppm standard was prepared by dispensing 2000 μL of stock solution using an automatic pipette into a 100 ml volumetric flask and filling to the mark with deionised water. Similarly, 10 ppm and 5 ppm standard were prepared by dispensing 1000 μL and 500 μL respectively. A 1 ppm standard was prepared by pipetting 5000 μL of 20 ppm standard into a 100 ml volumetric flask and filling to the mark with deionised water.

`

Table 3.2:Preparation of 1000 mg L-1 anion stock solution for IC calibration (as recommended by ASTM International, 2010)

Anion	Salt	Exact mass required per 1 L (g)	Recommended salt preparation prior to weighing
Bromide	Sodium bromide (NaBr)	1.287	Dry salt for 6 hours at 150°C and cool in a desiccator.
Chloride	Sodium chloride (NaCl)	1.648	Dry salt for 1 hour at 100°C and cool in desiccator.
Fluoride	Sodium fluoride (NaF)	2.210	None.
Nitrate	Sodium nitrate ($NaNO_3$)	1.371	Dry salt for 48 hours at 105°C.
Phosphate	Potassium dihydrogen phosphate (KH_2PO_4)	1.433	None.
Sulphate	Sodium sulphate (Na_2SO_4)	1.479	Dry salt for 1 hour at 105°C.

In order to prevent damage to the column, water samples often required dilution. The dilution factor was estimated based on the conductivity of the samples were measured. Dilutions were carried out by using a micropipette and 15 ml or 50 ml an array of volumetric flasks. For example, a solution with dilution by a factor of 100 was prepared by delivering 0.5 ml of sample into a 50 ml volumetric flask and filling to the mark with deionised water.

`

3.3.1.4 Inductively coupled plasma- optical emission spectroscopy (ICP-OES)

Inductively coupled plasma-optical emission spectroscopy (ICP-OES) was used to detect and quantify metal ions in the field water samples and prepared water samples. ICP-OES was used in this project as it allows simultaneous determination of the concentration of a variety of metallic elements and it exhibits less spectral interference than atomic absorption spectrophotometry (Baloyi, 2006).

In optical emission spectrophotometry, the sample is first subjected to very high temperatures and decomposes into individual excited atoms and ions. The excited atom or ion then emits visible or ultraviolet radiation at a wavelength which is ideally unique to that atom or ion (Baloyi, 2006). A peristaltic pump transports sample to a pneumatic nebulizer where an aerosol is generated and transported via the sample chamber into the ICP torch (Mike, 1987). Samples are filtered first to prevent blocking the nebulizer. The high temperatures (6000 to 9000 K) are achieved through Ohmic heating of argon plasma which is initially formed by a spark from a Tesla coil (Mike, 1987). A polychromator allows for the simultaneous detection of a variety of predetermined wavelengths of the photons emitted during excitation.

The spectral interferences that could lead to discrepancies between the measured and true values of a particular element include (ASTM International, 2010):

- The overlaps of a spectral line of the element of interest with that the spectral line of another element or band spectra of a molecule. Another spectral line for the analyte of interest would be selected if this interference was present.
- Contribution to the spectral line of interest from background. This can arise from recombination factors or from stray light from the line emission of high concentration elements. Application of background correction techniques could be applied adjacent to the spectral line of interest in order to compensate for these interferences.

`

Standard solutions for calibration of the analytes of interest were prepared in 100 ml volumetric flasks. Dilutions were undertaken in the same way as for the IC method.

Spectral line choices for the elements are summarised in the Appendix as Table A3. The Student's T-test at a 95% confidence level was employed for elements in which more than one spectral line was chosen. If the differences between the measurements were not significant, then an average value of the two spectral lines has been reported. In cases where the concentration difference between lines was significant then line that portrayed a better calibration, more consistency with dilutions, and often the lower value, has been reported. In these cases, it was likely that a spectral interference was occurring and where possible the likely interferent has been identified and reported in the description column of Table A3 in the Appendix.

3.3.2 Analysis of Solid Material

This section discusses the analytical techniques used to measure the physiochemical properties and mineralogy of the solid samples taken from the sampling sites.

3.3.2.1 Determination of physiochemical properties

Temperature, pH, redox potential, water content and particle size distribution were among the physiochemical properties that were determined for a few of the solid samples.

Increasing temperature of soil leads to microbial activity and increased volatilisation of some species (Paschke, 2002). The temperature of solid samples should be measured in the same way as the temperature of water samples, which is with an electronic platinum resistance sensor thermometer. A longer time is required for thermal equilibration and greater care is needed to prevent damage to the sensor (Paschke, 2002).

The pH of the samples should be measured in the field as the effects of aeration to the samples are unknown (Paschke, 2002). For water-rich sludge or muddy material, a pH electrode can be inserted directly into the sample; however for dry

`

samples a suspension of one part solid to 2.5 parts water was made and measured. The pH is an important characteristic in sediments as it governs the mobility of some trace elements such as aluminium, iron and manganese (Paschke, 2002). Instead of deionised water, a neutral salt solution such as 0.1 M KCl or 0.01 M $CaCl_2$ could have been used as it provides a constant, comparable ion activity (Paschke, 2002).

The redox potential was measured in the field using the same electrode system that was used for the water samples. The electrode was inserted into the sample and the reading was only taken once a stable measurement is obtained, some methods recommend waiting 30 minutes before recording. Redox measurements of solids are a mere indication and should not be regarded as quantitative measurements. The aerated nature of some samples or the aeration process in sampling introduces or releases gases that yield measurements questionable (Paschke, 2002). Similarly to environmental water measurements, the redox measurement is a combination of mixed potentials due to the presence of multiple sets of redox active ions and elements. Redox measurements can be reliable for flooded soils because of the absence of interfering gases (Paschke, 2002).

Particle size distribution is a physical property of solid material which was not taken into quantitatively determined during this project. Only a visual estimation of particle size was described. It is an important property in that it controls the sedimentation rate and packing density of material (Paschke, 2002). Gravel consists of particles between 1 and 8 cm, sand particles are between 63 µm and 1 cm, silt particles are between 2 and 63 µm and clay particles are less than 2 µm in diameter (Paschke, 2002).

3.3.2.2 Powder X-ray diffraction

Powder X-ray diffraction is a routine method for identifying crystalline minerals in solid material. X-ray diffractometers consist of an X-ray source, a sample holder associated with a goniometer and an X-ray detector (Nesse, 2000). In this project, a Bruker D2 Phaser desktop diffractometer which was fitted with a cobalt X-ray source and a LynxEye 1-D detector was used. Samples were crushed using an agate pestle and mortar and then packed onto a sample holder. A random

`

orientation of grains was made possible by using a side packing method in which a small amount of sample was placed in the holder, a glass slip covered the sample holder, the sample holder was tilted to 90° and then tapped on a rubber mat until the sample fell to one end. This method was repeated until the sample holder was full. Ten minute data collections were done with no spinning of the sample. The files were exported to DIFFRAC.EVA software where the peaks were matched to a database of PXRD patterns of standard minerals. Environmental samples contain a mixture of minerals and the potential for overlapping peaks complicate this procedure (Nesse, 2000). Furthermore, peak shift due to solid solutions and partially amorphous material also complicate this procedure. In samples were it was possible to allocate each peak in the patterns, a Rietveld refinement was used to determine their relative abundances.

3.4 Strategy for constructing geochemical models

In this project, geochemical modelling was used to better understand the evolution, transport and fate of metals released from tailings storage facilities. In order to prepare the models, the following guideline was observed and was adapted from that recommended by Zhu & Anderson (2002).

3.4.1 Establishment of the goals of the model

The goals of modelling aid in determining which type of model is required, the type of samples required and which parameters need to be measured (Zhu & Anderson, 2002). The modelling in this project aimed to better understand the processes highlighted in Figure 3.15.

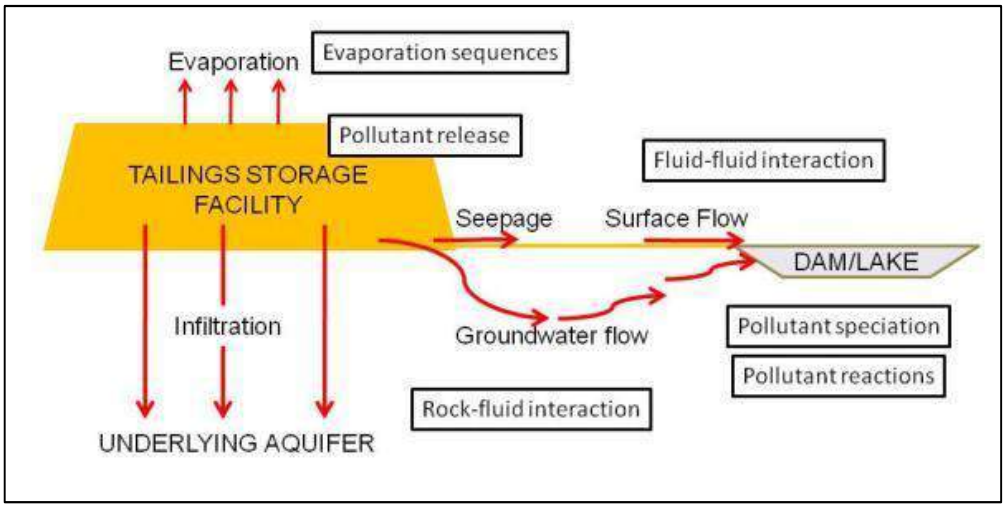

Figure 3.15: Processes of metal pollutant evolution and transportation from a tailings storage facility that were considered in geochemical models

3.4.2 Site selection and determination of the water flow system

The sites of the study have been described in the Sampling Sites section.

The direction of flow dictates the sequence in which the moving body of water will come into contact with different environs with unique mineral assemblages. The rate of flow is also an important parameter to consider as influences sample collection and type of geochemical model that would be ideal, i.e. a kinetic or equilibrium based model.

3.4.3 Compilation of field and laboratory data

The appropriate data that was obtained through the analysis of field samples was selected. The quality of this data was examined using statistical tests such as the Student's t-test and ANOVA.

3.4.4 Selection of geochemical models

There are several types of geochemical models and the selection of a particular model was based on the goal of the modelling. The types of models are described in greater detail in Chapter Two.

Speciation-solubility models were used to interpret the dispersion of elements within the water bodies shown in Figure 3.15 (incoming water, groundwater flow, surface flow and dam, lake or wetland).

`

Reaction path models and inverse mass balance models were extensively used in this project. The effect of tailings material on incoming water; the generation of pollutants (via dissolution of minerals or redox reactions); the reactions that occur along the flow path of the water bodies (rock-fluid and fluid-fluid interactions) and the reactions that occur when the pollutant enters natural waters (Figure 3.15) can be modelled. Reactions that occur to a pollutant once it is released in the system include dissolution, precipitation, co-precipitation, adsorption, desorption, complexation, redox transformation and ion exchange (Crawford, 1999).

Coupled mass transport models were the ideal models for evaluating the fate and transport of chemical constituents in the environment (Zhu and Anderson, 2002). These models combine transport equations with the models discussed above. A one-dimensional transport model was created for the transport of metal pollutants from a TSF (presented in Chapter Five).

3.4.5 Assemblage of chemical properties

The input for a geochemical model consists of the specific information which describes the system under study (for example the chemical constituents that have been either been analytically determined or hypothesized) and an appropriate database which includes the equations that are used to solve the model (Zhu & Anderson, 2002). The determination of the chemical constituents for the models has been discussed in the Sample Preparation and Analytical Techniques sections of this chapter. Databases include the thermodynamic, kinetic and surface properties that are used in describing chemical reactions. The type of activity coefficient model used is inherent in the choice of database. A discussion regarding the two predominant types of activity coefficient models and the common databases follows. In some instances, adding to or modifying the databases was required. Any adjustments and additions were stated in methodology of the journal article or in the text explaining the model.

`

3.4.5.1 Activity coefficient Models

The equilibrium constant equations that are employed by the modelling code require input of the activity of a species instead of its concentration. The concentration (c_i) and activity (a_i) of the species *i,* are related to one another through the activity coefficient (f_i):

$$a_i = f_i . c_i \qquad (3.5)$$

The activity coefficient should take into account the non ideal interactions of an ion with the solvent and other ions (Nordstrom, 2007). It is dependent on the ion; it is non-linear and varies with the ionic strength of the solution (Merkel & Planer-Friedrich, 2005). In an ideal, infinitely dilute solution, the activity coefficient approaches 1 and the concentration of the species is equal to its activity.

The saturation index (S.I.) of a mineral in the solution of concern is defined as:

$$S.I = \log\left(\frac{IAP}{K_{sp}}\right) \qquad (3.6)$$

where IAP is the Ion Activity Product and K_{sp} is the solubility product constant. Because the calculated activity of an ion is strongly dependent on the choice of method for determining the activity coefficient, the S.I. of a mineral will also depend on the choice of method (Sánchez España & Diez Ercilla, 2008). A positive S.I. value indicates that the mineral is supersaturated in solution and could precipitate from the solution (Zhu & Anderson, 2002).

There are two theories that are widely implemented to calculate the activity coefficient; the ion dissociation theory and ion interaction theory.

The ion dissociation theory and its related methods are based on the original Debye-Hückel equation (Debye & Huckel, 1923). This equation is only valid for solutions up to an ionic strength of 0.005 mol kg^{-1} (Merkel & Planer-Friedrich, 2005) :

$$\log(f_i) = -A . z_i^2 . \sqrt{I} \quad (3.7)$$

`

The factor A is the temperature dependent, empirically derived Debye-Hückel solvent parameter, z_i is the valence (ionic charge) of the species *i* and I is the ionic strength of the solution.

The Debye-Hückel extension includes an additional Debye-Hückel solvent parameter and a factor for the empirically fitted hydrated ion diameter (Nordstrom, 2007). The Güntelberg equation, the Davies equation and the B-dot or "WATEQ" Debye-Hückel equation are modifications of the Debye-Hückel equation (Merkel & Planer-Friedrich, 2005).

The theory of ion interaction is implemented by the Pitzer approach. This is a semi-empirical method that is based on the Debye-Hückel equation and includes virial coefficient polynomial equations (Pitzer, 1973). This method requires a number of parameters (virial coefficients) which have been fitted to allow for the modelling of brines. For example, Harvie and Weare (1980) reported the parameters for the Na–K–Mg–Ca–Cl–SO_4–H_2O system and more recently Accornero and Marini (2009) evaluated the Pitzer parameters for the aluminium species; Al^{3+}, $AlOH_2^+$ or AlO^+, with SiO_2 and CO_2. The Pitzer approach can be used for solutions of ionic strength up to 6 mol kg^{-1} (Merkel & Planer-Friedrich, 2005).

The "WATEQ" Debye-Hückel approach developed by Truesdell and Jones (1974) compares well with the more precise ion interaction (Pitzer) theory for salt water up to an ionic strength of 0.7 mol.kg^{-1} (Nordstrom, 2007) and can be applied for solutions up to 1 mol.kg^{-1} (Merkel & Planer-Friedrich, 2005). Merkel and Planer-Friedrich (2005) showed that these two approaches corresponded well with one another for calcium and sulphate ions as well as for chloride. However, there was significant deviation for sodium and hydrogen ions.

The differences between the two approaches for determination of activity coefficients has been summarised in Table 3.3. In short, the modified Debye-Hückel equations can be used for dilute solutions and there are extensive databases with the Debye-Hückel parameters that are readily available. The Pitzer approach is more complex and requires extensive parameters which might not be

`

readily available but this approach is needed for concentrated solutions. When Pitzer parameters are not available; they can be estimated but the accuracy of the determined activity coefficient will be compromised (Nordstrom, 2007).

Table 3. 3: Comparison of the models for determining ion activity coefficients

Aspect	Ion- Dissociation Approach	Ion-Interaction Approach
Underlying Equation	Debye-Hückel and its modifications	Pitzer equations (unscaled and MacInnes scaled versions)
Considerations (Sánchez España & Diez Ercilla, 2008)	Considers only long range electrostatic interactions	Also takes into account short range interactions by using virial coefficient equations
Ion pair interactions (Nordstrom, 2007)	Quantified explicitly through stability constants	Implicitly quantified through empirical fits with activity coefficient parameters
Ionic strength (Sánchez España & Diez Ercilla, 2008)	Effective ionic strength (I_e) is used (considers ion pairing, therefore always lower than I_s)	Total or stoichiometric ionic strength (I_s) is used (considers elements as free ions).
Application (Nordstrom, 2007)	Dilute waters	Works well for brines
Ionic strength validity (Merkel & Planer-Friedrich, 2005)	Up to 1 $mol.kg^{-1}$ (for WATEQ equation)	Up to 6 $mol.kg^{-1}$
Data Availability (Sánchez España & Diez Ercilla, 2008)	More complete data sets for a number of components and species	Limited parameters have been reported (Fe^{2+}, Ca^{2+}, Mg^{2+}, Mn^{2+}, Ba^{2+}, Sr^{2+}, Na^{+}, K^{+}, Li^{+}, B^{3+}, Cl^{-}, SO_4^{2-} and CO_3^{2-})
Examples of databases	minteq, wateq4f, phreeqc, llnl, thermo, thermo.com.V8. etc	H-M-W and phrqpitz

`

3.4.5.2 Common databases

The common databases that were of use in this project include phreeqc, wateq4f, thermo, thermo.com.V8.R6.230, llnl, minteq and phrqpitz. For clarity, the geochemical codes are written in uppercase (e.g. PHREEQC) and the databases are written in lowercase (e.g. phreeqc). The phreeqc database is similar in content to the wateq4f database (Parkhurst & Appelo, 1999). The difference in these databases lie in their activity coefficient models as discussed in the previous section. The thermo database is the common database for models run in Geochemist's Workbench. The llnl and thermo.com.V8 databases are the same databases but are presented in different formats. The llnl is suitable for PHREEQC whereas the thermo.com.V8 is suitable for Geochemist's Workbench. These databases were developed by the Lawrence Livermore National Laboratory. They are the most extensive databases however there was concerns regarding their internal consistency (Merkel & Planer-Friedrich, 2005). The minteq database is a database available in PHREEQC that was derived from MINTEQA2. This database contains an array of organic ligands and their mass –action equations for complexing metal ions.

3.4.6 Selection of a computer code

This decision is based on the processes that a code can simulate and the relevance of a code's database in terms of availability and accuracy.

The geochemical modelling programmes that were used in this project are PHREEQC Interactive, Geochemists' Workbench and Windermere Humic Acid Model (WHAM). PHREEQC Interactive (PHREEQCI) is free software made available by the United States Geological Survey (USGS) (Parkhurst and Appelo, 2013). Academic licences for Geochemists' Workbench and WHAM were purchased.

PHREEQC is an updated version of the original PHREEQE code developed by Parkhurst et al. (1980). The original PHREEQE code was capable of aqueous speciation, mass transfer and reaction paths while the updated PHREEQC code (Parkhurst & Appelo, 1999) is also capable of adsorption and ion exchange, kinetics, one dimensional transport and inverse modelling (Nordstrom, 2007). A

`

graphical user interface was been developed, PHREEQCI, and this software was used during this project (Charlton et al., 1997).

Geochemists' Workbench is a combination of 5 separate programs (Rxn, Act2. Tact, React and Gtplot) (Bethke, 1994). It has similar capabilities to Phreeqc (Nordstrom, 2007).

3.4.7 Construction of a model

A geochemical model is a combination of the chemical constituent data (the analyses and assumptions), the thermodynamic, kinetic and surface interaction parameter databases and the computer code. When presenting the models in this thesis, an outline of the goals, parameters, database, code and appropriate assumptions will be presented.

3.4.8 Verification and validation of models

Oreskes, Shrader-Frechette & Belitz (1994) suggest that to verify and validate a model in the traditional sense of the words is not possible. They suggest that often modellers use the terms validation and verification incorrectly; either as synonyms when the modeller shows that predictions match observational data or that modellers suggest that valid model is an accurate representation of reality.

Verification demonstrates that the correct modelling formalism was used (Rykiel 1996). To verify a model means that the model has been proven to be "true" (Oreskes, Shrader-Frechette & Belitz 1994). For a model to be proved "true", it should ideally be a closed system. In a closed system, all of the components of the system have been independently determined and are correct. However, models for natural scientific purpose are rarely closed because the input parameters that are required are incompletely known. The parameters are often estimated or applied from a different system (perhaps a smaller scale laboratory experiment). Therefore, the assumptions that are taken in building the conceptual model and the assumptions that are taken in the data collection for a model render the system under study as open (Oreskes, Shrader-Frechette & Belitz 1994). Thus, verification of a model of a natural system would require parameters, mathematical calculations and input data that are absolutely faultless with no assumptions made in the conceptual model. Such criteria are essentially

`

impossible to achieve for a natural system. If verification of a model is attempted, then verification errors are branched into two types namely mechanical errors (which involve debugging and correcting the computer and mathematical codes) and logical errors (which involves assessing the program logic and how accurately the code represents the ideas around which it is built) (Rykiel 1996).

Validation is used to determine if a model is acceptable for its intended use (Rykiel 1996). A validated model is one that performs under specific conditions with a certain level of accuracy that is required for its intended application (Rykiel 1996). Oreskes, Shrader-Frechette & Belitz (1994) suggest that only computer code of a model can be valid if it has no known or detectable flaws. Regarding the model however, the term "valid" cannot be used in description about results. The model itself might have no flaws but the model results might be invalid due to incorrect or insufficient input parameters (Oreskes, Shrader-Frechette & Belitz 1994).

However, we require some manner to determine and discuss whether or not a model is reasonable and provides a reasonable output. Thus, in my opinion, for natural system modelling, the terms "verification" and "validation" have taken on a more relaxed definition than that proposed by Oreskes, Shrader-Frechette & Belitz (1994) and have been used due to a lack of more appropriate terms. Using the approach of Rykiel (1996), it is understood that a validated model is not necessarily the best possible model for the system and a validated model is not expected to be completely truthful regarding the real system which it is simulating. A "valid" model simply performs with a level of accuracy for a specific system under specific conditions. If the conditions of the system change, then the model must be re-validated.

"Validation" can be seen as a means of testing a model. If the performance if a model during validation is not acceptable, then the model can be recalibrated, the accuracy input parameters and data can be investigated and the underlying conceptual model may be revised. Without the process of attempting to validate a model, the quality of the model cannot be determined.

`

There are several techniques that can be used to validate a model. The choice of technique is dependent on the model and on the developer and user. Before the techniques can be discussed, it is important to discuss the categories of validation. The technique of validation will depend on which category of validation is required. Validation can be subdivided into three categories (Rykiel 1996):

- Operational validation: this involves assessing how well the output of a model correlates with observed data. This type of validation does not concern itself with the internal structure of the model (a "black box" validation). Internally, the scientific structure of the model might be incorrect but the model could still give an accurate output. Therefore operational validation does not imply that the internal mechanics of a model are reasonable. However, if operational validation is not possible, then it could imply that there are underlying problems with the model

- Conceptual validation: this involves determining if the structural, mathematical and logical relationships underlying the model are sound. Either there must be scientific explanation for the relationships or reasonable justification for their simplification. A model is built for an intended purpose, so it might be reasonable to exclude some aspects that would lead to unnecessary complications in the model. These exclusions can be justified in this type of validation.

- Data validation: like the model, the data obtained for a system is also only a representation of the real system. The quality of the data and the quality of its interpretation must be assessed. A model might be a better representation of a system in which accumulation of data is hindered by measurement difficulties or in which data is biased by our perception of the system. However, it is unreasonable to expect a model to provide results that are better than input data.

Qualitative methods to test a model's validity include the face evaluations or a more formal Turing test. An expert's opinion might be biased by their preconceived ideas and thus statistical methods for validation are common and

`

cover a variety of tests and applications (Rykiel, 1996). Internal validity can be examined by using a test data set which yields consistent output (Rykiel, 1996).

3.4.9 Interpretation of modelling results

Following an analysis of the validity of a model, the results of the model's applicability of were assessed.

The accuracy of a model is dependent on the quality of the chemical analysis of water and solids, the accuracy and completeness of the database and the applicability of defined reactions and activity coefficient models (Zhu & Anderson, 2002). A model can be continuously improved on by iteratively eliminating assumptions or calibrating the model.

An environmental model is a simplified snapshot of a very complex system. It is not feasible to attempt the description of all of the aspects of the environment in a single model. As such, assumptions are made and with this a degree of uncertainty is inherent. Nevertheless, geochemical models provide useful insight into complex systems.

`

CHAPTER FOUR - EVOLUTION OF METAL POLLUTANTS FROM TAILINGS STORAGE FACILITIES

A metal pollutant that is strongly bound to the waste material is not likely to be as great an environmental concern as a metal that is easily mobilized by rainwater in the short term, however long term release does remain a concern. This chapter explores the combination of analytical techniques such as batch and sequential leaching with geochemical modelling in order to better understand a particular metal's association with the tailings and its subsequent release mechanisms from the material.

The work in this chapter focuses on the evolution of pollutants from an abandoned tailings storage facility. Dissolved metals emanating from active tailings storage facilities were also studied however the work undertaken as those sites have been incorporated into Chapter Five as the studies focused more on the transport of the metals.

Tailings storage facility footprints can pose as great or an even greater environmental risk as complete tailings storage facilities. Oxidation of sulphides occurs on the material of the tailings material because rainwater interacts with this outer surface and oxygen diffusion into the outer edge of the tailings material and not into the bulk material as discussed in Chapter Two- Literature Review. During reprocessing, the outer surface of the tailings is stripped away and fresh, unoxidised tailings material is exposed to the atmosphere. The acid forming, metal releasing reactions which are known to occur for complete, unprocessed TSF will occur on the remaining freshly exposed material.

4.1. Mineralogy of tailings material

An abandoned tailings storage facility located in the Central Rand goldfields was studied. The site has been partially reworked and since neglected. Oxidised and unoxidised tailings material and efflorescent crusts were sampled in the dry season of 2012.

`

Standard powder X-ray diffraction (PXRD) was employed to assess the mineralogy of the material. PXRD patterns are included as Appendix A1 and A2. The standard PXRD method used in this work has a detection limit of approximately 5% (D. Billing, 2012, pers. comm.). PXRD patterns of both oxidized and unoxidised tailings material indicated that the bulk mineralogy was alpha quartz. The patterns also showed a minor presence of an additional mineral phase. This mineral had a greater intensity in the unoxidised tailings material PXRD pattern. The peaks could potentially indicate chlorite-serpentinite ($(Mg,Al)_6(Si,Al)_4O_{10}(OH)_8$) or montmorillonite ($Na_{0.3}(Al,Mg)_2Si_4O_{10}(OH)_2.8H_2O$). However, given the small intensity of these peaks, their low angle occurrence (these peaks carry the greatest error in their position) and that this match is based on very few (two or three) small peaks, it is unlikely that this designation of minerals would be accurate. In the case, PXRD was not useful in determining the association of metal pollutants in the waste material as no mineralogy other than quartz was determined. Therefore, it was necessary to perform batch and sequential leaching studies on the sediments in order to gain insight into the mechanisms of metal pollutant release from the tailings.

4.2. Batch and Sequential Leaching of Tailings Material

The sampled oxidised and unoxidised tailings material was leached using batch and sequential methods. The batch leaching is presented in the paper "*Geochemical modelling of the evolution and fate of metal pollutants arising from an abandoned gold mine tailings facility in Johannesburg*". Sequential leaching using the BCR procedure is presented in the paper "*Fractionation of metals in gold mine tailings: implications for release and mobility to the surroundings*". The results from the sequential leaching were used to generate inverse models of the rainwater and sulphuric acid batch leachates. The inverse models and confirmatory forward models are presented in the third paper for this section, "*Leachability of metals from gold tailings by rainwater: an experimental and geochemical modelling approach"*. For details regarding the theory and methodology of the batch and sequential leaching, refer to Section 3.2.1.

`

4.2.1. Journal article 1: Geochemical modelling of the evolution and fate of metal pollutants arising from an abandoned gold mine tailings facility in Johannesburg

The paper "*Geochemical modelling of the evolution and fate of metal pollutants arising from an abandoned gold mine tailings facility in Johannesburg*" was published in the journal Water Science and Technology (2014, issue 69.5) and is included in the pages that follow. In this paper the batch leaching results of the oxidized and unoxidized tailings material were used to generate inverse geochemical models. The aim of this work was to determine the relative contributions of surface water runoff interacting with oxidized material and infiltrated water interacting with unoxidised material to the geochemistry of the pond water adjacent to the TSF. Prediction models of the fate of the pond water were also included in the paper. The significant achievement within this paper is that it was possible to correlate lab based data (batch leaching) with an environmental water body (the pond) by using geochemical modelling. It was found that the pond water on the site is comprised mostly of rainwater leaching the oxidized tailings with a smaller portion of sulphuric acid leaching unoxidised tailings. PXRD patterns of the tailings material and efflorescent crusts are included in the Appendix as Figures A1 – A15. An example PHREEQC script for the modelling in this work is included in the Appendix as Figure A16.

The author contributions to the work are as follows:

B.P.C. Camden-Smith – analytical work, geochemical modelling, author of paper

H. Tutu – supervisor and project coordinator

The doi reference for the article is 10.2166/wst.2014.028 and can be accessed via the permalink:

http://search.ebscohost.com/login.aspx?direct=true&db=a9h&AN=95030935&site=eds-live

`

4.2.2. Journal article 2: Fractionation of metals in gold mine tailings: implications for release and mobility to the surroundings

The paper "*Fractionation of metals in gold mine tailings: implications for release and mobility to the surroundings*" was submitted in March 2015 to the journal Toxicological and Environmental Chemistry. It is included in the pages which follow and is currently under review. This paper used the BCR sequential extraction scheme to categorise the metals of the tailings material into chemically unique reactive phases; namely 1) water soluble, acid soluble and exchangeable (salts and metal held by exchangeable sites in clays); 2) reducible (associated with oxidised phases such as iron and manganese oxides), 3) oxidisable (associated with organics or sulphides), and 4) residual (associated with unreactive minerals, commonly silicates). This paper formed the basis for the paper "*Leachability of metals from gold tailings by rainwater: an experimental and geochemical modelling approach*" published by WaterSA.

The contributions from the authors to this work are as follows:

B.P.C. Grover – analytical work, interpretation, supervised P. Mthombeni in lab and author of paper

P. Mthombeni – assisted with lab work as part of the undergraduate Chemistry Research Assistance Program

H. Tutu – supervisor and project coordinator

Fractionation of metals in gold mine tailings: implications for release and mobility to the surroundings

B.P.C. Grover, P. Mthombeni and H. Tutu

Molecular Sciences Institute, School of Chemistry, University of the Witwatersrand, Johannesburg, South Africa

Dr Hlanganani Tutu, University of the Witwatersrand, Address: 1 Jan Smuts Avenue, Braamfontein, Johannesburg, South Africa, Telephone: +27 11 717 6771, Email: hlanganani.tutu@wits.ac.za

Fractionation of metals in gold mine tailings: implications for release and mobility to the surroundings

The release of metals from tailings of an abandoned gold mine site near Johannesburg, South Africa, was investigated using sequential chemical extractions. The metals were leached according to their phase partitioning in the tailings. Leaching profiles for aluminum, calcium, cobalt, copper, chromium, iron, magnesium, manganese, nickel and uranium for oxidized and unoxidized tailings were compared. In the former, metals were found to be generally held in water-soluble and reducible (iron oxide) phases due to the oxidation of the tailings while in the latter the metals were found to be generally held in water-soluble, reducible and oxidizable (mostly sulfides) phases. Changes in metal partitioning were found to occur during the oxidation of tailings with elements held in oxidizable phases being transferred to water-soluble phases. The distribution of these metals in the water-soluble phases was found to corroborate their presence in the pond water collected at the site.

Keywords: sequential leaching; metal partitioning; metal mobility

Introduction

The release of low pH, high metal and sulfate water from tailings dumps within the Witwatersrand Basin gold fields has been of environmental concern for some time (Förstner and Wittmann 1979; Naicker, Cukrowska, and McCarthy 2003; Tutu, McCarthy, and Cukrowska 2008). Gold in the basin was discovered in 1886 and the farming community that occupied the land was transformed into a mining community (Durand 2012). After 128 years of nearly continuous mining, the basin has over 270 tailings storage facilities covering an area of 400 km^2 (Oelofse et al. 2007). Currently, the area hosts domestic, agricultural and industrial water users. Long-term exposure to increased metal and sulfate load of the affected ground and surface water could lead to a variety of negative environmental and health implications (Dudka and Adriano 1997; Durand 2012).

The potential release of metal pollutants from solid wastes is of greater environmental concern than their concentration in a bulk medium and this release is dependent on the mineralogy of the waste. However, knowledge of the bulk mineralogy alone does not provide an accurate indication of the potential release of metal pollutants from the waste as metal pollutants could exist in minor minerals that are below standard powder X-ray diffraction (PXRD) detection limits. A metal of interest can be associated with a single mineral phase or a combination of mineral phases. Moreover, the metal could be incorporated into the bulk mineralogy through solid solutions or could be adsorbed onto the surface of minerals such as iron and manganese oxides. The chemical behavior of the minerals hosting a metal affects the potential release of the metal with readily soluble minerals posing a greater threat than slow weathering minerals. Mineral hosts for metals include: water-soluble minerals such as readily soluble salts; acid-soluble minerals such as carbonates; minerals with ion-exchangeable properties such as clay minerals; minerals with potential to adsorb metals such as amorphous or crystalline iron oxides; sulfides and silicates (Leinz et al. 2000).

Batch leaching and sequential extraction methods have been used to characterize the chemical behavior of the mineral hosts of metals in contaminated sediments and waste materials (Rao et al. 2008). The most common sequential extraction methods have been the Tessier method (Tessier et al. 1979) and the Communities Bureau of Reference method (BCR) (Rauret et al. 1999). Modified variants of these methods have also been developed and used successfully (Schultz et al. 1998; Dybowska et al. 2005; Margui et al. 2006).

In this study, the release of metals from a partially reclaimed, abandoned tailings dump in Johannesburg, South Africa was investigated. The study investigated chemical partitioning or fractionation of metals in oxidized and unoxidized gold tailings. This

determined which metals were associated with: soluble minerals; reducible phases such as iron and manganese oxides; oxidizable phases such as organics or sulfides; and residual silicate phases. A modified BCR sequential extraction protocol was used to assess the partitioning and, subsequently, the potential release of metals as well as the changes in metal partitioning as a result of oxidation of gold tailings.

Materials and methods

Sampling

A partially reprocessed and abandoned gold tailings dump located within the Central Rand goldfield of the Witwatersrand Basin (Figure 1) was sampled during the dry season of 2012. This site hosted a tailings dump that was partially reprocessed in 2004. However, due to poor management, the facility was abandoned without further rehabilitation, leaving behind what is commonly termed a tailings footprint. When it rains, leachates drain into a pond adjacent to the footprint before seeping into an adjacent natural stream via shallow groundwater passages.

Oxidized and unoxidized portions of remnant tailings on the footprint were sampled. Oxidized tailings were orange brown while unoxidized tailings were grey in color with the latter being fine grained and more consolidated than the former. The samples were collected into polypropylene bottles using plastic trowels. Samples were air dried at 40°C for 48 h and ground using a pestle and mortar to a grain size less than 0.75 mm.

Water samples were collected from the tailings pond according to accepted methods (Wardencki and Namiesnik 2002). Field measurements including temperature, pH, oxidation-reduction potential (Eh), dissolved oxygen (DO) and electrical

conductivity (EC) were determined using field probes (Thermo Scientific, South Africa). The samples were filtered using 0.45 µm filter paper prior to anion and metal analysis.

Efflorescent crusts occurring between the tailings and the pond were collected and comprehensively characterized in a previous study (Camden-Smith et al. 2013).

Characterization

The mineralogy of the tailings samples was determined using a D2 Phaser powder X-ray diffractometer (PXRD) (Bruker, Karlsruhe, Germany). The samples were treated in two ways, namely: acid dissolution in an Anton Paar Multiwave microwave system (Vienna, Austria) and subjecting them to the BCR sequential extraction protocol (explained later). The metal content was then determined using inductively coupled plasma optical emission spectroscopy (ICP-OES) (Spectro Genesis, Kleve, Germany). The water samples were analyzed for metal and anion (largely sulfate) content using ICP-OES and ion chromatography (IC) (Metrohm 761 Compact Ion Chromatograph, Herisau, Switzerland), respectively.

Sequential extraction experiments

The leaching or extraction solutions as recommended by the BCR extraction scheme were utilized. The BCR extraction scheme was developed by the Standards, Measurements and Testing Programme (formerly the Community Bureau of Reference (BCR)) of the European Commission. The procedure was improved by Rauret and colleagues (1999) by standardizing the volume of acid required in the preparation of the leaching solution in the second step of the extraction. This improved BCR scheme is a popular leaching scheme and has certified reference materials available (Pueyo et al. 2001). The leaching procedure is summarized in Table 1. Solutions were checked

repeatedly in order to ensure that there was adequate exposure of the tailings to the leaching solutions. Samples of the oxidized and unoxidized tailings were prepared in triplicate and empty centrifuge tubes were used as procedural blanks and subjected to the same leaching and cleaning procedures. The samples were centrifuged after each step and metal content in the supernatants was determined by ICP-OES. As no certified reference materials (CRMs) for tailings could be obtained, the BCR 701 lake sediment CRM (Industrial Analytical, South Africa) was used to verify the extraction protocol.

Results

PXRD analysis of the tailings revealed that the bulk mineralogy constituted largely of quartz (SiO_2). Other minerals could not be detected because their peaks were either overshadowed by the silica peaks making it difficult to detect them or they were amorphous. The results for the total metal content in microwave acid-dissolved tailings and the percentage extractions from the BCR protocol are presented in Table 2. Unoxidized tailings were found to contain higher metal contents than oxidized tailings. The reduction was attributed to pyrite (FeS_2) and associated sulfides in the latter being exposed to natural weathering. This weathering process, catalyzed by the bacteria *Thiobacillus ferrooxidans*, is summarized by the following equation (Nordstrom, 1982):

$$FeS_{2\,(s)} + 7/2\ O_{2(aq)} + H_2O_{(aq)} \rightarrow Fe^{2+}{}_{(aq)} + 2SO_4{}^{2-}{}_{(aq)} + 2H^{+}{}_{(aq)} \quad (1)$$

The elevated acidity released (H^+) leads to the subsequent leaching of other constituent elements in the tailings.

Sequential extraction results

Sequential extraction results and certified values for the BCR 701 CRM are presented

in Table 3. The greatest percentage deviation from certified values was observed for the cadmium extracted in the reducible fraction (Step B) in which 5.7 mg kg^{-1} of cadmium was extracted. This was 51% more than the certified value of 3.7 mg kg^{-1}.

The leaching profiles for the major elements in the oxidized and unoxidized tailings are presented in Figures 2 and 3, respectively while those for the minor elements are presented in Figures 4 and 5, respectively.

The majority of aluminum mobilized from the oxidized tailings was released in the first leach step (Figure 2). This step targets the water-soluble, acid-soluble and exchangeable fraction. More aluminum was leached during the first leach step from the oxidized than from the unoxidized tailings (Figure 3). Efflorescent crusts sampled from the same site in another study (Camden-Smith et al. 2013) were found to be predominantly made up of aluminum sulfates. A greater percentage of extractable aluminum was found to be present in the reducible phase of unoxidized tailings and as such was not readily available. Calcium and magnesium were mostly present in a readily soluble phase in the oxidized and unoxidized tailings (Figure 2 and 3). A small percentage of calcium and magnesium was leached from the reducible phase of unoxidized tailings (Figure 3). Iron portrayed a different leaching profile to that of other metals (Figures 2 and 3). Although the iron-bearing efflorescent mineral coquimbite ($Fe_2(SO_4)_3.9H_2O$) was found at the site (Camden-Smith et al. 2013), it appears that the majority of iron present in the tailings was not present as sulfate salts. The reducible iron phase was present in both the oxidized and unoxidized leachates. This iron was in the form of iron oxides. Iron was also leached from the oxidizable phases of both tailings samples and was likely to be associated with sulfide minerals (in particular, pyrite). In the oxidized tailings, sulfur was mainly present in the water-soluble, acid-

soluble and exchangeable form (Figure 2). The crusts collected from the area were all sulfate efflorescent crusts (Camden-Smith et al. 2013). The crusts were readily soluble, making a strong correlation with the high concentration of easily mobilized sulfur in the oxidized tailings. In the unoxidized tailings, sulfur is predominantly present in two forms, namely readily soluble and oxidizable (Figure 3). The readily soluble fraction mobilized in the first leach step was sulfur in the form of sulfate and suggests that the unoxidized tailings could have been partially oxidized or that the sulfates had leached from the oxidized tailings above them. The oxidizable sulfur liberated in the third leach step comes from sulfide minerals. These sulfide minerals give the unoxidized tailings the grey coloration.

Copper exhibited a similar leaching profile to aluminum for the oxidized tailings with most of it found to be present as a readily soluble phase (Figure 4). Similar amounts of total leachable copper were extracted from the oxidized (Figure 4) and unoxidized tailings (Figure 5). The fractionation of copper in the two tailings samples differed, with the unoxidized tailings containing marginally less readily soluble copper and more reducible copper (Figure 5) compared to the oxidized tailings. Cobalt, manganese and nickel portrayed similar leaching profiles (Figure 4 and 5). The majority of extractable cobalt, manganese and nickel present in the oxidized and unoxidized tailings were removed as readily soluble fractions during the initial leach step. Significantly more metals were leached from the unoxidized than from oxidized tailings. This is plausible as oxidized tailings tend to have their metal content depleted over time due to natural weathering and subsequent leaching associated with their oxidation. Unoxidized tailings were found to contain a portion of reducible cobalt, manganese and nickel which was not observed in the oxidized tailings. This leach step

is expected to target metals associated with iron and manganese oxides. As indicated earlier, this fraction could be due to ingress of leachates from oxidized tailings. No uranium was observed to be leached from the oxidized tailings (Figure 4). Uranium in the unoxidized tailings was leached in the first two leach steps (Figure 5), suggesting that it was associated with the readily soluble sulfate and iron and manganese oxides.

In the natural environment, the oxidized tailings are leached by rainwater resulting in readily soluble fractions being washed off into the adjacent tailings pond or nearby wetland. Only a small percentage of aluminum (4% from oxidized and 1% in unoxidized tailings) was leached during the sequential extractions. The majority of aluminum in the samples is held in aluminosilicates, rendering it less readily accessible due to the slow weathering of the silicate minerals. A large amount of the sulfur present in the oxidized tailings (61%) was leached during the sequential extractions.

Pond water analysis

The pond water collected at the tailings footprint had an average pH of 3.7, temperature of 15.7°C, EC of 3.16 mS cm^{-1}, Eh of 0.618 V and a dissolved oxygen content of 8.0 mg L^{-1}. Sulfate and chloride were the only major anions detected, with average concentrations of 3550 mg L^{-1} and 85 mg L^{-1}, respectively. Table 4 presents concentrations of some of the metals determined in the sample. Elevated concentrations of aluminum (209.2 mg L^{-1}), manganese (36.1 mg L^{-1}), nickel (21.5 mg L^{-1}) and zinc (25.0 mg L^{-1}) were obtained while the concentration of iron was relatively low (2.1 mg L^{-1}).

The study by Camden-Smith et al. (2013) showed that the minerals present in the crusts were: alunogen ($Al_2(SO_4)_3.17H_2O$), pickeringite ($MgAl_2(SO_4)_4.22H_2O$), epsomite ($MgSO_4.7H_2O$), coquimbite ($Fe_2(SO_4)_3.9H_2O$) and ($MgFe_4(SO_4)_6(OH)_2.20H_2O$). Traces of cobalt (0.2 – 0.6% of total metal content), copper (0.3- 0.9 %), manganese (0.3-1.2%) and nickel (0.2-0.9%) were found.

Discussion

Metal fractionation changes during oxidation of tailings

In unoxidized tailings, the majority of extractable aluminum is present as a reducible phase (that is, associated with iron and manganese oxides). Upon oxidation of the tailings, the extractable aluminum became associated with a readily soluble phase. The presence of aluminum sulfate containing crusts at the study site suggested that this readily soluble phase is a sulfate salt. In both the unoxidized and oxidized tailings, extractable copper was found to be held in water-soluble, reducible (associated with oxides) and oxidizable (associated with sulfides) phases. During the oxidation of tailings, this copper is transferred into a more soluble phase (likely a sulfate salt). Cobalt, manganese and nickel were held as readily soluble phases in both the unoxidized and oxidized tailings. Higher concentrations of metals were extracted from the unoxidized tailings than the oxidized tailings and this was likely as a result of rainwater percolating through the exposed oxidized tailings, transporting significant proportions of metals to the inner unoxidized tailings. Nickel and cobalt sulfides were oxidized in the final step of the extractions and could have been included into residual pyrite through solid solutions or occurred as individual minerals. The occurrence of water-soluble and oxidizable phases in the unoxidized tailings suggests that the tailings could have been partially oxidized. Only a small amount of iron was readily water-

soluble from both tailings samples. The results for sequential extraction of unoxidized tailings showed that there were comparable proportions of iron oxide and iron sulfide in them, further confirming the possibility of partial oxidation. The orange brown coloration of the oxidized tailings is due to the presence of iron oxide. The findings showed that only 6% and 16% of iron is environmentally extractable from oxidized and unoxidized tailings materials, respectively (Table 2). The rest of the iron is held in phases that are not easily reduced or oxidized. Of the metals studied, only copper showed a significant association with the reducible iron oxide phases in the oxidized tailings.

Mobility of metals from tailings

Metal mobility is dependent on a variety of processes; including dissolution and precipitation reactions, complexation with organic and inorganic ligands, adsorption and desorption by solids (in particular, iron and manganese oxides) and redox reactions (Reeder, Schoonena and Lanzirotti 2006). The mineralogy and association of metals with various mineral phases influence their release. The pH, redox nature, ionic strength and chemical characteristics of a leaching or extraction solution are some of the most important factors determining the rate at which a mineral is saturated with respect to the solution. Sequential extractions have been used to determine the association of metals within various mineral phases of a solid e.g. soil, sediment and tailings. Metals which are leached in the first leach step are easily leachable and could potentially be mobilized with rainwater. Metals leached in the second leach step (reducible fraction) and third leach step (oxidizable fraction) would require more drastic redox changes to mobilize. In the environment, metals associated with the reducible phases (iron and manganese oxides) would require a reducing leach such as an organic-rich waste stream or wetland

stream to be mobilized. On the other hand, metals associated with the oxidizable phase (associated with organics and sulfides) require oxidation to become soluble. Metals associated with the organic fraction that are extracted in the third leach step are generally considered insoluble (Filgueiras, Lavilla and Bendicho 2002). These leach steps can be catalyzed by acid or bacteria in the environment, thereby not requiring as harsh conditions as they would in laboratory experiments in order to release metals. Based on the above sequential extractions, aluminum, cobalt, manganese, nickel and zinc were easily leached from tailings since they were leached in the water-soluble phase of the extractions. These metals were also found to be in high concentration in the pond water that was sampled on the site. Iron was present as a reducible and oxidizable phase in the tailings, suggesting that it was less water-soluble, a phenomenon that was corroborated by its low concentrations in the pond water. The Fe^{2+} released following the oxidation of pyrite (Equation 1), is oxidized during its transport to Fe^{3+} which is precipitated out of solution as a ferrihydrite (nominally $5Fe_2O_3.9H_2O$ with the formula $Fe(OH)_3$ used as a surrogate (Blowes and Ptacek 2003)) according to the following reaction (Nordstrom 1982):

$$Fe^{2+}_{(aq)} + 5/2H_2O + 1/4O_{2\ (aq)} \rightarrow Fe(OH)_{3(s)} + 2H^{+}_{(aq)} \qquad (2)$$

The adsorption of metals on the hydrated ferric oxide mineral surface is a means of natural attenuation for metals and these metals are those identified in the reducible phase of the BCR protocol. The oxidation of the ferrous species to the insoluble ferric species and the subsequent precipitation ferric minerals at the site is likely to have led to a low concentration of iron in the pond water.

Conclusion

Sequential extraction was used to gain insight into the mineralogical phases with which metals in gold mine tailings are associated. These phases were essentially those that

could not be detected using PXRD due to either their low abundance or amorphous nature. Aluminum, copper, cobalt, manganese and zinc were present as water-soluble phases in the oxidized tailings, suggesting that they were likely to be sulfate salts. Sequential leaching revealed that iron leached from oxidized tailings was associated with iron oxides while in unoxidized tailings it was found to be present in oxide and sulfide phases. The iron oxides, formed as a result of precipitation and maturation of iron hydroxides, were found to provide adsorption sites for the other metals, in particular copper, thus a natural attenuation mechanism. Metal partitioning was found to be influenced by the oxidation of tailings, with most of them being transferred to the water-soluble sulfate phase. This was substantiated by the corresponding elevated concentration of these metals in the rainwater runoff pond at the study site. These findings would be important for risk assessment and planning for remediation of contaminants.

Acknowledgements: The authors would like to thank Mr Thuthuka Mabaso for his assistance with ICP-OES and Professor Dave Billing for his assistance with PXRD. The authors acknowledge the advice of Professor Gustaf Olsson and the facilitators at the YWP-ZA Publication Workshop. This work was supported by the US National Academy of Sciences (through the PEER Program) and the South African National Research Foundation.

References

Blowes, D.W., C.J. Ptacek, J.L. Jampor and C.G. Weisener. 2003. "9.05- The Geochemistry of Acid Mine Drainage." In *Treatise on Geochemistry*, edited by H.D. Holland, K.K. Turekian, 149-204. Pergamon: Oxford. doi:10.1016/B0-08-043751-6/09137-4

Camden-Smith, B., R. Johnson, R. Richardson, D. Billing, and H. Tutu. 2013. "Investigating the potential impact of efflorescent mineral crusts on water quality: complementing analytical techniques with geochemical modelling." In *Reliable Mine*

Water Technology, Vol I, edited by A. Brown, L. Figueroa, and C. Wolkersdorfer, 281 - 287. Denver, Colorado, USA: Publication Printers

Dudka, S., and D. Adriano. 1997. "Environmental impacts of metal ore mining and processing: A review." *Journal of Environmental Quality* 26 (3): 590 - 602. doi:10.2134/jeq1997.00472425002600030003x

Durand, J. 2012. "The impact of gold mining on the Witwatersrand on the rivers and karst system of Gauteng and North West Province, South Africa." *Journal of African Earth Sciences* 68: 24-43. doi:10.1016/j.jafrearsci.2012.03.013

Dybowska, A., M. Farago, E. Valsami-Jones and I. Thornton. 2005. "Operationally defined associations of arsenic and copper from soil and mine waste in south-west England." *Chemical Speciation and Bioavailability* 17 (4): 147-160. doi: 10.3184/095422906783438811

Filgueiras, A.V., I. Lavilla, and C. Bendicho. 2002. "Chemical sequential extraction for metal partitioning in environmental samples." *Journal of Environmental Monitoring,* 4(6): 823-857. doi: 10.1039/B207574C

Förstner, U., and G. Wittmann. 1979." Metal accumulations in acidic waters from gold mines in South Africa." *Geoforum* 7 (1): 41-49. doi: 10.1016/0016-7185(76)90056-7

Leinz, R., S. Sutley, G. Desborough, and P. Briggs. 2000. "An Investigation of the Partitioning of Metals in Mine Wastes Using Sequential Extractions." In *Proceedings from the Fifth International Conference on Acid Rock Drainage,* 1489-1499. Littleton, Colorado: The Society for Mining, Metallurgy, and Exploration Inc.

Marguí, E., I. Queralt, M. L. Carvalho, and M. Hidalgo. 2007. "Assessment of metal availability to vegetation (Betula pendula) in Pb-Zn ore concentrate residues with different features." Environmental Pollution 145 (1), 179-184. doi: 10.1016/j.envpol.2006.03.028

Naicker, K., E. Cukrowska, and T.S. McCarthy. 2003. "Acid mine drainage arising from gold mining activity in Johannesburg, South Africa and environs." *Environmental Pollution* 122(1)**:** 29-40. doi: 10.1016/S0269-7491(02)00281-6

Nordstrom, D.K. 1982. "Aqueous pyrite oxidation and the consequent formation of secondary iron minerals." In *Acid Sulfate Weathering*, edited by J.A. Kittrick, D.F. Fanning and L.R. Hossner, 37-56. Madison: Soil Science Society of America

Oelofse, S., P. Hobbs, J. Rascher, and J. Cobbing. 2007. "The pollution and destruction potential of mining waste Witwatersrand: A West Rand Case Study." In *10th International Symposium on Environmental Issues and Waste management in Energy and Mineral Production*, 11-13. Bangkok: Mine Planning and Equipment Selection

Pueyo, M., G. Rauret, D. Luck, M. Yli-Halla, H. Muntau, P. Quevauviller and J.F. López-Sánchez. 2001. "Certification of the extractable contents of Cd, Cr, Cu, Ni, Pb

and Zn in a freshwater sediment following a collaboratively tested and optimised three-step sequential extraction procedure." *Journal of Environmental Monitoring*, 3(2), 243–250. doi: 10.1039/B010235K

Rao, C., A. Sahuquillo, and J. Lopez Sanchez. 2008. "A review of the different methods applied in environmental geochemistry for single and sequential extraction of trace elements in soils and related materials." *Water, Air & Soil Pollution* 189: 291–333. doi: 10.1007/s11270-007-9564-0

Rauret, G., J. Lopez-Sanchez, A. Sahuquillo, R. Rubio, C. Davidson, A. Ure, and Ph. Quevauvillier. 1999. "Improvement of the BCR three step sequential extraction procedure prior to the certification of new sediment and soil reference materials." *Journal of Environmental Monitoring,* 1(1): 57-61. doi: 10.1039/A807854H

Reeder, R.J., M.A.A. Schoonen, and A. Lanzirotti. 2006. "Metal Speciation and Its Role in Bioaccessibility and Bioavailability." *Reviews in Mineralogy and Geochemistry*. 64(1): 59-113. doi: 10.2138/rmg.2006.64.3

Schultz, M., W. Burnett, K. Inn,and G. Smith. 1998. "Geochemical partitioning of actinides using sequential chemical extractions: Comparison to stable elements." *Journal of Radioanalytical and Nuclear Chemistry*, 234 (1): 251-256. doi: 10.1007/BF02389780

Tessier, A., P. Campbell, and M. Bisson. 1979. "Sequential Extraction Procedure for the Speciation of Particulate Trace Metals." *Analytical Chemistry*, 51 (7): 844-851. doi: 10.1021/ac50043a017

Tutu, H., T.S. McCarthy, and E. Cukrowska. 2008. "The chemical characteristics of acid mine drainage with particular reference to sources, distribution and remediation: The Witwatersrand Basin, South Africa as a case study." *Applied Geochemistry*, 23(12): 3666-3684. doi: 10.1016/j.apgeochem.2008.09.002

Wardencki, W. and J. Namiesnik. 2002. "Chapter 2. Sampling water and aqueous solutions." In *Sampling and sample preparation for field and laboratory: fundamental and new directions in sample preparation*, edited by J. Pawliszyn, 33-60. Amsterdam: Elsevier Science B.V.

Titles for Figures:

Figure 1. Modified Google Earth image of the edge of the partially reprocessed gold tailings dump

Figure 2. Major elements leached from oxidized tailings using the modified BCR sequential extraction protocol

Figure 3. Major elements leached from unoxidized tailings using the modified BCR sequential extraction protocol

Figure 4. Minor elements leached from oxidized tailings using the modified BCR sequential extraction protocol

Figure 5. Minor elements leached from unoxidized tailings using the modified BCR sequential extraction protocol

Titles for Tables:

Table 1. The BCR sequential extraction protocol

Table 2. Total metal content in unleached tailings and percentage of metals leached from sequential extractions

Table 3. The BCR 701 CRM certified values compared to experimental values. Standard deviations are calculated for the triplicate experimental values. Concentrations are in mg kg^{-1}

Table 4. Metal content in the pond water sample (concentrations are in mg L^{-1}, analysis performed in triplicate)

Table 1: The BCR sequential extraction protocol

Step	Targeted Phase	Leaching solution	Volume (ml)	Leaching conditions
A	Water soluble, exchangeable and acid soluble	0.11 M acetic acid	40	Overnight at room temperature
B	Reducible (associated with iron and manganese oxides)	0.5 M hydroxylamine hydrochloride	40	Overnight at room temperature
C	Oxidizable (associated with organic material and oxides)	1) H_2O_2	10	1 hour at room temperature, 1 hour at 85°C and then reduced to 3 ml
		2) H_2O_2	10	1 hour at 85°C and then reduced to 3 ml
		3) 1 M ammonium acetate	40	Overnight at room temperature
D	Residual (associated with silicates)	1) Hydrochloric acid	5	Microwave assisted complete digestion with acid regia and hydrofluoric acid (approximately 1.5 hours)
		Nitric acid	2	
		Hydrofluoric acid	1	
		2) Deionised water	<100	Volume made up to 100 ml

Table 2: Total metal content in unleached tailings and percentage of metals leached from sequential extractions

		Al	Cu	Co	Fe	Mn	Ni	S	U
Oxidized Tailings	Total (mg kg^{-1})	23.4	0.032	0.56	18.6	0.23	0.11	4.5	0.19
	Standard deviation	1.5	0.003	0.81	1.0	0.01	0.01	0.4	0.03
	% extracted in sequential leach	4	35	3	6	9	24	61	0
Unoxidized Tailings	Total (mg kg^{-1})	33.4	0.08	0.01	31.7	0.37	0.17	12.1	0.36
	Standard deviation	1.2	0.01	0.002	1.9	0.02	0.01	0.6	0.05
	% extracted in sequential leach	1	13	>100	16	37	34	19	23

Table 3: The BCR 701 CRM certified values compared to experimental values. Standard deviations are calculated for the triplicate experimental values. Concentrations are in mg kg^{-1}

	Cd	Cr	Cu	Ni	Pb	Zn
BCR Step A						
Certified Value	7.3	2.26	49.3	15.4	3.18	205
Experimental Value	8.3	2.6	51	19	3.9	200
Standard deviation	0.1	1.0	3	1	1.0	8
BCR Step B						
Certified Value	3.77	45.7	125	26.6	126	114
Experimental Value	5.7	55	130	31	107	116
Standard deviation	0.1	1	3	2	3	4
BCR Step C						
Certified Value	0.27	143	55	15.3	9.3	46
Experimental Value	0.3	97	48	16	13	35
Standard deviation	0.1	13	6	0.3	4	2

Table 4: Metal content in the pond water sample (concentrations are in mg L-1, analysis performed in triplicate)

	Al	Bi	Ca	Co	Cr	Cu	Fe	K	Li	Mg	Mn	Na	Ni	U	Zn
Sample	209.2	5.9	0.9	11.4	0.5	5.5	2.1	15.4	0.8	203.4	36.1	23.0	21.5	2.8	25.0
Standard Deviation	19.6	0.1	0.0	0.2	0.0	0.1	0.0	0.3	0.0	32.2	2.5	1.0	0.3	0.5	1.7

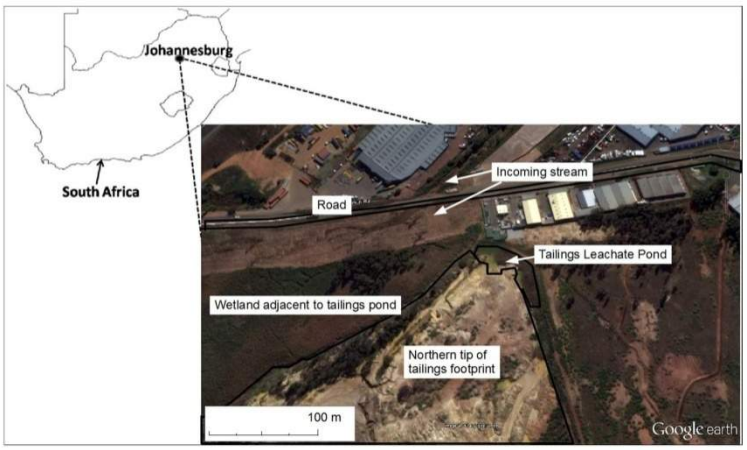

Modified Google Earth image of the edge of the partially reprocessed gold tailings dump
379x225mm (96 x 96 DPI)

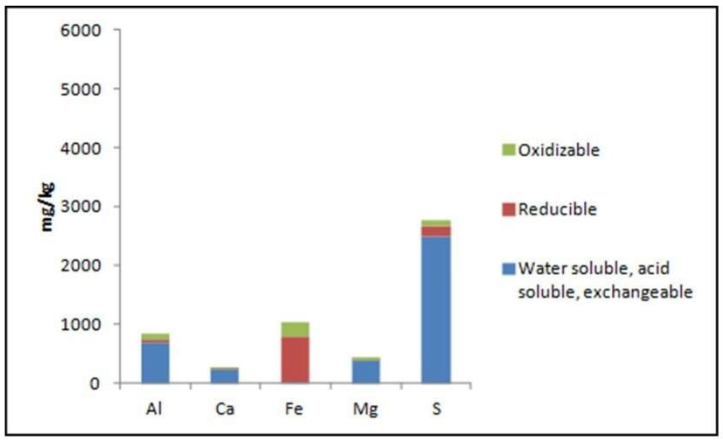

Major elements leached from oxidized tailings using the modified BCR sequential extraction protocol
127x76mm (96 x 96 DPI)

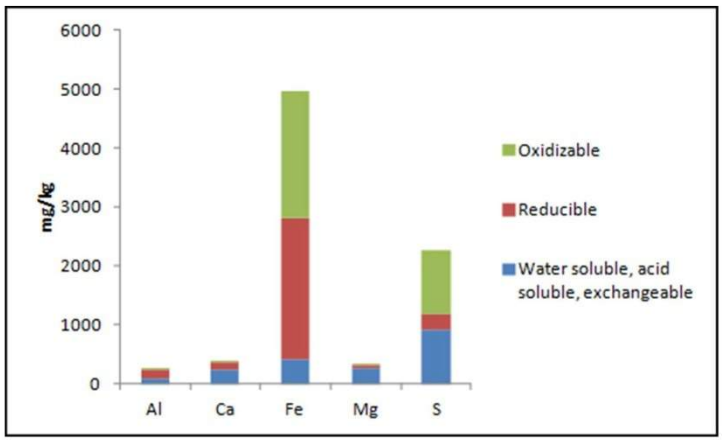

Major elements leached from unoxidized tailings using the modified BCR sequential extraction protocol
127x76mm (96 x 96 DPI)

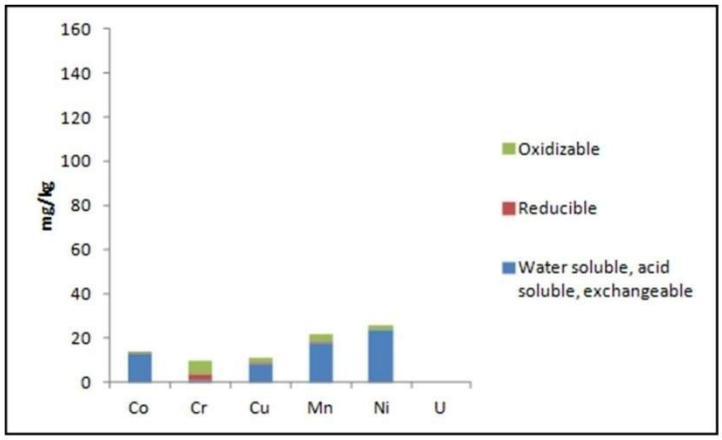

Minor elements leached from oxidized tailings using the modified BCR sequential extraction protocol
127x76mm (96 x 96 DPI)

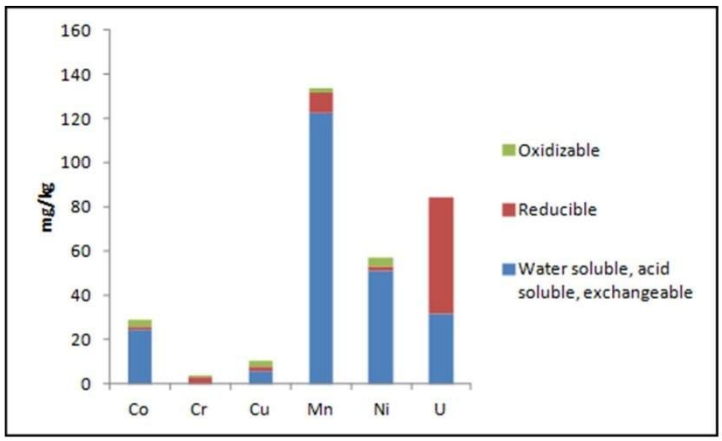

Minor elements leached from unoxidized tailings using the modified BCR sequential extraction protocol
127x76mm (96 x 96 DPI)

`

4.2.3. Journal article 3: Leachability of metals from gold tailings by rainwater: an experimental and geochemical modelling approach

The paper, "*Leachability of metals from gold tailings by rainwater: an experimental and geochemical modelling approach*" was published in WaterSA, January 2016. This paper used inverse geochemical modelling of the rainwater and sulphuric acid leachates to deduce a list of potential reactive minerals. These two particular leachates were considered for this paper as they were deemed important given the results of the paper "*Geochemical modelling of the evolution and fate of metal pollutants arising from an abandoned gold mine tailings facility in Johannesburg"*. One of the most common challenges for inverse modelling is the selection of minerals when setting up the model. The mineralogy used in the inverse models presented in the following paper was deduced from the PXRD as well as the BCR extractions presented in the paper "*Fractionation of metals in gold mine tailings: implications for release and mobility to the surroundings"*. In the introduction to the paper, the bacteria were referred to as *Thiobacillus ferrooxidans,* it was reclassified in 2000 as *Acidithiobacillus ferooxidans*.

The list of reactive minerals can be used in risk assessment models of the site. The pure end members of the minerals as stated in the paper are unlikely to occur as such in the environment. The minerals are more likely to exist as solid solution minerals; however the use of the pure members simplifies the model and its future applications in predicting release from the abandoned TSF.

The contributions of the authors are as follows:

B.P.C. Grover - analytical work, geochemical modelling, author of paper

R.H. Johnson - advisor on geochemical modelling

H. Tutu - supervisor and project coordinator

The article can be accessed via the permalink:

http://ref.scielo.org/2q9rd9

`

CHAPTER FIVE- DISTRIBUTION PATHWAYS OF POLLUTANTS FROM TAILINGS STORAGE FACILITIES: TRANSPORT, DISPERSAL AND FATE

The focus of this chapter is on the water aided transport and dispersal of metal pollutants from tailings storage facilities (TSFs). TSFs are also sites for air and dust pollution and windblown dust from the sites affects the surrounding study regions, as shown in work by Cukrowska et al. (2013), Ojelede et al. (2012), and Wright et al. (2012).

Following their dissolution from tailings storage facilities, metals enter the environment through groundwater and surface water pathways. Surface AMD and groundwater AMD could have different chemistry due to their origin or their subsequent transport mechanisms. For example, surface drainage could originate from leaching the surface and dissolution of salt crusts as compared to groundwater drainage originating from infiltrating acidic water leaching unoxidised material. Surface water is exposed to atmospheric gases whereas groundwater moves slower and interacts to a much greater degree with solid material in the aquifer. Metal content in the released plumes is decreased during transportation due to dilution during mixing with surrounding water bodies, natural remediation (through biotic or abiotic processes), and active or passive treatment facilities. Metals could also be temporarily held during the dry season as efflorescent crusts. These crusts dissolve during the first rain of the wet season and can release an acidic, metal rich pulse into surrounding streams. In the sections which follow the combination of geochemical modelling and analytical techniques was used to study the transport of metal pollutants from TSFs in groundwater systems (Section 5.1), in surface water systems (Section 5.2) and their storage in temporary sinks such as efflorescent crust formations (Section 5.3.1). In order to study the impacts of more permanent sinks, a recently installed AMD treatment plant was studied (Section 5.3.2). This pump-and-treat plant treats underground AMD resulting from the flooding of mined out or abandoned workings in the Central Rand Goldfield. The plant is not treating AMD resulting

`

from TSFs, however the study did allow for comparison of underground AMD resulting from the oxidation of host rock with TSF AMD resulting from the oxidation of waste material. Furthermore, better understanding of the fate of metals from underground AMD through active treatment will be beneficial should TSF AMD be treated in a similar manner.

5.1 Groundwater systems

The groundwater system studied is located in the West Rand Goldfield (West Wits), in a study site referred to as the Vaal site. The TSFs in this area belong to Anglo Gold Ashanti and groundwater plumes from the site affect the Schoonspruit ("spruit" is the Afrikaans term for a stream) and the Vaal River (GCS Pty Ltd, 2011). The geology of the region was introduced in the Methodology (Section 3.1.1.2). A perched aquifer was hosted in weathered dolomite and underlain by Ventersdorp lavas in the western section of the study site. Surface water emanating from the TSF is captured in a 600 000 m^3 emergency dam and treated. Therefore, the main concern at this TSF was the sulphate rich groundwater plumes. Figure 5.1 shows the predicted extent of the sulphate plumes in the region (GCS Pty Ltd, 2011). Plume 1 was studied in this work by analysing water sampled from monitoring boreholes in the site and solid material was sampled at a freshly dug trench adjacent to the facility and at a newly drilled borehole 500 m from the TSF (Figure 5.1). Water samples from three boreholes within plume 3 were also collected.

`

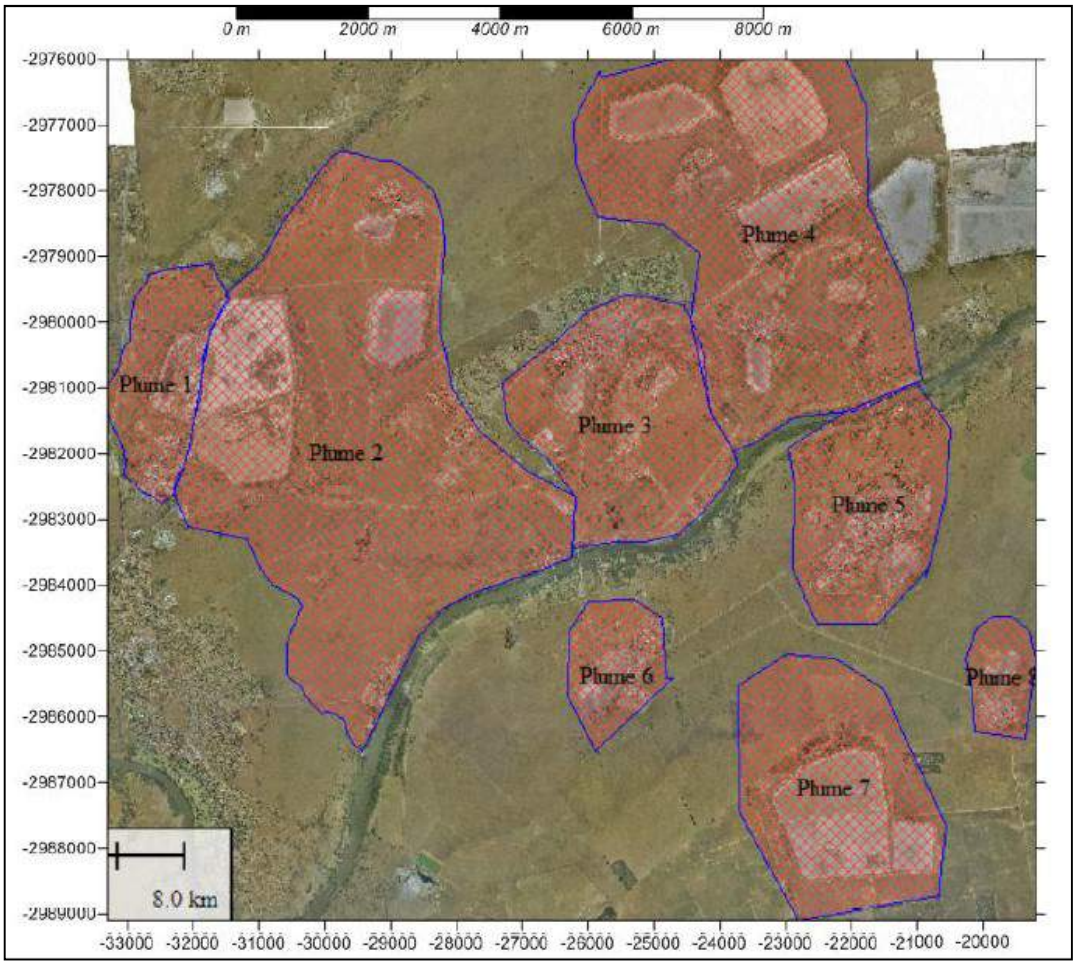

Figure 5.1: Map of sulphate plumes at the Vaal study site. Boreholes in the vicinity of Plume 1 were sampled (Figure extracted from report by GCS (Pty) Ltd, 2011)

In order to study the transport of metals within the plume, speciation-solubility models of the groundwater in plume 1 were compiled and sequential extractions of the solid material were undertaken. The findings of this study are summarized in the IMWA 2014 conference proceedings paper, "*The release and transport of metals arising from gold mining tailings storage facilities in the Witwatersrand, South Africa*" which follows in Section 5.1.1. Additional results are included and discussed in the text following the paper. The insights gained through that work combined with flow data from the GCS (Pty) Ltd (2011) report were used to construct a one dimensional reactive transport model with PHREEQC, presented in Section 5.1.2.

`

5.1.1. Conference proceedings 1: The release and transport of metals arising from gold mining tailings storage facilities in the Witwatersrand, South Africa

This paper was published in the peer reviewed conference proceedings of the 2014 International Mine Water Association Meeting that was held in Xuzhou, China and titled "An Interdisciplinary Response to Mine Water Challenges." The proceedings were edited by W. Sui, Y. Sun and C. Wang and published by the China University of Mining and Technology. Given the condensed nature of the proceedings, additional results and discussion have been included. The paper and the additional work formed the basis for the development of a one dimensional reactive transport model. The paper demonstrates how sequential extractions and speciation-solubility geochemical modelling complement one another in providing insight into the chemical reactions which occur during transport of a metal and sulphate rich solution from a TSF. The PHREEQC script for the geochemical modelling in this section is included in the Appendix as Figure A17.

The contributions of the authors to the work presented in the paper are as follows:

Bronwyn Camden-Smith	– sampling and analytical work, geochemical modelling, supervised P. Mthombeni in the lab, author of the article
Papi Mthombeni	– assisted with lab work as part of the undergraduate School of Chemistry Research Assistantship Program
Raymond H. Johnson	– advisor on geochemical modelling
Isabel M. Weiersbye	– advisor on study site
Hlanganani Tutu	– supervisor and project coordinator

The article can be viewed on the IMWA website at the following link:

https://www.imwa.info/docs/imwa_2014/IMWA2014_Camden-Smith_157.pdf

`

Due to length constraints of the paper, it was not possible to include a full description of the metal partitioning. Additional results and discussion have been included here to provide a more complete description as the results have been used in the compilation of the reactive transport model presented in Section 5.1.2.

The purpose of this study was to assess metal speciation and transport within the plumes emanating from the TSFs using selected borehole data. This study was in no way intended to be a complete assessment of the water quality in the region but was complementary to the regular assessments of the water quality conducted by the mining company. The current transport models for the site (done by consulting companies for the mining company) assumed that sulphate transport was conservative while metal transport was not taken into account.

The BCR leaching procedure allowed for an internal check in which the sum of the analysed components of the three leaches and the residual was compared to the analysis of the unleached material (Table 5.1). The extracted and residual total for calcium, copper, iron, magnesium and manganese were within 10% of the unleached potential of the material. Aluminium had the greatest difference between total potential leached and total leached. Additionally, in the BCR extraction of the solids aluminium values were the most varied with the highest relative standard deviations. Therefore, the aluminium content within the samples was either not homogenous or there were inconsistencies in the samples which led to variation in the analysis of aluminium. For example, aluminium forms hydroxide colloids in solution and during filtration of samples these colloids may be excluded from the solution; pH differences in the samples affects the speciation of aluminium and thus the percentage of aluminium held in colloidal phases would vary.

`

Table 5.1: BCR sequential extraction results for the borehole sample (sampled at 10 m). Values are the average of three replicates and analytical error <10%

	Al	Ca	Cd	Co	Cr	Cu	Fe	K	Mg	Mn	Ni	Zn
	g kg^{-1}	g kg^{-1}	g kg^{-1}	g kg^{-1}	g kg^{-1}	g kg^{-1}	g kg^{-1}	g kg^{-1}	g kg^{-1}	g kg^{-1}	g kg^{-1}	g kg^{-1}
BCR A	0.03	2.34	<0.01	<0.01	<0.01	<0.01	<0.01	0.07	1.04	0.03	<0.01	<0.01
BCR B	3.33	4.54	<0.01	0.03	0.01	0.01	6.08	0.07	3.01	1.54	0.03	0.02
BCR C	4.06	0.12	<0.01	0.01	<0.01	0.01	7.42	0.04	3.33	0.06	0.02	0.02
Residual	58.61	1.15	0.02	0.01	0.05	0.15	91.56	12.63	11.79	0.25	0.16	0.10
Total from extracted	**66.02**	**8.16**	**0.03**	**0.05**	**0.06**	**0.18**	**105.1**	**12.81**	**19.17**	**1.88**	**0.21**	**0.14**
Total from unleached	**80.02**	**7.53**	**0.01**	**0.07**	**0.08**	**0.17**	**105.4**	**15.95**	**20.93**	**1.91**	**0.16**	**0.12**

Results for the sequential extraction of the sediments adjacent to the TSF and 500 m from the TSF in the sulphate plume are summarised in Figures 5.2-5.8. Each figure is comprised of 2 bar graphs. The graph on the left refers to the partitioning in sediments collected from a freshly excavated pit close to the TSF and the graph on the right refers to the partitioning in the sediments obtained during drilling of a research borehole 500 m from the TSF within the predicted plume.

Extractable aluminium was not present in a readily soluble phase except for a small percentage in the lower region of the pit close to the TSF (Figure 5.2). Aluminium partitioning is evenly distributed between reducible (associated with iron or manganese hydroxides) and oxidisable (associated with sulphides or organics) phases (Figure 5.2).

In the upper section of the pit adjacent to the TSF, calcium was mostly partitioned into the water soluble, exchangeable or acid soluble phase (6.0 mg kg^{-1}) (Figure 5.3). In this section calcium was associated with carbonate minerals such as calcite or dolomite or associated with sulphate minerals such as gypsum. The high percentage of sulphate in the readily soluble fraction (water soluble, acid soluble or exchangeable) supports the presence of gypsum. The lower section of the pit was within the water table. In the lower section of the pit, calcium was associated with the reducible phase of the material. The presence of dolomite is expected

`

given the geology of the area, however grains might be coated with iron hydroxide and the calcium rich core would only be leached following the dissolution of the iron hydroxides in the reducible leach step. This could explain the high calcium content in the reducible phase; alternatively calcium was adsorbed onto the iron hydroxides. Extractable calcium within the borehole samples taken within the plume was distributed between a readily soluble phase (1.9 – 2.7 mg kg^{-1}) and reducible phases (4.5 – 5.8 mg kg^{-1}). The dissolution of calcite and precipitation of gypsum within the same water body was also observed by Sracek et al. (2010) and summarised as the following reaction :

$CaCO_3$ (s) + $2H^+$ + SO_4^{2-} + $2H_2O$ → $CaSO_4.2H_2O$ (s) + H_2CO_3 … (reaction 5.1)

Copper was evenly distributed between the reducible and oxidisable phases (Figure 5.4).

Magnesium was present in all three of the leachable BCR phases in the lower pit sample and in the borehole samples (Figure 5.5). Magnesium is not present in the reducible and oxidisable phases in the upper pit section.

Extractable manganese was largely associated with the reducible phase (Figure 5.6). This phase likely contained manganese in an oxidised form analogous to iron oxides/hydroxides or manganese was included into or adsorbed onto iron oxides/hydroxides. Adjacent to the TSF, a small amount of manganese (0.1 – 0.3 mg kg^{-1}) was readily soluble whereas further from the facility, manganese was not readily soluble. The amount of manganese leached from the borehole solid samples in the plume increased with depth.

Extractable nickel from the pit adjacent to the TSF had different partitioning in the upper and lower sections (Figure 5.7). In the upper section it was mostly associated with the oxidisable fraction (0.1 mg kg^{-1}, 34% of total Ni). In the lower, wet section of the pit nickel was associated largely with the reducible section (0.06 mg kg^{-1}, 26% of total Ni). In the borehole samples taken in the plume 500 m from the TSF, the nickel concentration shows no variation with depth and was evenly distributed between reducible and oxidisable fractions.

`

Adjacent to the TSF, extractable zinc was partitioned in all three of the extractable phases (Figure 5.8). More zinc was leached from the sediments in the lower section of the pit than in the upper section. In the borehole samples, zinc showed a similar trend to nickel in that it was near evenly distributed between the reducible and oxidisable fractions.

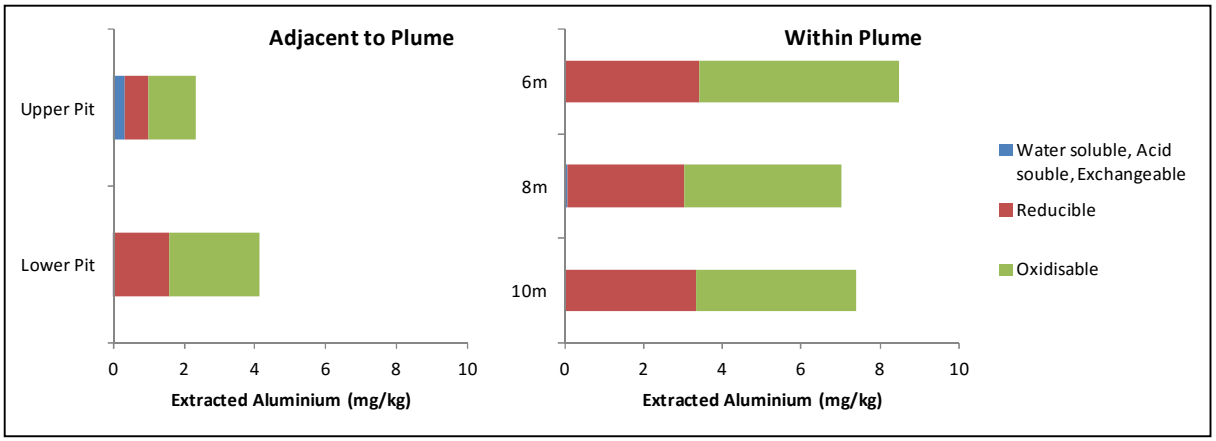

Figure 5.2: Aluminium partitioning in sediments impacted by underground AMD plume

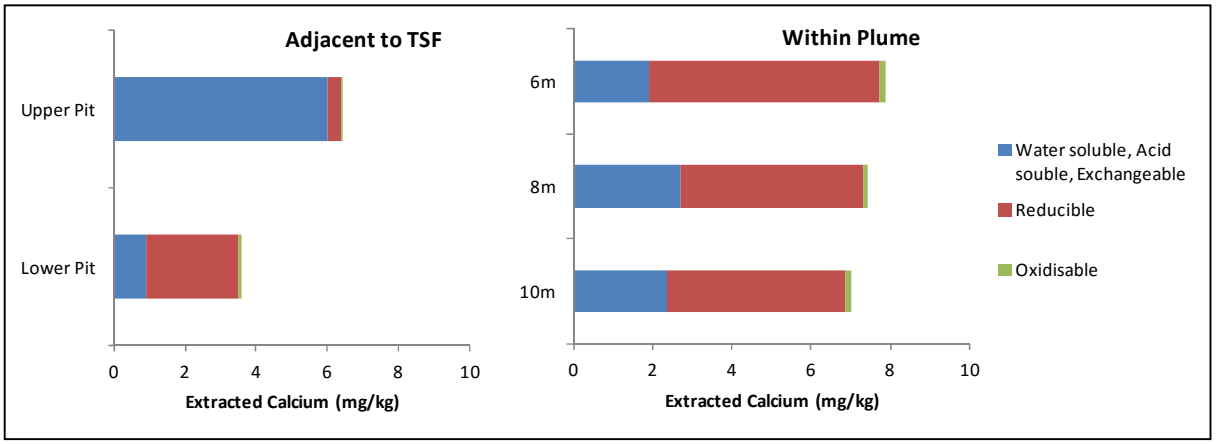

Figure 5.3: Calcium partitioning in sediments impacted by underground AMD plume

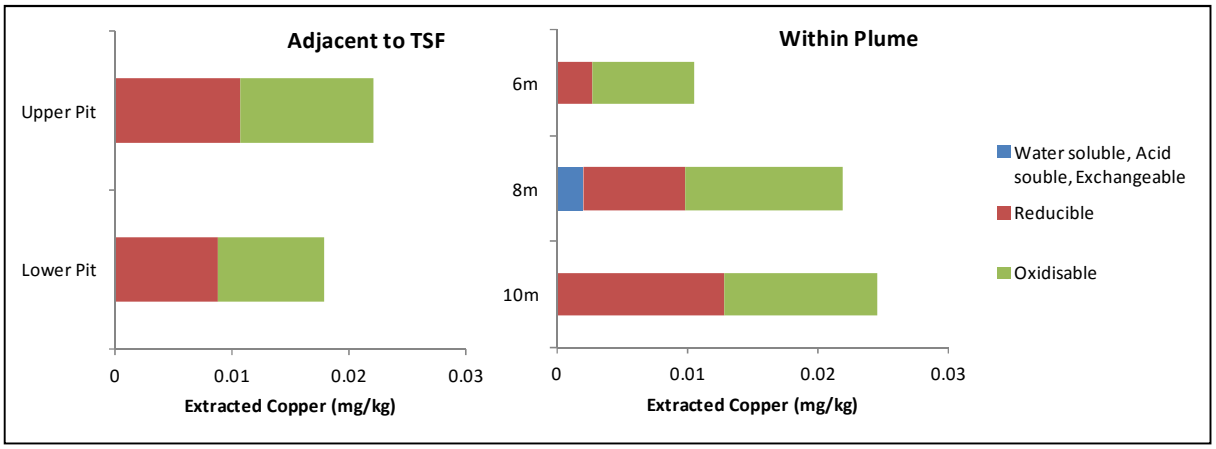

Figure 5.4: Copper partitioning in sediments impacted by underground AMD plume

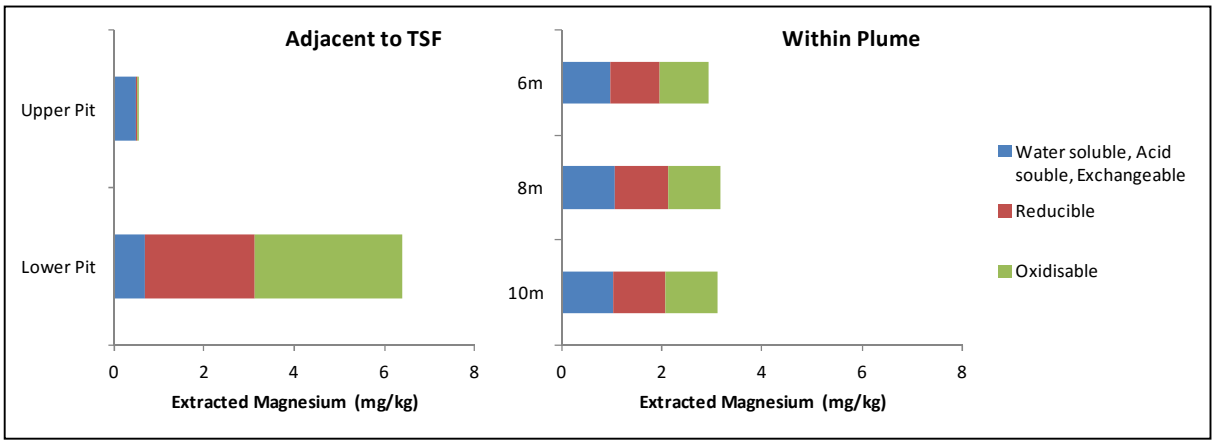

Figure 5.5: Magnesium partitioning in sediments impacted by underground AMD plume

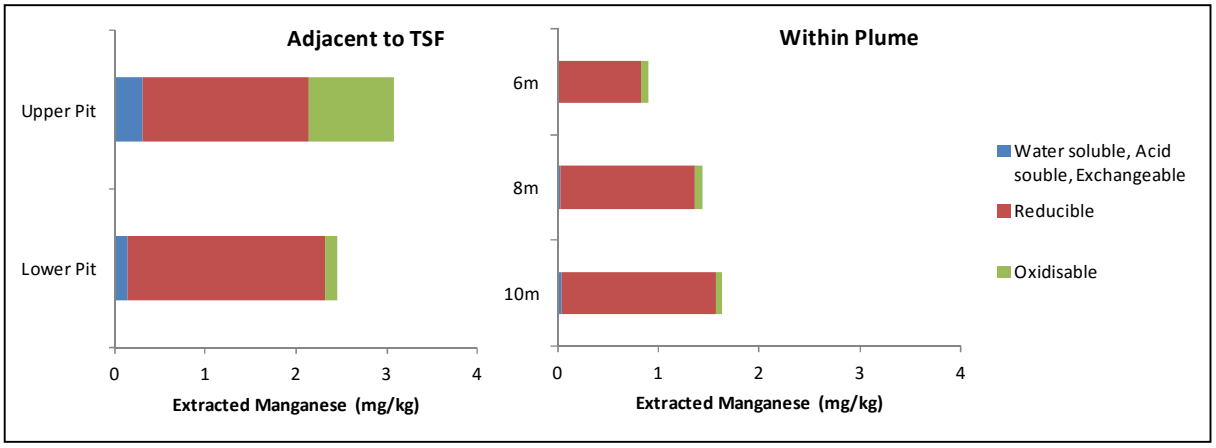

Figure 5.6: Manganese partitioning in sediments impacted by underground AMD plume

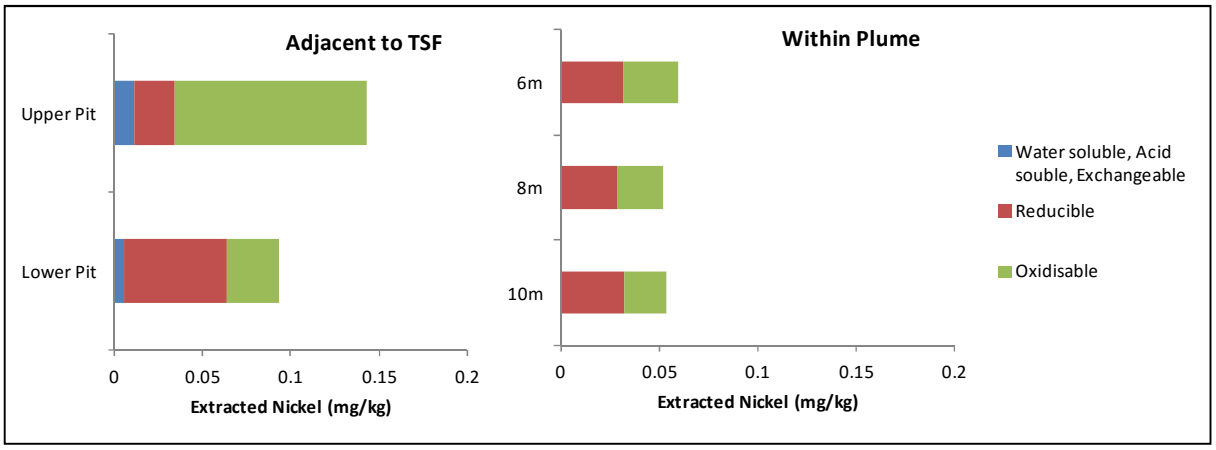

Figure 5.7: Nickel partitioning in sediments impacted by underground AMD plume

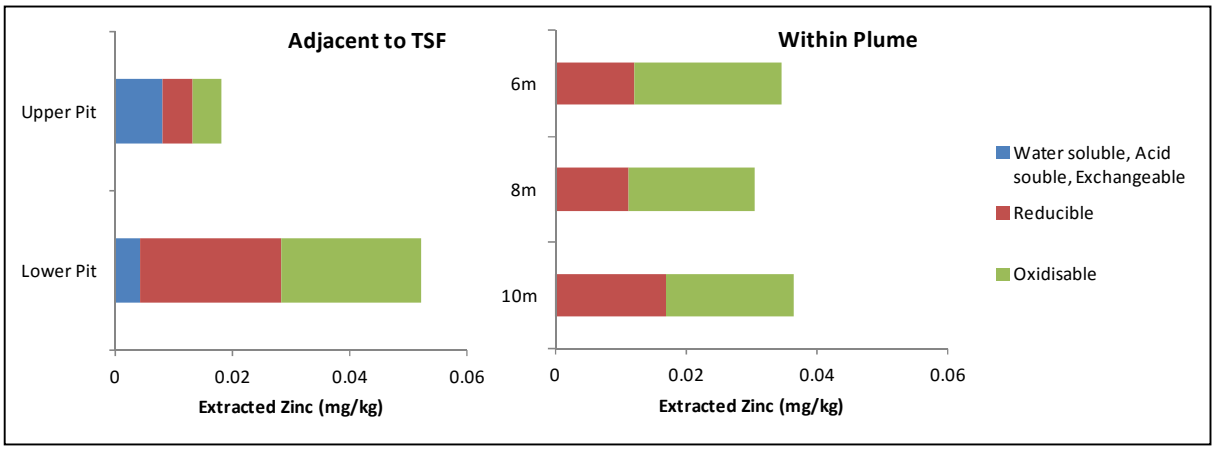

Figure 5.8: Zinc partitioning in sediments impacted by underground AMD plume

The IMWA conference paper, *"The release and transport of metals arising from gold mining tailings storage facilities in the Witwatersrand, South Africa"* included water analyses for two of the boreholes sampled. The one borehole (termed Borehole A in the publication) was situated close to the TSF, near to the freshly excavated pit. The second borehole (termed Borehole B in the publication) was the same borehole from which the solid samples were taken from at the beginning of the dry season. Seven other boreholes were sampled during the same trip (see Figure 5.9 and Figure 5.10 which are smaller scaled versions of the map included in the sampling site description in Section 3.1.1.2).

`

Three transects were sampled. Boreholes A, B and C sample the plume emanating from the facility towards the north (Figure 5.9). Boreholes D, E and F form a second transect going east towards the Schoonspruit (Figure 5.9). The position of the pit close to borehole A is also shown in Figure 5.9. Boreholes G and H were on the northern and southern respective ends of a tailings footprint situated adjacent to a land fill site and borehole I was situated to the south of this footprint (Figure 5.10). The boreholes were closed and locked except for boreholes C and E. Borehole C had a rusted casing and was open; hence it was excluded from the IMWA publication. Borehole E was in better condition but was also open and unlocked and was beginning to rust. The open boreholes are more likely to be diluted by rainfall or contaminated by human activities.

Field measurements of water samples included temperature, pH, Eh, conductivity and dissolved oxygen (summarized in Table 5.2). The pH was found to increase with increasing distance away from the TSF, as noted in borehole sets A, B and C and D, E and F. The Eh, on the other hand, remained approximately constant. It is important to note that the field measurements were taken in the sample bottle as *in situ* measurements were not possible. Therefore, Eh and dissolved oxygen concentrations could be affected by interaction of the sample with atmospheric oxygen. Efforts were made to minimize this interaction including carefully decanting the sample into the sample bottle and by taking field measurements shortly after collection. The depth at which the water table was intersected during sampling is also included in Table 5.2. The water table was closer to the surface near to the TSF (boreholes A and D) and was intersected deeper in boreholes further away from the TSF (boreholes C and F). Conductivity of the samples obtained close to the TSF were higher than samples further away from the TSF, the greatest being borehole A with 8.33 $mS.cm^{-1}$. There was no distinct trend observed in the alkalinity determinations of the samples.

`

Figure 5.9: Boreholes sampled for water at the end of the dry season at the active western TSF situated in plume 1. Solid sampling was undertaken at Pit and Borehole B.

Figure 5.10: Boreholes sampled for water at the end of the dry season at the eastern TSF footprint situated in plume 3.

`

Table 5.2: Field measurements and alkalinity determinations of borehole samples from plume 1 and plume 3

Borehole	Depth	Temperature	pH	Eh	Conductivity	Dissolved Oxygen	Alkalinity
	m	°C		mV	mS cm^{-1}	mg L^{-1}	mg $CaCO_3$ L^{-1}
A	2.50	21.0	4.01	391	8.33	2.10	nd
B	7.57	22.1	6.67	400	3.93	3.07	148
C	8.21	22.4	7.76	402	1.88	2.02	226
D	2.35	19.5	5.73	395	5.69	2.70	62
E	6.49	20.7	6.07	391	1.63	2.79	21
F	7.27	22.0	7.47	397	3.25	6.22	169
G		23.5	6.70	403	4.31	2.68	296
H		22.8	7.47	405	2.20	3.40	34
I		22.7	6.88	403	2.85	1.44	250

nd = not determined

Table 5.3 includes the ion chromatography and ICP-OES analytical results of the borehole samples. Borehole water close to the TSF showed elevated concentrations of sulphate (5065 mg L^{-1} in borehole A and 3442 mg L^{-1} in borehole D). Sulphate concentrations were lower in the plume. The open boreholes C and E had considerably lower sulphate, calcium and magnesium values than the other samples within the plume. This could be due to dilution by rainwater through surface flow. The high iron value in borehole E could be attributed to the newly rusted borehole casing. A general observation regarding the data presented in Table 5.3 for the plume to the west (boreholes A, B and C and boreholes D, E and F) was that as distance from the tailings increased, the metal content within the plume decreased. Aluminium was present only in borehole A and not detected elsewhere. Cobalt, manganese, magnesium, nickel, potassium, sodium and zinc were in higher concentrations in borehole A and borehole D than elsewhere in plume 1.

From these analyses, it was ascertained that solute transport in the region does not appear to be conservative. The construction of speciation-solubility models aimed to provide insight into the reactions which transform the water chemistry during transport away from the TSF.

`

Nitrate concentrations were higher in boreholes G, H and I than in the other samples (Table 5.3). These samples were taken from a tailings footprint that was adjacent to a landfill, a likely nitrate source. Although the tailings had largely been removed from the site; the presence of sulphate and minor concentrations of manganese, nickel and zinc indicated that the water quality beneath this facility was still compromised; either by leaching of the landfill or remnant tailings material or a combination thereof.

`

Table 5.3: Anion and metal concentrations within borehole samples from plume 1 and plume 3

Borehole	Analysed concentrations (mg L^{-1})													
	Cl	NO_3	SO_4	Al	Ca	Co	Cu	Fe	K	Mg	Mn	Na	Ni	Zn
A	425	15	5065	52	605	6.2	0.4	7.5	52	640	322	705	7.9	3.6
B	230	BDL	2202	BDL	640	0.3	0.1	0.0	12	393	1.8	63	BDL	BDL
C	183	BDL	431	0	66	0.1	0.0	0.1	20	166	0.3	43	BDL	BDL
D	336	BDL	3442	BDL	603	0.1	0.1	3.5	18	559	162	300	1.2	0.2
E	106	BDL	655	0	134	BDL	0.1	7.0	5	136	0.5	28	BDL	BDL
F	140	3	1761	BDL	626	0.1	0.1	0.1	7	290	0.7	38	BDL	0.0
G	140	38	2278	BDL	813	0.5	0.1	BDL	38	224	8.6	225	0.5	2.1
H	147	12	796	BDL	133	BDL	0.1	BDL	16	103	0.3	148	BDL	BDL
I	143	19	1151	BDL	401	0.5	0.1	BDL	21	124	0.0	155	BDL	BDL

BDL = Below Detection Limit

`

Speciation-solubility models of the borehole water samples were compiled in PHREEQC using the LLNL database. Table 5.4 summarises the charge balances and the saturation indices that were close to zero for each sample. The reported values in Table 5.4 are for solutions modelled in chemical equilibrium; this was achieved by running a “mix” function of each sample. For the reactive transport model, the modelling approach used by PHREEQC assumes chemical equilibrium and this step would be the first step undertaken. Therefore, using the “mix” function upfront allows the modeller to better understand the saturation states of the solutions used in the reactive transport model.

The charge balances are an indication of the accuracy of the chemical analyses (Freeze and Cherry, 1979; Zhu and Anderson, 2002). A positive charge balance indicates that there was an abundance of cations in the analysis and a negative charge balance indicates an abundance of anions. A large absolute charge balance could potentially indicate that an abundant species was not included in the analysis. In this case, the charge balances are of an acceptable level (< 15 %) with the exception of borehole H (charge balance of 18.1%, Table 5.4). Organic ligands and cyanide were not quantified during the analyses.

Minerals that were in equilibrium with the solutions were identified by their saturation indices being close to zero (Table 5.4). These minerals could have potentially been precipitating from the solution or been in a great enough abundance in the solid material that the solution could dissolve enough of the mineral to reach equilibrium. This list does not include all the minerals that impact the chemistry of the groundwater. Minerals in a low abundance in the solid material may dissolve but the saturation index will remain negative as there was not enough of the mineral present for equilibrium to be reached. These minerals could not be determined as easily as the minerals with saturation indices close to zero. Close inspection of saturation indices could be used and inverse modelling could be useful should quantification of the minerals be required.

`

Table 5.4: Charge balance and selected saturation indices of borehole water samples

Borehole	Charge Balance	Saturation Indices					
		Calcite	Diaspore	Dolomite	Gypsum	$Fe(OH)_3$	Magnesite
A	8.8		0.08		0.06	-0.50	
B	14.7	-0.16		-0.76	-0.05	-0.34	-0.68
C	2.2	0.35	2.21	2.46	-1.36	0.51	0.46
D	11.4	-1.63		-3.53	0.00	1.19	-1.98
E	11.9	-2.31	2.72	-4.89	-0.82	1.70	-2.66
F	18.1	0.71		0.86	-0.09	0.18	0.07
G	11.0	0.25		-0.29	0.08		-0.62
H	-1.4	-0.50		-1.35	-0.81		-0.93
I	5.7	0.17		-0.39	-0.32		-0.64

A concern with the inspection and interpretation of changing saturation indices for metal transport was that the dilution effect of infiltrating rainwater was not taken into account. This is a valid concern as the sediments overlying the aquifer were fractured dolomite (GCS Pty Ltd, 2011). In order to estimate the amount of infiltrated water an inverse model was compiled.

The chemistry of the infiltrating rainwater for the inverse model was approximated by defining the rainwater used in the leaching experiments and equilibrating it with atmospheric oxygen and carbon dioxide. The solution was then equilibrated with dolomite (the model calculated that 8.4×10^{-5} mol of dolomite per litre was dissolved, this equates to 16 mg per litre). The final pH of the modelled infiltrated rainwater was 9.88, the pe was 11.21 and the charge balance was 6.7%.

The PHREEQC inverse model was set up as follows (refer to the script in Figure 5.11):

`

- In step 1, the solutions for boreholes A and B were defined. Metals that were in low concentration were excluded in order to minimize the amount of phases needed.
- In step 2, the “mix” function was applied as in previous cases.
- In step 3, the infiltrating rainwater solution was estimated as described above.
- In step 4, the inverse model was defined. The infiltrating rainwater and borehole A solutions were defined as the initial solutions and borehole B as the final solution. The minerals that were identified in the speciation-solubility models were defined as phases. Additional phases were required for the balancing of metals (Al, Cu, Mn, Ni, and Zn) defined in the initial solution. Hydroxide phases were selected as it was possible that these metals would interact with iron hydroxide surfaces either through solid solution or surface adsorption. Halite was also included as a phase. Potassium, lithium, sodium and chloride were set as balances. Due to the unknowns in this run, such as rainwater chemistry, the uncertainties were set very high (0.3, 0.4 and 0.5, respectively). Using these uncertainties, the models of the solutions were able to converge. While such high uncertainties were not ideal, they helped in making the model to provide an insight into the extent to which rainwater might be infiltrating the system.

`

```
# Step 1) Defining initial borehole solutions

SOLUTION_SPREAD
    -temp      22
    -units     mg/l
 Description       pH        pe  O(0)          Alkalinity         Cl     S(6)      Al       Ca      Co      Cu      Fe      K        Mn     Na       Ni     Zn      Mg     Number
                                                as Ca0.5(CO3)0.5
           A      4.01    6.6079   2.1                           425     5065    51.8      605    6.16    0.42     7.5    52.2     321.5    705    7.935    3.6     640          2
           B      6.67      6.76  3.07                   148     230     2202             639.5   0.295   0.085   0.025     12   1.7925   62.5                    393          3

END

# Step 2) Mixing borehole solutions for chemical equilibrium

MIX 1
    2    1
SAVE solution 5
END

MIX 2
    3    1
SAVE solution 6
END

# Step 3) Estimating the infiltarting rainwater solution.

EQUILIBRIUM_PHASES 1
    O2(g)     -0.7 10
    CO2(g)    -3.5 10
SOLUTION_SPREAD
    -units     mg/l
     Description          Number   pH       pe     Temperature      Cl     S(6)     Ca      K      Mg      Na
 Rainwater Leach               4  4.3     7.34           19.5     2.5      3.5    1.0     2.8     0.1     0.3

SAVE solution 7
END

USE solution 7
EQUILIBRIUM_PHASES 2
    Dolomite  0 10

SAVE solution 8
END

# Step 4) Compiling inverse model with infiltarting rainwater and borehole A as initial solutions

INVERSE_MODELING 1
    -solutions     8        5        6
    -uncertainty   0.3        0.4      0.5
    -phases
        Dolomite
        Calcite
        Gypsum
        Fe(OH)3(a)
        Magnesite
        Diaspore
        Pyrochroite
        Ni(OH)2
        Zn(OH)2-a
        Cu(OH)2
        Kaolinite
        Quartz
        Halite
    -balances
        Cl          0.9      0.2      0.2
        K           0.9      0.2      0.2
        Li          0.9      0.2      0.2
        Na          1        0.7      0.7
    -minimal
    -tolerance         1e-10
    -mineral_water     false
    -multiple_precision     true
    -mp_tolerance 1e-12
    -censor_mp 1e-20
END
```

Figure 5.11: Input for inverse model between borehole A with infiltrating rainwater and borehole B

Six inverse models were proposed. Table 5.5 summarises the mineral transfers in the models. In inverse models 1 and 2, the ratio of infiltrating rainwater to borehole A required to make one unit of borehole B solution was 0.70 to 0.30. For inverse models 3-6, this ratio was 0.68 to 0.32. Minerals with a positive quantity have dissolved into solution and minerals with a negative quantity have precipitated from solution.

In all of the inverse models, the hydroxide minerals ($Fe(OH)_3$, diaspore, pyrochroite, $Ni(OH)_2$ and $Zn(OH)_2$) precipitate from solution (Table 5.5). There was a decrease in the concentration of the metals within this range of hydroxides from the TSF to the borehole (Table 5.3).

The inverse models predicted the dissolution of carbonate minerals. Inverse models 1 and 2 predicted the dissolution of magnesite ($MgCO_3$), models 3 and 4

`

the dissolution of calcite ($CaCO_3$) and models 5 and 6 the dissolution of dolomite ($CaMg(CO_3)_2$). The dissolution of magnesite in models 1 and 2 did not allow for a related increase in the calcium content, resulting in the prediction of dissolution of a relatively large amount of gypsum (11.4 mmol). Given that the geology of the aquifer is dolomite rich, the magnesite and calcite dissolution models were discarded as base models for the construction of the one dimensional reactive transport model.

Models 1 and 2 predicted the same amounts of carbonate and hydroxide mineral dissolution and precipitation. However, they differ in the behaviour of diaspore, kaolinite and quartz. Model 1 accounts for the absence of aluminium and silica in borehole B by precipitating kaolinite and dissolving quartz whereas model 2 allows for the precipitation of diaspore with no dissolution or precipitation of silicates. The same observation was noted in models 3 and 4 as well as models 5 and 6.

These results are a direct product of the selection of minerals for inverse models. It was possible that choosing different minerals would have yielded a completely different set of inverse models. The use of sequential extraction of solid material provided some insight into which type of minerals could be selected for inverse modelling. However, the choice of minerals remains at the discretion of the modeller and therefore carries the potential for significant error.

`

Table 5. 5: Results of inverse modelling between borehole A with infiltrating rainwater and borehole B

Mineral	Formula	Inverse Models (mineral amounts in mmol/l)					
		1	2	3	4	5	6
Calcite	$CaCO_3$			4.31	4.31		
Diaspore	AlOOH		-0.57		-0.62		-0.62
Dolomite	$CaMg(CO_3)_2$					2.16	2.16
$Fe(OH)_3(a)$	$Fe(OH)_3$	-0.04	-0.04	-0.04	-0.04	-0.04	-0.04
Gypsum	$CaSO_4.2H_2O$	11.43	11.43				
Halite	NaCl	1.88	1.88	1.66	1.66	1.66	1.66
Kaolinite	$Al_2Si_2O_5(OH)_4$	-0.29		-0.31		-0.31	
Magnesite	$MgCO_3$	4.09	4.09				
$Ni(OH)_2$	$Ni(OH)_2$	-0.04	-0.04	-0.04	-0.04	-0.04	-0.04
Pyrochroite	$Mn(OH)_2$	-1.72	-1.72	-1.85	-1.85	-1.85	-1.85
Quartz	SiO_2	0.57		0.62		0.62	
$Zn(OH)_2$ (a)	$Zn(OH)_2$	-0.02	-0.02	-0.02	-0.02	-0.02	-0.02

The inverse modelling was rerun using only the major metal concentrations; Al, Ca, Fe, K, Na and Mg. The metals arising from the AMD input and that were likely to interact with the iron hydroxide precipitates were excluded (Co, Cu, Mn, Ni, Zn). Similar models to the six described above were yielded. The quantities of calcite, diaspore, dolomite, $Fe(OH)_3$, gypsum, halite, kaolinite, magnesite and quartz were the same as those in Table 5.5.

5.1.2 One dimensional reactive transport model of a metal and sulphate plume emanating from an active TSF

A one dimensional reactive transport model was developed for the Vaal site described in Section 5.1.1. The aim of this model was to describe the chemical reactions that have occurred within the plume since the introduction of AMD into the plume. The model outputs were compared to the analysed concentrations at Borehole B to determine how well the model performed.

A simple reactive transport model could later be modified to provide a more accurate description of the site and additional sampling could allow for calibration

`

and testing of the model. Furthermore, it can be used for hypothetical studies such as the installation of permeable reactive barriers or the inlet of alternative solutions (for example, municipal waste).

5.1.2.1 Input considerations

The model was iteratively built up from a flow path that dissolved dolomite and precipitated metal hydroxides (model A) to a model which contained reactive surfaces (model B) and exchange sites (model C). The results of the individual iterations are presented and a discussion regarding their assumptions and merits follows. The models were repeated at a high dolomite content (labelled as models A(high), B(high) and C(high)) and a low dolomite content (labelled as models A(low), B(low) and C(low)). The particulars for the input files for the models are outlined below:

For model A:

- The plume under study was approximately 500 m long; therefore the model used 50 cells of 10 m each
- Average hydraulic conductivity of dolomite is 2.53 m day^{-1} according to GCS Pty Ltd (2011). According to the hydraulic head map the difference in head (Δh) was between 10 and 20 m. Using Darcy's Law, the calculated flow rate for the area would be 0.1 m day^{-1}. This correlated to the reported seepage into the Schoonspruit (GCS Pty Ltd, 2011). Therefore, each time step corresponded to 100 days and a 50 year simulation required 183 time steps.
- In order to approximate the groundwater conditions prior to influx of AMD, rainwater was equilibrated with atmospheric gases (oxygen and carbon dioxide), 50 cells containing dolomite were then equilibrated with this solution.
- The incoming AMD feed water (solution 0) was defined as the solution analysed from Borehole A.
- The reactive mineralogy for each cell was defined using the "equilibrium phases" data block. Dolomite was present in each cell with initial amounts of 0.02 mol for model A(high) and 0.002 mol for model A(low).

Halite was present with an initial amount of 0.032 mmol, because of the high solubility of halite it was found that all of the halite dissolved within the first flush. Diaspore, $Fe(OH)_3$ (a), gypsum, $Ni(OH)_2$, pyrochroite and $Zn(OH)_2$ were allowed to precipitate.

- The Wateq4f database was used.
- PHREEQC script for the basic model A is shown in Figure 5.12

```
#Assuming that the original aquifer had a composition similar to that of rainwater in equilibrium with dolomite

EQUILIBRIUM_PHASES 501
    O2(g)     -0.7 10
    CO2(g)    -3.5 10
SOLUTION_SPREAD
    -units    mg/l
     Description         Number   pH      pe    Temperature      Cl     S(6)     Ca      K      Mg      Na
 Rainwater Leach            501  4.3    7.34           19.5     2.5      3.5    1.0    2.8     0.1     0.3

SAVE solution 502
END

USE solution 502
EQUILIBRIUM_PHASES 502
    Dolomite  0 10

SAVE solution 1-50
END

SOLUTION_SPREAD
    -temp     22
    -units    mg/
 Description        pH         pe  O(0)          Alkalinity          Cl     S(6)        Al      Ca    Co      Cu      Fe      K       Mg     Mn         Na   Number
                                              as CaO.5(CO3)0.5                                                                                    pe
    VRM 38 A      4.03    6.6248   3.1                              410     4720    52.875   569.5   5.9     0.291  5.975    49.4    596.5  330     622.5      0

END
# 10m cells,  average hydraulic conductivity for dolomites is 2.53 m/day. Delta h is between 10 and 20 (according to head map), distance 500 m. Using Darcy law:
# flow rate is 0.1m/day.
# (This correlates with the reported seeapge into the Schoonspruit river). Therefore, each step is 100 days
# a time step of 100 days, means that for a 50 yr simulation, 183 time steps are required
TRANSPORT
    -cells                50
    -shifts               183
    -lengths              50*10
    -dispersivities       50*0.1
    -print_frequency      10
    -punch_frequency      5

EQUILIBRIUM_PHASES 1-50
    Diaspore  0 0 precipitate_only
    Dolomite  0 0.02
    Fe(OH)3(a) 0 0.00 precipitate_only
    Gypsum    0 0 precipitate_only
    Halite    0 0.000032
    Ni(OH)2   0 0 precipitate_only
    Pyrochroite 0 0 precipitate_only
    Zn(OH)2-a 0 0 precipitate_only
```

Figure 5.12: Input for basic reactive transport model (model A)

For model B, the following reactive surface consideration was added to the input from model A:

- In each cell, a surface was defined that corresponded to the amount of $Fe(OH)_3$ (a) that was precipitated in the cell. The area defined for the mineral was determined from the commonly used 600 m^2 g^{-1}.
- Figure 5.13 includes the script added to that shown in Figure 5.12

```
SURFACE 1-50
    Hfo_sOH Fe(OH)3(a)      equilibrium_phase 0.005  53300
    Hfo_wOH Fe(OH)3(a)      equilibrium_phase 0.2

#Area for HFO determined from 600 m2/g, therefore 53300 m2/mol
```

Figure 5.13: Additional input script for the inclusion of reactive surface modelling into the reactive transport model (model B)

`

For model C, the following exchange surface consideration was added to the input from model B:

- An exchange surface was defined in each cell. The concentration for the X species was averaged from the cation exchange capacity determinations for the pit samples and the borehole samples. The initial exchange surface was equilibrated with rainwater-dolomite solution which was used in the first step of the model.
- The PHREEQC input script for the addition of this consideration to model B is included as Figure 5.14.

```
EXCHANGE 1-50
    X       0.044
    -equilibrate with solution 1
    -pitzer_exchange_gammas true
```

Figure 5.14: Additional input script for the inclusion of cation exchange surfaces into the reactive transport model (model C)

5.1.2.2 Modelled reactive transport output

There was little variation in the output of the A(high), B(high) and C(high) models. The dissolution of dolomite and change in pH dominate the chemistry in these models (Figures 5.15-5.20). In the low dolomite content of these models, the addition of cation exchange surfaces in model C(low) retards the acidification of the aquifer relative to models A(low) and B(low) (Figures 5.15-5.20).

Figures 5.15 and 5.16 show the pH profile of the aquifer at 15 years and 50 years into the simulation, respectively. The three lines in the foreground of each plot indicate the pH in the high dolomite content aquifer and the three lines in the background represent the low dolomite content aquifer. The initial pH of the incoming acidic drainage from the tailings facility was 4.0. As expected, the high dolomite content aquifer has a greater neutralising capacity than the low dolomite content aquifer. At 15 years the model predicts that the neutralising capacity within the low dolomite aquifer has been depleted and the aquifer is acidic up to 300 m away from the TSF (Figure 5.15). At 50 years into the simulation, the low dolomite aquifer has no neutralising capacity remaining and the entire aquifer is acidic (Figure 5.16). The introduction of exchange sites in to the model (model C(low)) of the low dolomite content aquifer predicted that the acidic plume was

retarded with respect to the model A(low) and B(low) (Figure 5.15). The high dolomite content aquifer offers better resistance to the migration of the acidic plume by neutralising the acidic water, only the first 50 m and 200 m of the plume has no neutralising capacity remaining 15 years and 50 years into the simulation respectively.

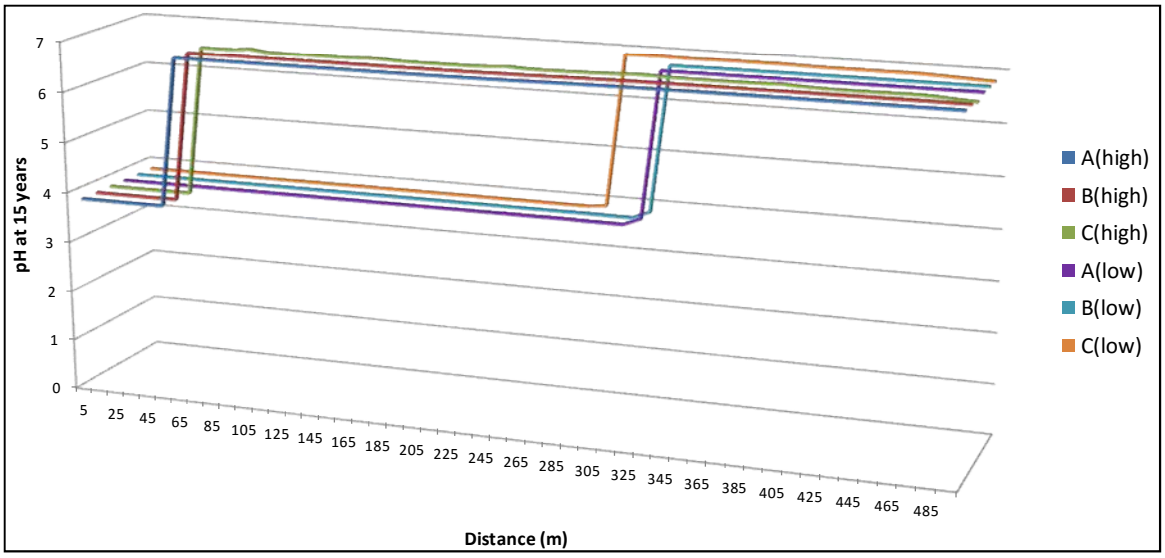

Figure 5.15: 1-D PHREEQC reactive transport modelled output of pH within the plume at 15 years (55 steps). Models with high dolomite content are in the foreground and low dolomite models are set further back

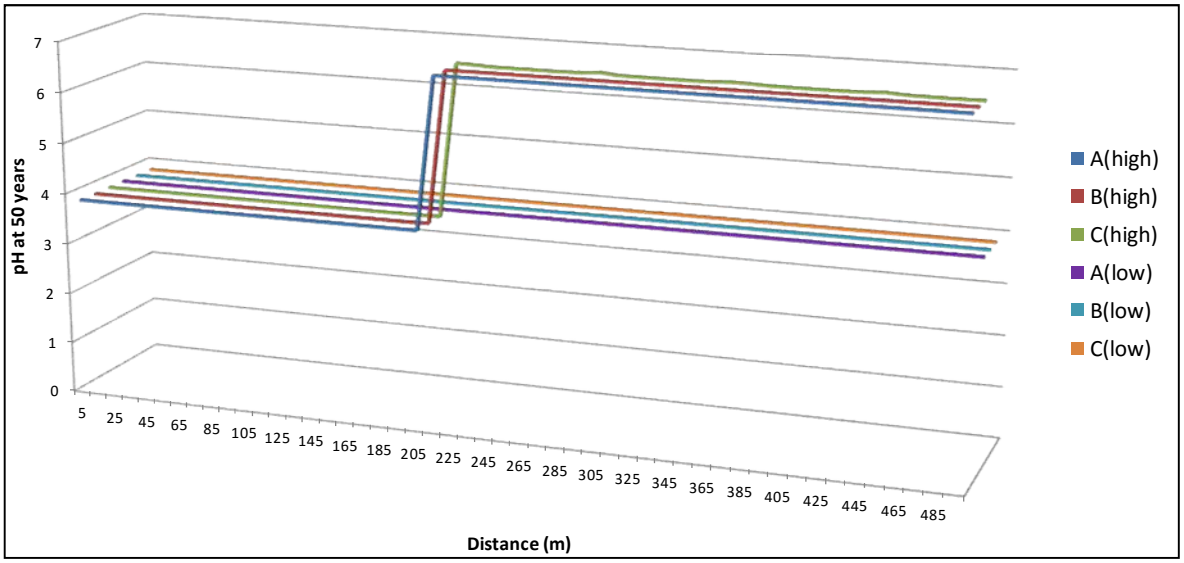

Figure 5.16: 1-D PHREEQC reactive transport modelled output of pH within the plume at 50 years (180 steps)

`

The dissolved iron content in the groundwater within the aquifer at 15 years and 50 years into the simulation are portrayed in Figures 5.17 and 5.18. The iron content correlates in an inverted manner with the pH graphs in Figures 5.15 and 5.16. The high dolomite content aquifer retards the progression of dissolved iron more successfully than the low dolomite aquifer; 15 years into the simulation the iron content is restricted to 60 m from the TSF in the high dolomite content aquifer compared to the 310 m in the low dolomite content aquifer (Figure 5.17). Correspondingly, more ferric hydroxide was predicted to have precipitated within the high dolomite content aquifer (Figure 5.19 and Figure 5.20). The ferric hydroxide precipitation curves have a sinusoidal shape and this could indicate that the time step or cell length of the simulations should be adjusted (Figure 5.19 and Figure 5.20).

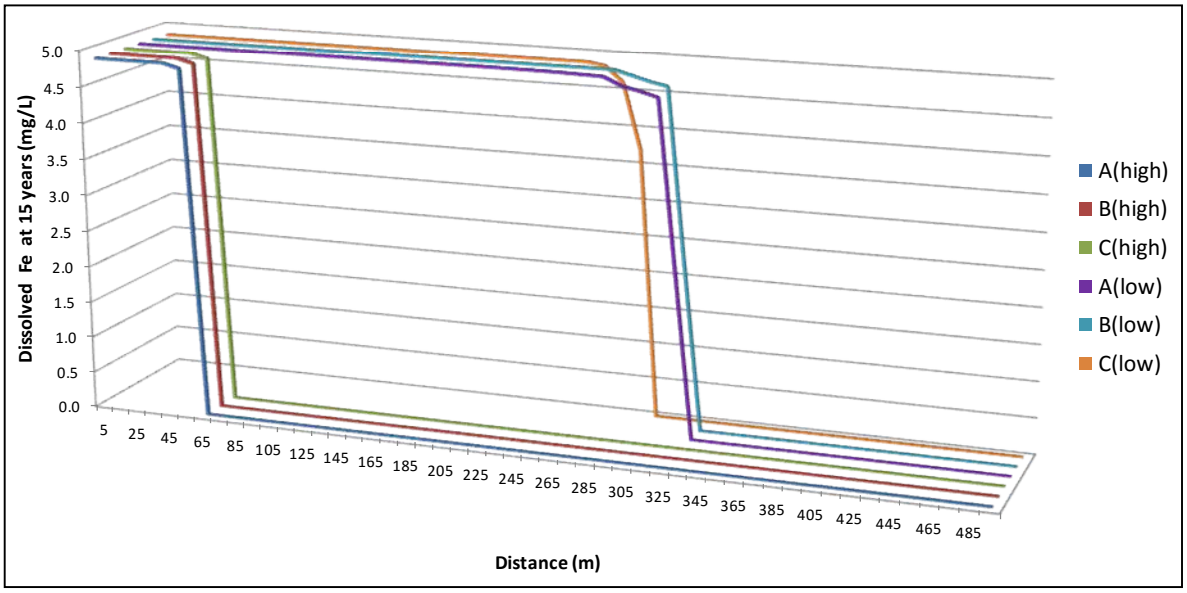

Figure 5.17: 1-D PHREEQC reactive transport modelled output of dissolved iron within the plume at 15 years (55 steps)

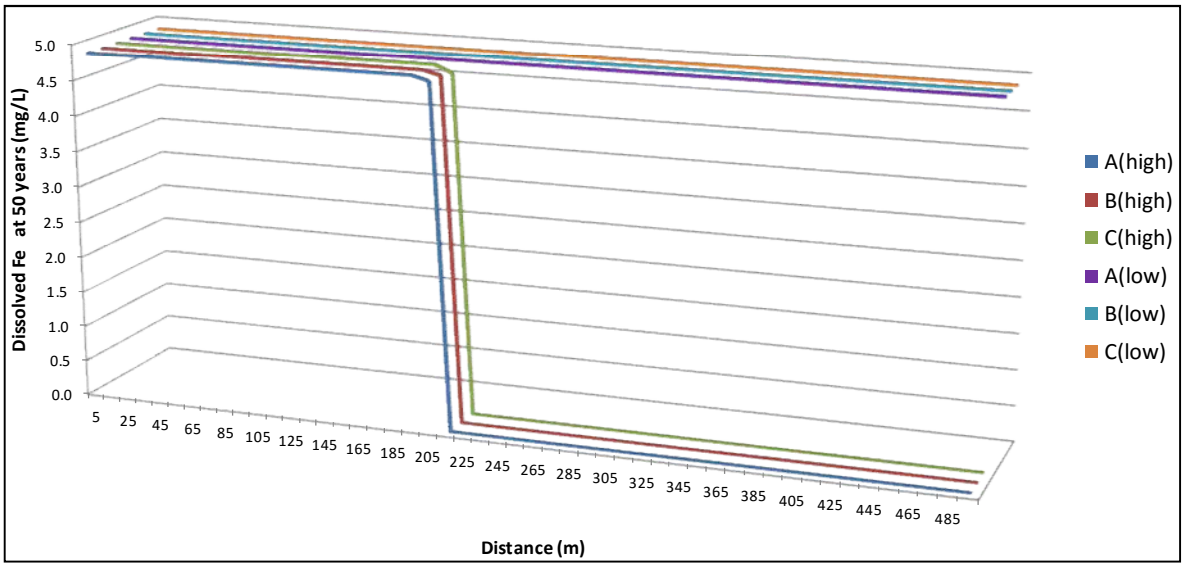

Figure 5.18: 1-D PHREEQC reactive transport modelled output of dissolved iron within the plume at 50 years (180 steps)

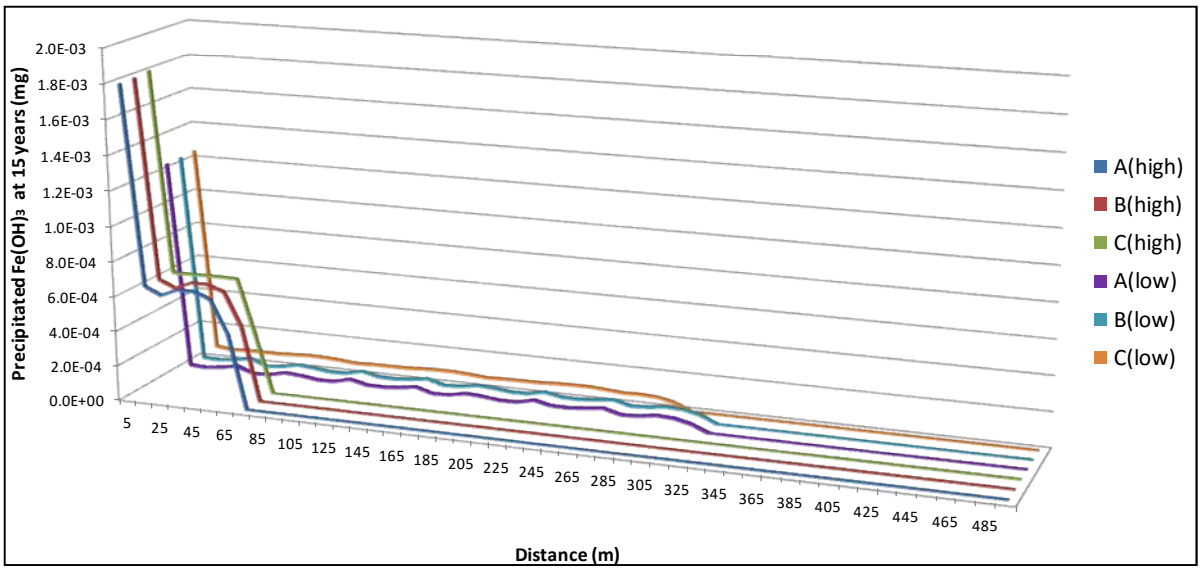

Figure 5.19: 1-D PHREEQC reactive transport modelled output of precipitated iron hydroxide from the plume at 15 years (55 steps)

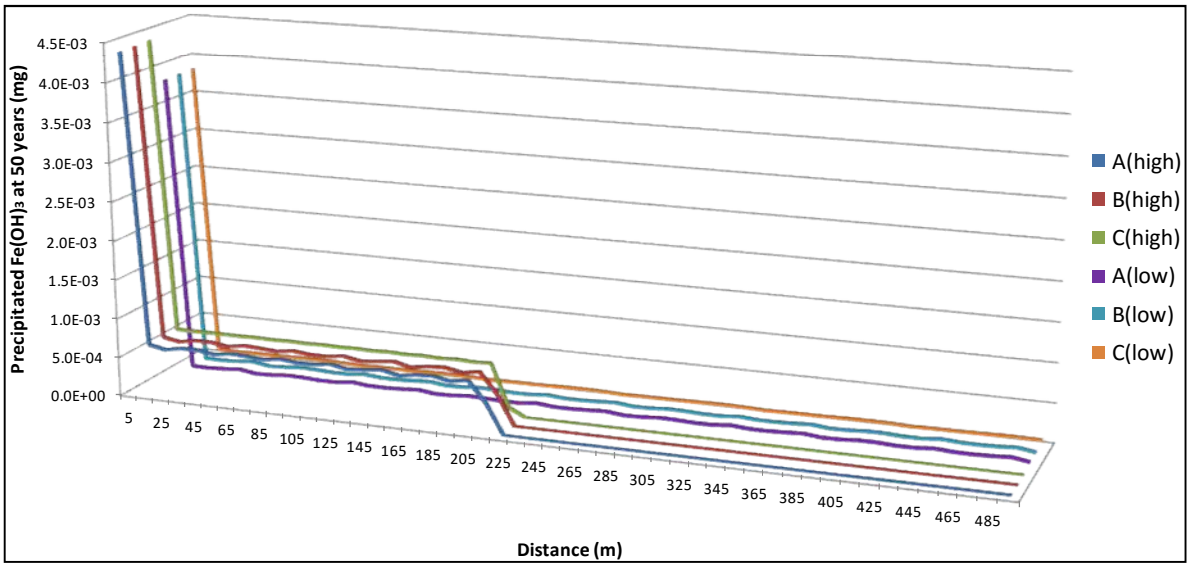

Figure 5.20: 1-D PHREEQC reactive transport modelled output of precipitated iron hydroxide from the plume at 50 years (180 steps)

5.2 Surface water systems

Metals emanating during rainwater leaching of TSFs can be transported in small streams into main water ways such as rivers. TSFs in the Witwatersrand often have a rainwater runoff pond on site to collect the leachate. In some cases, this water is pumped directly from the pond for processing as mentioned for the TSF studied in Section 5.1. Alternatively, the water seeps via surface or shallow groundwater passages into adjacent streams as observed at the abandoned partially processed tailings footprint in Chapter 4. At the study site discussed in the first part of this section (Section 5.2.1), a TSF undergoing reprocessing, the surface leachates have a fate that was a combination of the two. The leachates were collected in a rainwater pond close to the site and seeped down slope into a pollution control dam. Water from the pollution dam was pumped and treated or, an occasion when the dam wall has been compromised entered the nearby wetland. For photos and more information regarding the site, please refer to Chapter 2. In the second part of this section (Section 5.2.2), water samples from various surface waterways in residential and industrial Soweto, south of Johannesburg, were analysed. The metal content within the waterways was interpreted using statistical and geochemical modelling techniques to evaluate whether acid mine drainage had a chemically unique profile in the area.

`

5.2.1 Conference proceedings 2: Chemical Transformations of Metals Leaching from Gold Tailings

This paper was presented at the 10th International Conference on Acid Rock Drainage & IMWA Annual Conference 2015 in Santiago, Chile. The theme of the conference was "Agreeing on solutions for more sustainable mine water management". The proceedings were compiled by A. Brown, C. Buckman, J. Burgess, M. Carballo, D. Castendy, L. Figueroa, L. Kirk, V. McLemore, J. McPhee, M. O'Kane, R. Seal, J. Wiertz, D. Williams, W. Wilson and C. Wolkersdorfer. The publication carries the ISBN number 978-956-9393-27-3. In this work, a flow path for metal pollutants from the TSF was identified. Water and solid samples from the rainwater runoff pond, small stream tributaries into the pollution control dam, the pollution control dam and the wetland were collected in two sampling trips. BCR sequential extractions were performed on the solid samples as part a BSc Honour's project by Nicole Pretorius. Speciation- solubility models and inverse geochemical models of the site were constructed and interpreted with the aid of the sequential extractions. The paper demonstrated that metal partitioning within in the solid samples changed with increasing distance from the TSF and that sequential extractions can be useful in determining mineral selection for inverse models. Example PHREEQC scripts for the geochemical modelling undertaken for this paper are included in the Appendix as Figures A18 and A19.

The contributions of the authors to the work presented in the paper are as follows:

Bronwyn Camden-Smith	– sampling and analysis of water samples, geochemical modelling, co-supervised the BSc Honours project of N. Pretorius, author and presenter of the article
Nicole Pretorius	– performed sequential extractions and analysis as part of BSc Honours project
Anthony Turton	– study site coordinator and advisor, assisted with sampling

`

Peter Camden-Smith – advisor on geology and hydrology at study site, assisted with sampling

Hlanganani Tutu – supervisor and project coordinator

The proceedings are available on the IMWA website at the link:

https://www.imwa.info/imwa-meetings/proceedings/293-proceedings-2015.html

5.2.2 Occurrence and distribution of metals in surface water systems

Water sampling of several surface water bodies within Soweto, a mining impacted suburban and industrial region located in southern Johannesburg, was undertaken in September 2012. A map of the locations sampling sites is included in Section 3.1.1.4. During this sampling excursion, samples of spillages from TSF control dams, trench water surrounding TSF, natural streams following adjacent to TSF and through residential areas, a dam adjacent to a TSF and a lake in a residential area were sampled (Table 5.6). Field blanks were prepared by filling sampling bottles with deionised water and were transported and analysed in the same manner and at the same time as samples. Table 5.7 presents field electrode measurements and laboratory alkalinity determinations which were completed within 24 hours of sampling. Anion concentrations were determined using IC and dissolved metal content was determined using (Table 5.8).

Sample spill 1 was collected from a stream that has formed from spillage from a small water retention dam adjacent to the TSF. Sample spill 2 was collected downstream from spill 1 (Table 5.6, Figure 5.21). The small spillage stream from which these samples were collected decants into a larger stream flowing parallel to a main road. The road and the stream separate the TSF from a residential area to the north of the TSF (Figure 5.21). The samples taken from the spillage catchment stream (Spill 1 and 2) alongside the TSF were acidic (pH 4.07 and 5.57 respectively) (Table 5.7). The spill samples had elevated concentrations of sulphate, iron and manganese (Table 5.8). Sample spill 1 had a quantifiable concentration of uranium (3.8 mg L^{-1}, Table 5.8).

`

`

Table 5.6: Description of Soweto sampling sites

Sample ID	Sample site description
Spill 1	Adjacent to tailings, spillage from water retention dam, enters stream further down
Spill 2	Spillage from tailings water retention dam. Water flows on concrete bricks (potential neutralising effects). Down stream of Spill 1. Spillage stream enters natural stream (Stream 1) after bridge
Stream 1	Near the suburb of Riverlea, stream prior to passing the dumps near FNB stadium (water before entry of spillage, Spill 1)
Stream 2	Natural stream, down stream after mixing, lots of organic material, additional tailings outwash nearby
Stream 3	River from New Canada, lots of soap bubbles, soap scum and froth. Cow dung= used as drinking water by stock. Light yellow, clear water. Upstream of Stream 4. Near rapids.
Stream 4	River from New Canada, lots of soap bubbles, soap scum and froth. Large quantities of cow faeces suggest it is used as drinking water by live stock. Light yellow water.
Stream 5	Stream in the residential suburb of Nooitgesig. Tributary to the river from which Stream 3 and Stream 4 samples were taken. Small stream with steep banks, lots of litter near the river. Tailings in the distance (upstream). Medium to dark green water, very turbid.
Trench 1	Orange trench water. Upstream from trench 3
Trench 2	Trench water close to outlet pipe. Upstream from trench 3
Trench 3	Direct from pipe which feeds water into trench. Upstream of pipe water is orange, downstream from pipe water is green
Trench 4	Green trench water adjacent to tailings. Downstream from trench 3
Trench 5	Tailings trench water
Tailings paddock	Very small flow of water, adjacent to possible unmaintained tailings paddock. Slow flowing. Downstream from reprocessing site. Orange, turbid water.
Fleuhof Dam 1	Fleuhof dam
Fleuhof Dam 2	Fleuhof dam (near inlet)
Florida Lake	Florida Lake
Field blank 1	Filtered and stored blank
Field blank 2	Filtered and stored blank

`

Table 5.7: Field determined physio-chemical parameters and lab based alkalinity titrations of Soweto water samples

Sample ID	Temperature	pH	ORP (standard)	Conductivity	Dissolved Oxygen	Alkalinity	
	°C		mV	mS cm^{-1}	mg L^{-1}	mg $CaCO_3$ L^{-1}	Standard Deviation
Spill 1	20.3	4.07	446	2.56	8.2	bdl	-
Spill 2	21.4	5.57	418	4.37	6.4	bdl	-
Stream 1	19.6	6.20	439	0.66	4.8	118	0.6
Stream 2	21.5	5.90	415	0.69	6.1	19	1.3
Stream 3	19.0	6.32	408	0.96	5.6	95	1.3
Stream 4	19.5	6.23	410	1.01	5.7	102	0.8
Stream 5	21.0	6.37	399	1.19	3	146	4.7
Trench 1	19.1	3.39	530	4.79	5.2	bdl	-
Trench 2	20.3	3.55	492	4.69	4.0	bdl	-
Trench 3	19.1	9.55	382	3.61	2.9	144	0.9
Trench 4	20.9	3.35	500	4.44	4.7	bdl	-
Trench 5	19.6	3.50	483	4.65	5.1	bdl	-
Tailings paddock run off	26.3	2.80	499	11.34	2.2	bdl	-
Fleuhof Dam 1	20.2	5.50	461	0.42	not measured	37	0.9
Fleuhof Dam 2	23.0	5.70	450	0.41	not measured	36	0.3
Florida Lake	20.9	5.88	445	0.19	not measured	54	0.8

bdl = below detection limit of alkalinity titrations (less than 10 mg $CaCO_3$ L^{-1})

`

Table 5.8: Quantification of anion and metal concentrations in Soweto water samples

	IC and ICP-OES Analysis (mg L^{-1})																						
Sample ID	**F**	**Cl**	**Br**	**NO_3**	**SO_4**	**Al**	**Ba**	**Bi**	**Ca**	**Co**	**Cr**	**Cu**	**Fe**	**K**	**Li**	**Mg**	**Mn**	**Na**	**Ni**	**Rb**	**Si**	**Sr**	**U**	**Zn**
Spill 1	bdl	59	bdl	bdl	2525	2.28	0.02	0.61	429	1.83	bdl	0.13	214.5	11.92	bdl	121.7	75.35	91.45	2.02	0.35	0.32	0.62	3.80	bdl
Spill 2	bdl	75	bdl	bdl	3625	0.47	0.03	0.73	305	1.97	0.01	0.21	222.5	41.80	bdl	210.9	95.15	139.9	1.50	0.36	0.35	0.96	bdl	bdl
Stream 1	bdl	28	bdl	bdl	154	0.14	0.04	0.03	10.1	0.23	bdl	bdl	0.91	11.90	bdl	19.70	3.65	30.75	0.19	0.28	0.26	0.19	bdl	bdl
Stream 2	bdl	13	bdl	bdl	324	0.04	0.06	0.03	66.8	0.18	bdl	bdl	1.15	12.80	bdl	20.20	5.25	16.65	0.26	0.18	0.17	0.17	bdl	bdl
Stream 3	bdl	34	bdl	bdl	303	0.03	0.04	0.02	43.5	0.50	bdl	bdl	Bdl	14.20	bdl	24.30	3.65	38.85	0.98	0.30	0.27	0.22	bdl	bdl
Stream 4	bdl	36.5	bdl	bdl	313	0.02	0.04	0.02	45.3	0.46	bdl	bdl	0.02	14.60	bdl	24.40	4.00	39.10	0.82	0.29	0.27	0.22	bdl	bdl
Stream 5	bdl	39.5	bdl	bdl	333	0.04	0.03	0.03	41.9	0.23	bdl	bdl	2.28	16.10	bdl	21.90	5.25	50.35	0.19	0.32	0.29	0.22	bdl	bdl
Trench 1	bdl	75	bdl	bdl	4095	56.85	0.06	0.50	116	2.19	0.12	0.59	398.5	49.50	0.52	104.6	41.15	160.6	2.78	1.95	1.74	0.68	12.03	0.55
Trench 2	bdl	60	bdl	bdl	4055	47.5	bdl	0.39	147	1.65	0.14	0.35	302.0	49.50	0.21	81.00	22.85	156.6	2.05	1.47	1.32	0.74	bdl	0.42
Trench 3	bdl	64	bdl	bdl	2066	0.06	0.05	bdl	166	1.06	bdl	bdl	0.40	71.00	bdl	0.86	0.01	172.8	bdl	0.37	0.34	0.94	bdl	bdl
Trench 4	bdl	62.5	bdl	bdl	3664	55.3	0.07	0.32	116	1.92	0.14	0.56	289.0	44.70	0.53	110.7	18.09	150.2	2.43	2.04	1.82	0.66	8.35	0.21
Trench 5	bdl	Bdl	bdl	bdl	2570	57.9	bdl	0.57	129	2.37	0.19	0.40	319.5	39.60	0.23	131.6	40.00	145.4	1.95	1.48	1.33	0.67	bdl	bdl
Tailings Paddock run off	bdl	Bdl	bdl	bdl	16980	560	bdl	6.90	169	18.10	1.55	9.00	3060	9.70	1.02	453	96.95	69.40	22.30	7.10	1.97	0.58	36.00	30.20
Fleuhof Dam 1	bdl	16.2	bdl	bdl	133	0.37	0.03	bdl	25.6	bdl	bdl	bdl	0.18	6.40	bdl	11.65	0.13	14.80	bdl	bdl	0.09	0.12	bdl	bdl
Fleuhof Dam 2	bdl	16.6	bdl	bdl	129	0.21	0.03	bdl	26.9	bdl	bdl	bdl	0.02	5.75	bdl	11.65	0.07	12.65	bdl	bdl	0.10	0.12	bdl	bdl
Florida Lake	bdl	14	bdl	bdl	17	0.05	0.04	bdl	15.7	bdl	bdl	bdl	0.19	3.48	bdl	6.42	0.03	7.88	bdl	0.21	0.19	0.07	bdl	bdl
Field blank 1	bdl	bdl	1.90	bdl	Bdl	bdl	bdl	bdl	bdl	bdl	bdl	bdl	Bdl	bdl	bdl	bdl	bdl	bdl	bdl	bdl	bdl	bdl	bdl	bdl
Field blank 2	bdl	bdl	0.90	bdl	Bdl	bdl	bdl	bdl	bdl	bdl	bdl	bdl	Bdl	bdl	bdl	bdl	bdl	bdl	bdl	bdl	bdl	bdl	bdl	bdl
Detection limits						0.05	0.02	0.01	0.05	0.02	0.01	0.03	0.01	0.19	0.12	0.01	0.01	0.21	0.01	0.12	0.14	0.01	0.08	0.06

bdl = below detection limit

`

The spillage stream from the TSF enters the natural stream downstream from where sample stream 1 was taken. Sample stream 2 was taken down stream from the spillage stream inlet (Table 5.6, Figure 5.21). There was tailings material nearby sample stream 2 as seen in Figure 5.21 by the light yellow sand patch east of the sample location. Therefore, sample stream 1 was relatively unaffected by the TSF (ground water flow in the area was unknown) and sample stream 2 was directly affected by both the spillage stream from the TSF and leaching of tailings material in close proximity to it. Stream 1 had a slightly higher pH than sample stream 2 (6.20 and 5.90 respectively, Table 5.7) and more notably sample stream 1 had a much higher alkalinity (118 mg $CaCO_3$ L^{-1}) than sample stream 2 (19 mg $CaCO_3$ L^{-1}) (Table 5.7). There was an increase in sulphate, calcium iron and manganese concentrations samples stream 1 and stream 2 (Table 5.8).

Figure 5.21: Modified Google Earth image of tailings spillage stream and stream showing flow directions (sampling undertaken in September 2012, satellite imagery from 3 October 2012)

`

The stream from which the samples stream 3 and stream 4 were taken flow to the west of a residential area (Figure 5.22). The water body is used by the neighbouring community for washing of clothes and for drinking water by livestock. As a result of the washing of clothes, the rapids in the river where sample stream 3 was taken were filled with soap foam and soap scum on the day of sampling (Figure 5.23). Further downstream where sample stream 4 was collected there was calmer water and fewer bubbles. A tributary enters the stream between samples stream 3 and 4. This tributary was sampled further upstream where road access to the stream was possible (Figure 5.22). The tributary flows along the southern edge of a TSF and through an industrial and residential area before joining the main river. There was a large amount of litter around the tributary. The chemical analyses of the samples stream 3, 4 and 5 show little variation; the pH values average 6.3 with a standard deviation of only 0.07, the samples have similar ORP and conductivity measurements (Table 5.7) as well as similar chloride, sulphate, calcium and magnesium concentrations (Table 5.8). However, the tributary (sample 5) has a lower dissolved oxygen concentration than the stream possibly owing to the rapids at sampling site of sample stream 3 (Table 5.7). Additionally, the iron content in the tributary sample was higher than that within the stream samples (2.28 mg L^{-1} compared to below detection and 0.02 mg L^{-1} respectively, Table 5.8). The manganese and sodium concentrations within the tributary sample were also higher than those within the stream (Table 5.8).

Figure 5.22: Modified Google Earth map showing the relative positions of a sampled stream and its sampled tributary. The tributary flows along the southern edge of a TSF and through a residential area (sampling undertaken in September 2012, satellite imagery from 1

Figure 5.23: Photograph showing foam and rapids at the sampling site of sample stream 3

`

The trench samples were collected from the southern edge of the same TSF from the samples spill 1 and spill 2 were collected from (Figure 5.24). The water in the trench flows eastwards and then likely towards the retention dam. The TSF is 1.0 km wide as measured from sample Trench 1 to sample Trench 5. Trench 3 was taken from a pipe which was draining into the trench. The pH of this sample was alkaline (pH 9.55) whereas the samples within the trench had an average pH of 3.45. Upstream of Trench 3 the water was orange and directly below the outlet the water green (Figure 5.25). Sample Trench 3 had an alkalinity of 144 mg $CaCO_3$ L^{-1} whereas the alkalinity in the other trench samples was below quantification limits for the titration. The chemical reactions occurring at this junction are under further investigation. Decant of cyanide rich effluent from TSF has been observed. Therefore, the precipitation of blue-green ferricyanide minerals could be responsible for the observed colour change (H. Tutu, personal communication, 2013*).* The sulphate concentrations in Trench 1 and 2 samples are comparatively higher than the other samples (>4000 mg L^{-1}) and the concentration of sulphate decreases along the channel from Trench 1 to Trench 5 (excluding the decant sample) (Table 5.8). Trench samples 1, 2, 4 and 5 had an average aluminium concentration of 54.4 ± 4.7 mg L^{-1} however the decant from the pipe had a very low concentration of aluminium (<1 mg L^{-1}). Similar trends were noted for iron, magnesium, manganese and nickel (Table 5.8). The Trench 3 decant sample contained higher concentrations of calcium (166 mg L^{-1}), potassium (71 mg L^{-1}) and sodium (173 mg L^{-1}) than the samples obtained within the trench (Trench 1,2, 3 and 4, Table 5.8).

Figure 5.24: Modified Google Earth image showing positioning of trench samples along the southern edge of a TSF (sampling undertaken in September 2012, satellite imagery from 3 October 2012)

Figure 5.25: Photograph showing colour change in trench surrounding TSF. Water is flowing from left to right. Before the outlet, water was orange with a pH of 3.5; water decanting from the pipe has a pH of 9.6; water after the pipe is blue/green with a pH of 3.6

`

A sample from a seepage flowing across the edge of a tailings footprint or paddock was obtained (Figure 5.26). The sample had a very low ph of 2.8 and a high conductivity (11.34 mS cm^{-1}) which corresponded to the high metal and sulphate concentrations within the sample (Table 5.8). The sample relatively high concentration of aluminium (560 mg L^{-1}), cobalt (18.10 mg L^{-1}), chromium (1.55 mg L^{-1}), copper (9.00 mg L^{-1}), iron (3060 mg L^{-1}), manganese (97.0 mg L^{-1}), nickel (22.3 mg L^{-1}) and uranium (36.0 mg L^{-1}) (Table 5.8). The sample was collected downstream from a tailings reprocessing site and the leachates from the freshly exposed tailings material were draining into the sampled paddock seepage stream (Figure 5.27).

Figure 5. 26: Modified Google Earth map showing the relative positions of samples from Fleuhof dam, Florida Lake and the tailings paddock. (sampling undertaken in September 2012, satellite imagery from 9 December 2012)

`

Figure 5. 27: Photograph of seepage emanating from freshly exposed residual tailings material following reprocessing of the TSF

Two samples were collected from Fleuhof dam and one sample from Florida Lake (Figure 5.26). The samples were not representative of the water quality of the entire dam but were intended to give an indication of metal content of the water body. The dam and lake samples had an average pH of 5.7 and low conductivity. Fleuhof dam has a TSF on the north-western bank, sampling took place on the north eastern bank and a residential area lies to the east of the dam (Figure 5.26). The Fleuhof dam samples had a higher concentration of sulphate (131 mg L^{-1}) than the Florida lake sample (17 mg L^{-1}) which was bordered by residential and industrial zones. Fleuhof dam also had higher calcium and sodium concentrations than the Florida Lake sample (Table 5.8). The dam and lake samples were compared with the SANS 241:2011 standards for drinking water quality. The pH fell within the acceptable range of between 5 and 9.7. The conductivity was also acceptable in that it was lower than 1.70 mS cm^{-1}. The anion content was acceptable, in particular the sulphate concentration was less than 500 mg L^{-1}. Aluminium content (limit was 0.300 mg L^{-1}) was borderline within the Fleuhof Dam sample but was acceptable within Florida Lake. Iron and manganese was within the 2 mg L^{-1} and 0.5 mg L^{-1} respective limits. Other metal content in the samples (Co, Cr, Cu, Ni, U) were below the detection limit of the equipment and were not quantified.

`

The field blank samples were analysed at the same time at the collected water samples with IC and ICP-OES. All of the metal concentrations were below the detection limit and only small amounts of bromide were detected in the anion analysis. This illustrates that there was a low risk of contamination of collected water samples from sampling containers as well as during transport, filtering and analysis.

A piper diagram for the Soweto water samples was compiled using Geochemist's Workbench Student software (Figure 5.28). The lower right triangle of the piper diagram demonstrates clearly that the trench water samples, Stream 2 sample and tailings paddock sample are sulphate rich. The Fleuhof dam samples plot at 70% meq sulphate and 20% meq (bi)carbonate whereas as the Florida lake sample contains less sulphate and 60% meq (bi)carbonate. The projection of the cation and anion triangles onto the diamond show that the trench samples clump together (red shapes) except for the Trench 3 which was a sample of the decant coming from the drainage pipe. The spillage samples (blue shapes) project onto close to the tailings paddock samples. Stream 1, the sample prior to spillage stream entering the stream, projects at 50% calcium and magnesium and 60% sulphate and chloride. Stream 2, a sample from downstream Stream 1 and affected by the spillage stream and residual tailings material, projects closer to the spillage samples at above 90% sulphate and chloride due to its low alkalinity (Table 5.7). Stream 3 and Stream 4 samples overlap on the projected diamond and along with Stream 5 project into the moderate region of the diamond.

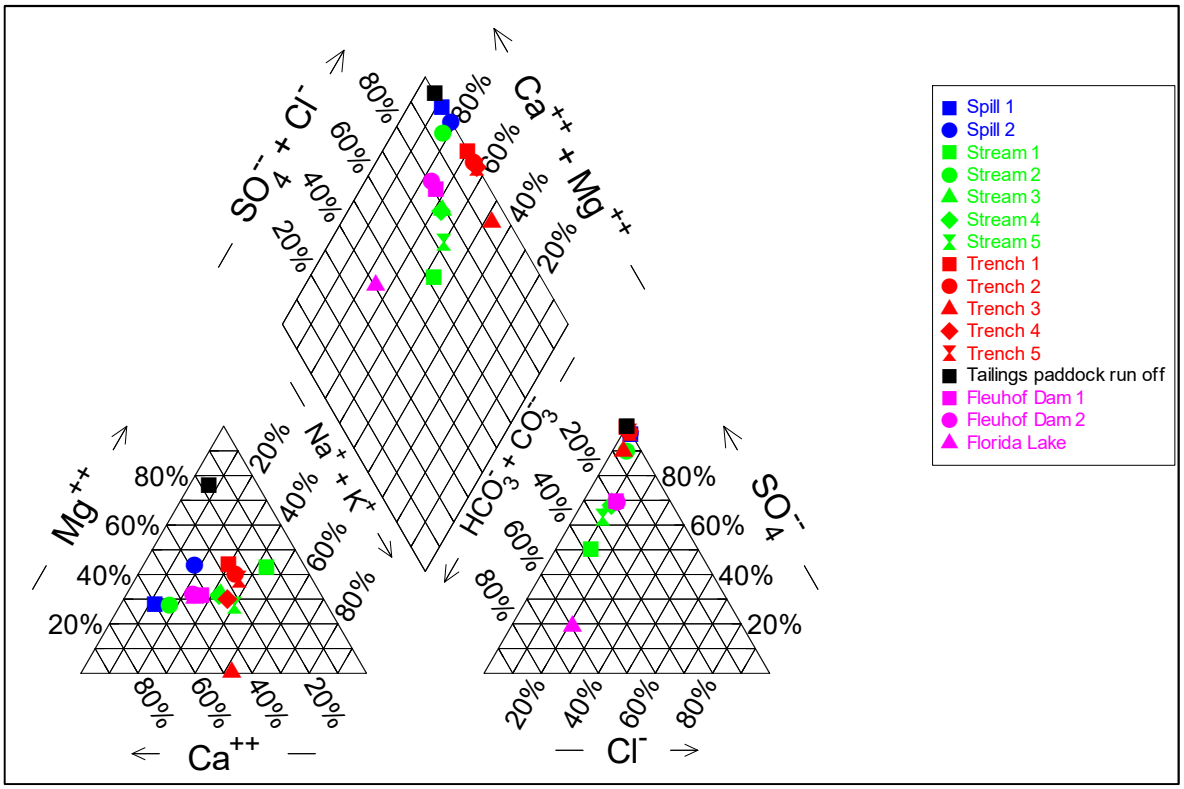

Figure 5.28: Piper diagram plot of Soweto samples

A principal component analysis (PCA) of the Soweto samples was performed using XLSTAT, a Microsoft Excel Plug-in software created by Addinsoft SARL and available from https://www.xlstat.com/en/. A Pearson (n) type of PCA was performed. A plot of eigenvalue and cumulative variability vs. principal components (scree plot) shows that the first four principal components described 95% of the variability within the data with the first value describing 58% (Figure 5.29). Factor loadings of the first four principal factors are summarised in Table 5.9. Factor 1 is loaded with conductivity, sulphate, the transition metals as well as lithium, magnesium and uranium and to a lesser extent the pH. A similar trend was observed in factor analysis by Cukrowska et al. (2004) in which the conductivity, sulphate and heavy metals contributing to factor 1 was attributed to solubility nature of minerals within the tailings material. Alkalinity was a major contribution to factor 2 and dissolved oxygen was the major contributor to factor 3. These factors affect both dissolution of minerals and speciation of metals within the resulting leachates and waterways. The fourth factor was loaded with

pH and ORP and accounts for the redox equilibrium effects on the mobility of dissolved species (Cukrowska et al., 2004).

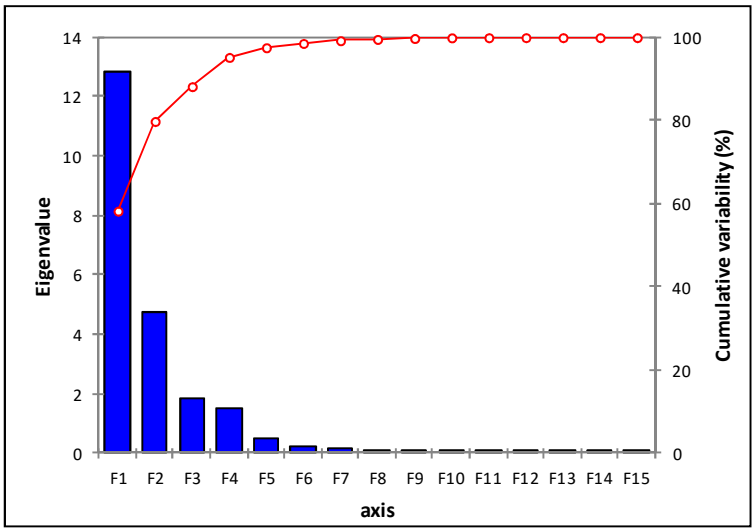

Figure 5.29: Scree plot of Pearson principal component analysis of Soweto samples

`

Table 5.9: Factor loading of the first four principal components for the Soweto samples

	F1	F2	F3	F4
pH	**-0.601**	-0.106	-0.446	**-0.599**
ORP (standard)	0.550	0.203	0.157	**0.774**
Conductivity	**0.943**	0.301	-0.075	-0.033
Dissolved Oxygen	-0.483	0.014	**0.821**	0.091
Alkalinity	0.034	**0.795**	-0.219	0.320
Cl	-0.149	**0.855**	0.013	-0.088
NO_3	0.000	0.000	0.000	0.000
SO_4	**0.994**	0.042	-0.026	-0.062
Al	**0.968**	-0.229	-0.090	-0.031
Ca	0.317	0.587	0.578	-0.416
Co	**0.979**	-0.154	-0.025	-0.121
Cr	**0.965**	-0.236	-0.089	-0.042
Cu	**0.956**	-0.260	-0.070	-0.093
Fe	**0.981**	-0.177	-0.022	-0.061
K	0.068	**0.887**	-0.405	-0.028
Li	**0.916**	0.078	-0.134	0.327
Mg	**0.950**	0.075	0.212	-0.113
Mn	**0.718**	0.322	0.523	-0.245
Na	0.278	**0.918**	-0.152	0.020
Ni	**0.974**	-0.199	-0.015	-0.077
Sr	0.399	0.872	-0.020	-0.225
U	**0.953**	-0.115	-0.036	0.072
Zn	**0.932**	-0.313	-0.080	-0.136

Transition metals (Co, Fe, Ni, Cr, Cu and Zn) as well as aluminium and uranium group along the positive side of the first principal component axis in the negative quarter of the second principal component (Figure 5.30). Alkali metals and alkali earth metals excluding lithium and magnesium group along the second principal component axis along with alkalinity.

`

The observations or samples were plotted on the first two principal component axes and examined for trends. It was noted that the samples obtained from the trench and from the spillage stream (samples presenting leachates from the TSF) grouped together along the near to the second principal component axis (the vertical axis in Figure 5.31). The samples obtained from the streams and from Florida Lake and Fleuhof Dam were closely grouped together in the lower left quadrant of the plot. The tailings paddock sample had a unique chemistry in that it had a very high conductivity, low pH and high metal content (Table 5.7 and 5.8). This samples contributed 80% towards the first principal component and thus on a plot of first two principal component lies far to the right (Figure 5.31).

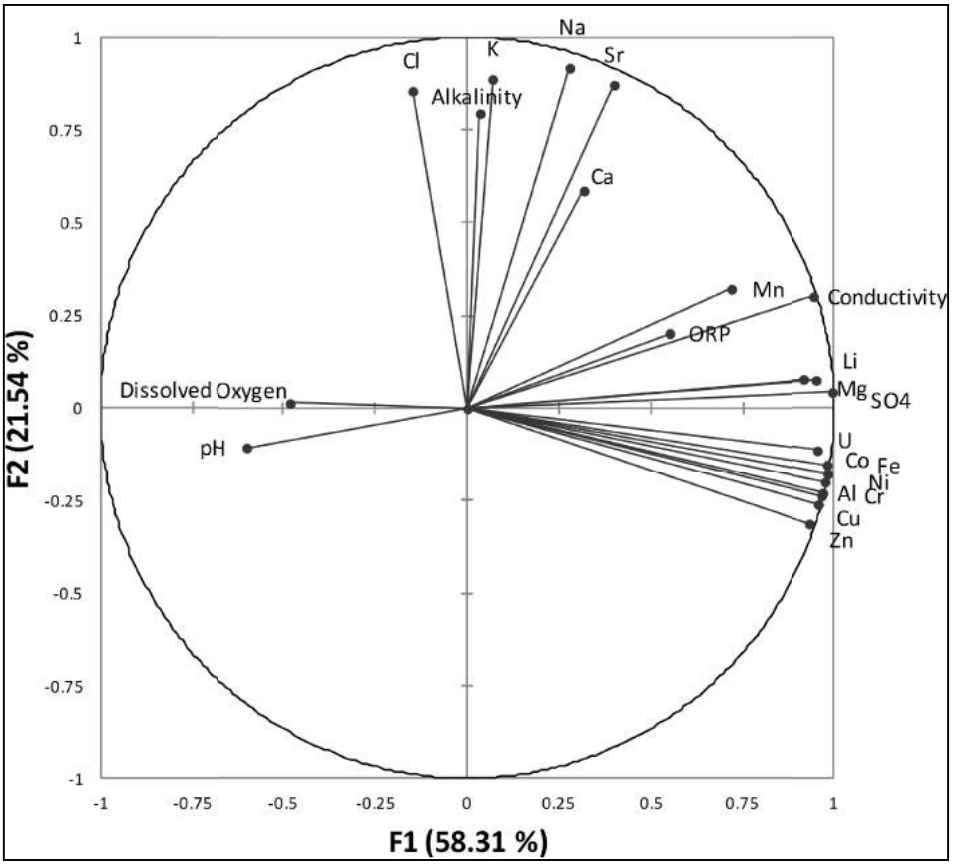

Figure 5.30: Analysed variables plotted on first and second principal component axes showing a grouping of transition metals along the first axis and a partial grouping of alkali and alkali earth metals along the second axis

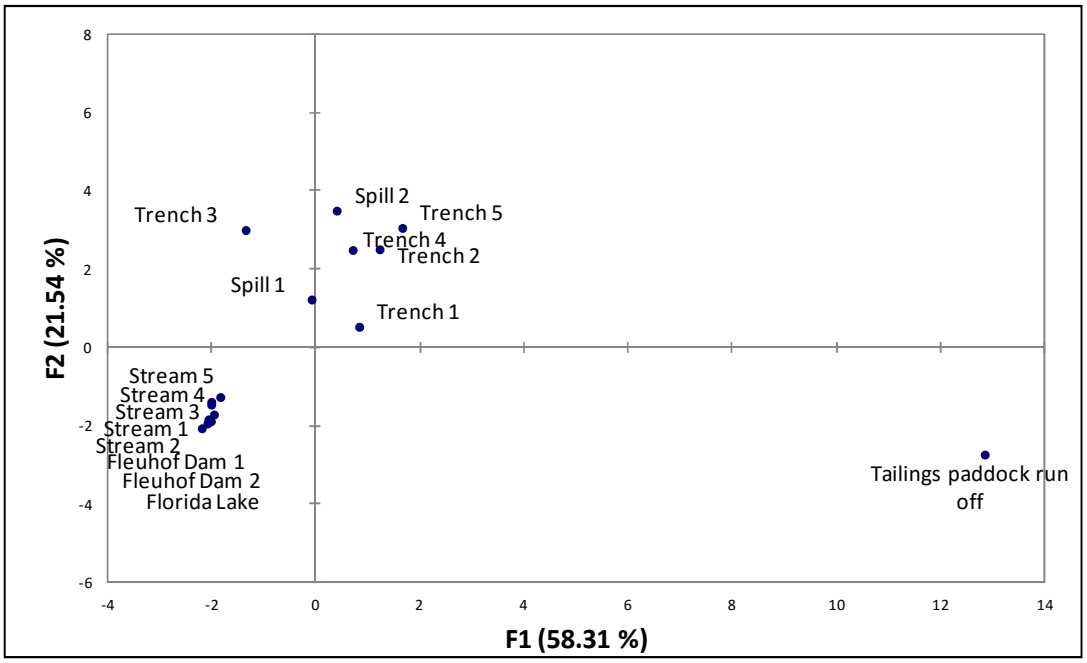

Figure 5.31: Observations (samples) plotted on first and second principal component axes showing a grouping of acidic samples taken from within the trenches or near to trenches surrounding TSF and lesser polluted streams and dams

Speciation-solubility models were constructed for water samples in Geochemist's Workbench using the extensive themo.com.V8.R6.dat database with no modifications. The database is equivalent to the llnl.dat database used in PHREEQC. For samples with concentrations below the detection limit, half of the detection limit was used as input (Table 5.8).

The models predicted that the ferric containing oxide minerals,$CoFe_2O_4$, hematite (Fe_2O_3), goethite (FeOOH) and magnetite (Fe_3O_4) were supersaturated in most of the models. Goethite and hematite in particular are not expected to precipitate at surface temperature due to slow growth kinetics and amorphous $Fe(OH)_3$ is commonly used as a proxy for ferric mineral precipitation (Zhu and Anderson, 2002). A selection o-f minerals that were close to saturation (saturation index (S.I.) between -2 and 0) or supersaturated in solution (S.I. greater than 0) were selected for representation in Figures 32-36. These minerals were in equilibrium or were close equilibrium with the solution and could provide insight into which minerals were precipitating from solution or were in great enough abundance in

associated solid material to dissolve into solution and reach equilibrium. The minerals were grouped into sulphate, hydroxide and carbonate minerals.

In the two TSF spillage samples alunite, jarosite were supersaturated (S.I. > 0) and gypsum was close to saturation in both samples (Figure 5.32). Spill 2 had a higher pH and correspondingly the hydroxide minerals amorphous $Fe(OH)_3$ and gibbsite (aluminium hydroxide) were supersaturated (Figure 5.32).

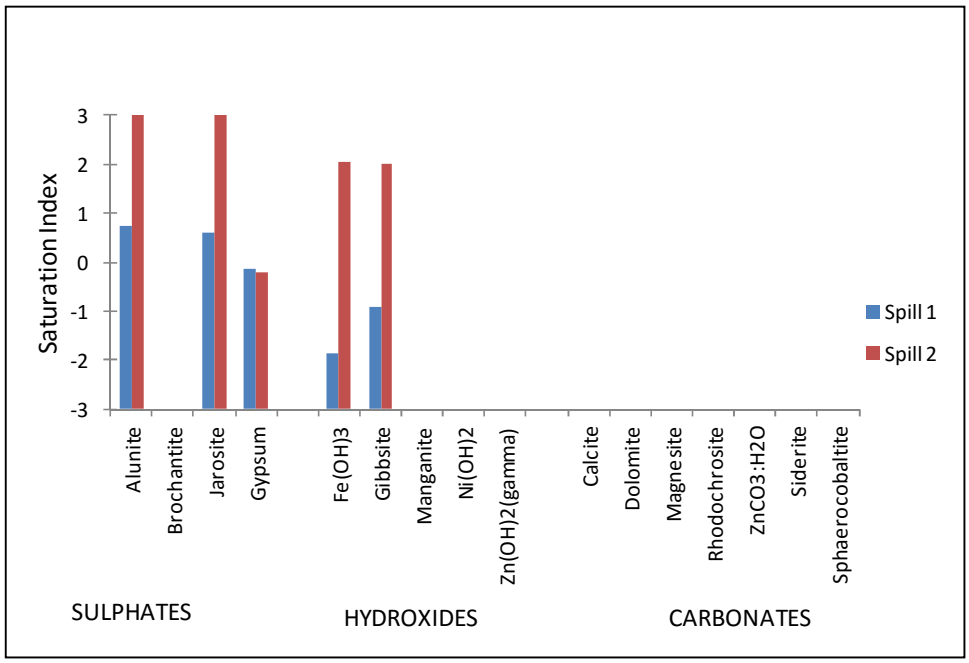

Figure 5.32: Geochemist's Workbench calculated saturation indices of a selection of minerals within the spillage stream samples

The stream samples had a selection of carbonate minerals, including calcite and dolomite, which were close to saturation (Figure 5.33). The inclusion of alkalinity measurements into the model made these determinations possible. Amorphous iron hydroxide and gibbsite (aluminium hydroxide) were supersaturated. Stream samples 3 and 4 had low concentrations of iron and correspondingly were not supersaturated with respect to jarosite.

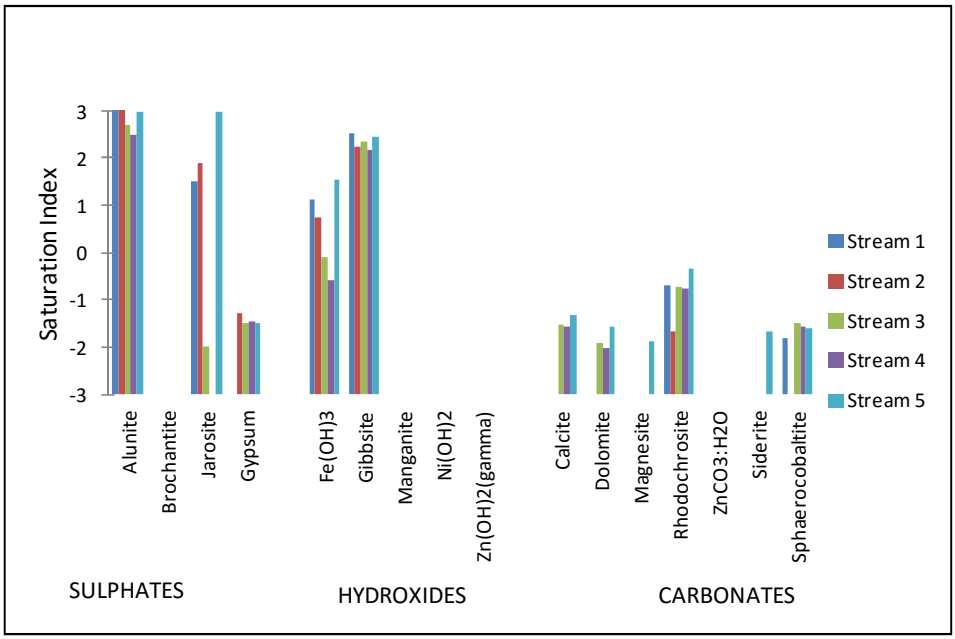

Figure 5.33: Geochemist's Workbench calculated saturation indices of a selection of minerals within the stream samples collected in Soweto

Trench sample 3 had a wider selection of minerals that were close to saturation than the other trench samples, including carbonate minerals and manganese, nickel and zinc hydroxides (Figure 5.34). This sample came from the pipe draining into the trench and had a high pH. Similar to the spill samples; alunite, jarosite, gypsum and gibbsite were close to saturation in the trench samples 1, 2, 4 and 5. The trench samples 2, 3, 4 and 5 had unacceptable, high charge balances of 44 -50%. Clearly an analyte was missing from these analyses and given the colour precipitate around the samples, cyanide species should be quantified in the future.

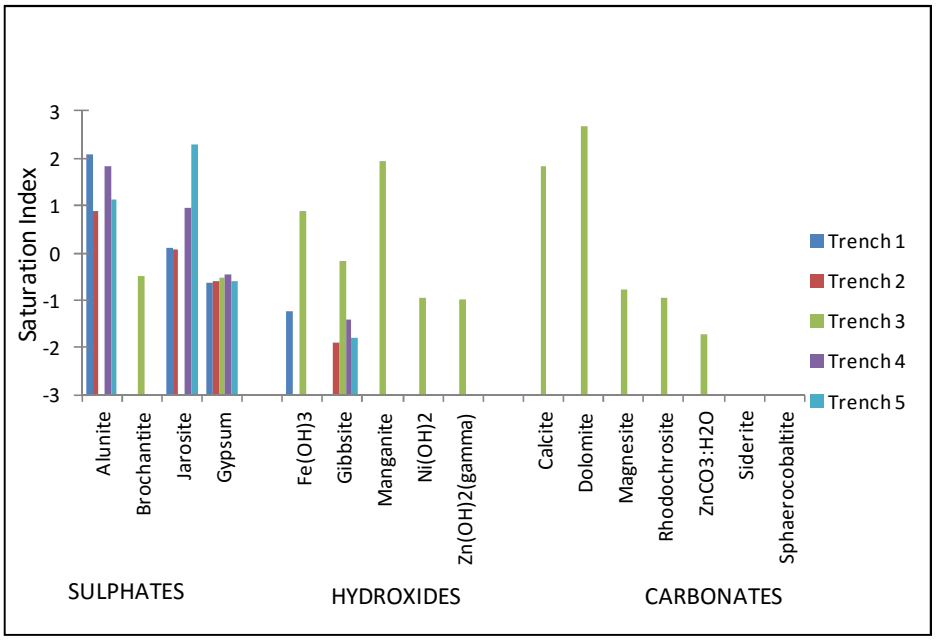

Figure 5.34: Geochemist's Workbench calculated saturation indices of a selection of minerals within the samples collected from a trench collecting leachates bordering a TSF in Soweto

The low pH, metal rich tailings paddock sample had very few minerals close to saturation within it (Figure 5.35). Alunite, jarosite and gypsum were close to saturation as observed in the AMD trench samples. However, due to the high conductivity and inferred ionic strength of the sample, the Debye-Hückel model for calculating activity coefficients might not be valid and a Pitzer model would be more appropriate. Unfortunately, the current Pitzer databases do not contain an extensive suite of acid mine drainage minerals.

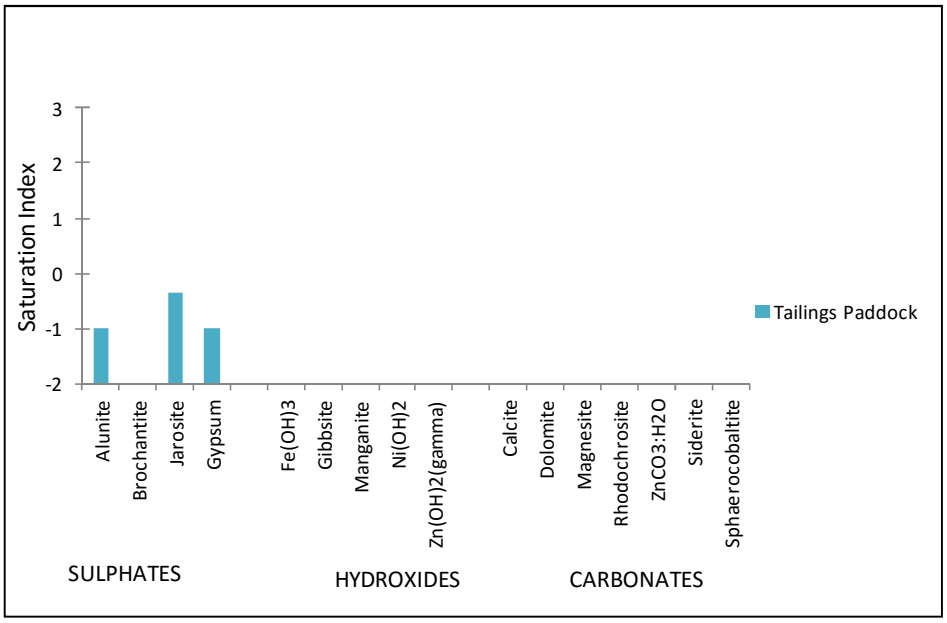

Figure 5.35: Geochemist's Workbench calculated saturation indices of a selection of minerals within the tailings paddock run off sample

The dam and lake samples were close to saturation with alunite, amorphous $Fe(OH)_3$ (Figure 5.36) . Fleuhof samples 1 and 2 were also close to saturation with gypsum and Fleuhof sample 1 was close to saturation with jarosite. Even though these samples had measurable alkalinity content, they were not close to saturation with any carbonate minerals (Figure 5.36)

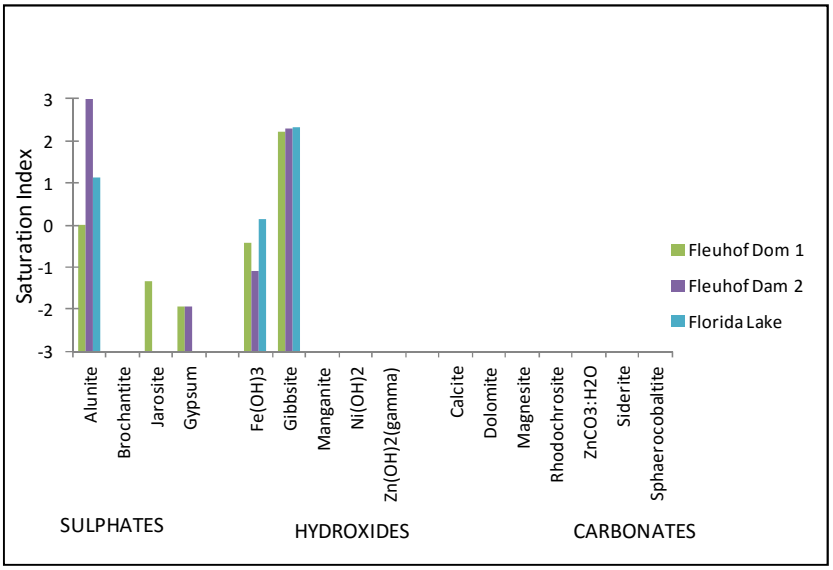

Figure 5.36: Geochemist's Workbench calculated saturation indices of a selection of minerals within dam and lake samples collected within Soweto

`

The principal component analysis in this section was more useful at distinguishing between groups of AMD samples and less polluted stream and dam samples to than the analysis of a selection of saturation indices. In the AMD samples obtained from the spillage, tailings paddock and trench, alunite, jarosite and gypsum were close to saturation. However, in the stream samples these same minerals were also often close to saturation. The major difference was observed in samples in with high alkalinity because a suite of carbonate minerals were close to saturation. The second principal factor was loaded with alkalinity. Therefore, a combination of chemometric and geochemical modelling might be the good approach to understanding water variation and chemistry in a region. Geochemical modelling can assist with identifying missing analytes and minerals of interest and chemometric or statistical methods can be used to differentiate types of waterways even if they have a similar saturation indices profile.

`

5.3 Temporary and Permanent Sinks

Metal pollutants released from tailings storage facilities have a variety of potential fates depending of the nature of their release and the chemistry within the surrounding environment. Following their release metals from tailings, the distance with which they travel and impact of metal pollutants is dependent on their carrying water body and on the physical and chemical reactions which occur during transport. Metals transported in small, shallow surface ways that evaporate will be temporarily held in efflorescent crusts before dissolving and being transported again by rainwater (Harris et al., 2003; Lottemoser, 2005; Nordstrom, 2008). Metals that enter larger streams will be transported further from the TSF and can be diluted, precipitate within the stream, adsorb onto reactive surfaces, be taken up by biological organisms or transport conservatively (Chapman et al., 1983; Blowes et al., 2003). Surface or groundwater routes can enter wetlands which have been extensively researched for their ability to remove metals from incoming flow (Machemer and Wildeman, 1992; Mays and Edwards, 2001; Johnson and Hallberg, 2005; Sheoran and Sheoran, 2006; Cukrowska, 2015) Shallow, natural wetlands are common features on the Witwatersrand due to the sustained water input from underground pumping activities and drainage released from TSF. Wetlands, both natural and constructed, have been used to treat AMD arising from tailings storage facilities within the Witwatersrand goldfields (Cukrowska et al., 2015). Passive and active treatment options for acid mine drainage have been utilised worldwide in efforts to curb the release of metals into residential, industrial, and flora and fauna conservational areas (a selection of AMD treatment reviews include Brown et al., 2002; Kalin et al., 2005; Johnson and Hallberg, 2005). In this section, the precipitation and dissolution of efflorescent crusts at an abandoned tailings storage facility and metal removal within an active treatment plant treating AMD arising from mine workings were investigated.

`

5.3.1 Evaporation barriers

Metals released from tailings storage facilities can be stored temporarily as efflorescent crusts. Efflorescent crust is the general name given to the collection of coloured minerals that are known to precipitate from ion rich solutions or brines and have now been exposed and dehydrated by the atmosphere. The salts reflect the chemical composition of the water from which they were precipitated and play an important role in the transport and storage of metals released during the weathering of mineralised sources (Jambor, Nordstrom and Alpers, 2000). Efflorescent crusts contribute to soil pollution surrounding tailings storage facilities (Weiersbye et al., 2006). Efflorescent crust formation is not unique to an acid mine drainage environment. For example, it is commonly formed by the capillary evaporation of groundwater brines from pans or sabkhas giving rise to large thick halite salt pans (Warren, 2006). Efflorescent crust associated with mining activities is not a recent phenomenon and was described by Agricola in the mid 1500's (Jambor, Nordstrom and Alpers, 2000).

The water table is elevated under tailings and this could feed ponds where the surface intersects the water table. The evaporation of this water along with capillary evaporation, leads to the formation of multicoloured efflorescent crusts (Naicker, Cukrowska and McCarthy, 2003). The colour is dependent on the salt composition, for example white crust indicates the presence of calcium (gypsum), pink indicates cobalt or manganese and green indicates nickel or iron (Naicker, Cukrowska and McCarthy, 2003). Yellow salts could indicate the presence of uranium (Naicker, Cukrowska and McCarthy, 2003) or ferrichydroxysulphate (Younger, 2002). The precipitation of magnesium and zinc rich minerals generally occur first and are later followed by manganese and calcium rich minerals (Diehl, Hageman and Smith, 2008). These mineral crusts are significantly more soluble than the primary minerals from which they are derived and are not preserved past the first thunderstorms at the start of the wet season (Sutton, 2008). The quick dissolution of these salts into surface water at the start of a rainy season leads to a spike in the metal concentration and a lower pH of discharging waters (Nordstrom, 2011).

`

Two articles relating to ability of efflorescent crusts to act as temporary sinks for metal pollutants have been compiled. The first was published in the peer reviewed conference proceedings of the 2013 International Mine Water Association (IMWA) conference. The second was submitted to Environmental Science and Pollution Research in July 2016 and has been accepted for publication.

5.3.1.1 Conference proceedings 3: Investigating the potential impact of efflorescent mineral crusts on water quality: complementing analytical techniques with geochemical modelling

In the peer reviewed conference proceedings article, "*Investigating the potential impact of efflorescent mineral crusts on water quality: complementing analytical techniques with geochemical modelling*", the formation and dissolution of efflorescent crusts was investigated. The composition of crusts was studied by dissolving a selection of crusts and analysing their composition. The resulting solution was then allowed to evaporate over a period of time and the solid products were analysed using PXRD. The evaporation of the solutions was modelled using PHREEQC. The comparison of analytical and geochemical modelling results was presented at the 2013 International Mine Water Association (IMWA) conference, "Reliable Mine Water Technology", held in Golden, Colorado, USA. Sample PHREEQC scripts for the solubility analysis and mineral precipitation aspects for the evaporation modelling discussed in this work are included in the Appendix as Figures A20 and A21.

The contributions of the authors are as follows:

B.P. Camden-Smith - analytical work, PXRD and interpretation geochemical modelling, author of paper

R.H. Johnson – advisor on geochemical modelling work

R. Richardson – assisted with PXRD and interpretation

D.G. Billing – assisted with PXRD and interpretation

H. Tutu - supervisor and project coordinator

The proceedings can be accessed via the link:

`

https://www.imwa.info/imwa-meetings/proceedings/278-proceedings-2013.html

5.3.1.2 Journal article 4: Mineralogy and geochemistry of efflorescent minerals on mine tailings and their potential impact on water quality

This paper was published in Environmental Science and Pollution Research. Efflorescent crusts were dissolved in a step wise manner in deionised water with measurements of pH and Eh taken after every addition. Geochemical modelling with PHREEQC then aimed to reproduce the experiment. This gave insight into the effect of minor metal quantities on the pH of crust solutions, for example a small portion of iron present in aluminium and magnesium rich crusts lowered pH more than the major cations. Geochemical modelling was used to deduce the minor mineralogy that impacts the quality of water following the dissolution of the crusts. Traditionally, mineralogy has been determined through the use of PXRD. The combination of the two techniques provides both bulk mineralogy and reactive mineralogy.

The dissolved crust solutions were compared with the rainwater and sulphuric acid leachates of oxidised and unoxidised tailings respectively as well as the pond water on the site. It was noted that the aluminium and magnesium crusts found of the surface of the tailings correlated well with the pond water and the rainwater leachate of oxidized tailings. The crusts which were collected from a borehole spillage and the sulphuric acid leach of unoxidised tailings were both iron rich. This led to the conclusion that were two types of drainage disseminating from the site and that these drainages have unique chemistry. The surface drainage emanating from the site is aluminium and magnesium rich whereas the shallow ground water drainage is iron rich. An example of the PHREEQC script for the modelling used in this paper is included in the Appendix as A22.

The contributions of the authors were as follows:

B.P.C. Grover – analytical work, geochemical modelling, author of paper

R.H. Johnson – advisor on geochemical modelling work

D.G. Billing – assisted with PXRD and interpretation

I.M. Weiersbye – study site advisor

`

H. Tutu – supervisor and project coordinator

The doi reference for the article is 10.1007/s11356-015-5870-z and it can be accessed via the link:

http://link.springer.com/article/10.1007/s11356-015-5870-z

5.3.2 AMD Treatment Plants

At present, there are two active plants (both high density sludge (HDS) treatment facilities) operating on the Witwatersrand for treatment of AMD released from tailings storage facilities. The one is in the West Rand while the other has been commissioned within the Central Rand. During the treatment process lime is added to AMD, the solution is aerated and an iron rich sludge is produced. This sludge contains significant concentrations of other metals that were extracted during from the metal rich, acidic mine drainage. The trace metal removal process at this site was studied by constructing a series of forward reaction models. Although there are no current publicised plans to treat tailings AMD using an HDS facility, the active treatment plant does give insight into the potential fate of metals released from tailings storage facilities should they be treated in a similar manner. The draft paper describing the AMD treatment process is presented below.

5.3.2.1 Journal article 5: Investigating the removal of trace metals in a high density sludge treatment plant using a geochemical modelling approach

This paper will be submitted to the IWA journal "Water Science and Technology" in 2016. The paper was compiled for and presented at the 4th South African Young Water Professionals Biennial and 1st African IWA Young Water Professionals conference held at the Council for Scientific and Industrial Research (CSIR) in Pretoria, South Africa from 16 to 18 November 2015. The paper received the WISA (Water Institute of South Africa) Mine Water Division Award for the best mine water related paper at the conference. The PHREEQC script for modelling discussed in this paper is included in the Appendix as Figure A23.

The contributions of the authors were as follows:

B.P.C Grover - Analytical work and geochemical modelling, author of article

`

P.M. Camden-Smith - Organised and assisted with sampling, advisor on site

H. Tutu - Project co-ordinator and advisor

INVESTIGATING THE REMOVAL OF TRACE METALS IN A HIGH DENSITY SLUDGE TREATMENT PLANT USING A GEOCHEMICAL MODELLING APPROACH

Bronwyn P.C. Grover[1], Peter M. Camden-Smith[2] and Hlanganani Tutu[1]*
[1]Molecular Sciences Institute, School of Chemistry, University of the Witwatersrand, 1 Jan Smuts, Johannesburg, South Africa
[2]Camden Geoserve, Boksburg, South Africa
*E-mail: hlanganani.tutu@wits.ac.za

ABSTRACT

Treatment of underground acid mine drainage using high density sludge treatment procedures is a common technique. A PHREEQC geochemical model of a high density sludge treatment facility located within the Witwatersrand goldfield was iteratively developed in order to better predict the removal of trace metals within acid mine drainage. Water and sludge samples from an active facility were collected and analysed. Incoming AMD water samples were used as input for the model and outgoing treated water samples were used to test the model's accuracy. The mineralogy of the sludge was predominantly gypsum. The model successfully determined the removal of trace metals (Al, Cu, Mn, Ni, U and Zn) from the mine drainage. The hydrated iron oxide surfaces in the model, both freshly precipitated and within the sludge, are responsible for the removal of Cu, Mg, Mn, Ni, U and Zn.

Keywords geochemical modelling, high density sludge; mine water treatment

INTRODUCTION

The Witwatersrand goldfields of South Africa have been mined for over 120 years. At the beginning of mining activities in the region, the water table was shallow as such most of the mines required water to be pumped out of the workings (Scott, 1995). Mine closure and the related cessation of water pumping have resulted in flooding of abandoned mine workings and the subsequent decant onto surface have generated a large amount of negative publicity for the region (McCarthy, 2011). The incoming water assists the oxidation of sulphides within the remaining underground mineralised regions and this releases acid, metals and sulphates into solution. The effects of decant of this water onto surface include the lowering of pH levels which will yield the water unfit for domestic use and aquatic life; the lower pH also promotes the dissolution of minerals containing toxic metals and radionuclides; and the

increase in sulphate concentration yields the water unsuitable for some agricultural and industrial purposes (Inter-Ministerial Committee, 2010). Groundwater supplies away from mining centres have also been affected through the possible circulation of water in open fractures and karst structures (Abiye, 2014). Measures have been taken to prevent acidic decant from the Central and Eastern basins following decant of acid mine drainage from the Western Basin near Krugersdorp in 2002 (Durand, 2012). These measures include the installation of pump and treat facilities such as high density sludge treatment plants.

High density sludge treatment plants are a common, widespread active AMD treatment option (Korstenbader and Haines, 1970; Wolkersdorfer, 2008). In short, an alkaline substance (often lime) is added to AMD to increase pH and the solution aerated to oxidise ferrous iron to less soluble ferric iron. An iron rich sludge is produced and there are various techniques, including dissolved air floatation or addition of floccuants, to reduce the water content of the sludge and make it as high density as possible to lessen disposable costs (Bosman, 1983; Johnson and Hallberg, 2005). The sludge is considered stable with low risk of metals leaching from it and entering the environment (Murdock et al., 1994) Instead of disposing the voluminous sludge generated, research efforts into recycling sludge have included the production of bricks (Huang et al., 2001).

In this paper, PHREEQC is used to model the treatment process at an active acid mine drainage treatment facility in South Africa. PHREEQC software is capable of performing a range of geochemical calculations including speciation and solubility calculations; batch and 1-D transport calculations involving reactions or equilibriums with gas, aqueous, solid mineral phases and surface-complexes; and inverse modelling (Parkhurst and Appelo, 2013). In a recently published article, Cravotta et al (2015) has described the development and utilization of the coupling of PHREEQC with AMDTreat 5.0+, software released by the U.S. Office of Surface Mining, Reclamation, and Enforcement (OSM). Cravotta et al (2015) simulated the addition of NaOH, CaO, $Ca(OH)_2$, Na_2CO_3 and NH_3 to coal mine drainage to estimate the treated water quality, chemical usage, volume of sludge produced and cost of treatment. Adsorption effects have not yet been incorporated into the model, however they are known to control the trace element concentrations in treatment systems (Cravotta et al., 2015)

This paper describes the development of a simple PHREEQC forward model for an existing acid mine drainage treatment facility. Using the model, this work aims to better understand

the reactions which occur within the facility and the removal of trace metal quantities (aluminium, cobalt, copper, manganese, nickel, uranium and zinc) from the incoming water.

METHODOLOGY

Sampling and Sample Preparation

An active acid mine drainage treatment facility was sampled shortly after the facility was opened. The plant aerates mine water, adds lime and generates and recycles high density sludge.

All of the samples reported here were collected on the same day during which the plant was functioning under normal operating procedures. Water samples of the unprocessed pumped mine water, processed water prior to discharge and water discharge into the environment were collected. Measurements of field chemical parameters (temperature, pH, electrical conductivity and redox potential) were conducted immediately after collection of the water samples (Paschke, 2002). Subsamples were filtered and subdivided on site with a portion being acidified (for metal analysis) and another portion left unacidified (for anion analysis) (Wardencki & Namiesnik, 2002). Alkalinity measurements were conducted within 24 h of sample collection. Sludge samples from the recycled sludge waste and gypsum crystallization tank were collected. These samples were centrifuged to separate water and solid material. Supernatant obtained from the centrifuged fractions was filtered and analysed in the same manner as the water samples. Solid samples of lime mixture used to treat the mine water were taken. Solid material was air dried between 35 – 45°C until constant mass. Daily water analyses provided by the plant were used to augment the analytical results from the sampling as well as to assess the variability of the incoming mine drainage and processed water.

Analytical Techniques

On site electrode field measurements were done with a calibrated multiprobe field meter (Thermo Scientific Orion Star). Metal analysis was undertaken using inductively coupled plasma-optical emission spectroscopy (ICP-OES) (Spectro Genesis, Kleve, Germany). Anion analysis was performed using chemically suppressed anion chromatography (IC) (Metrohm 761 Compact Ion Chromatograph, Herisau, Switzerland). Mineralogy of the dried solid samples was determined using D2 Phaser powder X-ray diffractometer (PXRD) fitted with a cobalt X-ray source and LynxEye 1-D detector (Bruker, Karlsruhe, Germany). Gran function plot, inflection point and fixed end point methods were used to quantify alkalinity (Gran

1952; ASTM International 2010; Rounds 2012). Measurements of pH for alkalinity assessment were undertaken using a calibrated Knick 766 Calimatic pH probe (Knick, Germany).

Geochemical Modelling

Speciation-solubility and forward geochemical modelling was undertaken using the USGS software, PHREEQC with the wateq4f database (Parkhurst and Appelo, 2013). Samples were equilibrated using a 1:1 "mix" function and then iterative forward modelling commenced. The iterative improvement of a forward geochemical model is presented in this work. The model starts with the incoming pumped mine water and allows for a series of reactions to occur (including dissolution of pentlandite (lime), degassing of carbon dioxide, influx of oxygen, precipitation of minerals, adsorption of species onto iron surfaces). A charge balance was applied to sulphate because there was analytical uncertainty in its value as it required numerous dilutions given its high concentration. The model aims to correlate the observed discharge water with the modelled output water. The initial solubility-speciation modelling of all of the water samples provides insight into which minerals are likely to precipitate during the process and this is incorporated into the forward modelling. An annotated example of the final PHREEQC input file for the forward model is included as Supplementary Material section (available in the online version of the manuscript).

RESULTS AND DISCUSSION

Analytical and Mineralogical Results

Table 1 summarises the field based measurements of temperature, pH, Eh and conductivity of the water and centrifuged water samples. Mine Water 1 and 2 samples were taken from separate incoming pipes close to the pumps. Processed Water 1 and 2 samples were taken from the holding tanks for the processed water. The Stream Discharge sample was taken from the stream created by discharge of the processed water. This water flows through a nearby a series of natural reed beds. The Gypsum Crystallisation and Recycled Sludge samples were centrifuged from sludge collected at the respective tanks. The presented Eh measurement has been calculated from the field measured oxidative-reductive potential (ORP) measurement. The lab pH measurements presented in Table 1 are measurements that were taken after the samples had been transported and stored. The difference in the pH measurements, especially for the processed water and stream discharge samples, is attributed to the degassing of carbon

dioxide following the filtering, transport and storage. This highlights the importance of field based measurements for accurate determination of pH. However, alkalinity was measured within 24 hours of collection as on site facilities were not available. Unfortunately, this increased pH for the processed water samples brings doubt into the accuracy of the alkalinity measurements. Alkalinity results presented are for the Gran function plot method with the exception of the sample AMD Feed 2, in which the average of the other two techniques is reported (Table 1). There was good correlation in the various alkalinity methods with the exception of the AMD Feed 2 sample.

Table 2 summarises the anion and metal analyses for the water samples and centrifuged samples. It's clear that the plant is effective in reducing the metal load of the mine water prior to discharge. Incoming mine water is enriched in iron (Fe) (average concentration of 2100 mg L^{-1}). This is considerably reduced in the processed water samples. Metals of environmental concern that are reduced in the plant include cadmium (Cd), cobalt (Co), copper (Cu), manganese (Mn), nickel (Ni), uranium (U) and zinc (Zn). Aluminium (Al) has been observed at high concentrations in coal acid mine drainage (Waters and Webster-Brown, 2013; Chamier et al., 2015) and from AMD emanting from tailings storage facilities (Camden-Smith and Tutu, 2014). However, in the underground mine water sampled at this site, the Al value was low. This infers that the chemistry within surface and underground acid mine drainage are different within the Witwatersrand Basin and that they may require different treatment options. Chloride concentration appears to not be affected by the treatment processes as the concentration in the mine water and final processed waters are similar. There is a reduction in the sulphate values; however the processed water still contains a high concentration of sulphate.

Table 1: Electrode measurements and alkalinity results of water samples

Sample	Temperature °C	Field pH	Lab pH	Eh mV	Conductivity mS/cm	Alkalinity mg/L as CaCO3
Mine Water 1	27.5	5.15	5.28	258	5.77	29.6
Mine Water 2	27.8	5.00	5.17	261	5.45	27.7
Processed Water 1	26.8	5.67	8.77	261	4.46	28.5
Processed Water 2	26.7	6.67	8.87	262	4.29	28.7
Stream Discharge	27.1	6.03	8.27	272	4.53	32.3
Gypsum Crystallisation	18.0		5.58	279	4.33	
Recycled Sludge	17.8		6.02	275	3.55	

Table 2: Anion and metal analysis of water samples collected from mine drainage treatment plant. Concentrations are in mg/L.

Sample	Cl	SO_4	Al	Ca	Cd	Co	Cu	Fe	K	Mg	Mn	Na	Ni	Si	U	Zn
Mine Water 1	110	4550	0.15	1154	0.08	0.86	1.26	819	21	675	36	355	2.24	1.9	0.32	0.35
Mine Water 2	106	4746	0.17	1663	0.08	0.81	1.19	806	26	988	41	580	2.14	1.8	0.31	0.33
Processed Water 1	106	3066	nd	970	0.02	0.02	0.03	13	21	255	0.63	238	0.02	0.3	nd	0.02
Processed Water 2	104	2830	nd	937	0.01	0.02	0.02	0.03	18	195	0.43	271	Nd	0.3	nd	0.02
Stream Discharge	114	3236	nd	996	0.01	0.02	0.02	0.02	22	220	0.52	303	Nd	0.3	nd	0.03
Gypsum Crystallization	113	2276	nd	865	0.02	0.02	0.02	nd	42	308	0.04	329	Nd	0.4	nd	0.01
Recycled Sludge	142	3114	nd	557	0.02	0.01	0.02	nd	31	179	0.01	387	Nd	0.3	nd	0.00

"nd"= not detected

The mineralogy of the solid material was determined by PXRD. It was revealed that the lime added to treat the mine water mostly lime with a small amount of calcite. The mineralogy within the dried sludge from the gypsum crystallization tank was predominantly gypsum, with small percentages of calcite and beta-quartz and the mineralogy within the recycled sludge was gypsum with a small percentage of calcite.

Iterative Forward Modelling

The model was improved in an iterative manner by comparing the modelled output with the treated water samples. The development of the initial model to the final model has been summarised and included as Supplementary Material. The final conceptual model for this site is presented as Figure 1. In this model, the AMD feed is first equilibrated by using a "mix" function. In Step 2, it reacts with portlandite while simultaneously being equilibrated with atmospheric oxygen and allowing for carbon dioxide to degas. The reaction with portlandite is done using the "equilibrium" function. The maximum amount portlandite allowed to react with one litre was calculated from the rate of lime addition as advised by the plant.

In Step 3, the precipitation of minerals and adsorption onto the freshly precipitated iron surfaces occurs. Gypsum, amorphous ferric hydroxide, gibbsite, $Cu(OH)_2$ and pyrochroite ($Mn(OH)_2$) were selected as minerals that were allowed to precipitate from solution. These minerals were supersaturated at the end of Step 2. From the selected hydroxide minerals, only amorphous ferric hydroxide and gibbsite precipitated. $Cu(OH)_2$ and pyrochroite were no longer supersaturated in this step as the concentrations of the metals were reduced by adsorption onto the fresh iron surface. Calcite, dolomite and rhodochrosite ($MnCO_3$) were

also supersaturated in Step 2 and remain supersaturated in this step. However, they were not allowed to precipitate in the model as the precipitation of divalent carbonates is kinetically hindered (Langmuir, 1997; Cravotta et al., 2015). In the AMD Treat models by Cravotta et al (2015), the precipitation of carbonates was only allowed to occur when they were highly supersaturated, that is the saturation index was greater than 2.5. The saturation indices of dolomite and rhodocrosite remained below 2.0. Adsorption onto the freshly precipitated ferric surface was allowed. The strong sites of the fresh surface were mostly occupied by manganese (91% for AMD feed 1 and 93% for AMD feed 2) and weak sites were occupied by magnesium ions (46% in AMD feed 1 and 50% for AMD feed 2).

Step 4 of the final conceptual model attempts to calculate the surface of the iron surfaces within the sludge. The sludge also contains a polymeric coagulant, but for now the effect of the polymer will be assumed to be only physical and not to behave as an adsorptive chemical surface. It was assumed that approximately 2.24 mol of HFO materials interacts with 1 litre of solution. The only treatment that the sludge received at the plant is that is was rinsed with clean water before being reused. In the model, fresh HFO surface was equilibrated with the final treated water and then rinsed several times until there was little change in the metal loading of the surface (in the model included in the Supplementary Material, 8 times) with the treated water. This was done to provide a reasonable quantity of surface that is loaded with metals.

In Step 5, this final surface was reacted with the solution from Step 3 and the predicted chemical constituents of this modelled solution were compared with the quantified constituents in the treated water. The final surface of the ferric sludge contained calcium on the strong sites (95% occupation) and various ions occupying the weak sites (58% hydrogen species, 18% magnesium and 16% sulphate species). The adsorption of the magnesium onto the sludge is predicted to be the main mechanism of the metal's removal from the solution. Magnesium bearing minerals remain undersaturated throughout the process.

Table 3 compares the model output to the analysed processed water. Sodium is conservative though out the model as sodium bearing minerals remain undersaturated. Therefore, the sodium in the output of the model correlates to the sodium input. The model successfully determines the removal of trace metal concentrations. The clear discrepancies between the sampled and modelled water are with respect to the calcium and sulphate concentrations. The saturation indices of gypsum in the processed water samples as well as the final modelled

solutions were between 0.22 and 0.28. The sulphate output from the plant varied between 2800 and 3600 $mg.L^{-1}$ during the month of sampling.

The model assumes that there is little variation in the incoming water chemistry. However, the untreated and treated water were collected from the site on the same day and it is possible that the untreated water does not fully represent the chemistry of the treated water prior to processing. Despite this, the model is still useful for determining the minerals of interest and estimating the removal of trace metals using the sludge. Further classification of the sludge will lead to improvements in the model, especially if an adequate sequential leaching scheme of the sludge is used to determine which metals co-precipitated with gypsum and which metals are associated with the ferric mineral surfaces. The model could also be improved by taking into account the potential adsorptive effects of the flocculants.

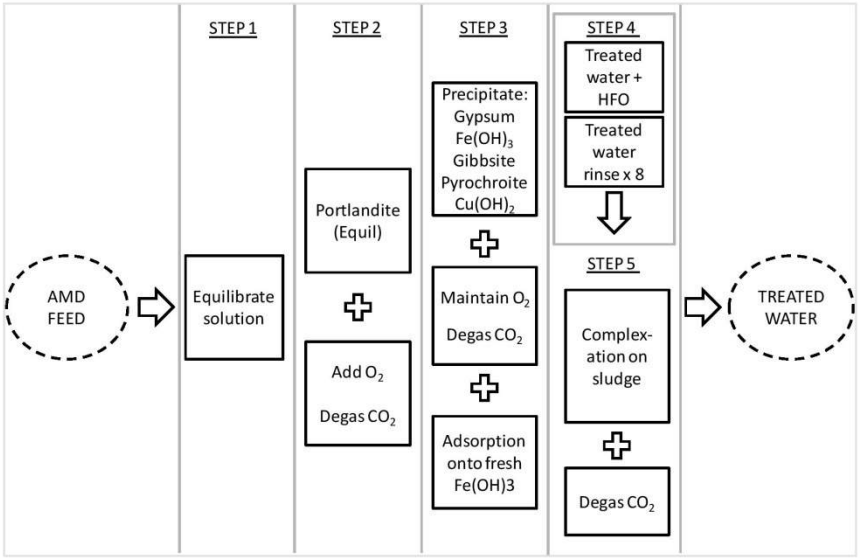

Figure 1: Final forward geochemical model for an acid mine drainage treatment plant

Table 3: Comparison of processed and modelled water

	Processed Water	Modelled Water
pH	5.6 – 6.7	7.2 - 7.3
SO_4	2830 – 3236	3550 – 4600

Al	Nd	0.02
Ca	937 – 996	825 – 866
Cu	0.02 – 0.03	0.00
Fe	0.02 – 13	0.002
K	18 – 22	21-25
Mg	195 – 255	215 – 312
Mn	0.4 - 0.6	0.1 – 0.2
Na	238 – 303	357-586
Ni	nd – 0.02	0.00
U	Nd	0.00
Zn	0.02 – 0.03	0.00

CONCLUSIONS

A simple PHREEQC geochemical model of the addition of an active high density sludge treatment facility was produced. In this model, lime (pentlandite) is added acid mine drainage and the solution is aerated (equilibrated with atmospheric gases). Hydroxides of aluminium, iron, copper and manganese were allowed to precipitate. The freshly precipitated iron surfaces adsorb manganese and magnesium. The surface of the recycled sludge was estimated by rinsing a mass of hydrated iron oxide with treated until the surface composition was constant. This surface was then bought into contact with the partially treated water in order to estimate the surface effects of the recycled sludge. There was good correlation between modelled output water and treated water from the facility. The model predicts the reduction in trace metals (Al, Cu, Mn, Ni, U and Zn).

ACKNOWLEDGEMENTS

This work was supported by the US National Academy of Sciences (through the PEER Program) and the South African National Research Foundation. The authors would like to thank the AMD treatment plant for their cooperation in this work.

REFERENCES

Abiye T.A. 2014 Mine water footprint in the Johannesburg area, South Africa: analysis based on existing and measured data. *South African Journal of Geology*. **117**(1), 87-96.

ASTM International. 2010 D1067-06: Standard test Methods for Acidity or Alkalinity of Water. In: *Annual Book of ASTM Standards Section 11 Water and Environmental Technology* Vol. 11.01. ASTM International, Baltimore.

Bosman D. J. 1983 Lime treatment of acid mine water and associated solids/liquid separation. *Water Science & Technology*, **15**(2), 71-84.

Camden-Smith B. P. C. and Tutu H. 2014 Geochemical modelling of the evolution and fate of metal pollutants arising from an abandoned gold mine tailings facility in Johannesburg. *Water Science & Technology*, **69**(5), 1108-1114.

Chamier J., Wicht M., Cyster L. and Ndindi N. P. 2015 Aluminium (Al) fractionation and speciation; getting closer to describing the factors influencing Al 3+ in water impacted by acid mine drainage. *Chemosphere*, **130**, 17-23.

Cravotta III C. A., Means B. P., Arthur W., McKenzie R. M. and Parkhurst, D. L. (2014). AMDTreat 5.0+ with PHREEQC titration module to compute caustic chemical quantity, effluent quality, and sludge volume. *Mine Water and the Environment*, **34**(2), 136-152.

Durand J. F. 2012 The impact of gold mining on the Witwatersrand on the rivers and karst system of Gauteng and North West Province, South Africa. *Journal of African Earth Sciences*, **68**, 24-43.

Gran G. 1952 Determination of the equivalence point in potentiometric titrations. *Analyst*, **77**(920), 661–671.

Huang C., Pan J., Sun K. and Liaw C. 2001 Reuse of water treatment plant sludge and dam sediment in brick-making. *Water Science & Technology*, **44**(10), 273-277.

Inter-Ministerial Committee 2010. *Mine water management in the Witwatersrand Gold fields with special emphasis on acid mine drainage*.,Report to the Inter-Ministerial Committee on Acid Mine Drainage, Department of Water Affairs, Pretoria, South Africa
Johnson D. B. and Hallberg K. B. 2005 Acid mine drainage remediation options: a review. *Science of the total environment*, **338**(1), 3-14.

Kostenbader P. D. and Haines G. F. 1970 High density sludge treats acid mine water. *Coal Age,* September, 90-97

Langmuir D. 1997 *Aqueous environmental geochemistry*. Prentice Hall, Upper Saddle River.

McCarthy T. S. 2011 The impact of acid mine drainage in South Africa. *South African Journal of Science*, **107**(5-6), 01-07.

Murdock D. J., Fox J. R. W. and Bensley J. G. 1994 Treatment of acid mine drainage by the high density sludge process. In *International Land Reclamation and Mine Drainage Conference and the Third International Conference on the Abatement of Acidic Drainage,* Pittsburh*,* 241-249

Parkhurst D. L. and Appelo C. A. J. 2013 Description of input and examples for PHREEQC version 3—A computer program for speciation, batch-reaction, one-dimensional transport, and inverse geochemical calculations: U.S. Geological Survey Techniques and Methods. http://pubs.usgs.gov/tm/06/a43/ (accessed on 31 May 2015).

Paschke A. 2002 Chapter 7. Physiochemical properties of aqueous and solid environmental matrices. In *Sampling and sample preparation for field and laboratory: fundamental and new directions in sample preparation,* J. Pawliszyn (ed.), Elsevier Science B.V, Amsterdam, pp 219-239.

Rounds S. A. 2012 Alkalinity and acid neutralizing capacity (version 4.0). In *National field manual for the collection of water-quality data*, F.D Wilde and D.B Radtke (eds.) U.S. Geological Survey Techniques of Water-Resources Investigations. http://water.usgs.gov/owq/FieldManual/Chapter6/section6.6/ (accessed on 31 May 2015).

Scott R. 1995 *Flooding of Central and Grand Rand Gold Mines: an investigation into controls over the inflow rate, water quality and the predicted impacts of flooded mines*. Report 486/1/95, Water Research Commission Report, South Africa.

Wardencki W. and Namiesnik J. 2002 Chapter 2. Sampling water and aqueous solutions. In *Sampling and sample preparation for field and laboratory: fundamental and new directions in sample preparation,* J. Pawliszyn (ed.), Elsevier Science B.V, Amsterdam, pp 33-60.

Waters A. S. and Webster-Brown J. G. 2013 Assessing aluminium toxicity in streams affected by acid mine drainage. *Water Science & Technology*, **67**(8), 1764-1772.

Wolkersdorfer, C. 2008 *Water management at abandoned flooded underground mines: fundamentals, tracer tests, modelling, water treatment*. Springer Science & Business Media, Heidelberg

`

5.4 Overview of modelling

The modelling techniques used in this thesis were summarised and published by InTech Publishers as a book chapter in the book, "Research and Practices in Water Quality" edited by Teang Shui Lee, published on 9 September 2015 (ISBN 978-953-51-2163-3). The book is available for download from http://www.intechopen.com/books/research-and-practices-in-water-quality/geochemical-modelling-of-water-quality-and-solutes-transport-from-mining-environments.

5.4.1 Book chapter: Geochemical modelling of water quality and solutes transport from mining environments

The book chapter provides an introduction to acid mine drainage and includes basic examples on speciation-solubility models, forward reaction models, inverse models and reactive transport models.

In the forward modelling section of the book chapter, the pond water is equilibrated with atmospheric gases. In iron rich solutions, the Eh is governed by the iron speciation and the equilibration with atmospheric gases should be avoided. However, due to a lack of redox equilibrium data and kinetic data detailing the necessary redox reaction (Fe2+/Fe3+) it was not feasible to define the Eh by the iron redox couple and so the oxygen equilibration was used. In future work, analytical techniques to quantify the ferrous and ferric species should be employed so that they are input into the model as separate entities instead of total iron.

The contributions of the authors of the book chapter are as follows:

B.P. Camden-Smith – analytical work, geochemical modelling and writing the chapter

R.H. Johnson – advisor on geochemical modelling work

P. Camden-Smith – advisor, assisted with sampling

H. Tutu - supervisor and project coordinator

`

The book chapter was published by InTech, the doi reference number is 10.5772/59234 and it can be accessed via the link:

http://www.intechopen.com/books/research-and-practices-in-water-quality/geochemical-modelling-of-water-quality-and-solutes-transport-from-mining-environments

`

CHAPTER SIX- GENERAL CONCLUSIONS AND RECOMMENDATIONS

The Witwatersrand Basin has been an important gold mining region, contributing significantly to the economic growth of South Africa. The mining has however resulted in the release of large volumes of waste which is contained in tailings storage facilities (TSFs). The release of metals from these facilities into surface and groundwater systems is of concern.

This research was aimed at assessing the release of these pollutants, their behaviour in water, their subsequent transport and their fate. The study has comprehensively used analytical and geochemical modelling to understand these processes that govern the distribution of metals. Further, chemometric (statistical) analysis was employed to gain insight into the water chemistry and its variability.

Batch and sequential leaching experiments of tailings materials illustrated that the suite of constituent metals included alkali and alkali earth metals as well as aluminium, cadmium, cobalt, copper, iron, manganese, nickel, uranium and zinc. Sulphate and minor amounts of chloride were also released during leaching of tailings material.

The release of metal pollutants from TSFs was found to be dependent on a number of factors, including the chemistry of the leaching solution. In the article "Geochemical modelling of the evolution and fate of metal pollutants arising from an abandoned gold mine tailings facility in Johannesburg*"* published in Water Science and Technology (2014), it was shown that an inverse model based on batch leaching results and the tailings pond water chemistry could be constructed. From this model, it was derived that the tailings pond water was a mixture of rainwater leachates of oxidised material and sulphuric acid leachates of unoxidised material. In this case, geochemical modelling was used to complement experimental results and to draw important information on the processes occurring in the real environment. It was shown that with further modelling, batch extractions could yield information about potential minerals which can be used for

`

reference in future case studies for the site. In the article, “Leachability of metals from gold tailings by rainwater: an experimental and geochemical modelling approach” published in WaterSA (2016), the batch leaching studies using the environmentally relevant leaching solutions rainwater and sulphuric acid were used in the compilation of inverse models. The inverse models were constructed to relate the final leachate and the blank leachate. The results from sequential extractions were used to aid in mineral selection, a process that usually presents some difficulty in inverse modelling. The resulting list of potential minerals was in some instances found to be missing in the actual tailings material because of the formation of solid solutions or the absence of other minerals in the databases. However, the modelled dissolution of the minerals was found to produce solutions of similar composition to those of the experimental solutions. These predicted minerals were postulated to be useful in estimating bulk metal release from the site.

Released metals can be transported in groundwater and surface water systems. Sequential extractions and speciation solubility models were used to investigate the groundwater transport of metals from an active tailings storage facility. The results showed that within the aquifer gypsum precipitates and calcium containing carbonates (calcite or dolomite) dissolve, a reaction that maintains the calcium concentration and increases the pH leading to the precipitation of metal hydroxides. Aluminium and iron hydroxides, in particular, precipitate during transport. Other metals were observed to bind onto the freshly precipitated iron surfaces with copper demonstrating a high affinity for these surfaces. These conclusions were then used to construct a one dimensional transport model for the transport of metals in the aquifer in area. It was observed that such a model would require additional sampling within the plume for validation and can be modified to include hypothetical circumstances, for example the installation of permeable reactive barriers.

Metals released into surface water systems were studied at a TSF undergoing reprocessing and the extent of metal distribution and factors affecting their concentrations were studied through regional sampling in the vicinity and the

`

parts of the township of Soweto. The TSF site was considered as a proxy for the general processes impacting on metal distribution in the vicinity of such sites. The results for sequential extraction of material along a flow path from the TSF to a pollution control dam and subsequently to a wetland showed that metals partitioning varied along the flow path. In the runoff pond, metals were found to be more associated with oxidisable phases (such as organics or sulphides), once released from this material, metals were transported via shallow groundwater paths to a pollution control dam in which the metals were found to be partitioned in a reducible phase (associated with iron oxyhydroxides) in the solid material.

The water samples emanating from such sites were found to mix with other water such as from domestic sources. Water draining from tailings facilities was found to portray unique chemical properties compared to the natural stream and dam water in the area. Principal component analysis was used to gain some insight into the variability of the water chemistry. Principal factors for the variation in the data were identified as solubility controls, alkalinity and dissolved oxygen. While analysis of saturation indices (using geochemical modelling) of the samples revealed that alunite, jarosite and gypsum were close to saturation in most of the samples, the distinct groups were found to be elaborated by chemometric (statistical) analysis. Therefore, a combination of these two techniques was found to be important in studying the distribution and associated chemistry of the water within the area.

During transport from TSFs, metals can be transported from and between temporary sinks before they are removed through a permanent sink. These sinks include efflorescent crusts, adsorption onto or precipitation within soil or bed material, wetlands and removal by active or passive treatment. The evaporation of shallow surface water bodies leads to the precipitation of efflorescent crusts. These crusts are quite common in the immediate vicinity around TSFs and can persist away from these sources as observed at groundwater seepage points and stream banks. The crusts essentially represent the solution from which they precipitate. These temporary sinks are discussed in the article “Mineralogy and geochemistry of efflorescent minerals on mine tailings and their potential impact

`

on water quality", published in Environmental Science and Pollution Research (2015). It was shown through geochemical modelling chemistry of the solutions resulting from the dissolution of efflorescent crusts that small amounts of metal pollutants within or existing as additional minerals to the bulk minerals could result in a significant impact on the chemistry of the water. Standard mineral identification techniques such as powder X-ray diffraction were found not to be capable of distinguishing minerals that occur in small amounts or that are in amorphous phases. Further, these techniques may not indicate the presence of metals incorporated through solid solutions. Therefore, for screening studies to identify impacted areas, one might identify the minerals and their constituents as harmless. Chemical analyses combined with geochemical modelling was used to assess the mineralogy of these minor minerals, thus providing useful information for studies where the potential release and impact of metals following the dissolution of the crusts are to be predicted. As mentioned earlier, one of the sinks for metals is a permanent type e.g. removal through active or passive treatment. In this part of the study, geochemical modelling was used to fingerprint the processes occurring in an active high density sludge treatment plant. The developed model was found to be potentially useful in future development of similar plants for treatment of AMD, for the optimisation of the costs and for prediction of material usage with respect to water chemistry.

While geochemical modelling has been shown to be a useful tool, there are various challenges that have been noted in this work. Firstly, a local thermodynamic equilibrium is assumed for modelling. Environmental samples can be in disequilibrium due to kinetic hindrances (for example, redox disequilibrium or a mineral being supersaturated and not precipitating). There is a lack of available, reliable kinetic data and as such kinetic modelling is not as utilised as it should be. Secondly, the formation of solid solutions within minerals, in particular for efflorescent salts, is a well known, widespread occurrence. Unfortunately there is little thermodynamic data available for these minerals and so the pure end members are used as proxies. There would be great difficulty in determining the thermodynamic data for solid solution minerals because of the many possible combinations that could occur. Thirdly, the commonly used

`

databases only contain surface data for hydrated ferric oxide. In this work, adsorption onto silica could have been useful. A database of sorption data for other minerals has been compiled by Helmholtz Zentrum Dresden Rossendorf called the RES^{3}T (Rossendorf Expert System for Surface and Sorption Thermodynamics (available from http://www.hzdr.de/db/RES3T.queryData). The data can be selectively included by the user into their operational databases as there are no PHREEQC or Geochemist's Workbench formats available at present.

Metal release, transport, distribution and remediation from these facilities are complex processes and will remain the subject of research on the Witwatersrand for decades to come. This research provides a repository of information about these processes involving metals. Such information is useful for risk assessment, designing remediation strategies and general public health aspects. The novelty of the work has been on the use of geochemical modelling to interrogate situations in which analytical work has fallen short. Complementing analytical work in this fashion has rarely been reported. Many modelling scripts have been written that will form important references in research, general geochemical modelling texts and teaching classes. Based on this, a geochemical modelling textbook is being compiled that will be used by researchers studying similar environments as well as for teaching environmental chemistry modules at the University of Witwatersrand and beyond. The findings for the study involving the water treatment plant have been communicated to the Trans Caledon Tunnel Authority, the parastatal that operates the AMD treatment plants. Their interest has been drawn to the potential cost optimisation and sludge reduction through geochemical modelling simulations.

`

REFERENCES

1. Abiye, T. (2014). Mine water footprint in the Johannesburg area, South Africa: analysis based on existing and measured data. *South African Journal of Geology, 117*(1), 87-96.

2. Accornero, M., & Marini, L. (2009). Empirical prediction of the Pitzer's interaction parameters for cationic Al species with both SiO2(aq) and CO2(aq): Implications for the geochemical modelling of very saline solutions. *Applied Geochemistry* (24), 747–759.

3. American Public Health Association. (1995). 3120 B. Inductively Coupled Plasma (ICP) Method. In A. D. Eaton, L. S. Clesceri & A. E. Greenberg (Eds.), *Standard methods for the examination of water and wastewater*. Baltimore: American Public Health Association; American Water Works Association; Water Environment Federation.

4. American Water Works Association. (1999). 2320 ALKALINITY #(1) *Standard Methods for the Examination of Water and Wastewater*: American Water Works Association, Water Environment Federation.

5. Anderson, P., Davidson, C. M., Duncan, A. L., Littlejohn, D., Ure, A. M., & Garden, L. M. (2000). Column leaching and sorption experiments to assess the mobility of potentially toxic elements in industrially contaminated land. *Journal of Environmental Monitoring, 2*(3), 234-239.

6. Apollaro, C., Marini, L., & De Rosa, R. (2007). Use of reaction path modeling to predict the chemistry of stream water and groundwater: a case study from the Fiume Grande valley (Calabria, Italy). *Environmental Geology, 51*, 1133-1145.

7. Appelo, C. A. J., van der Weiden, M. J. J., Tournassat, C., & Charlet, L. (2002). Surface complexation of ferrous iron and carbonate on ferrihydrite and the mobilisation of arsenic. *Environmental Science and Technology, 36*(14), 3096-3103.

8. ASTM International (Producer). (2010, June 15). ASTM D859 Standard Test Method for Silica in Water. Retrieved from http://solutions.ihs.com/document/abstract/UHLQHBAAAAAAAAAA

9. ASTM International. (2010). D1067-06: Standard test Methods for Acidity or Alkalinity of Water *Annual Book of ASTM Standards Section 11 Water and Environmental Technology* (Vol. 11.01). Baltimore: ASTM International.

10. ASTM International. (2010). D1976-07: Standard Test Method fo Elements in Water by Inductively-Coupld Argon Plasma Atomic Emission Spectroscoy *Anual Book of ASTM Standards Section 11 Water and Environmental Technology* (Vol. 11.01). Baltimore: ASTM International.

`

11. ASTM International. (2010). D4327-03 Standard Test Method for Anions in Water by Chemically Suppressed Ion Chromatograohy *Annual Book of ASTM Standards Section Eleven Water and Environmental Technology* (Vol. 11.01). Baltimore: ASTM International.

12. ASTM International. (2010). Standard Test Methods for Arsenic in Water *Annual Book of ASTM Standards Section 11 Water and Environmental Technology* (Vol. 11.01). Baltimore: ASTM International.

13. Bache, B. W. (1986). Aluminium mobilization in soils and waters. *Journal of the Geological Society, 143*(4), 699-706. doi: 10.1144/gsjgs.143.4.0699

14. Bakatula, E. N., Cukrowska, E. M., Chimuka, L., & Tutu, H. (2012). Characterization of cyanide in a natural stream impacted by gold mining activities in the Witwatersrand Basin, South Africa. *Toxicolological & Environmental Chemistry, 94*(1), 7-19.

15. Baloyi, J. N. (2006). *Spectral Interferences in ICP-OES.* Paper presented at the Analytical Challenges in Metallurgy, Randburg.

16. Benner, S. G., Blowes, D. W., Gould, W. D., Herbert, R. B., & Ptacek, C. J. (1999). Geochemistry of a permeable reactive barrier and acid mine drainage. *Environmental Science and Technology, 33*(16), 2793-2799.

17. Bethke, C. M. (1994). *The Geochemist's Workbench Version 2.0: A User's Guide to Rxn, Act2. Tact, React, and Gtplot*. Urbana: University of Illinois.

18. Bethke, C. M. (1996). *Geochemical reaction modelling: concepts and applications*. New York: Oxford University Press.

19. Bigham, J., & Nordstrom, D. K. (2000). Iron and aluminum hydroxysulfates from acid sulfate waters. *Reviews in Mineralogy and Geochemistry, 40*(1), 351-403.

20. Blowes, D., Ptacek, C., Jambor, J., & Weisener, C. (2003). The geochemistry of acid mine drainage. *Treatise on geochemistry, 9*, 149-204.

21. Blowes, D. W., Ptacek, C. J., Benner, S. G., Waybrant, K. R., & Bain, J. G. (1998). *Permeable reactive barriers for the treatment of mine tailings drainage water.* Paper presented at the Proceedings of the International Conference and Workshop on Uranium Mining and Hydogeology, Freiberg, Germany.

22. Bosman, D. (1983). Lime treatment of acid mine water and associated solids/liquid separation. *Water Science & Technology, 15*(2), 71-84.

23. Breit, G. N., Tuttle, M. L. W., Cozzarelli, I. M., Berry, C. J., Christenson, S. C., & Jaeschke, J. B. (2008). Results of the Chemical and Isotopic Analyses of Sediment and Gorund Water from Alluvium of the Canadian River Near a Closed Muncipal Landfill, Norman, Oklahoma, Part 2.

`

24. Brown, M., Barley, B., & Wood, H. (2002). *Minewater treatment: technology, application and policy*: IWA Publishing.

25. Brown, T., LeMay, H., & Bursten, B. (2006). *Chemistry The Central Science (Tenth Edition)*. United States: Pearson Prentice Hall.

26. Camden-Smith, B., Johnson, R. H., Camden-Smith, P., & Tutu, H. (2015). Geochemical Modelling of Water Quality and Solutes Transport from Mining Environments. In T. S. Lee (Ed.), Research and Practices in Water Quality: InTech. Retrieved from http://www.intechopen.com/books/research-and-practices-in-water-quality/geochemical-modelling-of-water-quality-and-solutes-transport-from-mining-environments. doi: 10.5772/59234

27. Camden-Smith, B., Mthombeni, P., Johnson, R. H., Weiersbye, I. M., & Tutu, H. (2014). *The release and transport of metals arising from gold mining tailings storage facilities in the Witwatersrand, South Africa.* Paper presented at the International Mine Water Association Proceedings: "Interdisciplinary Responses to Mine Water Challenges", Xuzhou, China.

28. Camden-Smith, B., Pretorius, N., Turton, A., Camden-Smith, P., & Tutu, H. (2015). *Chemical Transformations of Metals Leachings from Gold Tailings.* Paper presented at the Agreeing on solutions for more sustainable mine water management-Proceedings of the 10th ICARD and IMWA Annual Conference, Santiago, Chile.

29. Camden-Smith, B. P. C., Johnson, R. H., Richardson, R., Billing, D. G., & Tutu, H. (2013). *Investigating the potential impact of efflorescent mineral crusts on water quality: complementing analytical techniques with geochemical modelling.* Paper presented at the Reliable Mine Water Technology (Vol I). Denver, Colorado, USA.

30. Camden-Smith, B. P. C., & Tutu, H. (2014). Geochemical modelling of the evolution and fate of metal pollutants arising from an abandoned gold mine tailings facility in Johannesburg. *Water Science and Technology, 69*(5), 1108-1114. doi: 10.2166/wst.2014.028

31. Chamier, J., Wicht, M., Cyster, L., & Ndindi, N. P. (2015). Aluminium (Al) fractionation and speciation; getting closer to describing the factors influencing Al 3+ in water impacted by acid mine drainage. *Chemosphere, 130*, 17-23.

32. Chapman, B. M., Jones, D. R., & Jung, R. F. (1983). Processes controlling metal ion attenuation in acid mine drainage streams. *Geochimica et Cosmochimica Acta, 47*(11), 1957-1973. doi: http://dx.doi.org/10.1016/0016-7037(83)90213-2

33. Charlton, S. R., Macklin, C. L., & Parkhurst, D. L. (1997). PHREEQCI--a graphical user interface for the geochemical computer program PHREEQC.

`

34. Charlton, S. R., & Parkhurst, D. L. (2002). PHREEQCI—A Graphical User Interface to the Geochemical Model PHREEQC. Retrieved from ftp://brrftp.cr.usgs.gov/pub/dlpark/geochem/pc/phreeqc/PhreeqcI.FactSheet.pdf

35. Chatain, V., Blanc, D., Borschneck, D., & Delolme, C. (2013). Determining the experimental leachability of copper, lead, and zinc in a harbor sediment and modeling. *Environmental Science and Pollution Research, 20*(1), 66-74.

36. Clark, I., & Fritz, P. (1997). *Environmental Isotopes in Hydrogeology*. New York: Lewis Publishers.

37. Cocksedge, J. (1988). Design and production of synthetic rainwater, LR 684 (CS), Department of Trade and Industry, Warren Spring Laboratory: HMSO.

38. Cravotta III, C., Means, B. P., Arthur, W., McKenzie, R. M., & Parkhurst, D. L. (2014). AMDTreat 5.0+ with PHREEQC titration module to compute caustic chemical quantity, effluent quality, and sludge volume. *Mine Water and the Environment, 34*(2), 136-152.

39. Crawford, J. (1999). Geochemical Modelling – A Review of Current Capabilities and Future Directions. *Natur Vards Verket (Swedish Environmental Protection Agency)*. Retrieved from http://www.swedishepa.se/Documents/publikationer/afr-r-262-se.pdf

40. CSIR. (2009). Acid Mine Drainage in South Africa. Briefing Note 02/2009, from http://www.csir.co.za/nre/docs/BriefingNote2009_2_AMD_draft.pdf

41. Cukrowska, E., Lusilao-Makiese, J., Tutu, H., Chimuka, L., & Weiersbye, I. (2015). *Biogeochemical Cycle of Mercury in Wetlands Ecosystem Affected by Gold Mining in a Semi-arid area.* Paper presented at the Agreeing on solutions for more sustainable mine water management – Proceedings of the 10th ICARD & IMWA Annual Conference, Santiago, Chil.

42. Cukrowska, E., Lusilao-Makiese, J., Yalala, B., Tutu, H., & Chimuka, L. (2013). *Characterisation and modelling of mercury speciation in urban air affected by gold mining-assessment of bioavailability.* Paper presented at the E3S Web of Conferences.

43. Cukrowska, E. M., Govender, K., & Viljoen, M. (2004). Ion mobility based on column leaching of South African gold tailings dam with chemometric evaluation. *Chemosphere, 56*(1), 39-50. doi: http://dx.doi.org/10.1016/j.chemosphere.2004.01.036

44. Davidson, C. M., Hursthouse, A. S., Tognarelle, D. M., Ure, A. M., & Urquhart, G. J. (2004). Should acid ammonium oxalate replace hydroxylammonium chloride in step 2 of the revised BCR sequential extraction protocol for soil and sediment? *Analytica Chimica Acta, 508*(2), 193-199.

`

45. de Jager, F. S. J. (1986). The East Rand Goldfield and the South Rand Goldfield. In E. S. A. Antrobus (Ed.), *Witwatersrand Gold- 100 years* (pp. 111-172). Johannesburg: The Geological Society of South Africa.

46. Debye, P., & Huckel, E. (1923). On the theory of electrolytes. *Phys.Z*(24), 185-206.

47. Diehl, S. F., Hageman, P. L., & Smith, K. S. (2008). Chapter A: What is weathering in mine waste? Mineralogic Evidence for Sources of Metals in Leachates *Understanding contaminants associated with mineral deposits: U.S. Geological Survey Circular 1328*. Reston, Virginia: U.S. Geological Survey.

48. Dudka, S., & Adriano, D. C. (1997). Environmental Impacts of Metal Ore Mining and Processing: A Review. *Journal of Environmental Quality, 26*(3), 590-602.

49. Durand, J. F. (2012). The impact of gold mining on the Witwatersrand on the rivers and karst system of Gauteng and North West Province, South Africa. *Journal of African Earth Sciences, 68*, 24-43.

50. Dybowska, A., Farago, M., Valsami-Jones, E., & Tho, Dybowska, A., Farago, M., Valsami-Jones, E., & Thornton, I. (2005). Operationally defined associations of arsenic and copper from soil and mine waste in south-west England. *Chemical Speciation and Bioavailability, 17*(4), 147-160.

51. Dzombak, D., & Morel, F. M. M. (1990). Hydrous Ferric Oxide *Surface Complex Modeling*: Wiley-Interscience.

52. Engelbrecht, C. J. (1986). Chapter VI: The West Wits Line. In E. S. A. Antrobus (Ed.), *Witwatersrand Gold- 100 years* (pp. 199-224). Johannesburg: The Geological Society of South Africa.

53. Evangelou, V. P. (1998). Pyrite Chemistry: The Key for Abatement of Acid Mine Drainage. In W. Geller, H. Klapper & W. Salomons (Eds.), *Acidic Mining Lakes: Acid Mine Drainage, Limnology and Reclamation* (pp. 197-222). Berlin, Heidelberg: Springer Berlin Heidelberg.

54. Expert Team of the Inter-Ministerial Committee. (2010). Mine water management in the Witwatersrand Gold Fields with special emphasis on acid mine drainage. *Report to the Inter-Ministerial Committee on Acid Mine Drainage. Pretoria: Department of Water Affairs*.

55. Feather, C., & Koen, G. (1975). The mineralogy of the Witwatersrand reefs. *7*, 189-224.

56. Filgueiras, A. V., Lavilla, I., & Bendicho, C. (2002). Chemical sequential extraction for metal partitioning in environmental solid samples. *Journal of Environmental Monitoring, 4*, 823–857.

`

57. Förstner, U., & Wittmann, G. T. W. (1979). Metal accumulations in acidic waters from gold mines in South Africa. *Geoforum, 7*(1), 41-49.

58. Freeze, R. A., & Cherry, J. A. (1979). *Groundwater*. New York: Prentice-Hall.

59. Frimmel, H. E. (2005). Archaean atmospheric evolution: evidence from the Witwatersrand gold fields, South Africa. *Earth-Science Reviews, 70*, 1-46. doi: 10.1016/j.earscirev.2004.10.003

60. GCS (Pty) Ltd. (2011). Update of the Sulphate Groundwater Plume Delineation for the AngloGold Ashanti Vaal River and West Wits Operations: GCS (Pty) Ltd.

61. Gran, G. (1952). Determination of the equivalence point in potentiometric titrations. Part II. *Analyst, 77*(920), 661-671.

62. Grover, B., Johnson, R., Billing, D., Weiersbye, I., & Tutu, H. (2015). Mineralogy and geochemistry of efflorescent minerals on mine tailings and their potential impact on water chemistry. *Environmental Science and Pollution Research*, 1-11. doi: 10.1007/s11356-015-5870-z

63. Grover, B. P. C., Johnson, R. H., & Tutu, H. (2016). Leachability of metals from gold tailings by rainwater: an experimental and geochemical modelling approach. *WaterSA, 42*.

64. Grundl, T., & Delwiche, J. (1993). Kinetics of ferric oxyhydroxide precipitation. *Journal bf Contaminant Hydrology,, 14*, 71-97.

65. Hageman, P. L. (2007). U.S. Geological Survey field leach test for assessing water reactivity and leaching potential of mine wastes, soils, and other geologic and environmental materials *U.S. Geological Survey Techniques and Methods, Book 5, Chapter D3*. Reston, Virginia: U.S. Geological Survey.

66. Hammarstrom, J. M., Sibrell, P. L., & Belkin, H. E. (2003). Characterisation of limestone reacted with acid-mine drainage in apulsed limestone bed treatment system at the Friendship Hill National Historical Site, Pennsylvania, USA. *Applied Geochemistry, 18*, 1705-1721.

67. Harris, D. C. (2007). *Quantitative Chemical Analysis*. New York: W.H. Freeman and Company.

68. Harris, D. L., Lottermoser, B. G., & Duchesne, J. (2003). Ephemeral acid mine drainage at the Montalbion silver mine, north Queensland. *Australian Journal of Earth Sciences, 50*(5), 797-809. doi: 10.1111/j.1440-0952.2003.01029.x

69. Harvie, C. E., & Weare, J. H. (1980). The prediction of mineral solubilities in natural waters: the Na–K–Mg–Ca–Cl–SO4–H2O system from zero to high concentration at 25 C. *Geochim. Cosmochim. Acta*(44), 981–997.

`

70. Huang, C., Pan, J., Sun, K., & Liaw, C. (2001). Reuse of water treatment plant sludge and dam sediment in brick-making. *Water Science & Technology, 44*(10), 273-277.

71. Jager, F. S. J. d. (1986). The East rand Goldfield and The South Rand Goldfield *Witwatersrand Gold- 100 Years*. Johannesburg: The Geological Society of South Africa.

72. Jambor, J. L., Nordstrom, D. K., & Alpers, C. N. (2000). Metal-sulfate Salts from Sulfide Mineral Oxidation. *Reviews in Mineralogy and Geochemistry, 40*(1), 303-350.

73. Janisch, P. R. (1986). Gold in South Africa. *Journal of the South African Institute of Mining and Metallurgy, 89*(6), 273-316.

74. Johnson, D. B., & Hallberg, K. B. Pitfalls of passive mine water treatment. [journal article]. *Reviews in Environmental Science and Biotechnology, 1*(4), 335-343. doi: 10.1023/a:1023219300286

75. Johnson, D. B., & Hallberg, K. B. (2005). Acid mine drainage remediation options: a review. *Science of the Total Environment*(338), 3-14. doi: doi:10.1016/j.scitotenv.2004.09.002

76. Johnson, R. (2011). *Reactive Transport Modeling for the Proposed Dewey Burdock Uranium In-Situ Recovery Mine, Edgemont, South Dakota, USA*, Aachen, Germany.

77. Jones, A. M., Collins, R. N., & Waite, T. D. (2011). Mineral species control of aluminum solubility in sulfate-rich acidic waters. *Geochimica et Cosmochimica Acta, 75*(4), 965-977.

78. Kalin, M., Fyson, A., & Wheeler, W. N. (2006). The chemistry of conventional and alternative treatment systems for the neutralization of acid mine drainage. *Science of the Total Environment, 366*(2), 395-408.

79. Kempe, J. (1983). Review of water pollution problems and control strategies in the South African mining industry. *Water Science & Technology, 15*(2), 27-58.

80. Kostenbader, P., & Haines, G. (1970). High density sludge treats acid mine water. *Coal Age, September, 90*.

81. Langmuir, D., Hall, P., & Drever, J. (1997). *Environmental Geochemistry*: Prentice Hall, New Jersey.

82. Lednor, M. (1986). Chapter III: The West Rand Goldfield. In E. S. A. Antrobus (Ed.), *Witwatersrand Gold- 100 years* (pp. 49-110). Johannesburg: The Geological Society of South Africa.

83. Leinz, R. W., Sutley, S. J., Desborough, G. A., & Briggs, P. A. (2000). *An Investigation of the Partitioning of Metals in Mine Wastes Using Sequential*

Extractions. Paper presented at the In Proceedings from the Fifth International Conference on Acid Rock Drainage, Littleton, Colorado.

84. Lippard, S., & Bery, J. (1994). *Principles of Bioinorganic Chemistry*: University Science Books.

85. Lottermoser, B. G. (2005). Evaporative mineral precipitates from a historical smelting slag dump, Río Tinto, Spain. *Neues Jahrbuch fur Mineralogie - Abhandlungen: Journal of Mineralogy and Geoche, 181*(2), 183-190. doi: 10.1127/0077-7757/2005/0016

86. Macey, R., Oster, G., & Zahnley, T. (2009). Berkeley Madonna User's Guide.

87. Machemer, S. D., & Wildeman, T. R. (1992). Adsorption compared with sulfide precipitation as metal removal processes from acid mine drainage in a constructed wetland. *Journal of Contaminant Hydrology, 9*(1), 115-131.

88. Majzlan, J., Navrotsky, A., McCleskey, R. B., & Alpers, C. N. (2006). Thermodynamic properties and crystal structure refinement of ferricopiapite, coquimbite, rhomboclase, and Fe2(SO4)3(H2O)5. *Eur. J. Mineral., 18*, 175-186.

89. Maku, L. (2009). An Investigation of the Water Quality and Acid Mine Drainage at Khutala Colliery Block I: A Former Opencast Coal Mine Currently Under Rehabilitation (Honour's Project). Johannesburg: University of the Witwatersrand.

90. Margui, E., Queralt, I., Carvalho, M. L., & Hidalgo, M. (2006). Assessment of metal availability to vegetation (Betula pendula) in Pb–Zn ore concentrate residues with different features. *Environmental Pollution, 145*(1), 179-184.

91. Marsden, D. (1986). The current limited impact of Witwatersrand gold-mine residues on water pollution in the Vaal River system. *Journal of the South African Institute of Mining and Metallurgy, 86*, 481-504.

92. Mays, P., & Edwards, G. (2001). Comparison of heavy metal accumulation in a natural wetland and constructed wetlands receiving acid mine drainage. *Ecological Engineering, 16*(4), 487-500.

93. McCarthy, T. S. (2006). The Witwatersrand Supergroup. In M. R. Johnson, C. R. Anhaeusser & R. J. Thomas (Eds.), *The Geology of South Africa* (pp. 155-186): Geological Society of South Africa, Johannesburg/Council for Geoscience, Pretoria.

94. McCarthy, T. S. (2011). The impact of acid mine drainage in South Africa. *South African Journal of Science, 107*(5/6), 1-7.

95. Merkel, B. J., & Planer-Friedrich, B. (2005). *Groundwater Geochemistry*. Netherlands: Springer.

`

96. Mike, D. (1987). The application of inductively coupled plasmas to the analysis of natrual waters and acidic deposition *Chemical analysis in environmental research* (pp. 40-49): Institute of Terrestrial Ecology Symposium, 18.

97. Mossop, K. F., & Davidson, C. M. (2003). Comparison of original and modified BCR sequential extraction procedures for the fractionation of copper, iron, lead, manganese and zinc in soils and sediments. *Analytica Chimica Acta, 478*(1), 111-118.

98. Mphephu, N. F. (2004). *Geotechnical environmental evaluation of mining impacts on the Central Rand.* PhD, University of the Witwatersrand, Johannesburg.

99. Muetzelfeldt, R. I., & Massheder, J. (2003). The Simile visual modelling environment. *European Journal of Agronomy, 18*, 345-358.

100. Murdock, D., Fox, J., & Bensley, J. (1994). *Treatment of acid mine drainage by the high density sludge process.* Paper presented at the International Land Reclamation and Mine Drainage Conference and the Third International Conference on the Abatement of Acidic Drainage, Pittsburgh, PA.

101. Naicker, K., Cukrowska, E., & McCarthy, T. S. (2003). Acid mine drainage arising from gold mining activity in Johannesburg, south Africa and environs. *Environmental Pollution, 122*(1), 29-40. doi: 10.1016/S0269-7491(02)00281-6

102. Neculita, C.-M., Zagury, G. J., & Bussière, B. (2007). Passive Treatment of Acid Mine Drainage in Bioreactors using Sulfate-Reducing Bacteria: Critical Review and Research Needs. *Journal of Environmental Quality, 36*(1), 1-16.

103. Nengovhela, A., Yibas, B., & Ogola, J. (2007). Characterisation of gold tailings dams of the Witwatersrand Basin with reference to their acid mine drainage potential, Johannesburg, South Africa. *Water SA, 32*(4).

104. Nesse, W. (2000). *Introduction to Mineralogy*. New York: Oxford University Press.

105. Nordstrom, D. K. (2007). 5.02- Modeling Low-Temperature Geochemical Processes *Treatise on Geochemistry* (pp. 1-38). Pargamon: Oxford.

106. Nordstrom, D. K. (2008). Acid rock drainage and climate change. *Journal of Geochemical Exploration, 100*(2–3), 97-104. doi: http://dx.doi.org/10.1016/j.gexplo.2008.08.002

107. Nordstrom, D. K. (2009). Acid rock drainage and climate change. *Journal of Geochemical Exploration, 100*(2–3), 97-104. doi: http://dx.doi.org/10.1016/j.gexplo.2008.08.002

`

108. Nordstrom, D. K. (2011). Hydrogeochemical processes governing the origin, transport and fate of major and trace elements from mine wastes and mineralized rock to surface waters. *Applied Geochemistry, 26*, 1777-1791.

109. Nordstrom, D. K., & Campbell, K. M. (2014). Modeling Low-Temperature Geochemical Processes. In K. K. Turekian (Ed.), *Treatise on Geochemistry (2nd Ed)*. Oxford: Elsevier.

110. Nordstrom, D. K., Jenne, E. A., & Ball, J. W. (1979). Redox Equilibria of Iron in Acid Mine Waters *Chemical Modeling in Aqueous Systems* (Vol. 93, pp. 51-79): American Chemical Society.

111. Nordstrom, D. K., Mc Nutt, R. H., Puigdomenech, I., Smellie, J. A. T., & Wolf, M. (1992). Ground water chemistry and geochemical modeling of water-rock interactions at the Osamu Utsumi mine and the Morro do Ferro analogue study sites, Poços de Caldas, Minas Gerais, Brazil. *Journal of Geochemical Exploration*(45), 249-287.

112. Nordstrom, D. K., & Munoz, J. L. (1986). *Geochemical Thermodynamics*. Palo Alto: Blackwell Scientific Publications.

113. Nordstrom, D. K., & Southam, G. (1997). Geomicrobiology of sulfide mineral oxidation. *Reviews in mineralogy, 35*, 361-390.

114. Oelofse, S., Hobbs, P., Rascher, J., & Cobbing, J. (2007). *The Pollution and Destruction Threat of Gold Mining Waste on the Witwatersrand: A West Rand Case Study.* Paper presented at the 10th International Symposium on Environmental Issues and Waste management in Energy and Mineral Production (SWEMP, 2007), Bangkok.

115. Ojelede, M. E., Annegarn, H. J., & Kneen, M. A. (2012). Evaluation of aeolian emissions from gold mine tailings on the Witwatersrand. *Aeolian Research, 3*(4), 477-486. doi: http://dx.doi.org/10.1016/j.aeolia.2011.03.010

116. Oreskes, N., Shrader-Frechette, K., & Belitz, K. (1994). Verification, Validation and Confirmation of Numerical Models in the Eartch Sciences. *Science, 263*(5147), 641-646.

117. Parkhurst, D. L., & Appelo, C. (1999). *User's guide to PHREEQC (Version2)—A computer program for speciation, batch-reaction, one-dimensional transport, and inverse geochemical calculations.*

118. Parkhurst, D. L., & Appelo, C. A. J. (2013). Description of input and examples for PHREEQC version 3- A computer program for speciation, batch-reaction, one-dimensional transport, and inverse geochemical calculations. *U.S. Geological Survey Techniques and Methods* Retrieved 2 February 2015, 2015, from http://pubs.usgs.gov/tm/06/a43

119. Parkhurst, D. L., Plummer, L. N., & Thorstenson, D. C. (1980). PHREEQE—A Computer Program for Geochemical Calculations. *Water-Resour. Invest.* (pp. 80-96): USGS.

120. Paschke, A. (2002). Chapter 7. Physiochemical properties of aqueous and solid environmental matrices *Sampling and sample preparation for field and laboratory: fundamental and new directions in sample preparation*. Amsterdam: Elsevier Science B.V.

121. Pitzer, K. (1979). Theory: Ion Interaction Approach In R. M. Pytkowicz (Ed.), Activity Coefficients in Electrolyte Solutions: CRC Press, Boca Raton, FL.

122. Pitzer, K. S. (1973). Thermodynamics of electrolytes. Part I: Theoretical basis and general equations. *J. Phys. Chem.*(77), 268–277.

123. Pretorius, D. A. (1964). The Geology of the Central Rand Goldfield. In S. H. Haughton (Ed.), *The Geology of Some Ore Deposits in Southern Africa* (Vol. 1, pp. 63-108): Geol. Soc. S. Afr.

124. Pueyo, M., Rauret, G., Luck, D., Yli-Halla, M., Muntau, H., Quevauviller, P., & Lopez-Sanchez, J. F. (2001). Certification of the extractable contents of Cd, Cr, Cu, Ni, Pb and Zn in a freshwater sediment following a collaboratively tested and optimised three-step sequential extraction procedure. *Journal of Environmental Monitoring, 2*(3), 243–250.

125. Rao, C. R. M., Sahuquillo, A., & Lopez Sanchez, J. F. (2008). A Review of the Different Methods Applied in Environmental Geochemistry For Single and Sequential Extraction of Trace Elements in Soils and Related Materials. *Water, Air & Soil Pollution*(189), 291–333.

126. Rauret, G., Lopez-Sanchez, J. F., Sahuquillo, A., Rubio, R., Davidson, C., Ure, A., & Quevauviller, P. (1999). Improvement of the BCR three step sequential extraction procedure prior to the certification of new sediment and soil reference materials. *Journal of Environmental Monitoring,, 1*(1), 57-61.

127. Reeder, R. J., Schoonen, M. A. A., & Lanzirotti, A. (2006). Metal Speciation and Its Role in Bioaccessibility and Bioavailability. *Reviews in Mineralogy and Geochemistry, 64*, 59-113.

128. Reid, M. K., Spencer, K. L., & Shotbolt, L. (2011). An appraisal of microwave-assisted Tessier and BCR sequential extraction methods for the analysis of metals in sediments and soils. *Journal of Soils and Sediments, 11*(3), 518-528.

129. Robb, L. (2005). *Introduction to Ore-Forming Processes*. Singapore: Blackwell Science.

130. Rösner, T., & Van Schalkwyk, A. (2000). The environmental impact of gold mine tailings footprints in the Johannesburg region, South Africa. *Bulletin of Engineering Geology and the Environment, 59*(2), 137-148.

131. Ross, D. S., & Ketterings, Q. (1995). Recommended Methods for Determining Soil Cation Exchange Capacity *Recommended Soil Testing*

Procedures for the Northern United States (pp. 75-86). Newark: University of Deaware.

132. Rounds, S. A. (2012). Alkalinity and acid neutralising capacity (version 4.0). In F. D. Wilde & D. B. Radtke (Eds.), National field manual for the collection of water-quality data: U.S. Geological Survey Techniques of Water-Resources Investigations Retrieved from http://water.usgs.gov/owg/FieldManual/Chapter6/section6.6/.

133. Rull, F., Guerrero, J., Venegas, G., Gázquez, F., & Medina, J. (2014). Spectroscopic Raman study of sulphate precipitation sequence in Rio Tinto mining district (SW Spain). *Environmental Science and Pollution Research, 21*(11), 6783-6792.

134. Runkel, R. L., & Kimball, B. A. (2002). Evaluating Remedial Alternatives for an Acid Mine Drainage Stream: Application of a Reactive Transport Model. *Environmental Science and Technology, 36*(5), 1093-1101.

135. Rykiel, E. J. J. (1996). Testing ecological models: the meaning of validation. *Ecological Modelling*(90), 229-244.

136. SA Weather Bureau. (1998). Climate of South Africa. Weather Bureau Publication WB40. Pretoria.

137. South African National Standard: Drinking Water, Part 1: Microbiological, physical, aesthetic and chemical determinands, Local Government: Muncipal Structures Act (Act No 117 of 1998) and Water Services Act (Act No 108 of 1997) C.F.R. (2011).

138. Salmon, S. U., & Malmstrom, M. E. (2004). Geochemical processes in mill tailings deposits: modelling of groundwater composition. *Applied Geochemistry, 19*, 1-17.

139. Salomons, W. (1995). Environmental impact of metals derived from mining activites: Processes, predictions, prevention. *Journal of Geochemical Exploration, 52*, 5-23.

140. Sánchez España, J., & Diez Ercilla, M. (2008). Chapter 2: Geochemical modeling of concentrated mine waters: A comparison of the Pitzer Ion-Interaction Theory with the Ion-Association Model for the study of melanterite solubility in San Telmo Mine (Huelva, Spain) *Geochemistry Research Advances* (pp. 1-25): Nova Science Publishers, Inc.

141. Schultz, M. K., Burnett, W., Inn, K. G. W., & Smith, G. (1998). Geochemical partitioning of actinides using sequential chemical extractions. Comparison to stable elements. *Journal of Radioanalytical and Nuclear Chemistry, 234*(1-2), 251-256.

142. Scott, R. (1995). Flooding of Central and East Rand gold mines: An investigation into controls over the inflow rate, water quality and the

predicted impacts of flooded mines. South Africa: Water Research Commission.

143. Sheoran, A., & Sheoran, V. (2006). Heavy metal removal mechanism of acid mine drainage in wetlands: a critical review. *Minerals engineering, 19*(2), 105-116.

144. Singer, P. C., & Stumm, W. (1970). Acidic Mine Drainage: The rate determining step. *Science, 167*.

145. Soriano, M. A., & Fereres, E. (2003). Use of Crops for In Situ Phytoremediation of Polluted Soils Following a Toxic Flood from a Mine Spill. *Plant and Soil, 256*, 253-264.

146. Šráček, O., Černík, M., & Vencelides, Z. (2013). *Applications of Geochemical and Reactive Transport Modeling in Hydrogeology (1st edition)*. Olomouc, Czech Republic: Palacký University.

147. Stanton, M. R. (2008). Chapter D: Bacterial processes can influence the movement of metal contaminants in wetlands that have been affected by acid drainage *Understanding contaminants associated with mineral deposits: U.S, Geological Circular 1328*. Reston, Virginia: U.S. Geological Survey.

148. Stumm, W., & Morgan, J. J. (1996). Aquatic chemistry, chemical equilibria and rates in natural waters. *Env. Sci. Technol*.

149. Stumm, W., & Morgan, J. J. (1996). *Aquatic Chemistry: Chemical Equilibria in Natural Waters. 3rd ed*. New York: Wiley.

150. Sutton, M. (2008). Use of Remote Sensing and GIS in a Risk Assessment of Gold and Uranium Mine Residue Deposits and Identification of Vulnerable Land Use. Johannesburg.

151. Suttons, M., Weiersbye, I. M., Galpin, J. S., & Heller, D. (2006). A GIS-Based History of Gold Mine Residue Deposits and Risk Assessment of Post-Mining Land-Uses on the Witwatersrand Basin, South Africa. *Mining Closure*, 667-678.

152. Swanson, D., Barbour, S., & Wilson, G. (1997). *Dry-site versus wet-site cover design.* Paper presented at the Proceedings of 4th Int. Conference of Acid Rock Drainage p. 1595.

153. Terry, N., Sambukumar, S. V., & LeDuc, D. L. (2003). Biotechnological Approaches for Enhancing Phytoremediation of Heavy Metals and Metalloids. *Acta Biotechnol, 23*(2-3), 281-288.

154. Tessier, A., Campbell, P. G. C., & Bisson, M. (1979). Sequential Extraction Procedure for the Speciation of Particulate Trace Metals. *Analytical Chemistry, 51*(7), 844-851.

`

155. Tipping, E. (1994). WHAM—a chemical equilibrium model and computer code for waters, sediments and soils incorporating binding by humic substances. *Comput. Geosci.*(20), 973–1023.

156. Tonkin, J. W., Balistrieri, L. S., & Murray, J. W. (2002). Modeling Metal Removal onto Natural Particles during Mixing of Acid Rock Drainage with Ambient Surface Water. *Environmental Science and Technology, 36*(3), 484-492.

157. Turton, A. (2013). Debunking Persistent Myths about AMD in the Quest for a Sustainable Solution. *SAWEF Paradigm Shifter Series, 1*(1).

158. Tutu, H. (2006). *Determination and geochemical modelling of the dispersal of uranium in gold mine polluted land on the Witwatersrand Basin.* Ph.D Ph.D, University of the Witwatersrand, Johannesburg.

159. Tutu, H., Camden-Smith, B. P. C., Cukrowska, E. M., Bakatula, E. N., Weiersbye, I. M., & Sutton, M. S. (2011). *Mineral efflorescent crusts as sources of pollution in gold mining environments in the Witwatersrand Basin.* Paper presented at the International Mine Water Association Proceedings: "Mine Water – Managing the Challenges", Aachen, Germany.

160. Tutu, H., McCarthy, T. S., & Cukrowska, E. (2008). The chemical characteristics of acid mine drainage with particular reference to sources, distribution and remediation: The Witwatersrand Basin, South Africa as a case study. *Applied Geochemistry*, 3666-3684.

161. U.S. Environmental Protection Agency. (2002). Test methods for evaluating solid wastes, physical and chemical methods. Retrieved from http://www.epa.gov/epawaste/hazard/testmethods/sw846/pdfs/1312.pdf.

162. van der Lee, J., & De Windt, L. (2001). Present state and future directions of modeling of geochemistry in hydrogeological systems. *Journal of Contaminant Hydrology, 47*(2-4), 265-2852.

163. van der Sloot, H. A., & van Zomeren, A. (2012). Characterisation Leaching Tests and Associated Geochemical Speciation Modelling to Assess Long Term Release Behaviour from Extractive Wastes. *Mine Water Environ, 31*, 92-103.

164. Vorster, C. J. (2000). Gold Deposits of the Witwatersrand Basin Retrieved 12/08, 2015

165. Wardencki, W., & Namiesnik, J. (2002). Chapter 2. Sampling water and aqueous solutions *Sampling and sample preparation for field and laboratory: fundamental and new directions in sample preparation*. Amsterdam: Elsevier Science B.V.

166. Warren, J. K. (2006). *Evaporites- Sediments, resources and hydrocarbons*. New York: Springer.

`

167. Waters, A., & Webster-Brown, J. (2013). Assessing aluminium toxicity in streams affected by acid mine drainage. *Water Science & Technology, 67*(8), 1764-1772.

168. Weiersbye, I. M. (2008). An Overview of Phyto-technologies Applicable to Mine Remediation in Southern Africa. Johannesburg: University of the Witwatersrand.

169. Weiersbye, I. M., Margalit, N., Feingersh, T., G, R., Stark, R., Zur, Y., . . . Cukrowska, E. M. (2006). Use of Airborne Hyper-Spectral Remore Sensing (HSRS) to Focus Remediation and Monitor Vegetation Processes on Gold Mining Landscapes in South Africa. *Mine Closure*.

170. Werdmuller, V. W. (1986). Chapter II: The Central Rand. In E. S. A. Antrobus (Ed.), *Witwatersrand Gold- 100 years* (pp. 7 - 47). Johannesburg: The Geological Society of South Africa.

171. Wolkersdorfer, C. (2008). *Water management at abandoned flooded underground mines: fundamentals, tracer tests, modelling, water treatment*. Heidelberg: Springer Science & Business Media.

172. Wood, S. A., Taunton, A. E., Normand, C., & Gunter, M. E. (2006). Mineral-Fluid Interaction in the Lungs: Insights from Reaction-Path Modeling. *Inhalation Toxicology*, 975-984.

173. Wright, C. Y., Matooane, M., Oosthuizen, M. A., & Phala, N. (2014). Risk perceptions of dust and its impacts among communities living in a mining area of the Witwatersrand, South Africa. *24*(1), 22-27. Retrieved from http://reference.sabinet.co.za/webx/access/electronic_journals/cleanair/cleanair_v24_n1_a6.pdf

174. Yager, T. R. (2011). The Mineral Industry of South Africa *2009 Area Reports- International- Africa and the Middle East: U.S. Geological Survey Minerals Yearbook v.III* (pp. 349): U.S. Geological Survey.

175. Yibas, B., Pulles, W., Lorentz, S., Maiyana, B., & Nengovhela, C. (2012). *Oxidation process and hydrology of tailings dams: Implications for acid mine drainage from TSFs management - The Witwatersrand Experience, South Africa.* Paper presented at the International Mine Water Association.

176. Younger, P. L., Jayaweera, A., Elliot, A., Wood, R., Amos, P., Daugherty, A. J., & Johnson, D. B. (2003). Passive treatment of acidic mine waters in subsurface-flow systems: exploring RAPS and permeable reactive barriers. *Land Contamination and Reclamation, 11*(2), 127-135.

177. Zaluski, M., Trudnowski, J., Harrington-Baker, M., & Bless, D. (2003). *Post-mortem findings on the performance of engineered SRB field-bioreactors for acid mine drainage control.* Paper presented at the Proceedings of the 6th International Conference on Acid Rock Drainage, Cairns, QLD.

`

178. Zhu, C., & Anderson, G. (2002). *Environmental Applications of Geochemical Modeling*. Cambridge, United Kingdom: The Press Syndicate of the University of Cambridge.

179. Zygmunt, B., & Namiesnik, J. (2002). Sampling selected solid materials *Sampling and sample preparation for field and laboratory: fundamental and new directions in sample preparation*. Amsterdam: Elsevier Science B.V.

`

APPENDICES

List of appendices:

Table A.1: Summarised analysis procedure for chemical composition determinations of alkalinity and anions 197
Table A.2: Summarised analysis procedure for chemical composition determinations of metals 198
Table A.3: Spectral line wavelengths for ICP-OES analysis of metal concentrations 199

Figure A.1: PXRD pattern of unoxidised tailings material 203
Figure A.2: PXRD pattern of oxidised tailings material 203
Figure A.3: PXRD pattern of efflorescent crust 1 (original sample) 204
Figure A.4: PXRD pattern of efflorescent crust 1 after dissolution, filtration and evaporation 204
Figure A.5: PXRD pattern of efflorescent crust 2 (original sample) 205
Figure A.6: PXRD pattern of efflorescent crust 2 after dissolution, filtration and evaporation 205
Figure A.7: PXRD pattern of efflorescent crust 3 (original sample) 206
Figure A.8: PXRD pattern of efflorescent crust 3 after dissolution, filtration and evaporation 206
Figure A.9: PXRD pattern of efflorescent crust 4 (original sample) 207
Figure A.10: PXRD pattern of efflorescent crust 4 after dissolution, filtration and evaporation 207
Figure A.11: PXRD pattern of efflorescent crust 5 (original sample) 208
Figure A.12: PXRD pattern of efflorescent crust 6 (original sample) 208
Figure A.13: PXRD pattern of efflorescent crust 6 after dissolution, filtration and evaporation 209
Figure A.14: PXRD pattern of efflorescent crust 7 (original sample) 209
Figure A.15: PXRD pattern of efflorescent crust 7 after dissolution, filtration and evaporation 210
Figure A.16: Sample PHREEQC script for inverse modelling between pond sample and batch leachates (in Chapter 4.2.1) 211
Figure A.17: PHREEQC script for speciation solubility modelling of boreholes A and B (in Chapter 5.1.1) 212
Figure A.18: PHREEQC script for inverse modelling between pollution control dam and inlet streams 213
Figure A.19: PHREEQC script for forward modelling of mixing of inlet streams using the ratio derived from inverse modelling 214
Figure A.20: PHREEQC script for solubility analysis for evaporation modelling of dissolved crust solution 215
Figure A.21: PHREEQC script for mineral precipitation during evaporation modelling of dissolved crust solution 215
Figure A.22: Example PHREEQC script for forward modelling of the first and final model for efflorescent crust dissolution 216
Figure A.23: PHREEQC script for forward modelling of a high density sludge acid mine drainage treatment facility 217

`

Table A.1: Summarised analysis procedure for chemical composition determinations of alkalinity and anions

Analyte or parameter	Storage container and preservation (Wardencki, et al., 2002)	Maximum holding time	Standard method for analysis	Summarised procedure
Alkalinity	Polyethylene or borosilicate glass	24 hours	ASTM D1067-06	ASTM International, 2010
Anions				
Bromide				
Chloride	Polyethylene or borosilicate glass	15 days		
Fluoride	Polyethylene	7 days		
Nitrate	Polyethylene or borosilicate glass, 4°C	48 hours	ASTM D4327-03	Chemically suppressed ion chromatography (ASTM International, 2010)
Nitrite	Polyethylene or borosilicate glass, 4°C	24 hours		
Phosphate	Polyethylene or glass, 4°C	48 hours		
Sulphate	Polyethylene, 4°C	6 days		

`

Table A.2: Summarised analysis procedure for chemical composition determinations of metals

Analyte or parameter	**Storage container and preservation** (Wardencki, et al., 2002)	**Maximum holding time**	**Standard method for analysis**	**Summarised procedure**
Arsenic	Polyethylene or borosilicate glass; HCl (pH <2)	2 months	ASTM D1976-07	Inductively-Coupled Argon Plasma Atomic Emission Spectroscopy (ASTM International, 2010)
Aluminium Cadmium Chromium Cobalt Copper Iron Magnesium Manganese Nickel Vanadium Zinc	Polyethylene or borosilicate glass, HNO_3 (pH<1.5), 4°C	2 months	ASTM D1976-07	Simultaneous determination by inductively-coupled argon plasma atomic emission spectroscopy (ASTM International, 2010)
Lead Potassium Silica Sodium	(For Si: Polyethylene, 4°C)	7 days	3120 B	Inductively Coupled Plasma Method (American Public Health Association, 1995)
Uranium			D6239-09	

`

Table A.3: Spectral line wavelengths for ICP-OES analysis of metal concentrations

Element	Measured lines (nm)	Line of reported value (nm)	Description
Ag	328.06 and 338.289	Averaged	In most cases, values were below the detection limit.
Al	394.401 and 396.152	396.152	Standard Al solutions were prepared, less error associated with 369.152 nm line.
As	189.042 and 193.759	189.042	Al is a known interferent for the 193 nm spectral line. In cases where high Al concentration were measured, greater As values were detected for the 193 nm line but not for the 189 nm line.
Au	242.795 and 267.595	267.595	In most cases, values were below the detection limit.
Ba	230.424, 233.527 and 455.404	455.404	Blank checks gave positive values of 0.006 mg/L.
Be	313.042	313.042	
Bi	223.061	223.061	
Ca	393.366 and 396.847	Averaged	In high ionic strength solutions, measurements within calibration limits for the 393.366 nm line were noted but out of bounds for 396.847 nm line. However, upon dilution both spectral lines returned values within calibration boundaries which do not differ significantly. In these cases, the initial 393.366 nm measurement was neglected and the reported value is that of the diluted run.
Cd	214.438 and 226.502	226.502	Spectral line 214.438 nm provides higher positive measurements than 226.502 nm, especially in samples with high iron concentrations.
Ce	418.660 and 448.691	418.660	Values for the two lines were significantly different.
Co	228.616	228.616	
Cr	267.716	267.716	
Cs	455.531	455.531	
Cu	219.958, 224.700 and	224.700 nm and 324.754	The values for the 219.958 nm line were significantly different to the 224.700 nm and 324.754 nm lines.

`

Element	Measured lines (nm)	Line of reported value (nm)	Description
	324.754	nm were averaged	
Eu	381.967 and 420.505	420.505	Values for 381.967 were significantly higher than those of 420.505 nm.
Fe	238.204 and 259.941	Averaged	
Ga	417.206	417.206	
Gd	335.047 and 342.247	Averaged	In some cases, values for the two lines were significantly different and no value has been reported.
Ge	219.871 and 265.118	265.118	Values for the two lines were significantly different.
Hg	184.950 and 253.652	No values reported	Mercury required a specialised analysing technique and has been neglected.
In	230.606	230.606	
Ir	212.681 and 263.971	212.681	Values for 263.971 nm were significantly higher than those of 212.681 nm.
K	766.491	766.491	
Li	670.780	670.780	
Mg	279.553	279.553	
Mn	257.611 and 259.373	Averaged	
Mo	202.095	202.095	
Na	588.995 and 589.592	Averaged	
Ni	227.021 and 231.604	Averaged	
Os	225.585 and 228.226	228.226	Values for the two lines were significantly different. In most cases, values for the 228.226 nm were below the detection limit.
P	177.495 and 178.287	177.495	Values for the two lines were significantly different.
Pb	220.353 and 405.778	Averaged	In most cases, values for the 228.226 nm were below the detection limit.
Pd	340.458 and 360.955	360.955	Values for the two lines were significantly different.

`

Element	Measured lines (nm)	Line of reported value (nm)	Description
Pt	214.423 and 265.945	265.945	Values for the two lines were significantly different.
Rb	198.319	198.319	
Rh	343.489	343.489	
Ru	240.272	240.272	
S	180.731 and 182.034	Averaged	
Sb	217.581	217.581	
Sc	335.373 and 361.384	361.384	Values for the two lines were significantly different.
Se	196.090 and 207.479	196.090	Values for the two lines were significantly different.
Si	251.612 and 288.158	Averaged	In some cases, the values for the two lines were significantly different.
Sn	189.991	189.991	
Sr	407.771	407.771	
Ta	240.063	240.063	
Te	214.281	214.281	
Th	401.913	401.913	
Ti	334.941 and 336.121	Averaged	
Tl	190.864	190.864	
U	367.007, 385.958 and 409.014	385.958	The three spectral lines differ significantly from one another. The 385.958 nm line provided consistently lower concentrations and has been reported.
V	292.402 and 292.464	292.464	Iron is a known interferent for the 292.402 nm spectral line. Samples with high iron values had a higher concentration for the 292.402 nm line than the 292.464 nm line.
W	224.875	224.875	
Y	371.030 and 377.433	Averaged	
Zn	202.613 and 213.856	202.613	Copper is a know interferent for the 213.856 nm spectral line. Samples with high copper values had a significant difference between the zinc spectral lines.

`

Element	Measured lines (nm)	Line of reported value (nm)	Description
Zr	339.198 and 343.823	Averaged	In solutions with a high metal content, significant differences between the two spectral lines were noted. In such cases, the lower value was reported.

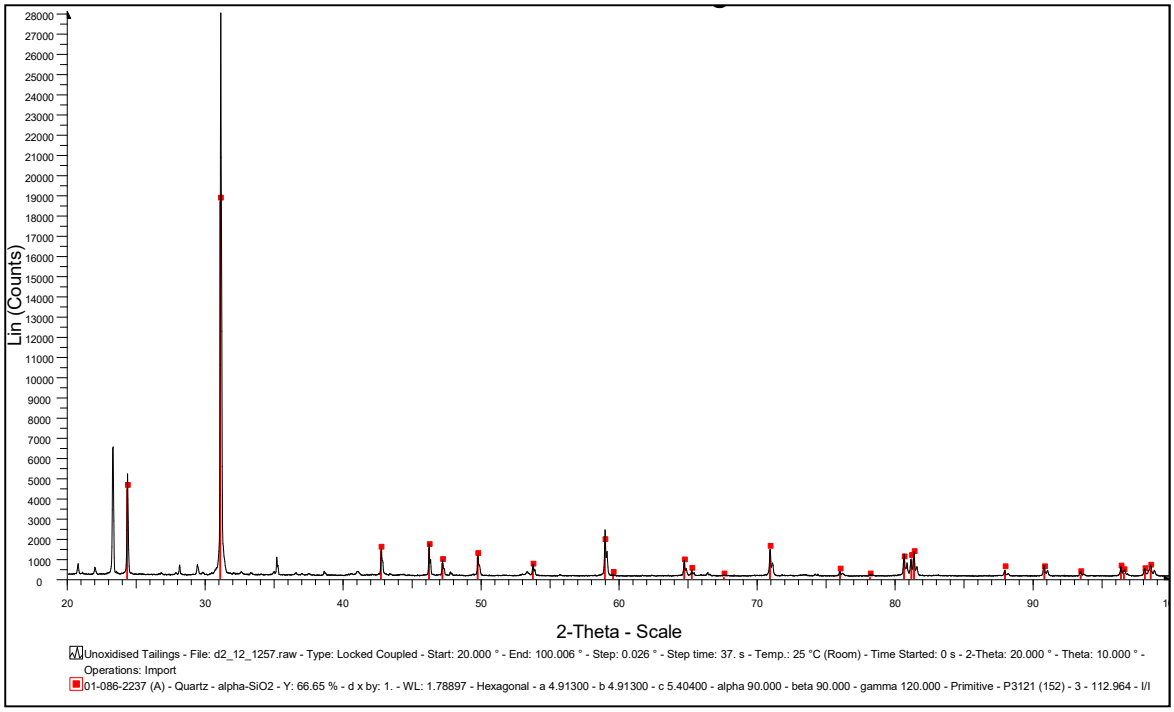

Figure A.1: PXRD pattern of unoxidised tailings material

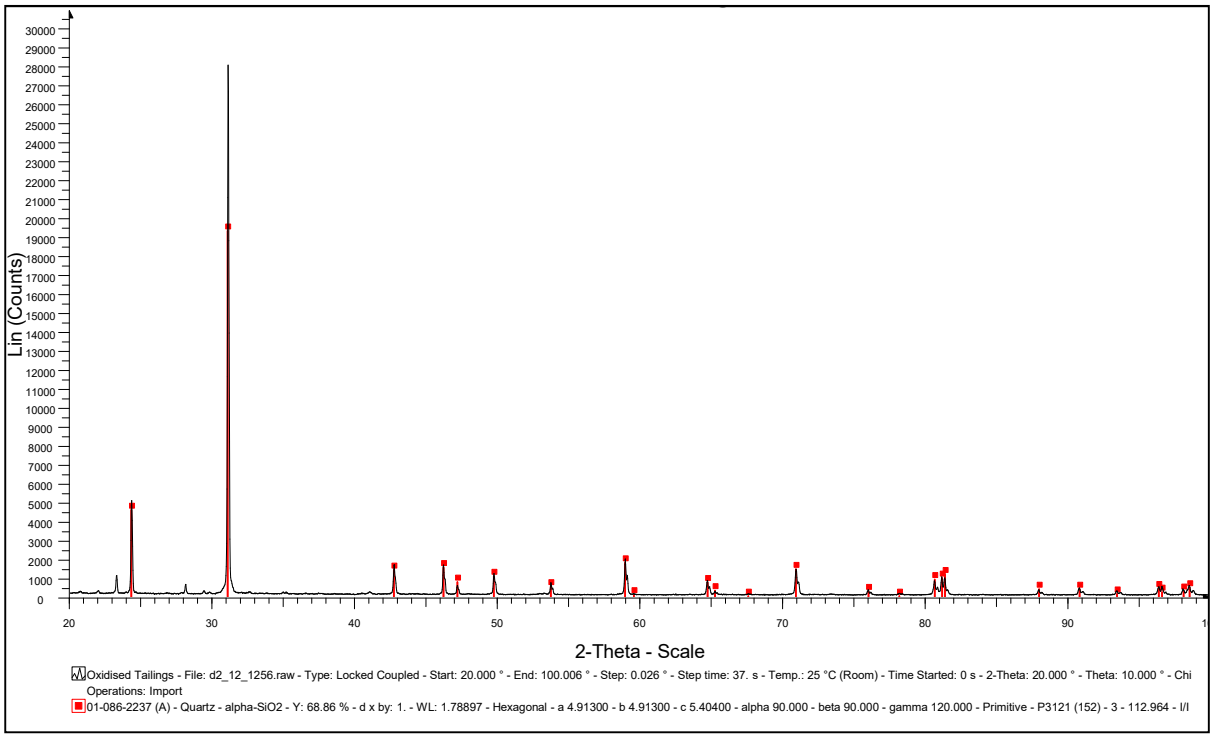

Figure A.2: PXRD pattern of oxidised tailings material

`

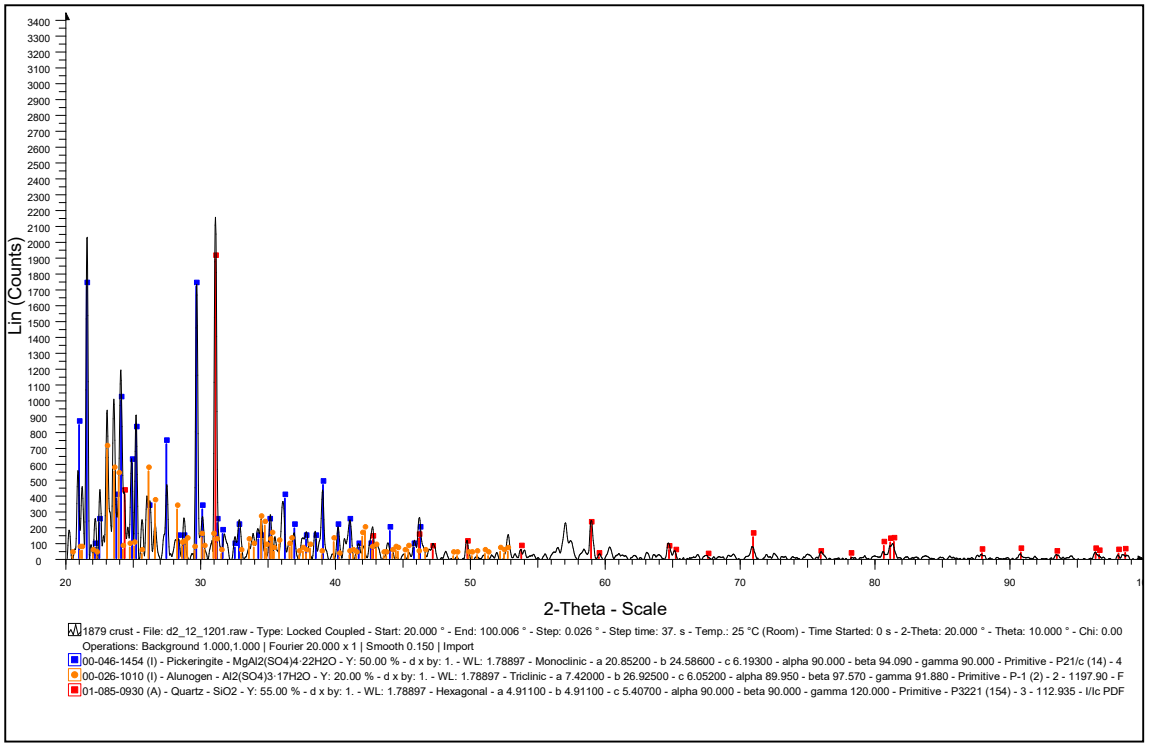

Figure A.3: PXRD pattern of efflorescent crust 1 (original sample)

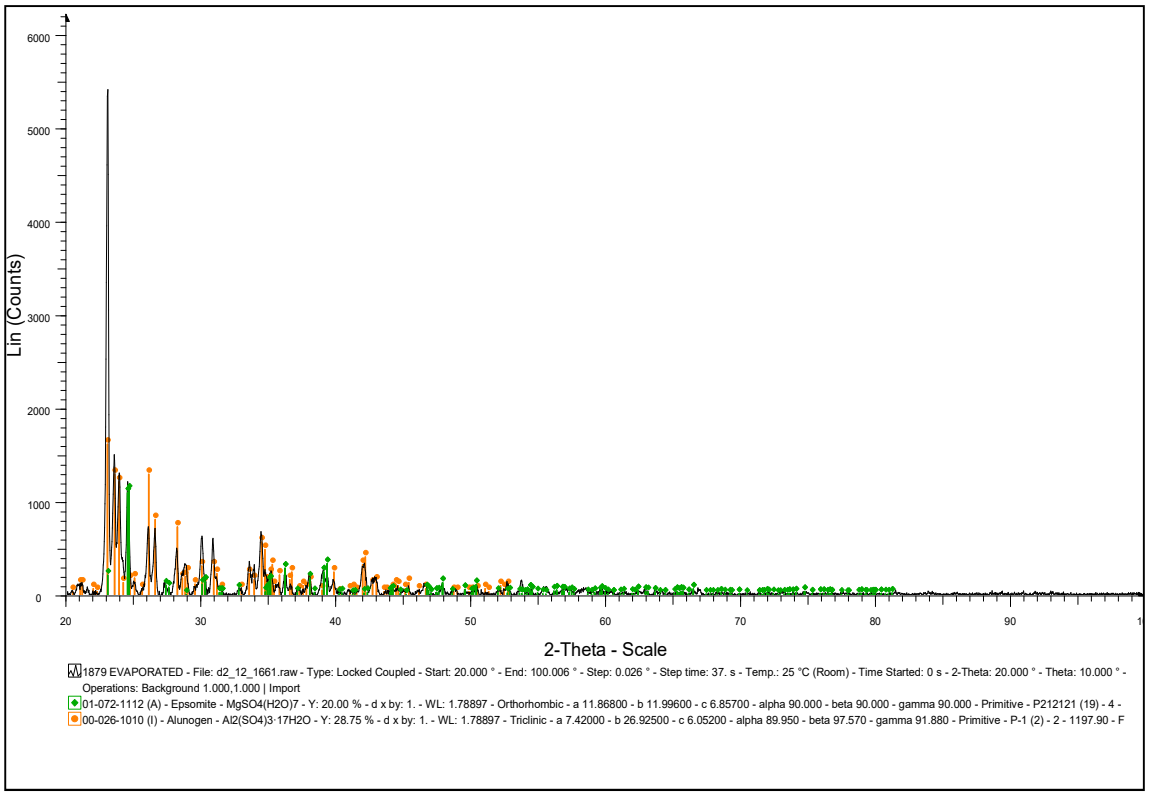

Figure A.4: PXRD pattern of efflorescent crust 1 after dissolution, filtration and evaporation

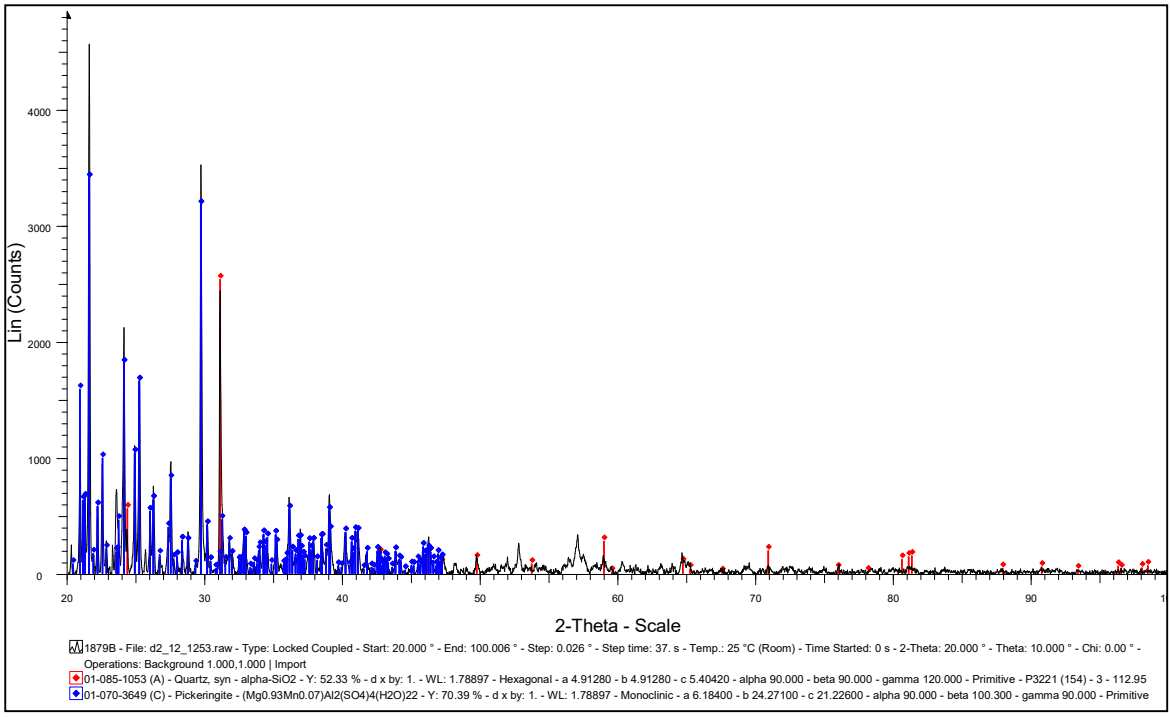

Figure A.5: PXRD pattern of efflorescent crust 2 (original sample)

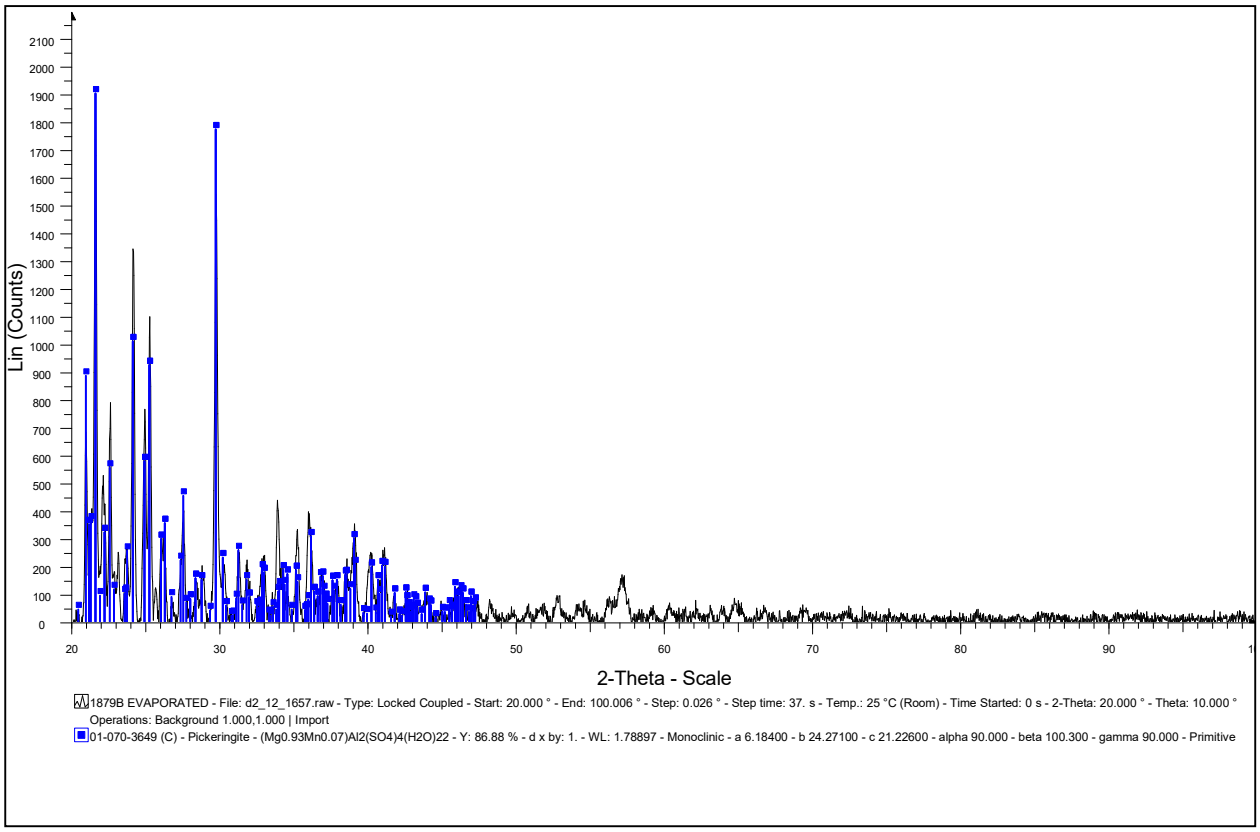

Figure A.6: PXRD pattern of efflorescent crust 2 after dissolution, filtration and evaporation

`

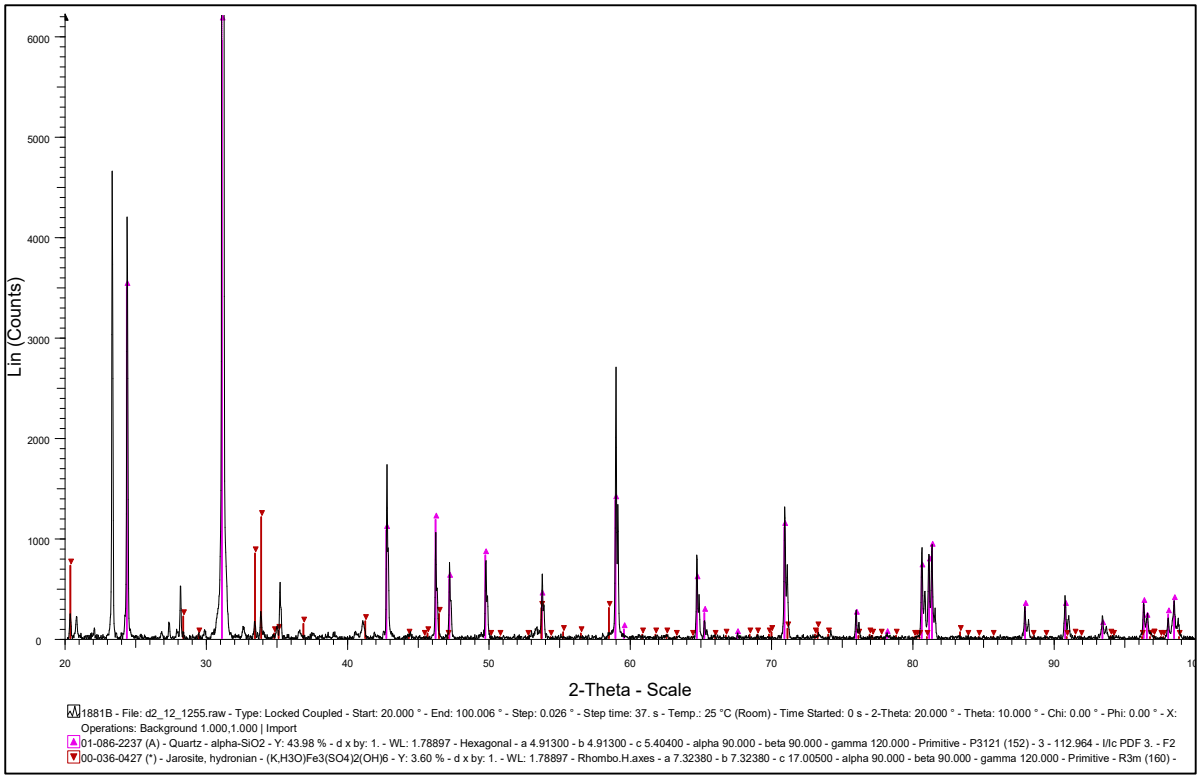

Figure A.7: PXRD pattern of efflorescent crust 3 (original sample)

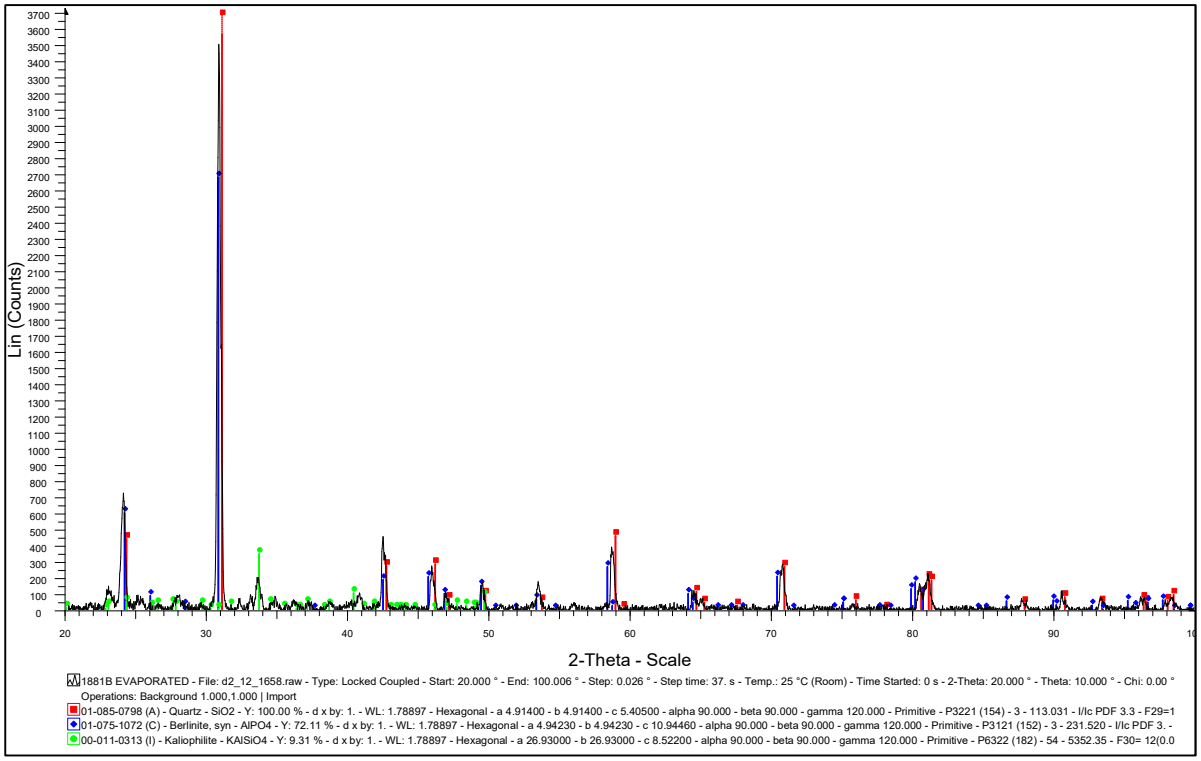

Figure A.8: PXRD pattern of efflorescent crust 3 after dissolution, filtration and evaporation

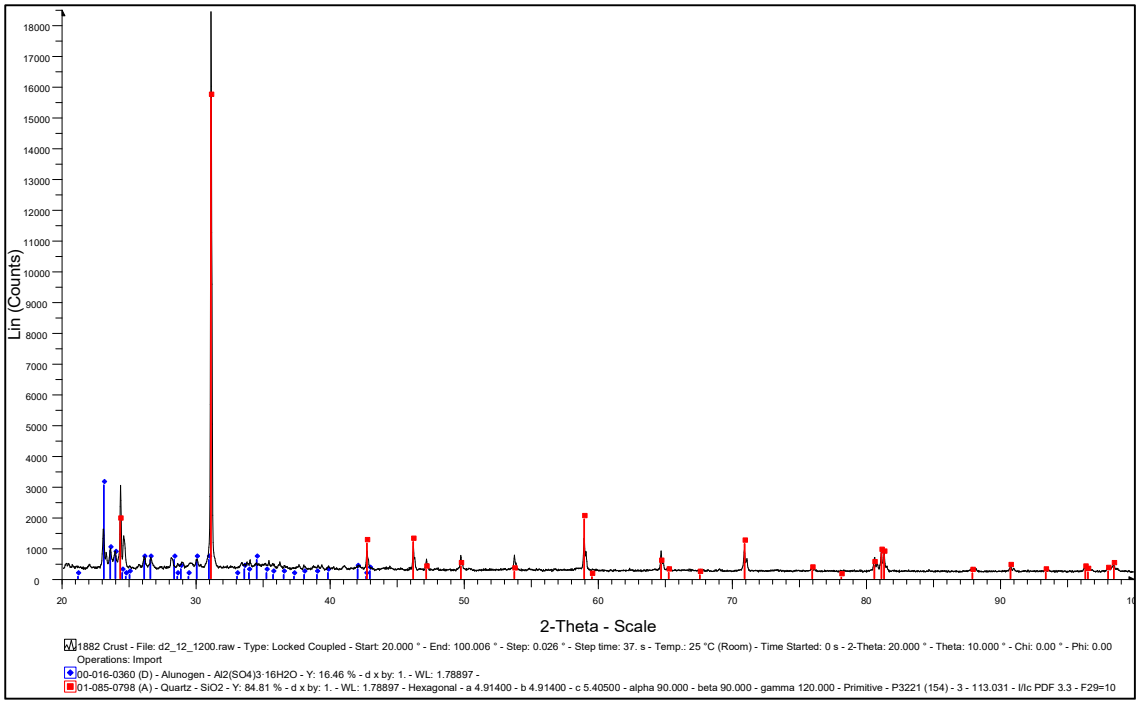

Figure A.9: PXRD pattern of efflorescent crust 4 (original sample)

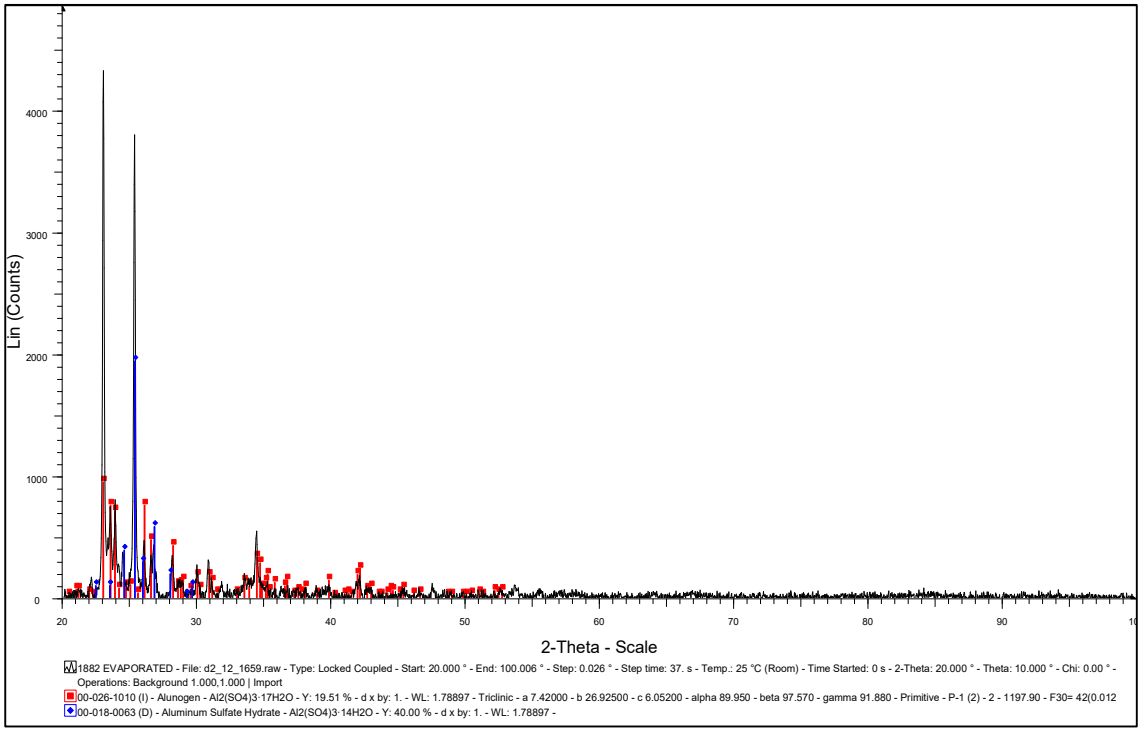

Figure A.10: PXRD pattern of efflorescent crust 4 after dissolution, filtration and evaporation

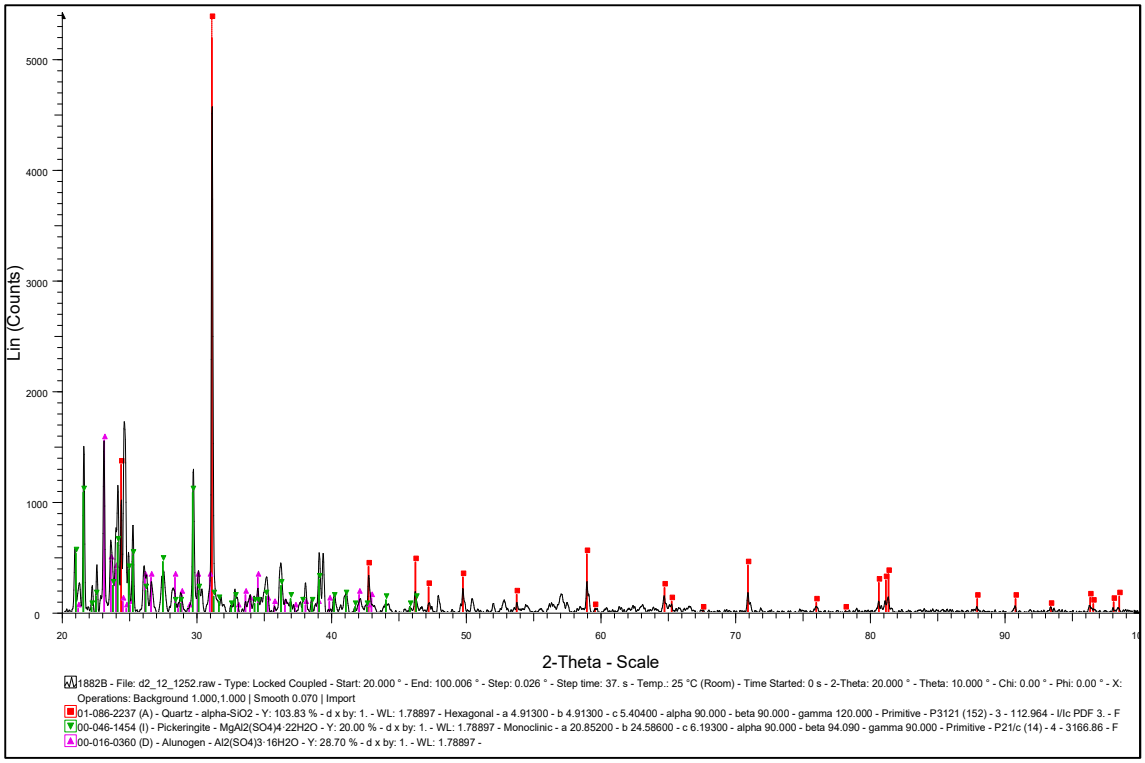

Figure A.11: PXRD pattern of efflorescent crust 5 (original sample)

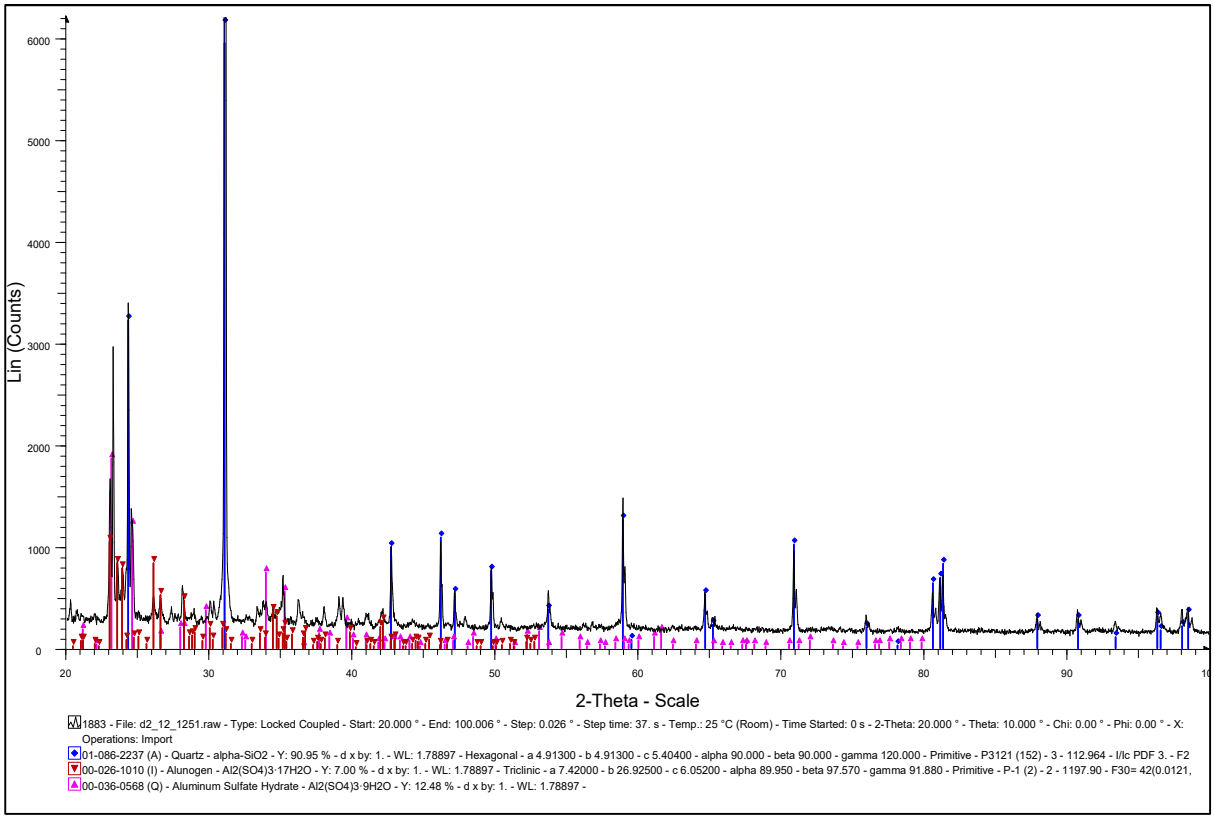

Figure A.12: PXRD pattern of efflorescent crust 6 (original sample)

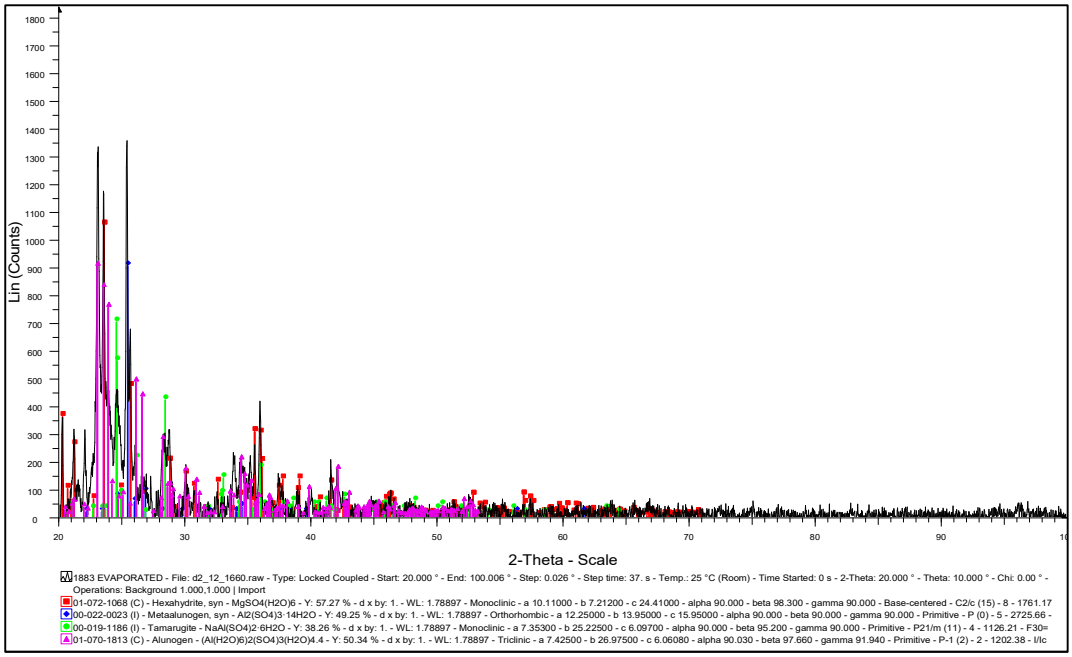

Figure A.13: PXRD pattern of efflorescent crust 6 after dissolution, filtration and evaporation

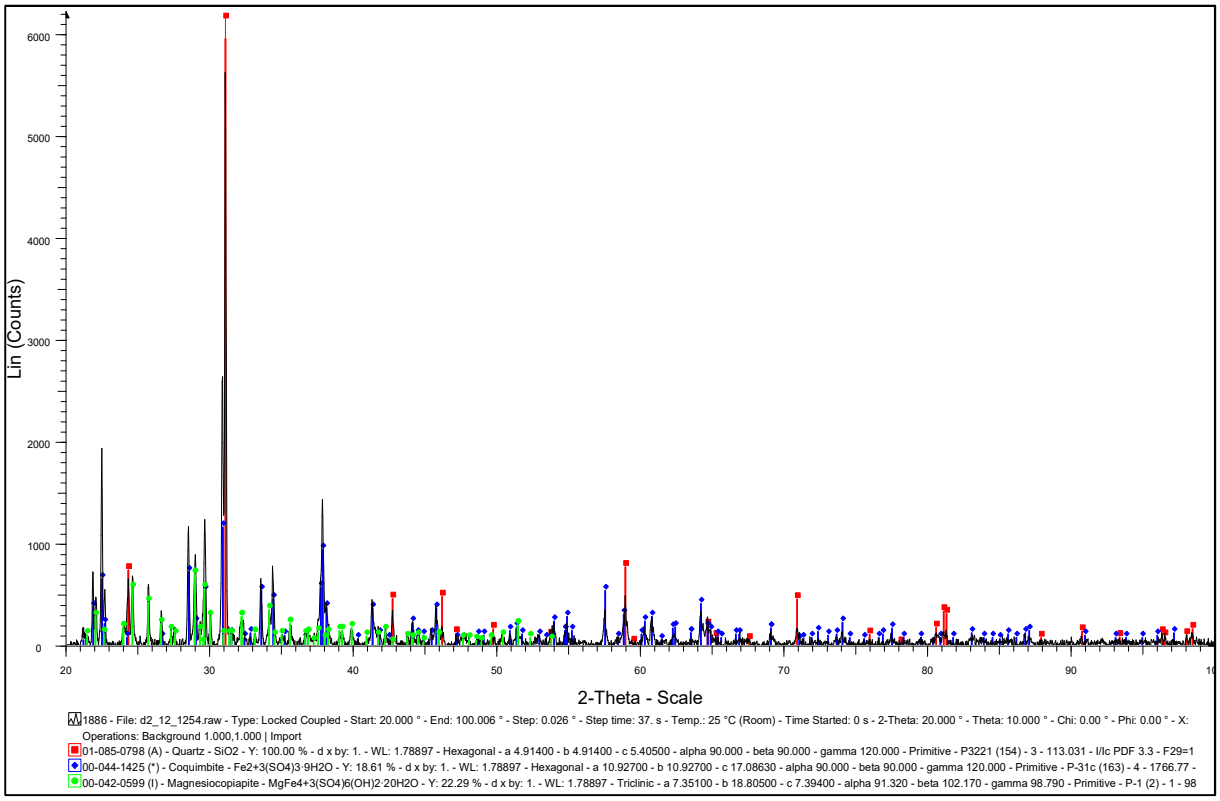

Figure A.14: PXRD pattern of efflorescent crust 7 (original sample)

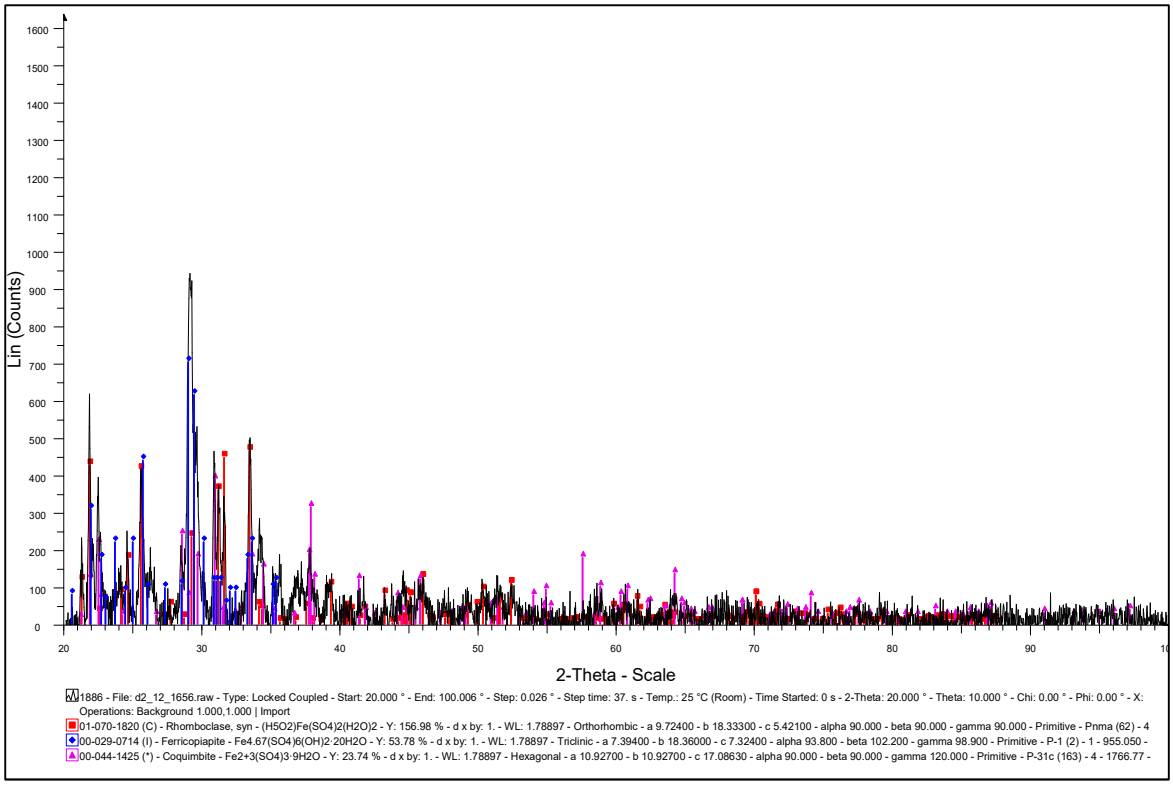

Figure A.15: PXRD pattern of efflorescent crust 7 after dissolution, filtration and evaporation

`

```
SOLUTION_SPREAD
    -units    ug/l
                Description      pH      pe     Number     Al        Ca          Co      Cu        Fe          K        Mg          Mn      Na      Ni      Si          S        Zn
                                                                                                                                                                as SO4 charge
          OT Deionised Water     3.7     7.2         1  18942    7367.5       408.7   298.0       0.0       320.8  12158.8       579.8     0.0   797.7    79.9       117445    172.2
          UT Deionised Water     4.1     7.2         2  10357    4358.3       713.4   126.9    5466.2       416.0  23369.7      2673.3   388.2  1848.3    96.9        78199   1235.8
     OT Artificial Rainwater     3.6     7.4         3  21675       0.0       469.2   291.2      25.6      3780.4  13964.5       655.4   126.5   903.0     0.1       108648    186.3
     UT Artificial Rainwater     3.9     7.3         4   1750   12578.0       840.2    62.5    2240.6      1910.4  14273.9      3249.9   622.3  2066.6     0.1        63407   2777.4
 OT Sulphuric Acid (pH 2.85)     2.9     7.6         5  26127    8923.0       458.4   438.1     958.9         0.0  15466.9       697.7     0.0   895.7   113.2       128963      0.0
 UT Sulphuric Acid (pH 2.85)     3.6     7.4         6   2663   16928.5       824.1   189.5   29839.2         0.0   9121.0      4520.9   338.2  2055.5   155.2        60984   1160.9
 OT Calcium chloride (0.01M)     3.7     7.1         7  12817   27554.8         0.0     0.0       0.0         0.0  15106.6       196.6     0.0     0.0     0.0       138372      0.0
 UT Calcium chloride (0.01M)     4.5     7.0         8   1484   18600.1         0.0     0.0    1191.1         0.0   6941.3      2267.7     0.0  1083.2     0.0        28976      0.0

SOLUTION_SPREAD
    -redox    Fe(2)/Fe(3)
    -units    mg/l
  pH        pe          S(6)          Al             Ca        Co          Cu       K      Mg      Mn          Na       Ni          Si          Zn     Number          Fe
                  as SO4 charge                                                                                                                          Fe(2)/Fe(3)
 3.7     10.44           3550   238.1666667    0.852666667     11.49   5.443333333    15.57   226.6   35.55   29.96666667    21.36   0.744166667    24.63333333         13          2.1

END
MIX 1
    1    1
SAVE solution 15

(in the original script, each solution was mixed and saved)


PHASES
Water
    H2O = H2O
    log_k     1
    delta_h   0 kJ
    -analytical_expression 1 0 0 0 0 0

INVERSE_MODELING 1
    -solutions      15      19      16      20      17      18      23
    -uncertainty    0.08    0.08    0.08    0.08    0.08    0.08    0.08
    -phases
        Water
        CdSO4:H2O
        Chalcanthite
        Epsomite
        Gypsum
        CoSO4:6H2O
        Quartz
        MnSO4
        NiSO4
        Goethite
        Al2(SO4)3:6H2O
        Jarosite
        Jarosite-Na
        Fe2(SO4)3
        Zn2SO4(OH)2
        ZnSO4:7H2O
        Alunite
    -tolerance          1e-010
    -mineral_water      false
    -multiple_precision     true
    -mp_tolerance 1e-012
    -censor_mp 1e-020
```

Figure A.16: Sample PHREEQC script for inverse modelling between pond sample and batch leachates (in Chapter 4.2.1)

```
# Inverse model of VRM 38 to Searsia D
SOLUTION_SPREAD
    -temp      22
    -units     mg/l
 Description        pH        pe              Alkalinity          Cl      S(6)        Al          Ca          Co          Cu          Fe          K          Mg          Mn          Na          Number
                                          as Ca0.5(CO3)0.5                                                                          pe
    VRM 38 A      4.03    6.6248                                  410      4720    52.875       569.5         5.9       0.291       5.975        49.4       596.5         330       622.5          1
   Searsia D      6.67      6.76                   148            230      2202                 639.5       0.295       0.085       0.025          12         393      1.7925        62.5          6

END
USE solution 1
MIX 1
    1    1
END
USE solution 6
MIX 2
        6       1

END
```

Figure A.17: PHREEQC script for speciation solubility modelling of boreholes A and B (in Chapter 5.1.1)

`

```
SOLUTION_SPREAD
    -units    mg/l
 Number         Description        Temperature      pH      pe      O(0)       Cl      S(6)      Al      Ca      Co      Cu      Fe      K      Mg      Mn      Na      Ni      U      Zn
      1               CAMS 1               23.8     2.7    10.6     6.5     13.0    2129.0    34.7    522.0    2.4     2.6     57.0    5.0    20.1     2.4     22.1    2.6     0.0    0.0
      2               CAMS 2               23.8     2.7    10.3     6.5     13.0    2256.0    53.4    531.3    2.5     2.6     51.6    5.3    29.8     3.5     31.6    4.5     0.0    0.0
      3            LC Dam 1                24.4     2.3    11.2     6.7     86.0    8000.0    528.8   582.5    14.5    6.3     322.5   3.0    225.0    74.5    79.3    25.6    0.0    0.0
      4            LC Dam 2                24.4     2.3    11.3     6.8     63.0    7401.0    467.5   550.0    13.3    5.9     312.5   2.5    212.5    66.9    72.2    23.0    0.0    0.0
      5      Muncipal Waste                24.4     4.3     8.4     6.8     658.0   4671.0    77.6    602.7    6.6     2.4     425.9   286.9  190.9    96.3    350.7   11.5    0.0    0.0
      6    25M4 (Porewater)                17.9     3.6     9.3             9.0     899.0     9.2    306.0    1.1     0.4     15.7    7.5    7.7      5.3     2.7     2.2     0.2    2.7
      7    25M5 (Porewater)                17.5     3.5     9.3             9.5     907.5     20.4   252.0    0.9     1.0     6.8     3.8    14.8     2.3     20.6    2.1     0.5    2.3
      8                25M6                25.6     3.4     7.6     5.6     17.5    1146.0    10.9    463.5    0.9     0.6     1.9     8.3    14.6     1.6     47.1    1.9     0.8    2.1
      9                25M7                23.8     3.4     7.7     7.0     15.0    982.5     9.6     335.7    0.8     0.4     5.1     5.0    13.1     1.6     33.3    2.1     0.5    1.8
     10                25M8                22.4     3.4     7.8     7.2     12.5    992.0     9.7     313.5    0.8     0.4     5.5     5.3    13.3     1.5     0.0     1.9     0.5    1.7
     11                25M9                26.5     2.7     11.6    6.7     36.0    2406.0    143.7   324.6    3.8     2.1     109.2   9.3    69.0     17.4    28.2    7.0     1.3    7.5
     12   25M10 (Porewater)                18.7     2.3     11.4    6.7     30.0    7800.0    495.0   265.5    7.2     8.2     1360.5  7.9    66.0     25.4    5.3     11.5    0.0    15.9
     13   25M11 (Porewater)                17.5     2.3     11.6    6.7     15.0    6840.0    447.8   191.3    7.5     7.8     1306.4  1.5    40.4     15.4    4.2     7.2     2.6    9.8
     14               25M12                25.8     3.5     9.3     3.6     28.0    3326.0    83.4    573.9    4.6     0.1     78.0    2.3    324.6    66.0    0.0     10.3    0.0    5.6
     15               25M13                25.1     3.0     9.1     4.7     8.0     2658.0    277.1   241.3    8.1     0.8     2.3     0.9    54.6     21.6    11.0    22.5    0.0    17.4
     16               25M14                26.6     2.7     11.4    6.8     36.0    2365.0    179.6   405.5    3.8     2.1     127.8   9.7    87.3     18.0    29.0    7.4     1.3    7.8
     17               25M15                28.1     2.6     11.0    4.0     98.0    6710.0    350.0   651.8    21.8    4.1     360.3   7.8    526.5    138.3   60.3    51.8    0.0    38.0
     18               25M17                25.8     2.7     10.9    6.6     36.0    2425.0    122.0   290.7    3.8     2.0     77.0    13.0   63.0     19.1    34.0    7.4     1.3    8.2
     19               25M18                24.3     2.7     10.3    6.4     35.0    2373.0    166.2   378.9    3.9     2.1     139.5   9.5    79.8     18.4    30.2    7.4     1.3    7.8


INVERSE_MODELING 1
    -solutions      14      15      18      16
    -uncertainty    0.07    0.07    0.1     0.1
    -phases
        Fe(OH)3
        Cd(OH)2
        Gypsum
        Chalcanthite
        Mn(OH)2(am)
        Epsomite
        UO2(OH)2(beta)
        NiSO4
        ZnSO4
        Bieberite
        H2O(g)
        Gibbsite
        Alunite

    -balances
        Cl(-1)      0.05    0.05    0.05    0.1
        Na          0.05    0.05    0.05    0.1
    -tolerance        1e-10
    -mineral_water    true
```

Figure A. 18: PHREEQC script for inverse modelling between pollution control dam and inlet streams

`

```
SOLUTION_SPREAD
    -units    mg/l
 Number         Description        Temperature      pH      pe      O(0)       Cl      S(6)       Al       Ca       Co       Cu       Fe        K       Mg       Mn       Na       Ni        U       Zn
      1                CAMS 1               23.8     2.7    10.6     6.5     13.0   2129.0     34.7    522.0      2.4      2.6     57.0      5.0     20.1      2.4     22.1      2.6      0.0      0.0
      2                CAMS 2               23.8     2.7    10.3     6.5     13.0   2256.0     53.4    531.3      2.5      2.6     51.6      5.3     29.8      3.5     31.6      4.5      0.0      0.0
      3              LC Dam 1               24.4     2.3    11.2     6.7     86.0   8000.0    528.8    582.5     14.5      6.3    322.5      3.0    225.0     74.5     79.3     25.6      0.0      0.0
      4              LC Dam 2               24.4     2.3    11.3     6.8     63.0   7401.0    467.5    550.0     13.3      5.9    312.5      2.5    212.5     66.9     72.2     23.0      0.0      0.0
      5        Muncipal Waste               24.4     4.3     8.4     6.8    658.0   4671.0     77.6    602.7      6.6      2.4    425.9    286.9    190.9     96.3    350.7     11.5      0.0      0.0
      6   25M4 (Porewater)                  17.9     3.6     9.3             9.0    899.0      9.2    306.0      1.1      0.4     15.7      7.5      7.7      5.3      2.7      2.2      0.2      2.7
      7   25M5 (Porewater)                  17.5     3.5     9.3             9.5    907.5     20.4    252.0      0.9      1.0      6.8      3.8     14.8      2.3     20.6      2.1      0.5      2.3
      8                25M6                25.6     3.4     7.6     5.6    17.5   1146.0     10.9    463.5      0.9      0.6      1.9      8.3     14.6      1.6     47.1      1.9      0.8      2.1
      9                25M7                23.8     3.4     7.7     7.0    15.0    982.5      9.6    335.7      0.8      0.4      5.1      5.0     13.1      1.6     33.3      2.1      0.5      1.8
     10                25M8                22.4     3.4     7.8     7.2    12.5    992.0      9.7    313.5      0.8      0.4      5.5      5.3     13.3      1.5      0.0      1.9      0.5      1.7
     11                25M9                26.5     2.7    11.6     6.7    36.0   2406.0    143.7    324.6      3.8      2.1    109.2      9.3     69.0     17.4     28.2      7.0      1.3      7.5
     12   25M10 (Porewater)                18.7     2.3    11.4     6.7    30.0   7800.0    495.0    265.5      7.2      8.2   1360.5      7.9     66.0     25.4      5.3     11.5      0.0     15.9
     13   25M11 (Porewater)                17.5     2.3    11.6     6.7    15.0   6840.0    447.8    191.3      7.5      7.8   1308.4      1.5     40.4     15.4      4.2      7.2      2.6      9.8
     14               25M12                25.8     3.5     9.3     3.6    28.0   3326.0     83.4    573.9      4.6      0.1     78.0      2.3    324.6     66.0      0.0     10.3      0.0      5.6
     15               25M13                25.1     3.0     9.1     4.7     8.0   2658.0    277.1    241.3      8.1      0.8      2.3      0.9     54.6     21.6     11.0     22.5      0.0     17.4
     16               25M14                26.6     2.7    11.4     6.8    36.0   2365.0    179.6    405.5      3.8      2.1    127.8      9.7     87.3     18.0     29.0      7.4      1.3      7.8
     17               25M15                28.1     2.6    11.0     4.0    98.0   6710.0    350.0    651.8     21.8      4.1    360.3      7.8    526.5    138.3     60.3     51.8      0.0     38.0
     18               25M17                25.8     2.7    10.9     6.6    36.0   2425.0    122.0    290.7      3.8      2.0     77.0     13.0     63.0     19.1     34.0      7.4      1.3      8.2
     19               25M18                24.3     2.7    10.3     6.4    35.0   2373.0    166.2    378.9      3.9      2.1    139.5      9.5     79.8     18.4     30.2      7.4      1.3      7.8

MIX 1
    14     0.34
    15     0.0692
    18     0.84

REACTION 1
    H2O(g)      -13.8
    1 moles in 1 steps
EQUILIBRIUM_PHASES 1
    Bieberite 0 0
    Epsomite  0 0
    Fe(OH)3   0 0.000304
    Gypsum    0 0
    Mn(OH)2(am) 0 0
    NiSO4     0 0
    ZnSO4     0 0


END
```

Figure A.19: PHREEQC script for forward modelling of mixing of inlet streams using the ratio derived from inverse modelling

`

```
SOLUTION_SPREAD
    -units    mg/l
 Description        Al   Ca      Co      Cr       Fe      K        Mg     Mn    Na        Ni     Tl     Zn       pe      pH    Temperature       S(6)
                                                                                                                                          as S
     Crust 6     571.5   39      12              204     27      492.5   22.5          17.5    100    14      10.2    2.82             24     2232.5

SAVE solution 6

EQUILIBRIUM_PHASES 6 Equilibrating with gases
    CO2(g)     -2 10
    O2(g)      -0.7 10


END
USE solution 6
EQUILIBRIUM_PHASES 6
    CO2(g)     -3.5 10
    O2(g)      -0.7 0
REACTION 6
    H2O(g)      -1
    53 moles in 53 steps

END
```

Figure A.20: PHREEQC script for solubility analysis for evaporation modelling of dissolved crust solution

```
SOLUTION_SPREAD

    -pe        10
    -units     mg/l
 Description        Al   Ca      Co      Cr       Fe      K        Mg     Mn    Na        Ni     Tl     Zn       pH    Temperature          S(6)
                                                                                                                                    as S charge
     Crust 6     571.5   39      12              204     27      492.5   22.5          17.5    100    14      2.82             24        2232.5

EQUILIBRIUM_PHASES 6 Equilibrating with gases
    CO2(g)     -2 10

SAVE solution 6
END
USE solution 6
EQUILIBRIUM_PHASES 6
    Alunite    0 0
    Anhydrite  0 0
    CO2(g)     -3.5 10
    Gypsum     0 0
    Jarosite(ss) 0 0
    Jarosite-K 0 0
    JarositeH  0 0
REACTION 6
    H2O(g)      -1
    53 moles in 53 steps

END
```

Figure A.21: PHREEQC script for mineral precipitation during evaporation modelling of dissolved crust solution

`

```
#Model 1:Adding only epsomite

SOLUTION 1
    temp      25
    pH        7
    pe        4
    redox     pe
    units     mmol/kgw
    density   1
O(0)      1 O2(g)      -0.7
    -water    1 # kg

REACTION 1
    Epsomite   1
    0.044090 moles in 6 steps

SELECTED_OUTPUT
    -file                  Mg
    -ph                    true
    -pe                    true
    -reaction              true
END

..... Other models were included

#Model 6: Adding minerals and allowing for precipitation of Fe(OH)3

PHASES
Coquimbite
    Fe1.47Al0.53(SO4)3:9.65H2O = 1.47 Fe+3 + 0.53 Al+3 + 3 SO4-2 + 9.65 H2O
    log_k     -0.4345
    delta_h   340.873 kJ

SOLUTION 1
    temp      25
    pH        7
    pe        4
    redox     pe
    units     mmol/kgw
    density   1
    O(0)      1 O2(g)      -0.7
    -water    1 # kg

REACTION 1
    Epsomite   0.044090
    Al2(SO4)3:6H2O 0.022377613
    Coquimbite 0.00198
        MnSO4      0.001115
    1 moles in 6 steps


SELECTED_OUTPUT
    -file                  Al, Fe, Mg, Mn FeOH3 ppt
    -ph                    true
    -pe                    true
    -reaction              true

EQUILIBRIUM_PHASES 1
    Fe(OH)3(a) 0 10 precipitate_only

END
```

Figure A.22: Example PHREEQC script for forward modelling of the first and final model for efflorescent crust dissolution

`

```
SOLUTION_SPREAD
    -units    mg/l
                Description      Al         Ca   Cd      Co      Cu      Fe(2)      K      Li         Mg      Mn         Na      Ni      Rb      Si      Sr       U      Zn      pH    Temperature      pe          Alkalinity      Cl          S(6)     O(0)    Number
                                                                                                                                                                                                                    as Ca0.5(CO3)0.5            as SO4 charge    as O2
                  AMD Feed 1     0.1     1153.8   0.1     0.9     1.3      819.0   21.1    0.5      675.0    36.2      355.0     2.2     1.8     1.9     0.5     0.3     0.4    5.28          27.5     4.4             29.6     110          4550      3.0         1
                  AMD Feed 2     0.2     1662.5   0.1     0.8     1.2      806.0   25.6    0.4      987.5    41.2      580.0     2.1     1.7     1.8     0.5     0.3     0.3    5.17          27.8     4.4             27.7     106          4746      3.0         2
            Processed water 1    0.0      970.0   0.0     0.0     0.0       13.2   21.4    0.4      255.0     0.6      237.5     0.0     0.1     0.3     0.4     0.0     0.0    5.67          26.8     4.4             28.5     106          3066        6         3
 Processed water 2 (dup of 1)    0.0      937.0   0.0     0.0     0.0        0.0   17.7    0.4      195.0     0.4      271.0     0.0     0.1     0.3     0.4     0.0     0.0    6.67          26.7     4.4             28.7     104          2830        6         4


PHASES
Ettringite
    Ca6Al2.02(SO4)2.79(OH)12.48:26H2O + 12.48H+ = 6Ca+2 + 2.02Al+3 +2.79SO4-2 + 38.48H2O
    log_k     61.82
# Step 1
MIX 1
    2    1
SAVE solution 5

END
MIX 1
    4    1
SAVE solution 6
END

USE solution 5
#Step 2
#Dosage rate of lime is 1.2 kg/m3, therefore 0.016 mol/L (1.2kg/1000L =0.012kg/L = 1.2 g/L = 0.016 mol/L)
EQUILIBRIUM_PHASES 1
    CO2(g)    -3.5 0
    O2(g)     -0.7 10
    Portlandite 0 0.016

SAVE solution 7
END
# Step 3
# Surface 4 using Dzombak and Morel parameters: 0.2 mol weak sites and 0.005 mol strong sites per mole Fe and 5.33e4m2/mol Fe. Allow precipitation and surface complexation onto fresh surface
# Look at minerals oversturated in simulation 3, these minerals are allowed to precipitate here (except carbonates unless SI>2.5)
USE solution 7
EQUILIBRIUM_PHASES 4
    CO2(g)    -3.5 0
    Cu(OH)2   0 0
    Fe(OH)3(a) 0 0
    Gibbsite  0 0
    Gypsum    0 0
    O2(g)     -0.7 10
    Pyrochroite 0 0
    Cu(OH)2   0 0

SURFACE 4
    Hfo_sOH Fe(OH)3(a)      equilibrium_phase 0.005  53300
    Hfo_wOH Fe(OH)3(a)      equilibrium_phase 0.2

SAVE solution 8
END
#Step 4
#Estimating composition of the sludge. Sludge is continually reworked at treatment site.
#2.24 mol of HFO, therefore (0.2*2.24) weak sites and (0.005*2.24) strong sites.

SURFACE 1
    Hfo_sOH    0.011     600       200
    Hfo_wOH    0.448

USE solution 6

SAVE surface 2

END
# Step 4, rinse 1
USE surface 2
USE solution 6

SAVE surface 3

.... This was repeated for a further 7 rinses

END
#Adding surface effect of sludge to the partially processed minewater solution

USE solution 8
USE surface 11
EQUILIBRIUM_PHASES 5
    CO2(g)    -3.5 0
```

Figure A.23: PHREEQC script for forward modelling of a high density sludge acid mine drainage treatment facility